Faculty of Engineering and Science

Enzyme-immobilized Polymeric Capsules for Removal of Synthetic Phenol

Chiong Tung

This thesis is presented for the Degree of

Doctor of Philosophy

of

Curtin University

November 2018

DECLARATION

To the best of my knowledge and belief this thesis contains no material previously published by any other person except where due acknowledgment has been made.

This thesis contains no material which has been accepted for the award of any other degree or diploma in any university.

Signature: ……..

Date: 12th November 2018

ACKNOWLEDGEMENT

First and foremost, I would like to extend my gratitude to the Almighty God for giving me the opportunity to embark on this PhD journey, and for his abundant grace and blessings throughout the journey so that I can accomplish this research in the best possible way.

I would also like to express my sincere gratitude and appreciation to my supervisors, Dr John Lau Sie Yon, Professor Michael Kobina Danquah and Dr Khor Ee Huey for giving me the opportunity to work under them. Their endless guidance and insightful advice have been of tremendous help to me in facing all the ups and downs in this research project. Their continuous encouragements have kept me moving forward to achieve my goal. Also, not forgetting their understanding and positive support throughout my pregnancy and maternity leave in the last year of research.

A special thanks to Curtin Malaysia Research Institute (CMRI) for the financial support especially in HDR monthly stipend and research funding of this project. I wish to thank the laboratory technicians, mainly Ms Magdalene Joing Bangkang and Ms Michelle Martin for their kind assistance especially during instruments breakdown or lack of chemicals in the laboratory. I also like to remember my colleagues for their valuable suggestions and kind support.

Last but not least, I am profoundly grateful to my beloved husband, David Ngu for his unconditional love and support in my PhD undertaking. Thank you for having faith in me and looking after our lovely children whenever I had to work overtime for experimental work. I am also indebted to my beloved parents for being caring and generous enough to stand by me to achieve whatever I have today.

PUBLICATION LIST

Journal paper

1. Chiong, T., S. Y. Lau, Z. H. Lek, B. Y. Koh, and M. K. Danquah. 2016. "Enzymatic Treatment of Methyl Orange Dye in Synthetic Wastewater by Plant-Based Peroxidase Enzymes." *Journal of Environmental Chemical Engineering* 4 (2): 2500-2509.
2. Chiong, T., S. Y. Lau, X. H. Zeng, and M. K. Danquah. 2017. "Synthesis of a peroxidase-encapsulated biopolymer for enhanced removal of phenolic compounds." (Submitted to Asia-Pacific Journal of Chemical Engineering – under review).

Conference paper

1. Chiong, T., S.Y. Lau, E.H. Khor, and M.K. Danquah. Peroxidase extraction from JP skin peels for phenol removal. 5th International Conference on Chemical and Bioprocess Engineering (ICCBPE 2015), Kota Kinabalu, Malaysia, 9-12 December, 2015.
2. Chiong, T., E.H. Khor, M.K. Danquah, and S.Y. Lau. Comparison of Two Agricultural Wastes for Phenol Removal via Peroxidase-Catalyzed Enzymatic Approach. 5th International Conference on Chemical and Process Engineering (ICCPE 2016), Jeju, Korea, 23-25 May 2016. MATEC Web of Conferences 69, 01002 (2016).

ABSTRACT

Apart from being the economic backbones of many countries, the rapid growth and development of industry sector also results in the discharge of huge volumes of industrial effluents. Amongst the various pollutants present in the effluents, phenol and its derivatives are regarded as priority pollutant due to their harmful and toxic characteristics even at low concentrations. Conventional technologies for phenol removal process are often challenged by lengthy start up / acclimatization period, huge volume of sludge, intensive cost and energy for adsorbent regeneration, and environmental concerns associated with the disposal of reagents used in the process. In view of this issue, the enzymatic approach has emerged as a promising alternative strategy for the treatment of phenol-containing wastewaters, owing to its substrates specificity, low energy requirements, more flexible operation conditions, and minimal environmental impacts.

In the literature, the potential of peroxidases, an enzyme that is ubiquitous in nature, in phenol degradation has been extensively explored with high removal efficiency. However, most of the studies conducted focused on horseradish peroxidase, soybean peroxidase and/or other microbial peroxidases under free enzyme condition. The major drawbacks of free enzymes are enzyme inactivation due to instability, and non-reusability. These challenges can be overcome by enzyme immobilization. Even that, the reports on continuous phenol treatment using immobilized peroxidases, either in packed-bed or fluidized-bed reactor, are limited. Therefore, this study aims to (1) extract and characterize peroxidase enzymes from local agricultural wastes in order to explore optimal applications in phenol treatment under varying physicochemical conditions, (2) to synthesize and biophysically characterize sodium cellulose sulphate / poly-dimethyl-dially-ammonium chloride (NaCS-PDMDAAC) polymeric capsules for effective peroxidase binding and enhanced mass transport, and (3) to experimentally study the performance of peroxidase-immobilized polymeric capsules for batch and continuous biodegradation of phenol.

The local agricultural wastes considered in this research project were *Luffa acutangula* (LP) and *Pachyrhizus erosus* (JP) skin peels. This research was conducted in several stages: extraction of Luffa peroxidase (LP) and Jicama peroxidase (JP) from their

respective skin peels, characterization of crude enzyme extracts using various analysis instrumentations, phenol degradation using the crude enzyme extracts, optimization of phenol removal process using design of experiment, synthesis of NaCS-PDMDAAC and immobilization of JP unto NaCS-PDMDAAC polymeric capsules, and application of enzyme-immobilized polymeric capsules for phenol degradation under batch and continuous process.

The crude enzyme extracts of LP and JP exhibited enzymatic activities of 1.38±0.03 and 1.57±0.02 U/mL respectively at the optimal extraction conditions of pH 7, 50% sample-to-buffer ratio (w/v) at 25 ºC for 30 min. Both peroxidases showed fair stability under varying pH and temperatures. The hydrodynamic sizes of LP and JP under stable configurations were found to be 127 and 365 nm, respectively, whereas their respective isoelectric points were at pH ~4.4 and ~4.9. Under free enzyme conditions, LP demonstrated >95% phenol removal efficiency under pH 7 and 6-8 mM H_2O_2 concentrations at 25-30 ºC. JP showed a comparable removal efficiency of 94.5% at pH 7 but over a wider range of H_2O_2 concentrations. JP also showed extended functionality up to 40 ºC. Under optimum operating conditions, the maximum removal for LP and JP was achieved in 16 and 13 h respectively. The performance of JP was further improved via optimization using factorial design and central composite design (CCD). Phenol removal efficiency of 95% was obtained after process optimization at pH ranging from 5.3 to 7 with H_2O_2 concentrations ranging from 4.3 mM to 7.9 mM at an enzyme loading equals to 3 mL. The proposed second order model was in good agreement with the experimental data according to Analysis of variance (ANOVA).

For immobilization, NaCS was successfully synthesized through cellulose sulphation process using cotton linter as source of cellulose. NaCS-PDMDAAC polymeric capsules of composition 2% NaCS and 6% PDMDAAC synthesized at 25 ºC gave uniform spherical capsules with mechanical strength of 1.12±0.35 N. The encapsulation efficiency of JP within this biopolymers was 87.4%, and the enzyme-encapsulated beads had an average diameter of 5.05±0.16 mm and a membrane thickness of ~31 µm. Immobilized JP demonstrated optimum working pH 6 over a broad range of H_2O_2 concentration, but required 15 h for optimal phenol removal efficiency of >95% due to diffusive mass transfer limitation. Nonetheless, JP-immobilized capsules maintained reusability up to 4 cycles at the highest removal efficiency of >95% with no regeneration.

The evaluation of JP-immobilized NaCS-PDMDAAC capsules in the customized fluidized bed column revealed that 109.6 mL/min was the optimum flow rate, giving a phenol removal efficiency of 96% after 8 h reaction with an average enzymatic activity of 0.13 U/mL. Increase of enzyme loading to 0.20 U/mL shortened the reaction time to 7 h with similar removal efficiency. Under continuous phenol removal process, JP-immobilized biopolymer capsules can be reused up to 8 cycles with a removal efficacy averaging at 95%. The results generated from this work demonstrate that immobilized JP in NaCS-PDMDAAC capsules holds great potential to be an alternative for phenol treatment under batch and continuous processes, and provide a basis for further product and process improvement in the future.

TABLE OF CONTENTS

LIST OF FIGURES

LIST OF TABLES

LIST OF ABBREVIATIONS

AAm-HEMA	acrylamide-2-hydroxyethyl methacrylate
4-AAP	4-aminoantipyrene
ABTS	2, 2'-azino-bis(3-ethylbenzothiazoline)-6-sulfonate
Al-PILC	Aluminium-pillared interlayered clay
ANOVA	Analysis of variance
AOP	Advanced oxidation process
BGP	Bitter gourd peroxidase
BOD_5	Biological oxygen demand
BSA	Bovine serum albumin
CCD	Central composite designs
CFD	Computational fluid dynamics
CLEAs	Cross-linked enzyme aggregates
CMC	Carboxymethyl cellulose
COD	Chemical oxygen demand
Con A	Concanavalin A
CSTR	Continuous stirred tank reactor
DOE	Design of experiment
EFB	Empty fruit bunch
FBR	Fluidized bed reactor
FTIR	Fourier transform infrared spectroscopy
GAC	Granular activated carbon
GO	Graphene oxide
GMA-MMA	Glycidylmethacrylate-co-methylmethacrylate
GRP	Growth related productivity
hFasL	Human Fas ligand
HRP	Horseradish peroxidase
HRT	Hydraulic retention time
JP	JP
LiP	Lignin peroxidase
LP	LP peroxidase
MnP	Manganese peroxidase

MWCO	Molecular weight cut-off
NaCS	Sodium cellulose sulphate
OFAT	One-factor-at-a-time
OSHA	Occupational Safety and Health Administration
PAC	Powdered activated carbon
PAN	Polyacrylonitrile
PANImG	Magnetite-modified polyaniline
PBR	Packed bed reactor
PBS	Phosphate buffered saline
PDMDAAC	Poly-dimethyl-dially-ammonium chloride
PEC	Polyelectrolyte complex
PEG	Polyethylene glycol
PEL	Permissible Exposure Limit
PUF	Polyurethane foams
RGO	Reduced graphene oxide
RL	Rhamnolipid
ROH	Phenolic substrate
RSM	Response surface methodology
PVP	Polyvinylpyrrolidone
SBP	Soybean peroxidase
TOC	Total organic carbon
TP	Turnip peroxidase
TS	Tea saponin
SEM	Scanning electron microscopy
TWA	Time-Weighted Average
UV	Ultra-violet
WHO	World Health Organization

NOMENCLATURE

AH_2	Aromatic molecule
$\cdot AH$	radical
E_i	Compound I
E_{ii}	Compound II
E_{iii}	Compound III
E-670	Verdohaemoprotein
E_i-H_2O_2	Intermediate enzyme-peroxide complex
E_N	Native peroxidase enzyme
$RO\cdot$	Phenoxy radical
V_o	Initial reaction rate
V_{max}	Maximum rate
K_m	Michaelis-Menten constant
S	Substrate
y	Predicted response
x	Experimental variable
β_o	Constant
β_j	Linear coefficient
β_{jj}	Squared coefficient
β_{ij}	Cross-product coefficient
ε	Model error
x_j	Linear term
x_j^2	Curvature term
$x_i x_j$	Interaction term
k	Number of factors
Cp	Replicate number of the central point
N	Number of experiments
R^2	Coefficient of determination
R^2_{adj}	Adjusted coefficient of determination

CHAPTER 1: INTRODUCTION

1.1 BACKGROUND

The rapid growth of industrial development in a country does not only benefit the country economically. It results in huge volumes of industrial wastewater. The presence of heavy metals and organic compounds in industrial liquid effluents adversely affects aquatic lives and human health if not treated properly before discharge. Among the numerous compounds generated by industrial activities, phenols and its derivatives are regarded as priority pollutants (Karam and Nicell 1997) owing to its toxicity and recalcitrant characteristic. Phenol and its derivatives are found in various industrial wastewaters such as petroleum refineries (6-500 mg/L), coking operations (28-3900 mg/L), coal processing (9-6800 mg/L), and petrochemicals manufacturing (2.8-1220 mg/L). Phenols are also present in the wastewater of plastics, wood products, paint, and pulp and paper (0.1-1600 mg/L) (Busca et al. 2008).

Phenol causes damages to the liver, kidney, lung and vascular system once it enters the human body (Said et al. 2013). Phenol can be absorbed through the skin, resulting in skin and eye burns upon contact. Comas, convulsions, cyanosis and even death are associated with over exposure to phenol (Michałowicz and Duda 2007). Apart from that, phenols also contribute to off-flavours in drinking water and food processing waters. The maximum permissible limit for chlorophenols (2 chlorophenol, 2,4-dichlorophenol, and 2,4,6-trichlorophenol) is set at 0.2 mg/L by the World Health Organization (WHO) (WHO 2011). Current Occupational Safety and Health Administration (OSHA) Permissible Exposure Limit (PEL) for phenol is 5 ppm as an 8-hour Time-Weighted Average (TWA) concentration (OSHA 2018). According to Wastewater Discharge Standards in Malaysia, the maximum permitted values of phenol are 0.001 and 1.0 mg/L for Standard A and Standard B respectively. For raw water quality, the permitted value is 0.002 mg/L (MWA 1994).

The most widely used technologies for the treatment of phenol-containing wastewaters are microbial degradation, adsorption, and chemical reaction. Although showing high phenol removal efficiencies, these treatment methods are also challenged with some recurrent drawbacks (Firozjaee et al. 2012; Gernjak et al. 2003; Busca et al. 2008). As a result, the enzymatic process has emerged as an alternative approach for phenol

degradation due to perceived advantages including low energy requirements, more flexible operation conditions, and minimal environmental impacts (Gómez et al. 2011). Enzymes have high substrates specificity, and can remove target pollutants selectively (Aitken 1993). Enzymatic treatment method has no delays associated with the acclimatization of biomass, and the volume of sludge produced is also low (Nicell, Al-Kassim, et al. 1993). Besides, enzyme-based process is capable of tackling compounds which are recalcitrant to conventional methods (Nicell, Bewtra, Biswas, St. Pierre, et al. 1993). Therefore, this approach can be integrated into conventional treatment methods either as secondary or tertiary treatment step to tackle bio-refractory compounds.

In this research, LP and JP extracted from their respective agricultural wastes are used in enzymatic-based phenol degradation. Various types of peroxidases have been evaluated for their feasibilities in phenol treatment. These include peroxidases from horseradish and soybean (Cooper and Nicell 1996; Nicell et al. 1992; Kinsley and Nicell 2000; Wilberg et al. 2002; Bódalo, Gómez, Gómez, Bastida, et al. 2006), turnip (Duarte-Vázquez et al. 2003), *Coprinus cinereus* (Ikehata et al. 2005), tomato hairy roots (González et al. 2008), bitter gourd (Ashraf and Husain 2010) and cauliflower (Deva et al. 2014). Once activated by H_2O_2, peroxidase catalyzes the oxidation of aromatic compounds to form free radicals, which polymerize spontaneously and precipitate out of solution due to low solubility. The precipitates can be separated by sedimentation and/or filtration techniques (Wilberg et al. 2002).

However, non-reusability of peroxidases under free enzyme condition have limited its application to a greater extent in peroxidase-based enzymatic technology. This is mainly due to the high cost of peroxidase available commercially. This disadvantage can be circumvented by immobilization technique. Immobilized enzymes demonstrate higher stability and enable a continuous process with product recovery (Shukla et al. 2004). Interruption of process reaction is also possible by removing the immobilized enzyme and thus controlling the product formation (Caramori and Fernandes 2004).

Peroxidases have been successfully immobilized on different supports, such as magnetite (Tatsumi et al. 1996), porous beads (Cho et al. 2008; Gómez et al. 2011; Chagas et al. 2015; Wang et al. 2015; Wang, Fang, et al. 2016), different polymers with diverse configurations (Zhang et al. 2010; Zhai et al. 2013), membranes (Vasileva

et al. 2009; Wang, Liu, et al. 2016), product precipitates (Feng et al. 2013), as well as encapsulation in natural marine polysaccharide K-Carrageenan (Shukla et al. 2004), calcium alginate (Alemzadeh and Nejati 2009; Quintanilla-Guerrero, Duarte-Vázquez, García-Almendarez, et al. 2008; Quintanilla-Guerrero, Duarte-Vázquez, Tinoco, et al. 2008) and phospholipid-templated titania particles (Jiang et al. 2014). These immobilized enzymes have demonstrated better pH and thermal stabilities, comparable or higher removal efficacy than its free enzymes counterpart, and also reusability in phenol degradation.

Sodium cellulose sulphate (NaCS) / poly [dimethyl(diallyl)ammonium chloride] (PDMDAAC), one of the commonly employed polyelectrolyte complex (PEC) systems, has been used to encapsulate microorganisms for various bioprocess productions (Förster et al. 1996; Zhao et al. 2006). NaCS-PDMDAAC polymeric matrix has also demonstrated successful employment in tissue engineering / gene transfer in medical systems (Lohr et al. 2002; Saller et al. 2002), membrane systems for salt rejection processes (Li and Yao 2009), and cell cultivations of yeast (Mei and Yao 2002), microalgae (Zeng, Danquah, Halim, et al. 2013) and recombinant proteins (Zheng et al. 2015). It was reported that the physical properties of NaCS-PDMDAAC polymeric carrier such as mechanical strength, opacity, pore diameter and mass transfer rate can be easily altered by varying the synthesis variables to suit different application purposes (Tan et al. 2011; Zeng et al. 2012; Chen et al. 2013).

Apart from giving high removal efficiency, effective wastewater treatment technologies should also ensure continuity in pollutant removal operation. In comparison with batch process, a continuous process demonstrates benefits in terms of ease of automation and control, leading to reduced operational cost and increase in throughput at consistent rate (Sheeja and Murugesan 2002). In this context, fluidized bed reactor (FBR) offers some excellent features such as low operating cost, high resistance to system upsets, high mass transfer rates, uniform particle mixing and uniform temperature distribution (Bello et al. 2017). These features have seen FBR's wide applications in wastewater treatment (Haribabu and Sivasubramanian 2016; Zhou et al. 2015; Mokhtar et al. 2011; Shet and Vidya 2016). Despite the enumerable studies of FBR for wastewater treatment, incorporation of peroxidase-based enzymatic approach onto this continuous system is limited (Trivedi et al. 2006a; Gómez et al. 2007).

Driven by the capability of plant peroxidase in oxidation and polymerization of phenol compounds, potential of immobilization using NaCS-PDMDAAC polymeric carrier, as well as lacking of information on peroxidase-based enzymatic approach in FBR, this project focuses on extraction of newly-sourced plant peroxidases from local agricultural wastes and immobilization of crude peroxidase extracts for continuous phenol removal from aqueous solution in a fluidized bed column. In particular, this thesis covers the identification and extraction of LP and JP from their respective plant skin peels. The crude enzyme extracts are characterized for their biophysical and biochemical properties, and are also evaluated for their efficacy in treating aqueous phenol solutions. The selected plant peroxidase will be subjected to optimization of phenol removal process via Design of Experiment, and subsequently immobilization unto NaCS-PDMDAAC polymeric matrix system. The biophysical characteristics of peroxidase-encapsulated NaCS-PDMDAAC polymeric capsules in terms of stability, encapsulation efficiency, hydrodynamic size and zeta potential, surface morphological analyses and binding characteristics are discussed herein. The efficacy of immobilized peroxidase in bioremediation of phenol is also compared with its free enzyme counterpart. Lastly, the potential application of peroxidase-immobilized polymeric capsules for continuous phenol treatment is explored using a customized fluidized bed column.

1.2 PROBLEM STATEMENTS / RESEARCH GAPS

Some problem statements and research gaps have been identified as follows:

1. Phenols are present in wastewater of various industries, and the concentration ranges from <10 to >6000 mg/L depending on the processes. Phenol is a hazardous organic pollutant because it is toxic even at low concentrations. Exposure to phenol results in adverse health effects to human, and presence of phenol in water can contribute to off-flavours in drinking and food processing waters besides endangering the species of the ecosystem.
2. Current technologies for phenol treatment suffer from certain recurrent drawbacks such as lengthy start-up procedure for microbial acclimatization, microbial growth inhibition due to high concentrations of phenolic compounds, high energy requirement for adsorbent preparation, intensive cost and energy for adsorbent

regeneration, and environmental concerns associated with the disposal of reagents used in the chemical oxidation.

3. Peroxidase-based enzymatic approach acts on phenol/phenolic compounds through oxidation in the presence of H_2O_2, resulting in insoluble polymer products which can be easily separated from solutions via filtration. However, free enzymes are usually challenged by susceptibility to inactivation, lack of long-term stability, difficulty in recovery, and non-reusability.
4. Most of the reported studies on peroxidases for phenol degradation are limited to batch operation mode (either in free or immobilized state). Batch operation is not practical in wastewater treatment as industrial effluents are generally released in bulk quantity continuously. The viability of peroxidase for continuous treatment of phenol should therefore be investigated in order to address its potential for large-scale application.
5. To overcome the aforementioned problem statements, this research project proposed the extraction of newly sourced plant peroxidases from local agricultural wastes, and immobilization of peroxidase onto NaCS-PDMDAAC polymeric capsules for phenol removal under batch and continuous processes. Amongst various families of peroxidases, plant peroxidases are chosen as candidates because the extraction process is simple and does not involve the complicated and lengthy cell cultivation steps. The plants being selected are also abundantly available in Malaysia throughout the year, so as to ensure continuous supply of agricultural bio-wastes for peroxidase extraction. NaCS-PDMDAAC as encapsulating materials has not been used for peroxidase immobilization. Biocompatibility between peroxidase and polymeric matrix system can be examined upon immobilization. Peroxidase encapsulated onto NaCS-PDMDAAC polymeric capsules will then be applied to phenol treatment from aqueous solutions under batch and continuous operating modes. For continuous phenol removal, the process will be conducted in a custom-made fluidized bed reactor.

1.3 RESEARCH QUESTIONS

1. Can newly-sourced crude peroxidase extracts from local agricultural wastes be used for biodegradation of phenol from aqueous solutions via enzymatic approach?
2. Can such peroxidase be successfully immobilized onto NaCS-PDMDAAC polymeric capsules?

3. Can peroxidase-immobilized NaCS-PDMDAAC polymeric capsules be an alternative for phenol removal under batch and/or continuous process?

1.4 OBJECTIVES

The main aim of this research is to develop a continuous bioprocess of phenol removal from aqueous solutions using newly-sourced plant peroxidase from local agricultural waste which is immobilized onto NaCS-PDMDAAC polymeric capsules. In particular, the objectives of this research are:

1. To extract and characterize peroxidase enzymes from local agricultural wastes in order to explore optimal applications in phenol treatment under varying physicochemical conditions.
2. To synthesize and biophysically characterize sodium cellulose sulphate / poly-dimethyl-dially-ammonium chloride (NaCS-PDMDAAC) polymeric capsules for effective peroxidase binding and enhanced mass transport.
3. To experimentally study the performance of peroxidase-immobilized polymeric capsules for batch and continuous biodegradation of phenol.

1.5 NOVELTY

Two newly-sourced plant peroxidases from local agricultural wastes for the treatment of phenol solutions are proposed. The non-seasonal plants ensure continuous supply of bio-wastes for peroxidase extraction. Combining the advantages of plant peroxidase and NaCS-PDMDAAC polymeric matrix, a novel system of agricultural waste peroxidase encapsulated in NaCS-PDMDAAC polymeric carrier is developed. This peroxidase-encapsulated polymeric capsules with enhanced enzyme functionality and reusability is newly explored for its performance in treating phenol-containing wastewater. The viability of this immobilized system for continuous phenol treatment is also explored and presented using a customized laboratory-scale fluidized bed column.

1.6 SCIENTIFIC MERITS AND SIGNIFICANCE OF RESEARCH

This research project will promote research contributions and scientific merits to bioprocess and biotechnology, environmental science and engineering as well as wastewater treatment. The findings from this research project would constitute new

knowledge on the characteristics of newly-sourced plant peroxidases and their behaviour in biodegradation of phenol from aqueous solutions. This project will also demonstrate that the efficiency of peroxidase-catalyzed enzymatic process can be improved through optimization. In addition, fundamental understanding of the characteristics of peroxidase-immobilized polymeric capsules as well as the efficacy of the immobilized enzyme for phenol treatment will be made available. Immobilization of peroxidase onto polymeric capsules can protect the encapsulated peroxidase from harsh environments without altering its enzymatic functionality, improve peroxidase stability and also ensure reusability. The concept of transforming an agricultural waste into a useful product for the treatment of another environmental waste offers a chain of green technology and value adding process. The novel peroxidase-encapsulated NaCS-PDMDAAC polymeric capsules is a new endeavour which possesses a significant potential to fit into existing bioremediation of phenol processing flowsheet in a continuous run.

1.7 THESIS LAYOUT

1. Chapter 1 gives an overview of conventional treatment methods employed in degradation of phenol from industrial effluents, and also the concept of immobilizing a newly-sourced plant peroxidase from local agricultural waste onto NaCS-PDMDAAC polymeric capsules for continuous phenol removal in a fluidized bed column.
2. Chapter 2 presents a review of various technologies available for phenol treatment, challenges faced by peroxidase-catalyzed enzymatic approach under free enzyme condition, different immobilization methods as well as the efficacy of immobilized peroxidases in phenol removal. Research gap is also emphasized at the end of Chapter 2.
3. Chapter 3 describes the research methodology used in this research, which includes extraction of plant peroxidase, physicochemical characterization of peroxidases, removal process of phenol from aqueous solution, synthesis of NaCS, encapsulation of crude peroxidase extracts onto NaCS-PDMDAAC polymeric capsules, characterization of peroxidase-encapsulated polymeric capsules and design of a fluidized bed column for continuous phenol removal using peroxidase-immobilized polymeric capsules.

4. Chapter 4 presents the results and discussions of this project, which include the following in-depth discussions:
   - Extraction of different plant peroxidases from local agricultural wastes under various extracting conditions, and biophysical characterization of these peroxidases.
   - Performance of crude plant peroxidase extracts in treating phenol under varying process parameters.
   - Optimization of phenol removal process using Design of Experiment for the selected plant peroxidase.
   - Synthesis of NaCS and formation of NaCS-PDMDAAC polymeric capsules, as well as encapsulation of selected plant peroxidase onto NaCS-PDMDAAC polymeric capsules.
   - Comparison of free and immobilized peroxidase in biodegradation of phenol.
   - The potential of immobilized peroxidase for continuous phenol removal process in a fluidized bed column.
5. Chapter 5 summarizes and highlights the key findings from this research in addition to reflections on the thesis objectives. Suggestions for future work towards further development of the peroxidase-immobilized polymeric capsules and enhancement of peroxidase's efficiency in biodegradation of phenol are also provided.

CHAPTER 2: LITERATURE REVIEW

2.1 OVERVIEW

The search for effective technologies for the treatment of phenol-containing industrial liquid effluents is an important research endeavour, and continues to be a challenging task in environmental science and engineering due to the several shortcomings suffered by conventional treatment methods. This has triggered research interests in developing improved alternatives for better process control and performance. The use of a ubiquitous enzyme called peroxidase for phenol treatment has gained much focus in the past owing to its substrates specificity and high catalytic functionality. Notwithstanding, peroxidase-based enzymatic approach is challenged by certain drawbacks including enzyme inactivation, enzyme cost and non-reusability. Therefore, the concept of enzyme immobilization and employment of immobilized enzyme in a column for continuous process holds a great promise to enhance the efficacy of peroxidase in this particular context. This chapter presents a critical review on existing technologies in removing phenol compounds from wastewater, the potential and challenges of peroxidase-based enzymatic method, various supports for enzyme immobilization as well as different configurations for continuous treatment of phenol. Problem statements and research gaps are also emphasized at the end of the chapter.

2.2 CURRENT TECHNOLOGIES FOR PHENOL TREATMENT

2.2.1 Microbial degradation

Biological method is appreciated as an inexpensive technique to treat wastewater containing phenolic compounds due to the presence of microorganisms which depend on phenolic compounds as source of carbon and energy for growth and reproduction. However, microbial growth can be inhibited at high concentrations of phenol. Approaches such as stepwise adaptation of microorganisms to higher phenol concentrations and/or procedures of genetic engineering are used to overcome this issue (Pradeep et al. 2015). Nonetheless, bioprocesses are generally preferred for large-scale treatment of industrial effluents because of the effectiveness in transforming the pollutants to non-toxic products in an environmental-friendly and cost-effective way (Krastanov et al. 2013).

Activated sludge reactors have been widely used to treat phenol in industrial wastewater due to the presence of various populations of microorganisms in the activated sludge. The effect of adaptation of mixed culture (activated sludge) on phenol biodegradation was studied by Marrot et al. (2006). The mixed culture was cultivated in an immersed membrane bioreactor with gradual adaption to increasing concentrations of phenol from 0.5 g/L to 3 g/L over a period of 4 months. When the acclimated sludge was taken for phenol degradation at different concentrations between 0.5 to 3 g/L, it was observed that more than 80 % of phenol degradation efficiency was achieved in less than 6 h for all experiments conducted. However, for complete phenol degradation, 54 h was required for an initial phenol concentration of 3 g/L. Inhibition effect of phenol as substrate due to toxic substrate metabolism was also observed at high phenol loading rate of 3.5 g/L.

An anaerobic biological process was carried out by Firozjaee et al. (2012) in a continuous stirred tank reactor (CSTR) with a consortium of mixed culture. The culture was acclimatized under anaerobic condition over a period of 2 months. Within the studied range of process parameters, it was noticed that 89% of initial phenol (100 mg/L) was removed at a hydraulic retention time (HRT) of 96 h, and the removal rate decreased with increasing inlet phenol concentration. A maximum biogas production rate of 2210 mL/d occurred at HRT of 96 h at 400 mg/L phenol. Anaerobic processes are known to have advantages such as elimination of aeration cost and recovery of methane.

Numerous species have been isolated from diverse microorganisms and characterized as phenol-degrading microorganisms. To this end, Agarry et al. (2008a) used an indigenous binary mixed culture of *Pseudomonas aeruginosa* and *Pseudomonas fluorescence* in a batch culture for phenol degradation. It was noticed that increase in initial phenol concentration resulted in increase of lag phase, leading to prolonged degradation process. Another Pseudomonas sp. SA01 was isolated from pharmaceutical wastewaters by Shourian et al. (2009). After an initial short lag phase, the isolated strain completed phenol decomposition of 0.7 g/L within 30 h. Significant inhibitory effect on bacterial growth was observed at phenol concentrations > 1 g/L. The optimum degradation pH was found to be 6.5.

Other microorganism species have also been reported to show high abilities in bioremediation of phenol. Liu, Xie, et al. (2016) successfully isolated a phenol-degrading bacterium strain PA from petrochemical wastewater. The strain was affiliated to *Acinetobacter calcoaceticus*, and achieved a 91.6% removal efficacy for an initial phenol concentration of 800 mg/L within 48 h, at optimum pH 8 and 30 ºC. Though suffering from inhibitory effect at phenol concentration above 800 mg/L, the strain still showed growth at 1700 mg/L phenol with a degradation rate of 46.2 %. A native bacteria strain isolated from coke oven processing also demonstrated high efficiency in removing phenol from wastewater. The optimum conditions for a maximal phenol removal rate of 97 % were found to be at pH 7, 30 ºC and 0.25 % supplemented glucose level (Chakraborty et al. 2010).

2.2.2 Adsorption

Adsorption via activated carbon is regarded as an effective method for phenol degradation because of its large surface area, micro-porous nature, high adsorption capacity as well as surface chemistry that reacts with molecules with specific functional groups (Wong et al. 2018). However, the relatively high cost of starting materials for commercial activated carbons such as wood and coals has made it less economically viable as adsorbent in pollution control applications. High regeneration cost and the generation of carbons fines are among other disadvantages associated with activated carbon, caused by the brittle nature of carbons used in removal of organic species (Lin and Juang 2009).

In recent years, special attention has been given to the use of cheaper raw materials to prepare activated carbon. For instance, Hameed and Rahman (2008) produced activated carbon from rattan sawdust through carbonization at 700 ºC under nitrogen atmosphere, soaking in potassium hydroxide (KOH), dehydration at 105 ºC, and pyrolysis under high purity nitrogen to a final temperature of 850 ºC. The activated carbon produced showed a maximum adsorption capacity of 149.25 mg/g, and its phenol removal efficiency was maximum and unaffected in the pH range of 3-8.

A highly porous carbon material was prepared from coconut spathe using KOH as activating agent and pyrolysed to 800 ºC under nitrogen atmosphere (Prashanthakumar et al. 2018). The maximum uptake of phenol, 2-chlorophenol and 4-chlorophenol were reported to be 120, 225 and 275 mg/g respectively within 15 min of contact time.

Desorption studies using sodium hydroxide (NaOH) showed that the adsorption and desorption efficiency decreased to 6 % after 5 cycles.

In contrast to the conventional preparation method through physical or chemical activation using a muffle furnace, Thue et al. (2017) produced activated carbons from wooden sawdust via microwave-assisted irradiation, using first-row transition metals (Co, Ni, Cu and Zn) as activating agents. Microwave irradiation greatly reduced the pyrolysis time of one cycle from few hours to less than 11 min including 5 min of cooling. Results showed that microwave-assisted activated carbon impregnated with Zn^{2+} showed higher pore volumes and surface areas, followed by Cu^{2+}, Co^{2+} and Ni^{2+}, independent of the ratio used. The adsorption capacities of the activated carbons for the tested adsorbates (2-nitrophenol and 4-nitrophenol) were in the order of $ZnCl_2$ > $CuCl_2$ > $CoCl_2$ > $NiCl_2$.

Apart from activated carbons, polymeric resins have also been viewed as a practical absorbent for efficient removal of aromatic pollutants although the bonding forces between the adsorbent and the adsorbate are weaker. This is beneficial for the regeneration process (Lin and Juang 2009). In a comparison study between non-functionalized resin and anion exchange resins with different strengths, Caetano et al. (2009) found that double contributions of adsorption and ion exchange mechanism enhanced the phenol uptake from aqueous solution. Three new porous copolymers in the form of microspheres but with different shape of pores and chemical structures were prepared via suspension polymerization method (Sobiesiak and Podkoscielna 2010). The copolymer which contained imide functional groups and was rich in carbonyl groups showed the strongest affinity towards phenol compounds.

2.2.3 Chemical oxidation

Chemical oxidation employs strong oxidants to destroy phenolic compounds. With low reagent and energy costs, this process could operate under mild temperature and pH conditions. Some of the commonly used chemicals for oxidative treatment of wastewater include ozone, chlorine, chlorine dioxide, chloramines, ferrate [Fe (VI)], and permanganate [Mn (VII)] (Villegas et al. 2016).

The oxidation of laboratory-synthesized potassium sulfatoferrate pellets on phenol was compared to pure potassium ferrate and other chemical oxidants (Peings et al. 2015).

It was noticed that the impurities in the pellets of potassium sulfatoferrate did not adversely impact its efficacy in phenol removal and mineralization. All the oxidants studied completely transform the phenol when used in greater than stoichiometric amounts. The effect of 2, 2'-azino-bis(3-ethylbenzothiazoline)-6-sulfonate (ABTS) on the oxidation of substituted phenols by potassium permanganate (Mn(VII) was evaluated by (Song et al. 2015). The oxidation kinetics of phenolic compounds were greatly enhanced due to the quick production of the stable radical cation [ABTS(•+)] from the oxidation of ABTS by Mn(VII).

Treatment of olive mill wastewater was carried out by Kallel et al. (2009) using spiral iron metal and hydrogen peroxide. The removal of phenolic compounds in the wastewater was 50% after 3 h reaction time under continuous presence of iron metal, acidic pH (2.0-4.0), and concentrated H_2O_2 (9.5 M) conditions. In the study using iron powder to treat coking wastewater, Chu et al. (2012) reported that 95% of total phenol was removed at an initial pH of < 6.5 and H_2O_2 concentration of 0.3 M in 1 h. The pH of the solution also decreased to 3.3 after 1 h.

Degradation of phenol from synthetic and petrochemical industries wastewater by photocatalytic UV/TiO_2 process was conducted by Nickheslat et al. (2013). For an initial phenol concentration of 40 mg/L, the removal efficiency was 60 % at pH 3 and 300 min. Choquette-Labbé et al. (2014) reported that 10 nm diameter TiO_2 particles operated at 37 °C resulted in the optimal degradation of phenolic compounds. Suzuki et al. (2015) developed a compact advanced oxidation process (AOP) reactor which generated ozone by UV irradiation, and concluded that the synergistic effect of using a combination of ozone, UV, and TiO_2 was due to the increased generation of •OH radicals during the oxidation process.

Babuponnusami and Muthukumar (2012) reported a similar observation whereby combination of UV irradiation and electrolysis using Fenton's reagent showed better performance amongst various types of AOPs. Phenol degradation efficiency was observed in the sequence of photo-electro-Fenton > ultrasonic-electro-Fenton > electro-Fenton > Fenton.

2.3 ENZYMATIC APPROACH FOR PHENOL REMOVAL PROCESS

As presented in the preceding section, microbial degradation, adsorption and chemical oxidation technologies are capable of removing phenol compounds from wastewater with high efficiency. However, it can also be noticed that there are some challenges associated with these current technologies. For microbial degradation process, lengthy start-up for microbial acclimatization which takes from weeks to months is unavoidable. Extreme high phenol concentration can also inhibit microbial growth which consequently affects the performance of microbial degradation process. As for adsorption, although cheaper absorbents have been successfully prepared from natural biomass, the synthesis of activated carbon generally involves carbonization and pyrolysis at extreme high temperatures, followed by physical or chemical activation. The exhausted activated carbons also need to undergo regeneration in order to ensure that adsorption process will be economically attractive. Regeneration of activated carbons is time consuming and expensive, and repetitive heating and cooling from regeneration cause loss of carbon due to oxidation and attrition (Busca et al. 2008). Chemical oxidation, on the other hand, involves the usage of excess reagents during oxidation process which will cause disposal problem after the reaction.

Taking these into consideration, research studies have been focused on finding alternative methods that are versatile for a wide range of reaction conditions with little or no environmental impacts post-treatment. There is a growing recognition that enzymatic treatment can be a potential alternative for phenol removal. Besides transforming the recalcitrant pollutants, enzymes also alter the characteristics of waste effluent for easier post treatment processes (Karam and Nicell 1997). Phenol solutions of high concentration can also be treated within a short time without dilution. This is favourable over biological method which requires wide space for its treatment plants (Nakamoto and Machida 1992). Other advantages of enzymatic treatment include application to bio-refractory compounds, operation over wide range of process conditions (such as contaminant concentrations, pH, temperature and salinity), absence of shock loading effects, absence of delays due to biomass acclimatization, and absence of biomass generation (Nicell, Bewtra, Biswas and Taylor 1993). Enzymes exhibit high substrates specificity and can be easily handled and stored (Wilberg et al. 2002).

2.3.1 Laccase

Laccases (benzenediol: oxygen oxidoreductase; EC 1.10.3.2) are monomeric, dimeric or tetrameric glycoproteins with four copper atoms (belonging to three types: 1, 2 or 3) per monomer distributed at three redox sites (Rodríguez Couto and Toca Herrera 2006). Type 1 (T1) copper is responsible for substrate oxidation and blue colour of the enzyme. In the presence of oxygen, laccases oxidize various aromatic and non-aromatic hydrogen donors and release radicals. The radicals can undergo further polymerization, hydration or hydrogen abstraction. For phenolic compounds, oxidation of phenolic compounds results in the formation of aryloxyradical which is further oxidized to quinone. Based on substrate and environmental conditions, the spontaneous reaction among quinone intermediates form soluble or insoluble coloured oligomers (Majeau et al. 2010).

Due to high enzyme production costs, the application of laccase for pollutants decontamination is limited to laboratory scale. Fungal laccase is considered the most studied group. The research study carried out by Aranda et al. (2006) revealed that laccase activity produced by *Pycnoporus cinnabarinus* and *Coriolopsis rigida* decreased the phenol content in olive-mill dry residues to 73% after 15 days. Phytotoxicity of the residues was also decreased after 5 and 15 days with *P. cinnabarinus* and *C. rigida* respectively which led to the plant growth of tomato. Laccase was also produced by *Trametes versicolor*. Ryan et al. (2007) demonstrated that the growth medium containing 10 g/L glucose and 10 g/L peptone resulted in the highest Growth Related Productivity (GRP) of laccase, and guaiacol further enhanced the laccase activity by 780%. Nonetheless, minimum 8 days of prior growth of culture was needed before the addition of phenolic effluent to ensure maximum phenol removal.

Surfactant has been reported to affect laccase activity and phenol degradation. Laccase activity was found to increase with increasing concentration of Triton X-100 and the optimal increase was about 17 % by 930 μM Triton (Zhang et al. 2012). The removal efficiencies of phenol with 155 mM Triton X-100 were 1.2 – 5.7 fold higher than those by control after 6 h for initial phenol concentrations of 50 – 600 mg/L. The hydrophobic interactions between Triton X-100 and laccase may have been the reason for the increase in laccase activity and better phenol removal. Also, biosurfactants –

tea saponin (TS) and rhamnolipid (RL) had stimulative effect on the production of laccase from *Penicillium simplicissimum* (Zhou, Yuan, et al. 2011). As a result, the efficiency of phenol removal was improved. These findings were supported by Liu, Zeng, Zhong, et al. (2012). They confirmed that dirhamnolipid (diRL) increased the activity of laccase from *T. versicolor* and improved the removal of phenol by 4.3 – 6.4 folds to that of control with 318 μM diRL within 24 h.

Purified laccase from a newly isolated ascomycete *Paraconiothyrium variabile* also demonstrated its potential in elimination of phenol. For an initial phenol concentration of 4 mM, a phenol removal efficiency of 96.3 % was attained by this purified laccase at pH 5 and 50 ^{o}C (Asadgol et al. 2014).

An alkaline-stable laccase from *Streptomyces psammoticus* was entrapped in alginate beads (Niladevi and Prema 2008). In comparison, copper alginate beads showed better performance by retaining 61 % of laccase activity than 42.5 % activity retained by calcium alginate beads. In a packed bed bioreactor, laccase-immobilized copper alginate beads achieved 95 % of total phenols removal initially at 30 min but reduced to 70 % after 6 h. After eight successive runs, the immobilized laccase maintained 50 % of its removal efficiency. The reduction in removal efficiency could possibly be attributed to leaching of enzyme coated on the capsule surface during the initial run. Liu, Zeng, Zeng, et al. (2012) reported that immobilization of laccase from *T. versicolor* into bimodal carbon-based mesoporous magnetic composites attained 78 and 84 % of phenol and *p*-chlorophenol removal respectively after 12 h of reaction, and mesoporous support contributed 20 % removal in the first hour via adsorption mechanism.

2.3.2 Tyrosinase

Similar to laccase, tyrosinase (EC 1.14.18.1) which is commonly obtained from button mushroom, requires the presence of biomolecular oxygen for activity. Also known as polyphenol oxidase, tyrosinase catalyzes the hydroxylation of mono-phenols to *o*-diphenols in the presence of oxygen molecules, followed by dehydrogenation of *o*-diphenols into reactive *o*-quinones that advance spontaneously to produce dark brown intermediates pigmentation (Halaouli et al. 2006).

The study by Wada et al. (1995) demonstrated that 100% removal was achieved for *p*-chlorophenol and phenol in 3 and 4 h respectively. The colour products were successfully removed by coagulants, with synthetic polymer coagulants being more effective than chitosan, attaining 95% colour removal at lower dosage compared to 90% by chitosan at higher dosage. A similar observation was reported by Ikehata and Nicell (2000), whereby complete transformation of phenol and 4-chlorophenol was achieved within 3 h.

Tyrosinase was extracted from common mushroom, *Agaricus bisporus* wastes by Pigatto et al. (2013). The crude extracts achieved phenol oxidation of 44.8% in olive mill wastewater after 100 min of reaction. Martínková and Chmátal (2016) conducted remediation of coking wastewater by the integration of cyanide hydratase and tyrosinase. The real coking wastewater which also contained cyanide was pre-treated with cyanide hydratase since cyanide was known as a strong inhibitor of tyrosinase. Thereafter, tyrosinase produced from *A. bisporus* was able to remove phenol from coking wastewater by 79 % in 8 h and proceeded to complete phenol degradation after 20 h.

Bayramoglu et al. (2013) covalently immobilized tyrosinase onto the pre-activated biosilica with an immobilization efficiency of ~76.6%. The immobilized tyrosinase achieved 87% phenol removal efficiency in 12 h as compared to 81% by free tyrosinase. The immobilized tyrosinase retained ~74% of its original activity after 10 cycles in the batch system. Xu and Yang (2013) demonstrated that immobilized tyrosinase as cross-linked enzyme aggregates (CLEAs) was able to achieve complete phenol conversion after 3 h reaction. However, tyrosinase CLEAs encapsulated in calcium alginate beads only attained 40 – 50 % phenol removal efficiency in a continuous stirred tank reactor. Similarly, cross-linked magnetic nanoparticles and tyrosinase aggregates on graphene oxide also displayed higher phenol degradation efficiency compared to free and covalently bonded tyrosinase over a wide pH and temperature range (Liu, Liang, et al. 2016). At 0.5 mM phenol concentration, the removal efficiency was 97% after 4 h. At 2 and 8 mM phenol concentrations, the removal efficiencies were 91.6% and 87.6% after 10 and 20 h respectively. The efficacy of magnetic tyrosinase aggregates on graphene oxide reduced to 56% after five cycles.

2.3.3 Peroxidase

Peroxidases (EC 1.11.1.X) are ubiquitous in nature and are widely distributed among animals, plants and microorganisms. They are categorized under oxidoreductases as they can catalyze the oxidation of various electron donors in the presence of hydrogen peroxide (H_2O_2) (Deepa and Arumughan 2002). Peroxidases are heme-containing glycoproteins constituting a single polypeptide chain, and ferriprotoporphyrin IX as a prosthetic group. Their molecular weight ranges from 30 to 150 kDa (Regalado et al. 2004).

Based on their structural and catalytic properties, these peroxidases are divided into three super-families. The first peroxidase super-family consists of enzymes in animals such as glutathione peroxidase, myeloperoxidase, thyroid peroxidase, eosinophil peroxidase, lactoperoxidase and prostaglandin endoperoxide synthase (Hiraga et al. 2001; Regalado et al. 2004). The second peroxidase super-family consists of catalases in animals, plants, bacteria, fungi and yeast. The third peroxidase super-family consists of peroxidases in plants, fungi, bacteria and yeast (Hiraga et al. 2001).

The third peroxidase super-family can be further classified into three different classes based on the amino acid homology and metal-binding capabilities. Class I consists of intracellular enzymes (EC 1.11.1.5/.6/.11) from mitochondria and chloroplasts such as cytochrome c peroxidase and ascorbate peroxidase. Class II includes extracellular fungal peroxidases (EC 1.11.1.13/.14) such as manganese peroxidase (MnP) and lignin peroxidase (LiP) whereas Class III comprises secretory plant peroxidases (EC 1.11.1.7) such as horseradish peroxidase (HRP) (Welinder 1992).

Peroxidases, such as lignin peroxidase and manganese peroxidase, have been applied to biopulping and biobleaching in the paper industry (de Souza-Cruz et al. 2004; Antonopoulos et al. 2001). Peroxidases also stimulate oxidation destruction of coloured compounds which is useful for decolourization of synthetic dyes (Kariminiaae-Hamedaani et al. 2007; Gholami-Borujeni et al. 2011; Jiang et al. 2014). The involvement of peroxidases in the synthesis of various polymers are also reported (Kim et al. 2003; Cruz-Silva et al. 2005). Besides, peroxidases have also found applications in the production of peroxidase-based biosensors (Jia et al. 2002; Zhang et al. 2004; Castillo et al. 2003), analysis and diagnostic kits (Agostini et al. 2002;

Sharma et al. 2002) as well as enzyme immunoassays (Zhuang et al. 2001; Kawatsu et al. 2002; Lee et al. 2013).

Another potential application of peroxidases which has generated great interest among researchers is in waste treatment. Numerous studies have been carried out to evaluate the feasibility of peroxidases in bioremediation of hazardous pollutants from wastewater. In the context of phenol-related pollutants, various peroxidases have successfully proven to be potential candidates for phenol degradation from wastewater in laboratory scale of work. The mechanism of peroxidase in polymerization and precipitation of aromatic compounds as well as performance of various peroxidases in degradation of phenol compounds are presented in the following sections.

2.4 MECHANISM OF ACTION OF PEROXIDASE FOR PHENOL REMOVAL

The one-electron oxidation of aromatic substrate (AH_2) catalyzed by peroxidase is usually depicted by the Chance-George mechanism (Henriksen et al. 1999):

$$E + H_2O_2 \rightarrow E_i + H_2O \quad (2.1)$$

$$E_i + AH_2 \rightarrow E_{ii} + {}^{\bullet}AH \quad (2.2)$$

$$E_{ii} + AH_2 \rightarrow E + {}^{\bullet}AH + H_2O \quad (2.3)$$

Initially, native peroxidase enzyme (E_N) is oxidized by H_2O_2 to form an unstable intermediate called Compound I (E_i), which has a haem structure of Fe IV = O-porphyrin π-cation radical. Compound I accepts an aromatic molecule into its active site and oxidizes it. The oxidized aromatic unit, now a free radical, is released from the catalytic site leaving the enzyme in the Compound II state (E_{ii}). Compound II then oxidizes a second aromatic molecule and releases a second free radical into the solution. The catalytic cycle is completed when the enzyme is returned to its native state. The free radicals generated diffuse from the enzyme into solution where they spontaneously react to form poly-aromatic products. Having less solubility than their monomeric precursors, these polymers tend to precipitate from solution (Nicell, Bewtra, Biswas and Taylor 1993).

The return of a free radical to the active centre of the enzyme and formation of bonding at/near the active site cause permanent inactivation. Such a bond blocks the active site or changes the critical geometric configuration of the enzyme, thus eliminating the enzyme's catalytic ability. Additionally, in the presence of excess H_2O_2, Compound II can be oxidized to Compound III (E_{iii}) according to:

$$E_{ii} + H_2O_2 \rightarrow E_{iii} + H_2O \tag{2. 4}$$

The formation of Compound III, which is catalytically inactive, is a non-terminal inactivation because Compound III decomposes spontaneously to native peroxidase according to:

$$E_{iii} \rightarrow E + O_2^- \tag{2. 5}$$

The decomposition of Compound III to the native state is significantly slow that, once Compound III is formed, the enzyme is severely hampered in carrying out the catalytic oxidation of aromatic substrates. As a result, accumulation of Compound III is regarded as a loss in catalytic efficiency (Nicell, Bewtra, Biswas and Taylor 1993).

Figure 2.1 illustrates the catalytic cycle of peroxidase and its postulated side reaction (Wright and Nicell 1999).

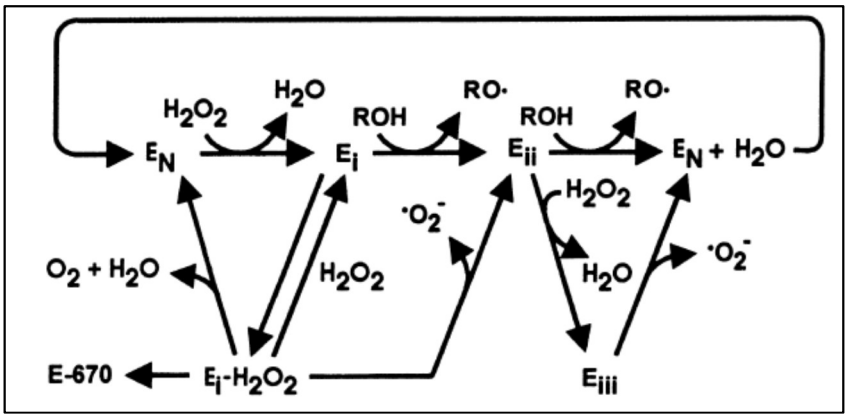

Figure 2.1: The catalytic cycle and side reactions of peroxidase (Wright and Nicell 1999).

According to Arnao et al. (1990), in the absence of reductant substrates such as phenolic and aromatic compounds, peroxidase / H_2O_2 system can behave as a catalase

system, where H_2O_2 acts either as an oxidant or a reductant. Compound I can react with H_2O_2 to form an intermediate enzyme-peroxide complex (E_i-H_2O_2):

$$E_i + H_2O_2 \leftrightarrow E_i - H_2O_2 \quad (2.\ 6)$$

From this E_i-H_2O_2 complex, they postulated that a competition is established between two catalytic pathways and a suicide inactivation pathway:

$$E_i - H_2O_2 \rightarrow E_{ii} + \cdot O_2^- \quad (2.\ 7)$$

$$E_i - H_2O_2 \rightarrow E_N + O_2 + H_2O \quad (2.\ 8)$$

$$E_i - H_2O_2 \rightarrow E - 670 \quad (2.\ 9)$$

In the absence of a reductant substrate, Compound II can be formed through reaction 2.7. Reaction 2.8 which represents a weak catalase reaction is minimal in the presence of stronger reducing agents. If there is excess of H_2O_2, peroxidase is converted to inactive verdohaemoprotein called E-670 (reaction 2.9). The catalytic pathways of 2.7 and 2.8 are important against the inactivation pathway 2.9.

According to Valderrama et al. (2002), the suicide inactivation process of peroxidase arises from the non-productive electron abstraction pathways, whereas substrate protection comes from the favourable partition of the oxidative equivalents towards the substrate. Rational reorganization of low-reduction-potential residues within the active site leads to peroxidases stabilization against H_2O_2.

2.5 PEROXIDASE-BASED PHENOL REMOVAL

2.5.1 Lignin peroxidase

Lignin peroxidase (LiP) was first reported from *Phanerochaete chrysosporium* with a molecular weight of 42 kDa by Tien and Kirk (1983) in 1983. It oxidized various recalcitrant aromatic compounds, polycyclic aromatic and phenolic compounds (Karam and Nicell 1997).

The work by Aitken et al. (1989) demonstrated that LiP from *P. chrysosporium* degraded phenol compounds in the order of pentachlorophenol > *o*-cresol > 2-chlorophenol > phenol > 2-nitrophenol. The degradation pathway of 2,4-

dichlorophenol by LiP involved several steps of oxidation and reduction which resulted in the removal of both chlorine atoms before the occurrence ring cleavage (Valli and Gold 1991). LiP from *Streptomyces viridosporus* T7A was found to oxidize phenolic compounds, but not non-phenolic ones (Spiker et al. 1992).

Three different bench scale bioreactors – mechanically mixed suspended bioreactor, upflow fixed-film bioreactor, and fluidized bed bioreactor were examined for their efficacy in degradation of pentachlorophenol (Kang and Stevens 1994). Increased LiP activity in a mechanically mixed suspended bioreactor improved pentachlorophenol degradation. Pentachlorophenol removal in the upflow fixed-film bioreactor was fast by following a quasi-first order steady state model. Effluent pentachlorophenol concentration varied slightly in the fluidized bed bioreactor at hydraulic residence times of 5 to 90 minutes.

Manimekalai and Swaminathan (2000) showed that phenol removal by LiP decreased from 80% to 50% due to the inhibitory effect of phenol on the biomass growth and enzyme synthesis. In addition, the removal rate of 4-chlorophenol was rather slow in this study, with 62% in ~10 days. On the other hand, despite immediate enzyme inactivation at the start of reactions, LiP continued to remove catecholic compounds from aqueous mixture in the order of 4,5-dichlorocatechol (95%) > 4-chlorocatechol (90%) > catechol (55%) > 4-methylcatechol (43%) after 1 h (Cohen et al. 2009).

2.5.2 Manganese peroxidase

Manganese peroxidase (MnP) catalyzes the oxidation of several mono-aromatic phenols and aromatic dyes in the presence of both divalent manganese and certain types of buffers. MnP first catalyzes the oxidation of Mn(II) to Mn(III) in the presence of Mn(III) stabilizing ligands. The resulting Mn(III) complexes can then oxidize organic substrates (Karam and Nicell 1997). However, the application of MnP in wastewater treatment is more limited than LiP due to the requirement of Mn(III) at high concentrations (Durán and Esposito 2000).

MnP produced from *P. chrysosporium* BKM F-1767 cultures has been shown to co-polymerize pentachlorophenol and ferulic acid in the presence of detergent (n-dodecyl-β-D-maltoside) and H_2O_2 (Ruttimann-Johnson and Lamar 1996). Banci et al. (1999) studied the oxidation of phenolic oligomers by MnP via transient-state kinetic methods.

MnP intermediate Compound I was found to be more reactive than Compound II, but the rate constants of both intermediate compounds were lower than those of LiP. They also concluded that Mn^{2+} was the only physiologically significant substrate despite MnP's ability to oxidize phenols.

An azlactone-functional copolymer derivatized with ethylenediamine and 2-ethoxy-1-ethoxycarbonyl-1,2-dihydroquinoline was used to immobilize MnP of *Lentinula edodes* covalently (Grabski et al. 1998). Mn(III)-chelate produced by immobilized MnP in enzyme bioreactor was supplied to chemical reaction vessel for the oxidation of 2,4-dichlorophenol and 2,4,6-trichlorophenol under a combination of enzyme and chemical system.

2.5.3 Other peroxidases

Treatment of aromatic contaminants from wastewater using fungal peroxidase from *Coprinus macrorhizus* was investigated by al-Kassim, Taylor, Nicell, et al. (1994). Results indicated that this fungal peroxidase was comparable to HRP in terms of its capability to oxidize aromatic compounds but was more susceptible to inactivation. Al-Kassim and team (Al-Kassim, Taylor, Bewtra, et al. 1994) further optimized the performance of this fungal peroxidase using batch, continuous and discontinuous semibatch reactors. Maximum phenol removal in a batch reactor was 53% while continuous addition of fungal peroxidase or H_2O_2 showed no positive impact on removal efficiency. 90% phenol removal was achieved when either fungal peroxidase or H_2O_2 was added discontinuously over a period of time.

Kauffmann et al. (1999) investigated the treatment of 10 different phenol compounds using *C. cinereus* in pH 6 and 7. Apart from 3-hydroxyphenol, the investigated phenols could be removed with high efficiencies (> 90%) at one or both of the pH conditions. Masuda et al. (2001) discovered that 12.2 U of *C. cinereus* peroxidase was needed to remove 1 mg of phenol, and excess peroxidase dose enhanced the operating conditions to a wider pH and temperature range.

Ikehata et al. (2005) also studied the efficacy of *Coprinus* sp. UAMH 10067 and *C. cinereus* UAMH 4103 in aqueous phenol treatment. Peroxidase from *Coprinus* sp. UAMH 10067 demonstrated better thermal and pH stability than the enzyme from *C. cinereus* UAMH 4103. *Coprinus* peroxidase also showed comparable phenol removal

efficiency with other reported plant peroxidases. This study also agreed with al-Kassim, Taylor, Nicell, et al. (1994) that *Coprinus* peroxidase was more susceptible to inhibition by H_2O_2.

Chloroperoxidase from *Caldariomyces fumago* has also been studied in the treatment of phenol. In comparison to HRP, chloroperoxidase showed lower removal efficiency in the treatment of phenols (Casella et al. 1994). In the oxidation of chlorinated phenols, chloroperoxidase completely removed phenol and 4-chlorophenol after 4 h under continuous electrogeneration of H_2O_2, while the removal efficiency of 2,4-dichlorophenol, 2,4,6-trichlorophenol and pentachlorophenol was 97, 93 and 88% under the same conditions. Electrogeneration also improved the enzyme half-life time in comparison to direct addition of H_2O_2 (La Rotta Hernández et al. 2007).

2.5.4 Plant peroxidase

In addition to the various biotechnological applications discussed in Section 2.3.3, plant peroxidases are also implicated in a number of physiological processes including auxin metabolism, lignin and suberin formation, cross-linking of cell wall components, defense against pathogens, and cell elongation (Hiraga et al. 2001; Passardi et al. 2005).

To date, HRP is undoubtedly the most established peroxidase for phenolic compounds removal owing to its high catalytic activity and robustness in a wide range of process conditions. Klibanov and co-workers are among the pioneers who proposed the use of HRP to remove various aromatic compounds from aqueous solutions. Over 30 different phenols and aromatic amines were removed from water via precipitation. The presence of easily removed phenols and aromatic amines (removal efficiency > 99%) also greatly enhanced the enzymatic precipitation of recalcitrant pollutants (Klibanov et al. 1980). Another study by Klibanov and Morris (1981) showed that HRP in the presence of H_2O_2 demonstrated high removal efficiency of carcinogenic aromatic amines due to enzymatic crosslinking. HRP was later applied to real coal-conversion aqueous effluents (Klibanov et al. 1983), and it was found that 97 – 99% phenol removal was achieved over a broad range of pH and phenol concentrations. Polychlorinated biphenyls was also enzymatically co-precipitated with the phenols, confirming their previous findings.

Since the initial demonstration of the potential of HRP by Klibanov's team, enzymatic approach using HRP has evolved tremendously due to its relatively non-substrate specific characteristics and high catalytic ability towards a variety of aromatic pollutants as well as robustness in a wide range of process conditions. Lab-scale demonstrations of HRP for biodegradation of phenolic compounds from aqueous solutions have been largely reported (Nicell et al. 1992; Nakamoto and Machida 1992; Wilberg et al. 2000). Kinetic models of HRP catalysis in steady-state, fully transient and pseudo-steady-state have been developed (Nicell 1994). Yu et al. (1994) examined the nature and fact of the reaction products from the oxidation and polymerization of phenol using HRP. They identified five dimeric and one trimeric products from the reaction at high phenol conversion. Three of the dimers were reaction intermediates, reaching a final concentration of < 1 mg/L when > 95% phenol removal was achieved. Nicell, Bewtra, Biswas, St. Pierre, et al. (1993) also affirmed that removal of bio-refractory compounds could be enhanced by co-precipitation with other substrates of HRP, which was in keeping with the findings by Klibanov et al. (1980).

In the employment of HRP onto phenol-containing wastewater, Cooper and Nicell (1996) demonstrated that ~97 – 99% of the phenolic contaminants were removed from foundry wastewater regardless of the purity of the enzymes used. While high purity HRP achieved > 65% removal of Chemical Oxygen Demand (COD), there was however, no reduction in COD with low purity HRP due to the presence of high concentration of organic matters in the enzyme solution. The work by Wagner and Nicell (2001a) revealed that phenol concentration in a petroleum refinery wastewater was successfully reduced to < 1.27 mg/L, along with 58% of COD, 78% of Biological Oxygen Demand (BOD_5) and 95% of toxicity removal. In another study, treatment of foul condensate from kraft pulping using HRP resulted in phenol content below 1 mg/L and toxicity drop of 46% (Wagner and Nicell 2001b).

Though effective in treating many phenolic compounds, HRP is costly in its purified form. This problem could be overcome by using a cheaper source. For example, Gillikin and Graham (1991) isolated peroxidase isozyme from soybean seed coat. Soybean seed coat is a by-product from the soybean industry and therefore is available in abundance. Soybean peroxidase (SBP) has proven to be effective in removing phenolic compounds from wastewater, with > 95% removal efficiency under optimum conditions (Caza et al. 1999; Kinsley and Nicell 2000). Characterization study of SBP

conducted by Wright and Nicell (1999) indicated that SBP is catalytically stable over wide ranges of pH and temperature. SBP was also found to be less susceptible to permanent inactivation by H_2O_2 but was catalytically slower than HRP. These findings were later confirmed by Bódalo, Gómez, Gómez, Bastida, et al. (2006). Low purity SBP has also been shown to give a 95% removal efficiency in the treatment of phenol from aqueous solution (Wilberg et al. 2002).

Research studies to compare the efficiency of different treatment methods for 4-chlorophenol removal from aqueous solutions have been carried out (Gomez et al. 2009; Gómez et al. 2011). Results showed that enzymatic approach using SBP attained 80 – 90% removal efficiency. AOPs achieved high conversion values in these studies but led to formation of toxic end-products. Furthermore, a continuous tank reactor was used to eliminate 4-chlorophenol and achieved almost 90% removal efficiency. A simplified steady-state design model was also formulated for this continuous tank reactor with good agreement between the theoretical and experimental values of steady-state conversion (Gómez et al. 2008). More recently, Triton X-100 has been shown to enhance the treatment of phenol in synthetic and high strength alkyd resin wastewater using crude SBP. This non-ionic surfactant reduced enzyme loading by 10 – 13 fold (Steevensz et al. 2014).

Apart from SBP, peroxidases from other plants have also been evaluated for their performances in treating phenolic wastewater. The optimal removal efficiencies of an industrial wastewater contaminated with 2, 4-dichlorophenol and other chlorinated phenols were 100, 96 and 99% for HRP, potato, and white radish peroxidase respectively (Dec and Bollag 1994). A neutral peroxidase isozyme was extracted from turnip root by Duarte-Vázquez et al. (2001). This turnip peroxidase (TP) exhibited high removal efficacy for various phenol derivatives, with > 95% removal within 10 min of reaction (Duarte-Vázquez et al. 2003). Peroxidases from tomato hairy roots demonstrated a removal efficiency of 95% for phenol (González et al. 2006) and 80% for 2, 4-dichlorophenol (González et al. 2008), respectively. For tobacco hairy roots, the phenol removal efficiency achieved was between 70% and 90% in 1 h treatment (Sosa Alderete et al. 2009). Bitter gourd peroxidase (BGP) which was more thermo-stable and retained greater fraction of catalytic activity in the alkaline pH range than HRP has also been reported (Fatima and Husain 2008). Treatment of *p*-bromophenol using BGP resulted in a maximum 94% removal efficiency after 2 h reaction as well

as low toxicity of the treated compound (Ashraf and Husain 2010). Deva et al. (2014), on the other hand, reported that peroxidase activity of cauliflower was greater in stem extract than in leaf extract. Phenol conversion of 93% was obtained after 3 h batch reaction using cauliflower peroxidase from stem extract.

Whilst these aforementioned peroxidases demonstrate efficacy for phenol removal, their sources (except SBP) fall within the human food chain, potentially creating competition with food supply logistics especially for large-scale operation. A number of peroxidases have been identified and isolated from various parts of plants including leaves, fruits and tubers. These include palm tree leaves (Deepa and Arumughan 2002; Al-Senaidy and Ismael 2011; Sakharov et al. 2001), rice leaves (Ito et al. 1991), cotton leaves (Triplett and Mellon 1992), tomato (Marangoni et al. 1989), strawberry (Civello et al. 1995), potato (Bernards et al. 1999) and sweet potato (Leon et al. 2002). These peroxidases were purified, and characterized in terms of stability, molecular weight as well as kinetic parameters. However, they have not been evaluated for feasibility in wastewater treatment. Moreover, some of these plant peroxidases may not be easily obtained in certain countries depending on the climate and agricultural potential. Therefore, identification of a suitable peroxidase which is available abundantly in a particular area is essential for the potential of biotechnology and bioengineering applications.

2.6 FACTORS AFFECTING PEROXIDASE-BASED PHENOL REMOVAL PROCESS

Extensive effort has been dedicated to making enzymatic treatment more economically viable. Factors affecting the performance of enzymatic process were investigated and the optimum operating conditions giving > 90% removal efficiency were reported.

2.6.1 Effect of pH

Being highly pH dependent, certain ionisable side chains of enzyme must be in specific configurations to ensure enyzme's functionality. At extreme pH conditions, disruption of protein structure may occur, leading to protein denaturation (Nicell, Bewtra, Biswas, St. Pierre, et al. 1993). Optimum operating pH for the degradation of phenol and other phenolic compounds from aqueous solutions has been reported for many peroxidases.

Using HRP, Klibanov and Morris (1981) discovered that peroxidase treatment for *o*-dianisidine was effective over a broad pH range with an optimum at pH 5.5. Good removal of phenolic compounds was accomplished via HRP-mediated enzymatic process over the pH range of 6 to 8 (Nicell et al. 1992). The optimum pH for phenol removal by HRP in the presence of PEG was determined at pH 8 (Wu et al. 1993). Substantial degradation of 2,4-dichlorophenol was observed between pH 3 and 8 with an optimum at pH 6 using minced horseradish root, whereas purified HRP attained maximum removal between pH 4 and 7 with the optimal at pH 5 (Dec and Bollag 1994). In the treatment of foul condensate from kraft pulping with HRP, Wagner and Nicell (2001b) stated that maximal phenol removal was obtained at pH of 9.2 which was the original pH condition of the wastewater. At limiting HRP doses, the optimum pH was 7, and the removal efficiency decreased markedly below pH 6.

Caza et al. (1999) reported that the optimum pH for various phenolic compounds treated with medium purity SBP ranged from pH 5 to 8. Similarly, the study by Wright and Nicell (1999) revealed an optimum pH of 6 to 9 for medium purity SBP. Kennedy et al. (2002) obtained an optimum pH of 8.2 and 6.2 for the removal of 2,4-dichlorophenol using SBP, in the absence and presence of PEG respectively. At extreme pH 2.5, nearly 90% of 2,4-dichlorophenol was removed using 1 U/mL SBP, indicating that SBP functionality is better retained than HRP in extreme acidic conditions. Peroxidase from tomato hairy root cultures achieved good phenol removal over pH range of 5 – 9 with an optimum pH of 7 (González et al. 2006).

The optimum operating pH for *C. macrorhizus* peroxidase in the treatment of phenol and 2-, 3- and 4-chlorophenols was found to be at pH 9 – 10. Relatively, the optimum pH of *C. macrorhizus* peroxidase was a unit higher than that of HRP in the treatment of the same compounds (al-Kassim, Taylor, Nicell, et al. 1994). Masuda et al. (2001) showed that the optimum operating pH of *C. cinereus* peroxidase for phenol removal was dependent on enzyme loading in the reaction mixture. Optimum pH for insufficient peroxidase dose was 9, but excess peroxidase dose worked well over a wide range of pH 5 – 9. On the contrary, the optimum pH values determined by other researchers for phenol removal using *Coprinus* peroxidase were different. Kauffmann et al. (1999) and Ikehata et al. (2005) reported an optimal at pH 8 and pH 7 respectively.

2.6.2 Effect of temperature

Enzymes are known to be susceptible to rapid inactivation at extreme temperatures. For HRP, the average number of turnovers decreased from 9300 in the range of 5 – 35 ºC to 4100 at 65 ºC. Hence, more enzymes were required to achieve the same degree of removal at elevated temperatures (Nicell et al. 1992).

Bódalo, Gómez, Gómez, Bastida, et al. (2006) showed that both commercial HRP and SBP exhibited comparable phenol removal at temperatures between 25 and 40 ºC. Peroxidase from tomato hairy root cultures achieved high phenol removal over temperature range of 40 – 50 ºC (González et al. 2006). The maximum removal of *p*-bromophenol was 91% at 40 ºC by using BGP (Ashraf and Husain 2010).

Using *C. cinereus* peroxidase, the phenol removal efficiency was improved with a decrease in the reaction temperature over the range of 0 – 70 ºC. Moreover, enzyme inactivation by free radicals was found to be more suppressed at 0 ºC than at 40 ºC (Masuda et al. 2002).

2.6.3 Effect of H_2O_2

Even though the presence of H_2O_2 is critical to peroxidase-catalyzed enzymatic reactions (as mentioned in Section 2.4), H_2O_2 concentration requires rigorous control for specific peroxidases as excess H_2O_2 has been reported to cause peroxidase inactivation. This form of H_2O_2 inactivation can be avoided if phenolic compounds and peroxide concentration are comparable.

For a near complete removal of *o*-dianisidine from solution using HRP, Klibanov and Morris (1981) discovered that only a 2-fold molar excess of H_2O_2 over the pollutant was required. A one-to-one stoichiometry of H_2O_2 to substrates was observed for reactions of pure aqueous phenol and its derivatives with HRP (Nicell et al. 1992; Wu et al. 1993). When real foundry wastewater was treated with HRP, the peroxide-total phenols stoichiometry was found to be slightly smaller at 0.85:1 (Cooper and Nicell 1996). An apparent stoichiometry of 1.14 and 1.24 mole H_2O_2 / mole total phenols was determined for samples of petroleum refinery wastewater (Wagner and Nicell 2001a). On the other hand, foul condensate from kraft recovery process required a molar ratio of 2.52 – 2.74 of H_2O_2/total phenols in the treatment using HRP (Wagner and Nicell 2001b). This difference was probably due to the presence of some phenolic compounds

which do not generate colour in the total phenol assay and hence not included in the total phenol assay results but consume peroxide during the treatment.

Wu et al. (1994) examined the effect of batch and semi-batch additions of the stoichiometric amount of H_2O_2 on removal of phenol (1 – 10 mM). It was noticed that the rate of phenol removal by HRP in the presence of PEG was controlled by the ratio between the maximum H_2O_2 concentration during the reaction and the initial HRP concentration (H_2O_{2max}/HRP_o). The optimum range of this ratio was determined to be 10 – 25 μmol/U.

Using SBP, Caza et al. (1999) demonstrated that the optimum ratios of H_2O_2/substrate ranged from 0.6 – 1.2 for the phenolic compounds being studied. For treatment of 4-chlorophenol, Caza et al. (1999) and Bódalo, Gómez, Gómez, Hidalgo, et al. (2006) reported an optimum stoichiometry ratio of 0.8 and 1 respectively.

Duarte-Vázquez et al. (2003) discovered that maximum phenolic removal was obtained at H_2O_2/phenolic molar ratio of 1.6. They also found that H_2O_2 concentrations >1.2mM inhibited peroxidase catalytic activity by irreversibly oxidizing the enzyme ferriheme group which is essential for peroxidase activity. The H_2O_2 concentrations required for maximum degradation also vary among different substrates. The optimal H_2O_2 concentrations for 2,4-dichlorophenol and phenol removal using peroxidases from tomato hairy roots were 1 and 0.1 mM respectively (González et al. 2008).

For microbial peroxidase from *C. macrorhizus*, Al-Kassim, Taylor, Bewtra, et al. (1994) found that H_2O_2/phenol stoichiometry was >1 if all H_2O_2 was added at the beginning of the reaction. Discontinuous addition of reactants conserved the 1:1 stoichiometry and also reduced the amount of peroxidase required to achieve 91% removal of phenol from 1.2 to 0.3 U/mL. Similarly, a ratio of H_2O_2/phenol close to 1 was found to be the most effective for *C. cinereus* peroxidase (Masuda et al. 2001).

2.6.4 Effect of additives

During the oxidation and polymerization process, a decrease in peroxidase activity is usually observed due to enzyme inactivation. Loss of enzyme activity will hamper the enzymatic process, leading to incomplete or low removal efficiency. Higher cost will

be incurred if more enzymes are to be supplied to the reaction system to maintain sufficiently high removal efficacy.

Klibanov et al. (1983) postulated that enzyme inactivation is a result of interactions between the phenoxy radicals and the enzyme's active site. Nakamoto and Machida (1992) elucidated that apparent inactivation of peroxidase during phenol polymerization reaction is mainly caused by adsorption of peroxidase by end-product polymer, leading to the hindrance of substrate from accessing the enzyme's active site. They demonstrated that additives such as PEG or gelatin suppressed enzyme adsorption and alleviated enzyme inactivation, thus allowing a reduction in the amount of peroxidase to 1/200. Wu et al. (1998) conducted a study on the protective effect of additives on HRP activity in the removal of phenol. Their results suggested that the interaction between enzyme and polymer products is minimized due to a higher affinity of additives towards polymeric products.

According to Wu et al. (1993), the presence of PEG reduced the amount of HRP required to attain > 95% phenol removal to 40- and 75-fold for 1 and 10 mM phenol solutions respectively. For 90% conversion of phenol, a reduction of 22- and 11- to 18-fold enzyme doses was observed for batch and CSTR configurations respectively in the presence of PEG (Nicell et al. 1995). In the treatment of foundry waste, Cooper and Nicell (1996) achieved a 22-fold reduction in HRP requirement for 99% phenol removal efficiency in the presence of 100 mg/L PEG. In the treatment of petroleum refinery wastewater, the use of PEG and chitosan resulted in a 4- and 25-fold reductions in HRP requirements, respectively (Wagner and Nicell 2001a). Chitosan had an adverse effect on phenol removal in concentrations exceeding 80 mg/L, while PEG showed no improvement or deterioration of treatment at higher doses. It was also noticed that higher H_2O_2 dose was required for treatments conducted in the presence of additives because of the increased significance of spontaneous decomposition of H_2O_2 when lower enzyme doses were employed.

Wu et al. (1997) compared the behaviour of several additives including PEG, gelatin and some polyelectrolytes in the removal of phenolic compounds from aqueous solution. It was found that excess gelatin and polyelectrolytes adversely affected the removal efficiency and also resulted in no formation of particles. At the end of reaction,

insignificant amount of PEG remained in the solution, but a considerable amount of gelatin was found in solution even at the minimum gelatin dose.

For SBP, it was noticed that the effect of PEG in terms of reduction of enzyme dosage was not as strong as in HRP (Caza et al. 1999). Kinsley and Nicell (2000) reported that PEG of high molecular weight provided maximum protection for enzymes. PEG_{35000} reduced SBP dosage by a factor of 4.2 for 95% phenol removal. This value was significantly much lower than those reported for HRP (Wu et al. 1993; Nicell et al. 1995; Cooper and Nicell 1996). It was also noticed that ~25% of the optimum PEG dose remained in the supernatant after the enzymatic treatment (Kinsley and Nicell 2000).

The PEG concentration required for maximum TP protection varied in the range of 100 – 200 mg/L, according to the phenolic compound being treated (Duarte-Vázquez et al. 2003). The study using peroxidases from tomato hairy roots showed that PEG (100 mg/L) increased the removal efficiency of phenol but not 2,4-dichlorophenol (González et al. 2008). According to Ashraf and Husain (2010), the removal efficiency of *p*-bromophenol was increased from 70% to 94% in the presence of 0.1 mg/mL of PEG. This amount of PEG also decreased the concentration of BGP required to attain the aforementioned removal efficiencies from 1.2 U/mL to 0.4 U/mL. It was also noticed that PEG prevented the inhibitory effect of sodium azide on BGP to some extent by showing a 32% removal efficiency, as compared to complete inhibition of BGP in the absence of PEG. For cauliflower peroxidase, the presence of PEG increased the phenol removal efficacy dramatically from 35% to > 90% (Deva et al. 2014). In the case of *Coprinus* peroxidase, the crude enzyme requirement for > 95% phenol removal was reduced by 20 – 33% in the presence of PEG. The effect of PEG was more profound on purified enzyme, with a reduction of 23-fold enzyme demand in the presence of PEG (Ikehata et al. 2005).

Mao et al. (2013) performed a research on HRP inactivation via heme destruction and investigated the influence of PEG on HRP inactivation. It was shown that heme destruction resulted in deprivation of the heme iron and oxidation of the 4-vinyl group in heme. It was also noticed that in the presence of PEG, heme consumption and iron releases due to HRP destruction were greatly controlled, indicating that heme destruction can be effectively suppressed by co-dissolved PEG.

As mentioned, the addition of additives have improved the removal efficiency of pollutants from solutions and also minimized the enzyme costs by reducing the amount of peroxidase required to attain high removal. However, the influence of additives on the quality of the final reaction solutions was not being addressed in these studies. Nicell et al. (1995), besides demonstrating a significant reduction of HRP requirement and enhancement of HRP catalytic lifetime for 90% removal of initial phenol, also noted that a higher residual absorbance due to by-products was produced in the presence of PEG. Their findings were later supported by Ghioureliotis and Nicell (1999). The presence of PEG increased the amount of soluble products at the end of the reaction, and this phenomenon was more prominent for HRP than SBP. Even so, PEG did not affect the residual toxicity of the treated solutions (Ghioureliotis and Nicell 1999). Nevertheless, a different scenario was observed by Wagner and Nicell (2002). They pointed out that the usage of PEG increased the toxicity of the solutions, but the toxicity dropped to a comparable level with those treated without additives 24 h after the reaction. On the other hand, solutions treated with chitosan demonstrated lower toxicities than solutions treated without chitosan. The elevated toxicity levels were likely caused by soluble reaction products. Wagner and Nicell (2002) also showed that increase of the retention time, addition of H_2O_2 after the completion of reaction, or lowering the rate of H_2O_2 addition, could be used to overcome these toxicity problems.

Summary of optimum operating conditions for various peroxidases giving >90% removal efficiency is presented in Table 2.1.

Table 2.1: Optimum operating conditions for various peroxidases with > 90% removal efficiency.

Peroxidases	Optimum operating conditions	Removal efficiency (%)	Reference
Horseradish	pH 5.5, 2:1 ratio of H_2O_2/*o*-dianisidine	~99% *o*-dianisidine	(Klibanov and Morris 1981)
	pH 6-8, 1:1 ratio of H_2O_2/substrate, < 35 ºC	>90%	(Nicell et al. 1992)
	pH 7-9	>90%	(Nicell, Bewtra, Biswas, St. Pierre, et al. 1993)
	pH 8, 1:1 ratio of H_2O_2/phenol, 0.03 – 0.25 g/L PEG	>95% phenol	(Wu et al. 1993)
	H_2O_{2max}/HRP_o = 10 – 25 µmol/U	>95% phenol	(Wu et al. 1994)
	0.85:1 ratio of H_2O_2/total phenols, 100 mg/L PEG	97-99%	(Cooper and Nicell 1996)
	1.14-1.24 ratio of H_2O_2/total phenols, 10-30 mg/L PEG, 60 mg/L chitosan	>90%	(Wagner and Nicell 2001a)
	pH 6-9.2, 2.52-2.74 ratio of H_2O_2/total phenols	>90%	(Wagner and Nicell 2001b)
Soybean	pH 5-8, 0.6-1.2 ratio of H_2O_2/substrate, 20-400 mg/L PEG	>90%	(Caza et al. 1999)
	pH 6-9	>90%	(Wright and Nicell 1999)
	PEG_{35000}/phenol = 35.2 mg/L.mM	95% phenol	(Kinsley and Nicell 2000)

	pH 8.2 (without PEG), pH 6.2 (with PEG), 1.2 g/L PEG_{3350}, 0.1 g/L PEG_{8000} 1:1 ratio of H_2O_2/4-chlorophenol	>95% >90%	(Kennedy et al. 2002) (Bódalo, Gómez, Gómez, Hidalgo, et al. 2006)
Turnip	pH 4-8, H_2O_2/phenolic = 1.6, 100-200 mg/L PEG	>95	(Duarte-Vázquez et al. 2003)
Tomato hairy roots	pH 7, 40-50 ºC, 5 mM H_2O_2	95% phenol	(González et al. 2006)
Bitter gourd	pH 5.5, 40 ºC, 0.75 mM H_2O_2, 0.1 mg/mL PEG	94% *p*-bromophenol	(Ashraf and Husain 2010)
Cauliflower	pH 7, 30 ºC, 2:1 ratio of H_2O_2/phenol, 150 mg/L PEG	>90% phenol	(Deva et al. 2014)
Coprinus macrorhizus *Coprinus cinerus*	pH 9-10, 1:1 ratio of H_2O_2/phenol (discontinuous addition of reactants) pH 8 pH 9, 1:1 ratio of H_2O_2/phenol, 0-60 ºC pH 7, 1.5 mM H_2O_2, 25 ºC, 200 mg/L PEG	>90% phenol >90% phenol ~100% phenol >95% phenol	(al-Kassim, Taylor, Nicell, et al. 1994; Al-Kassim, Taylor, Bewtra, et al. 1994) (Kauffmann et al. 1999) (Masuda et al. 2001) (Ikehata et al. 2005)

2.7 PROCESS OPTIMIZATION VIA DESIGN OF EXPERIMENT

Majority of the reported studies on peroxidase-catalyzed polymerization of phenol were conducted using one-factor-at-a-time (OFAT) approach to examine the effects of various process parameters on the removal efficiency. This approach involves varying one factor at a time while keeping other factors constant. No information of two-way interactions between the process parameters could be obtained.

Experimental design and optimization can be used to systematically study various problems encountered within a process, and to plan the experiments in such a way that useful information will be obtained (Lundstedt et al. 1998). One of the statistical approaches for process optimization is by using design of experiment (DOE).

Design of experiments (DOE) is a structured technique for the study of any situation which involves response that varies as a function of one or more variables. It is specifically designed to address complex problems where there are interactions between the variables (Mathews 2005). It usually starts with a screening step to identify the factors which have significant effects on critical variables, and followed by optimization to determine the best analytical conditions (Vera Candioti et al. 2014).

2.7.1 Screening designs

A screening experiment is conducted to identify the experimental variables and/or interactions between variables which have profound effect on the responses. Linear and second order models are common in full factorial or fractional factorial designs under screening step (Lundstedt et al. 1998).

A full two-level factorial design investigates a combination of k factors at two levels, resulting in a test plan consisting of 2^k experiment runs. The number 2 represents two levels of settings for each of the k factors, which are low and high level usually coded by (-1) and (+1) respectively (Soravia and Orth 2009). A zero-level (0), which is a centre with all variables set at their mid value, is also included. A number of centre experiments should always be included to detect any non-linear relationships in the middle of the intervals, and to determine confidence intervals through repetition (Lundstedt et al. 1998). 2^k factorial designs systematically analyse the effects of factor variations and dependence of these effects on other experimental settings. Both continuous variables such as pressure and temperature, and discrete or categorical

variables such as equipment or solvent type can be studied in factorial designs (Soravia and Orth 2009).

In situations where there are lots of possible combinations of test points due to many variables or many conditions per variable or both, it is impractical to run all combinations. In such cases, a fractional factorial design is often applied (Anderson and Whitcomb 2010). A full factorial 2^k design can be fractioned into a 2^{k-p} design with less number of experiment runs, where p denotes the number of independent design generators which are selected to fractionate the design. It should be noted that fractional designs are not able to consider all major and interaction effects separately because some of them are confounded (Vera Candioti et al. 2014).

Normal and half-normal probability plots are usually used to assess the significance of the effects. The effects that are negligible usually fall along a straight line on these plots, while significant effects lie far away from the straight line. Analysis of variance (ANOVA) should be used to examine the chosen variables from any graph analysis, and non-significant variables be removed from the initial model if needed (Vera Candioti et al. 2014).

Also, if a curvature is present in the factorial design based on ANOVA, the design needs to be augmented to fit a second-order model. Some available methods for augmentation are Central composite designs (CCD), Box-Behnken designs and Optimal designs. More experimental runs and sometimes more replicates are required in augmented designs.

2.7.2 Optimization designs

In some situations, the behaviour of an experimental system is not fully described by factorial designs which vary the experimental factors by only two level settings. Hence, it is compulsory to extend factorial designs and run extra experiments at other points in the experimental domain. Response surface methodology (RSM) is usually used for this purpose (Soravia and Orth 2009).

RSM was developed by Box and Wilson (1951). The key ideas in RSM were developed using linear polynomial models (mainly first- and second-order models) by assuming continuous response variables. They are to be normally distributed with constant error variances (Khuri 2006). Besides determining the optimum point, RSM

can also graphically illustrate the relationship between various experimental variables and the responses (Lundstedt et al. 1998). In most cases, the form of the relationship is unknown, and therefore a polynomial model is approximated. A first-order linear model for k independent variables is expressed by the simple relationship

$$y = \beta_o + \sum_{j=1}^{k} \beta_j x_j + \varepsilon \tag{2.10}$$

A polynomial of higher degree such as the second-order model must be used if a curvature exists in the system.

$$y = \beta_o + \sum_{j=1}^{k} \beta_j x_j + \sum_{j=1}^{k} \beta_{jj} x_j^2 + \sum_i \sum_{<j=2}^{k} \beta_{ij} x_i x_j + \varepsilon \tag{2.11}$$

where y is the predicted response; β_o a constant; β_j the linear coefficient; β_{jj} the squared coefficient; β_{ij} the cross-product coefficient; ε the model error; x_j the linear term; x_j^2 the curvature term; $x_i x_j$ the interaction term, and k is the number of factors (Montgomery 2017).

The most widely used designs in RSM are central composite, Box-Behnken, D-optimal and three level factorial design. Each design will be explained in the following sections.

2.7.2.1 Central composite design

Central composite design (CCD) is presented by Box and Wilson (1951). This design consists of a full factorial or fractional factorial design, a star design in which experimental points are set at a distance α from its center, and a central point (Bezerra et al. 2008). One of the advantages of CCD is that it can be built as an extension of a full factorial design (Ferreira et al. 2018).

There are three types of CCDs, namely circumscribed, faced and inscribed. The number of factors and the desired properties will determine the type of CCD used. For a full uniformly rotatable CCD, the number of experiments (N) required equals to $N=k^2+2k+C_p$, where k is the number of factor and C_p is the replicate number of the central point. All factors are studied in five levels (-α, -1, 0, +1, +α) (Bezerra et al. 2008). CCD provides accurate estimation over the entire design domain but requires a substantial number of experimental runs.

2.7.2.2 Box-Behnken design

Box-Behnken design can be employed for process modeling of three or more factors, with each factor being evaluated in three levels. This design is rotatable and all points lie on a sphere (Ferreira et al. 2018). It requires fewer runs than CCD, and the number of experiments is defined by $N=2k(k-1)+C_p$ (Vera Candioti et al. 2014). It enables experimental work to be done around extreme factor combinations by avoiding the corners of the design space. However, this may lead to poor estimation of extremes.

2.7.2.3 D-Optimal design

Optimal designs are usually used in fitting a non-standard model (polynomial model other than first- or second-order with normally distributed errors) or when restricted to running a specified number of test points. The most popular optimal design is the D-optimal, which seeks to maximize the determinant of the information matrix X'X of the design. This will minimize the volume of the joint confidence region on the regression coefficients. Since they focus on accurate estimates of the effects, D-Optimal designs are adequate for screening experiments on general (multilevel) factorials (Anderson and Whitcomb 2010).

2.7.2.4 Three-level factorial design

In comparison to other designs, the application of full three-level factorial design in RSM is limited owing to the large number of experiments required for this design ($N=3^k$), particularly when the factor number is greater than 2 (Bezerra et al. 2008).

2.7.3 Model evaluation

Many statistical tools can be used to justify whether a fitted model is sound. These include regression analysis, analysis of variance and graphical analysis.

Regression analysis allows a relationship to be fit between a series of experimental variables (x) and a response variable (y), which is especially relevant for data from response surface designs. The unknown β in a proposed model alongside their associated confidence bounds can be estimated by regression analysis. This enables one to predict an expected response and/or variability for that response, together with statistical confidence bounds, for a specified combination of the experimental variables based on the proposed model (Anderson and Whitcomb 2010).

Analysis of variance (ANOVA) is generally used to analyse and compare variability in different data sets. Within DOE, ANOVA can be used to complement regression analysis, as well as to compare the variabilities arise from the factors with those from the experimental errors. ANOVA can also provide information about the variability in the measured data with the model, and significance of a model (Soravia and Orth 2009). For the selected confidence level, a model is considered satisfactory when the regression is significant but the lack-of-fit is non-significant. Also, residual plots, the coefficient of determination (R^2) and the adjusted coefficient of determination (R^2_{adj}) are deemed important because they represent the percentage of variance explained by the model (Vera Candioti et al. 2014).

Graphical analysis is usually used to supplement the more formal statistical analysis. For example, half-normal probability plots and a formal analysis of variance provide similar information in terms of the relative importance of the individual sources of variation (Anderson and Whitcomb 2010).

Once a model is fit, the optimum point can be determined from the resulting response surface. The optimum conditions obtained can be validated through experimental runs.

2.7.4 Optimization of phenol removal processes

Optimization of experimental conditions using experimental design technique has been widely applied in various processes including phenol removal process. For instance, two-level full factorial design has been applied by Alam et al. (2009) in the production of powdered activated carbon (PAC) from oil palm empty fruit bunch (EFB) for adsorption of phenol. It was found that activation temperature in the range of 800 – 900 ºC had the most significant effect on adsorption capacity and activated carbon yield. EFB-based PAC produced at 900 ºC with CO_2 gas flow rate of 0.1 L/min and activation time of 15 min also demonstrated comparable phenol removal efficiency to commercial PAC. Also using factorial design, Rathinam et al. (2011) reported that the optimum conditions for phenol adsorption onto activated carbon from seaweed were pH 3, 150 mg/L initial phenol concentration, 10 g/L adsorbent, 75 strokes/min agitation speed, 50 ºC and 4 h, which corresponded to 98.31% of phenol uptake.

Optimization study has been employed in the preparation of activated carbon from coconut husk (Tan et al. 2008) and oil palm EFB (Hameed et al. 2009) in order to

investigate the effects CO_2 activation temperature, CO_2 activation time and KOH:char impregnation ratio on 2,4,6-trichlorophenol uptake and activated carbon yield. On the other hand, the efficacy of adsorptive removal of phenol using aluminium impregnated fly ash was found to be optimal at 13.63 g/l of adsorbent dose, 6.79 h of contact time, pH 5.65 and 34.44 ^oC for an initial phenol concentration of 200 mg/l. At these optimum conditions, the removal efficiency was 86.4% with 12.67 mg/g adsorption capacity (Chaudhary and Balomajumder 2014). The optimal conditions of phenol adsorption using ionic liquid immobilized in polymeric microcapsules were also established by RSM (Archana et al.). At the optimum conditions of 100ppm initial phenol concentration, pH 6 and 1g/100ml absorbent dosage, the removal of phenol and adsorption capacity were 92.5% and 9.07 mg/g respectively.

Statistical experimental designs were also used to optimize microbial degradation of phenol. Box-Behnken design was employed in the optimization of medium components and growth conditions to enhance phenol degradation by *P. putida*. Analysis results showed that 0.34 g/L glucose, 0.16 g/L yeast extract, 2.32 g/L ammonium sulfate and 0.48 g/L sodium chloride resulted in a phenol removal efficiency of 98% (Annadurai et al. 2008). Using *P. aeruginosa*, a phenol removal efficiency of 94.5% was obtained at optimum process conditions of 30.1 ^oC, aeration 3.0 vvm and agitation 301 rpm (Agarry et al. 2008b). Zhou, Yu, et al. (2011) demonstrated that the most important factors influencing phenol degradation by *Candida tropicalis* Z-04 were yeast extract, phenol, inoculum size, and temperature. Maximum phenol removal efficiency of 99.1% was obtained using 0.41 g/L yeast extract, 1.03 g/L phenol, 1.43% (V/V) inoculum size at 30.04 °C.

In an attempt to treat authentic wastewater solution having similar physicochemical characteristics as petroleum refinery effluents, a combination of microwave/H_2O_2 resulted in 75.7% phenol removal efficiency at the optimum conditions determined using CCD (Younis et al. 2014). Optimization study of electrochemical degradation of phenol on Pb/PbO_2 electrode showed that the most significant factors in this electrolysis were current density, temperature, initial phenol concentration and agitation speed (Yahiaoui et al. 2012). D-optimal design was applied to optimize photocatalytic degradation of phenol by new composite nano-catalyst (TiO_2/Perlite). The derived model predicted that UV irradiation time, initial pH, UV light intensity

and reaction temperature had significant effects on photocatalytic phenol degradation (Jafarzadeh et al. 2011).

Optimization studies related to peroxidase-catalyzed phenol oxidation, however, are limited. According to Ghasempur et al. (2007), temperature, pH, enzyme and H_2O_2 concentrations were significant factors in phenol degradation based on 2^{4-1} half-fractional factorial design. Using minimum HRP concentration at 0.26 U/mL, the optimum conditions for phenol degradation were at pH 7.12, 1.72 mM H_2O_2 concentration and 10 ^oC via CCD approach. For SBP, CCD showed that increased amount of soybean seed coats and higher H_2O_2 concentration led to higher phenol conversion, whereas the effect of PEG concentration on phenol conversion was negligible (Rezvani et al. 2012). Under optimum conditions of 1 mM initial phenol, 50 g/L soybean seed coats, 14 mM H_2O_2 and 0.8 g/L PEG, phenol conversion was 78% and 90-92% after 30 min and 2 h respectively. Kalaiarasan and Palvannan (2014) studied the effect of combinatorial polysaccharide additives (dextran and sodium alginate) on the stability of HRP, and RSM results showed that 10.08% of dextran, 0.41% of sodium alginate and 64 mM sodium acetate buffer (pH 4.2) gave optimal HRP stabilization at 65 ^oC with residual activity of 60.01%. The denaturation temperature of the stabilized HRP was 30 ^oC higher than that of the native enzyme. The stabilized HRP also exhibited better removal efficiency than native enzyme under acidic environment.

2.8 IMMOBILIZATION OF PEROXIDASE

Enzymatic wastewater treatment process is challenged by enzyme inactivation, which can happen through three pathways: (1) inactivation by H_2O_2; (2) sorption/occlusion by polymeric products; and (3) heme destruction (refer Section 2.6). Due to this problem, large amount of enzymes is required to attain high removal efficiency.

In addition to enzyme inactivation, enzymatic process is also usually hampered by lack of long-term operational stability of the enzymes as well as difficulty in recovery and reusability of the enzymes (Sheldon 2007). Some of the challenges encountered by soluble enzymes are stability against physical and chemical denaturants, susceptibility to attack by proteases, and activity inhibition. Soluble enzymes also cannot be used in continuous reactors (Husain and Ulber 2011). These challenges can be circumvented

by using immobilized enzymes, so that enzyme application in biotechnological processes can be more favourable.

According to Brena and Batista-Viera (2006), immobilized enzymes refer to enzymes physically confined or localized in a certain defined region of space with retention of their catalytic activities which can be used repeatedly and continuously. Immobilized enzymes not only can be handled more conveniently, they are also easily separated from the reaction mixture, thus minimizing/eliminating protein contamination of the products. They simplify the manipulation of biocatalysts as well as reaction process control. Immobilization of enzymes generally come with enhanced stability in terms of pH, temperature, contaminants, impurities and denaturants. Immobilization also facilitates the efficient recovery and reuse of expensive enzymes, and permits their application in continuous packed-bed or fluidized-bed operations. Rapid arrest of a particular reaction is also possible by removing the immobilized enzymes from the reaction medium (Sheldon 2007; Mohamad et al. 2015; Chagas et al. 2015).

There are various methods for enzyme immobilization, such as reversible physical adsorption, ionic linkages and affinity binding, as well as irreversible covalent bonds and entrapment (Brena and Batista-Viera 2006). Sheldon (2007) distinguished the immobilization techniques into three basic types: binding to a support (carrier), entrapment (encapsulation), and cross-linking. It is crucial to bear in mind that the choice of immobilization method could alter the chemical and physical characteristics of enzymes upon immobilization. The stability of enzymes and also their kinetic properties have been observed to be impacted by the changes of the microenvironment imposed upon them by the supporting matrix (Mohamad et al. 2015). Immobilization may also cause some distortion on the enzyme's active site, hence reducing the overall mobility of the enzyme groups (Mateo et al. 2007). Therefore, proper development of immobilized biocatalysts depends on fundamental factors such as choice of immobilization supports, conditions and methods of immobilization. An ideal support material for immobilization should be resistant to compression and microbial attack, hydrophilic, inert, biocompatible, and inexpensive (Brena and Batista-Viera 2006). For enzyme immobilization onto support via multipoint covalent attachment, the support should possess large internal surface for good geometrical congruence with the enzyme surface and a high superficial density of reactive groups. The protein reactive groups as well as the immobilization support should not hinder the reaction,

but have good stability to sustain the lengthy enzyme-support reaction (Mateo et al. 2007).

Immobilization of peroxidases on different supports via various immobilization methods have been studied extensively (Shukla et al. 2004; Bindhu and Abraham 2003; Caramori and Fernandes 2004; Kulshrestha and Husain 2006b; Sahare et al. 2014). For instance, ammonium sulphate precipitated HRP was immobilized on wool activated by 2% cyanuric chloride (Mohamed et al. 2013). The wool-HRP demonstrated better stability towards denaturants such as pH, heat, metal ions, urea, proteolytic enzyme, detergent and water-miscible organic solvent.

Zhao et al. (2009) prepared HRP microcapsules based on layer-by-layer polyelectrolyte deposition. After immobilizing HRP molecules into $CaCO_3$ microparticles, the $CaCO_3$ templates were coated by polyelectrolyte via alternate electrostatic adsorption of poly(allylamine) and poly(styrene sulfonate). HRP-containing microcapsules were obtained after dissolving the $CaCO_3$ templates in ethylenediaminetetraacetic acid (EDTA) solution. Leakage of HRP from the microcapsules was negligibly small.

In a different study, partially purified BGP was immobilized onto calcium alginate-starch hybrid via surface immobilization and entrapment. Concanavalin A (Con A) was either layered on calcium alginate-starch beads for surface immobilization, or complexed with BGP followed by cross-linkage with glutaraldehyde for entrapment into calcium alginate-starch beads. Comparatively, entrapped crosslinked Con A–BGP demonstrated better stability than surface immobilized BGP by retaining 75% of the initial activity after 7 repeated use whereas surface immobilized BGP only retained 69% (Matto and Husain 2009).

Monier et al. (2010) reported that immobilization of HRP on modified chitosan beads resulted in higher relative activity over 45 ^{o}C and better stability over a wider pH range than free HRP. The immobilized HRP retained 65.8% residual activity after being used for 6 cycles continuously. Upon storage, HRP immobilized with dendronized polymer on commercial glass slides showed better retention in enzymatic activity as compared to HRP immobilized with the help of α-poly-D-lysine (Fornera et al. 2011). Barbosa et al. (2012) demonstrated that HRP immobilized on magnetite-modified polyaniline (PANImG) can be used for 13 cycles while maintaining 50% of its initial activity. In

the adsorption of SBP onto activated carbon, the highest immobilization yield was obtained at pH 5 and 50 ^{o}C (Zheng and Jiang 2014).

The aforementioned work focused on the characteristics study of peroxidases after immobilization. The performance of immobilized peroxidases in the treatment of phenolic compounds from aqueous solutions is also widely available. In the following sections, some of the researches available in literature will be presented according to the immobilization methods being employed.

2.8.1 Adsorption

Acting as a reversible immobilization method, adsorption involves physical attachment of the enzymes on the support material via hydrophobic interactions, van der Waals forces, or hydrogen bonding (Nisha et al. 2012; Eş et al. 2015). Enzyme adsorption usually results from soaking of the support in an enzyme solution for a certain period of time to allow adsorption, or drying of a solution of enzyme on the electrode surfaces followed by rinsing (Datta et al. 2013; Mohamad et al. 2015). Immobilization by adsorption is a mild and easy to perform process as no reagents are required during the activation step. The catalytic activity of the enzyme is usually well preserved. However, this method may suffer from enzyme leakage due to the weak physical bonding between the enzyme and the carrier (Brena and Batista-Viera 2006; Nisha et al. 2012).

Tatsumi et al. (1996) successfully immobilized crude HRP on magnetite by physical adsorption which resulted in a 20-fold purification rate. It was found that desorption of peroxidase from magnetite was not affected by ionic strength but ion type, whereby 44% of the immobilized enzyme was desorbed in phosphate solutions. Nonetheless, nearly 100% removal was observed when this immobilized HRP was used to treat chlorophenol-containing solutions. More than 90% of total organic carbon (TOC) and adsorbable organic halogen (AOX) were also removed in the treatment.

HRP was adsorbed onto aluminium-pillared interlayered clay (Al-PILC) with immobilization yield of > 99% (Cheng et al. 2006). In the treatment of phenol, the immobilized HRP exerted > 90% removal efficiency over a broad pH range from 4.5 to 9.3. The high storage stability of this immobilized enzyme has seen it demonstrating an average of 95% phenol removal efficacy during 2 weeks of storage time. After 5

weeks of storage, the removal efficacy retained was 81%, and gradually decreased to 36% after 8 weeks. However, the immobilized HRP did not show good reusability. The efficiency of phenol removal during second cycle was only 50% of the first, and decreased to 5% on the fourth cycle due to rapid loss of enzyme activity during repeated use.

It was previously mentioned that phenolic precipitates adsorbed and inactivated enzyme molecules (Nakamoto and Machida 1992). However, Feng et al. (2013) explained differently of SBP fate during the reaction. They found that SBP was actually immobilized *in situ* in an active form with reduced enzyme specific activity rather than being inactivated. Although SBP activity remaining on the precipitate was only 20% of the initial value, the precipitate was able to achieve > 95% phenol removal for two consecutive cycles without any fresh SBP addition at the beginning of reactions. Removal efficiency in the subsequent cycles decreased, probably due to the increased irreversible inactivation of SBP. In the case with 0.5 U/mL fresh SBP addition, the removal efficiency of the precipitate remained constant at > 95% at the end of each cycle. This research study opens a new endeavour for enzyme immobilization in the absence of commonly used immobilization materials.

2.8.2 Covalent bonding

Irreversible enzyme immobilization via covalent bonding is normally chosen when enzyme is undesired in the product formed (Brena and Batista-Viera 2006; Nisha et al. 2012). Support materials most commonly used for covalent bonding include porous glass, porous silica, agarose, poly(vinyl chloride) and ion exchange resins (Nisha et al. 2012; Mohamad et al. 2015). The coupling process can be performed in two ways: (1) addition of a reactive functional group to the polymer to activate the matrix, and (2) modification of the polymer backbone to produce an activated group. Electrophilic groups generated via the activation process react with the strong nucleophiles on the proteins. The covalent coupling of the enzyme to the matrices usually involves amino acid side chains such as lysine (ε-amino group), cysteine (thiol group), and aspartic and glutamic acids (carboxylic group) (Brena and Batista-Viera 2006). Enzyme leakage is minimal because of the stable bonding between enzyme and support material. However, both enzyme and (often costly) support are rendered unusable if the enzyme is irreversibly deactivated (Sheldon 2007).

Turnip peroxidase (TP) was covalently bound to silica and utilized for phenol removal from industrial wastewater. This immobilized TP showed 95% phenol removal efficiency, while alginate encapsulated TP and polyacrylamide gel entrapped TP demonstrated a removal efficiency of 50 and 60.4% respectively (Singh and Singh 2002).

SBP and HRP were immobilized on glutaraldehyde-activated aminopropyl glass beads by Gómez et al. (2006), and their characteristics as well as efficacy in phenol removal were compared. Immobilized SBP retained all its activity even after 60 days of storage while immobilized HRP retained 81.5% after 45 days. The initial reaction rates of HRP were higher than SBP, but SBP was able to achieve higher removal conversion at low enzyme doses with longer treatment period. Immobilized SBP was less susceptible to inactivation, giving a removal efficiency of > 95% at H_2O_2/phenol molar ratio of 1.5 as compared to 76% by immobilized HRP for an initial phenol concentration of 2 mM. However, when this same immobilized derivatives were used in the treatment of 4-chlorophenol, a slightly different findings was observed (Bódalo et al. 2008). Immobilized SBP achieved 95% conversion after 30 min while immobilized HRP required 60 min for conversion of 90%.

HRP was covalently coupled onto acrylamide-2-hydroxyethyl methaacrylate (AAm-HEMA) copolymers through the activated hydroxyl and amino groups. More than 2-fold increase in activity of bound enzyme was observed through the activation process, and no conformation change occurred during enzyme immobilization. The immobilized HRP achieved 80% of phenol removal at the optimum conditions in a fixed bed reactor (Shukla and Devi 2005).

Also using glutaraldehyde as coupling agent, Bayramoğlu and Arıca (2008) covalently immobilized HRP onto magnetic poly(glycidylmethacrylate-co-methylmethacrylate) (poly(GMA-MMA)) beads. The immobilized HRP retained 79% of activity upon immobilization, and maintained 84% of its initial activity after 56 days storage period. The immobilized HRP attained 86 and 59% of phenol and *p*-chlorophenol removal respectively, at pH 7 and 25-35 ºC. Cho et al. (2008) investigated the catalytic conversion of phenol in a membraneless electrochemical reactor using immobilized HRP on porous Celite beads. Degradation of phenol by electrochemical method in the absence of an ion exchange membrane was much less compared to the

electroenzymatic method using immobilized HRP, with 0.9-4.4% and 93% respectively.

Polyacrylonitrile (PAN), a synthetic polymer with good mechanical stability, has been used to immobilize HRP for the treatment of 2,4-dichlorophenol from wastewater (Wang et al. 2015). PAN-based beads were modified through a sequential processing with NaOH, HCl, ethylenediamine, chitosan and glutaraldehyde, before immobilization of HRP onto the activated beads by covalent crosslinking. About 90% of 2,4-dichlorophenol was removed by immobilized HRP at the optimum conditions of pH 7 and H_2O_2/substrate ratio of 1. This immobilization system also demonstrated high removal efficiency (> 90%) for phenol treatment (Wang, Fang, et al. 2016).

In a separate study, Wang, Liu, et al. (2016) immobilized HRP onto PAN ultrafiltration membrane, and almost 100% phenol conversion was achieved by HRP-immobilized membranes for initial phenol concentrations of 1-10 mg/L at pH 6 using 30 mM H_2O_2. For high concentrated solutions, the removal efficiency was improved by successive cycles of oxidation. Also using PAN ultrafiltration membrane, Vasileva et al. (2009) immobilized HRP via two methods – adsorption onto non-modified membrane and covalent linkage onto modified membrane. Higher specific activity was observed on HRP immobilized onto modified membranes than that of non-modified membranes, which corresponded to 73.32 and 31.25 U/cm^2 respectively. Phenol oxidation of 95.4% was achieved by immobilized HRP on modified membrane for an initial phenol concentration of 100 mg/L.

Graphene oxide (GO), a novel nanostructured material, was used to immobilize HRP. The GO-immobilized HRP showed better pH and thermal stability. Overall, the GO-immobilized HRP displayed high removal efficiency for 2,4-dimetheoxyphenol and 2-chlorphenol in comparison to soluble HRP (Zhang et al. 2010). On the other hand, the covalent bonding between HRP and functionalized reduced graphene oxide (RGO) resulted in an immobilized derivative with improved stability in pH, thermal and storage. For high phenol concentration (2500 mg/L), immobilized HRP exhibited 100% removal efficiency whereas free HRP only acquired 55%. The reusability of HRP was also improved, retaining 70% of initial activity after 10 cycles (Besharati Vineh et al. 2018).

Nanotubes have the potential to serve as reliable enzyme supports due to the hollow and porous structure as well as the large surface-to-volume ratio (Martin and Kohli 2003). However, the high cost of nanotube supports have limited its application for enzyme immobilization on a large-scale. Zhai et al. (2013) explored the potential of an inexpensive halloysite nanotube as immobilization support for HRP. Chitosan, with abundant amino groups, could effectively bond to the negatively charged outer surface of halloysite nanotube. Chitosan-halloysite hybrid-nanotubes exhibited excellent capacity for HRP immobilization through crosslinking by glutaraldehyde. The activity of immobilized HRP was well maintained even after 35 days of storage. About 98.8, 94.3 and 78% of phenol was degraded after 30 min reaction using immobilized HRP.

In another study, chitosan beads were used as immobilization support for SBP, using glutaraldehyde as crosslinking agent (Chagas et al. 2015). After immobilization, the optimum pH of SBP remained unchanged at pH 6, but its enzyme activity became more dependent on temperature. Enzymatic oxidation of synthetic phenolic solutions and real coffee processing wastewater using immobilized enzyme resulted in 79 and 32.7% removal efficacy respectively. Low removal efficiency in real wastewater could be due to the high complexity of the coffee processing effluent.

2.8.3 Bioaffinity binding

Enzyme immobilization via bioaffinity binding involves creating different bioaffinity bonds between an activated support and a specific group on the protein surface. An affinity tail that has no impact on the activity or folding of the protein is placed at a specific position of the protein sequence. Strong affinity bonds between the enzyme structure and a support matrix functionalized with the complementary affinity ligand are created through these affinity tails (Andreescu et al. 2006). Affinity binding can be achieved in two ways: (1) pre-coupling of the matrix to an affinity ligand for target enzyme, or (2) conjugating the enzyme to an entity that develops affinity towards the matrix (Sardar et al. 2000). Bioaffinity binding is advantageous in terms of ease of immobilization, absence of chemical modification, control orientation of enzyme and minimal conformational changes (Costa et al. 2005). Besides, this immobilization method can also be employed for simultaneous purification and immobilization of enzymes directly from the crude homogenate or partially purified enzyme preparation (Akhtar et al. 2005; Kulshrestha and Husain 2006a).

Akhtar et al. (2005) demonstrated that partially purified bitter gourd peroxidase (BGP) can be immobilized on Con A-adsorbed Sephadex G 50, resulting in high yield of immobilization and markedly higher stabilization of the immobilized enzyme against several types of denaturants. Immobilized BGP was later used in the treatment of 14 different phenols (Akhtar and Husain 2006). Immobilized BGP exhibited higher removal efficiency than free BGP, but pyrogallol and phloroglucinol were recalcitrant to the action of BGP. For the treatment of 2,4-dichlorophenol and a phenolic mixture in stirred batch reactor, immobilized BGP attained 98% removal for both solutions after 8 h. Soluble BGP only achieved 66 and 70% removal for 2,4-dichlorophenol and phenolic mixture respectively, with no further removal observed after 3 h.

Dalal and Gupta (2007a), on the other hand, immobilized HRP on Con A-adsorbed Sephadex beads by bioaffinitiy layering, and found that alternate layering of three layers of Con A and peroxidase each presented the most efficient design. In the absence of PEG, 60 U/mL of immobilized HRP was required to fully degrade *p*-chlorophenol in 4 min. The presence of PEG significantly reduced the enzyme concentration (0.05 U/mL) but increased the reaction time (60 min) for complete degradation. The reusability of the immobilized HRP was enhanced by withdrawing the biocatalysts from the reaction medium after 10 min, which resulted in repeated 5 cycles of usage of the biocatalysts without any loss of activity.

2.8.4 Entrapment

Entrapment of enzyme refers to the inclusion of an enzyme in a polymer network (gel lattice) such as an organic polymer or a silica sol-gel, or a membrane device such as a hollow fiber or a microcapsule (Sheldon 2007), which permits the penetration of substrate and products but not the enzyme (Nisha et al. 2012). Entrapment improves mechanical stability and minimizes enzyme leakage (Shen et al. 2011). Due to the absence of chemical interaction between the enzyme and the polymer, denaturation is often avoided (Mohamad et al. 2015). This method also allows modification of the encapsulating materials in order to produce immobilized enzymes with optimal properties such as high encapsulation and low leakage (Alemzadeh and Nejati 2009). Enzyme entrapment is usually performed through gelation of polyanionic or polycationic polymers by the addition of multivalent counter-ions. Some of the

commonly employed polymers for entrapment are alginate, carrageenan, polyacrylamide, gelatin and collagen (Mohamad et al. 2015).

Degradation of 2,6-dichlorophenol was carried out using *C. cinereus* peroxidase covalently entrapped in polyacrylamide gel (Pezzotti et al. 2004). Complete removal was achieved within 6 h of reaction using immobilized enzyme, while free enzyme only attained 65 – 70% conversion even after 24 h.

Trivedi et al. (2006b) investigated the removal of phenol using SBP encapsulated within hybrid (silica sol-gel/alginate) particles. The hybrid biocomposites has higher mechanical strength than pure alginate encapsulation. The encapsulated SBP retained almost 90% enzyme activity after 3 weeks storage at 4 ºC. Under optimized conditions, the encapsulated biocatalysts attained 85% phenol polymerization. Regeneration with solutions such as 5% (v/v) ethanol and 10% (v/v) dimethylformamide promoted repeated usage of the encapsulated biocatalysts. Without regeneration, product inhibition on the biocatalysts became more severe resulting in loss of enzymatic activity of the particles.

Turnip peroxidase (TP) modified with methoxypolyethylene glycol exhibited an enhanced stability in organic solvents, as well as increased thermal stability of about 4 times than that of its free counterpart, in aqueous buffer at 70 ºC. Modified TP immobilized in alginate beads can be effectively reused for 17 cycles with phenol removal efficiency of > 65% (Quintanilla-Guerrero, Duarte-Vázquez, Tinoco, et al. 2008). In a further study, Quintanilla-Guerrero, Duarte-Vázquez, García-Almendarez, et al. (2008) immobilized TP on two different supports – crude TP in calcium alginate beads, and purified TP on Affi-Gel 10 via covalent bonding through the peroxidase amino groups. The operative stability of TP was enhanced by the presence of PEG, and immobilized TP also showed better thermal stability than free enzyme. Though experiencing loss of peroxidase activity due to enzyme leakage, alginate-encapsulated TP showed higher removal efficiency than covalently immobilized TP in the treatment of synthetic phenolic solutions, owing to the PEG-TP confinement within the alginate matrix. Nevertheless, both immobilized enzyme preparations exhibited > 90% effective phenol removal during the first 10 reaction cycles in the treatment of real effluents from paint industry.

According to Chai et al. (2004), higher sodium alginate concentration or lower calcium chloride ($CaCl_2$) concentration led to smaller diameter and membrane thickness of the capsule. Increasing sodium alginate or $CaCl_2$ concentration increased the compression intensity of the capsule. The study conducted by Alemzadeh and Nejati (2009) revealed that lowering $CaCl_2$ concentration resulted in an increase of capsule leakage. 1% w/v of sodium alginate solution and 5.5% w/v of calcium chloride hexahydrate produced the best gelatin condition for encapsulation of HRP. After 5 consecutive cycles of reaction, the phenol removal efficiency of the encapsulated HRP decreased to 75%, presumably due to clogging of the membrane pore and accumulation of radicals and dimmer within the capsules causing enzyme inactivation.

HRP was encapsulated in phospholipid-templated titania particles through the biomimetic titanification process (Jiang et al. 2014). Apart from showing improved pH and thermal stability as well as high tolerance against inactivating agents, the encapsulated HRP also demonstrated 93 and 88% removal efficiencies for phenol and 2-chlorophenol respectively. The removal efficiency decreased to ~50% after 6 and 8 consecutive operations for phenol and 2-chlorophenol respectively.

In short, immobilization improves the stability of peroxidases from many aspects including pH, thermal, storage and against some denaturants. Due to the introduction of carriers, the overall catalytic activity of the immobilized enzymes are generally lower than the free enzymes. Nonetheless, the immobilized enzymes are capable of attaining high removal efficiency in the treatment of phenol/phenolic compounds from aqueous solutions or even actual industrial effluents. In some cases, immobilization also enhances the purity of the peroxidases. One of the most significant contributions of immobilization is the reusability of enzymes which greatly reduces the enzyme cost in the long run. Some of the reported studies of immobilized peroxidases for the degradation of phenol/phenolic compounds are summarized in Table 2.2 according to immobilization methods.

Table 2.2: Peroxidases immobilized on various supports for the degradation of phenol/phenolic compounds.

Peroxidase	Immobilization support	Pollutants	Removal efficiency (%)	References
Adsorption				
Horseradish	Magnetite	Chlorophenols	100	(Tatsumi et al. 1996)
Horseradish	Al-PILC	Phenol	>90	(Cheng et al. 2006)
Soybean	Product precipitate	Phenol	>95	(Feng et al. 2013)
Covalent bonding				
Horseradish	Alumina beads	Phenol	54	(Vasudevan and Li 1996)
Turnip	Silica, calcium alginate, polyacrylamide gel	Phenol	95, 50, 60.4	(Singh and Singh 2002)
Horseradish	Aminopropyl glass beads	*p*-chlorophenol	25	(Lai and Lin 2005)
Horseradish	AAm-HEMA copolymer	Phenol	80	(Shukla and Devi 2005)
Horseradish and soybean	Aminopropyl glass beads	Phenol	>90	(Gómez et al. 2006)
Horseradish and soybean	Aminopropyl glass beads	4-chlorophenol	>90	(Bódalo et al. 2008)
Horseradish	Magnetic poly(GMA-MMA) beads	Phenol, *p*-chlorophenol	86, 59	(Bayramoğlu and Arıca 2008)
Horseradish	Porous Celite beads	Phenol	93	(Cho et al. 2008)
Horseradish	Polyacrylonitrile (PAN) ultrafiltration membrane	Phenol	95.4	(Vasileva et al. 2009)
Soybean	Aminopropyl glass beads	4-chlorophenol	70	(Gomez et al. 2009)
Soybean	Aminopropyl glass beads	4-chlorophenol	80-90	(Gómez et al. 2011)
Horseradish	Polyacrylonitrile (PAN)-based beads	2,4-dichlorophenol	90	(Wang et al. 2015)
Horseradish	PAN-based beads	Phenol	>90	(Wang, Fang, et al. 2016)

Horseradish	PAN ultrafiltration membrane	Phenol	100	(Wang, Liu, et al. 2016)
Horseradish	Graphene oxide	Phenolic compounds		(Zhang et al. 2010)
Horseradish	Functionalized reduced graphene oxide	Phenol	100	(Besharati Vineh et al. 2018)
Horseradish	Chitosan-halloysite hybrid-nanotubes	Phenol	90	(Zhai et al. 2013)
Soybean	Chitosan beads	Synthetic phenolic solution, coffee processing wastewater	79, 32.7	(Chagas et al. 2015)
Bioaffinity binding				
Bitter groud	Con A-Sephadex G 50	Phenol and phenol derivatives	>90	(Akhtar and Husain 2006)
Horseradish	Con A-Spehadex beads	*p*-chlorophenol	100	(Dalal and Gupta 2007b)
Entrapment				
Horseradish peroxidase	Polyacrylamide gel	Pentachlorophenol	63.5	(Zhang et al. 2007)
Coprinus cinereus	Polyacrylamide gel	2,6-dichlorophenol	100	(Pezzotti et al. 2004)
Soybean	Silica sol-gel / alginate beads	Phenol	85	(Trivedi et al. 2006b)
Modified turnip	Calcium alginate beads	Phenolic compounds	90	(Quintanilla-Guerrero, Duarte-Vázquez, Tinoco, et al. 2008)
Turnip	Calcium alginate beads and Affi-Gel 10	Phenolic compounds	90	(Quintanilla-Guerrero, Duarte-Vázquez, García-Almendarez, et al. 2008)
Horseradish	Calcium alginate beads	Phenol	90	(Alemzadeh and Nejati 2009)
Horseradish	Phospholipid-templated titania particles	Phenol, 2-chlorophenol	93, 88	(Jiang et al. 2014)

2.9 SODIUM CELLULOSE SULFATE / POLY [DIMETHYL(DIALLY)AMMONIUM CHLORIDE] AS ENCAPSULATING MATERIALS

Among the various polymers suitable for entrapment, alginate is one of the most frequently used polymers due to its high biocompatibility and simple gelation with calcium ions. However, alginate gels might suffer uncontrollable and unexpected dissolution by the loss of divalent ions into surrounding fluids (Eş et al. 2015). The instability of alginate beads in the presence of chelating agents such as citric acid and phosphate (Chen et al. 2005) and the probable leakage of intracapsular contents (Quintanilla-Guerrero, Duarte-Vázquez, García-Almendarez, et al. 2008) has triggered interests in the development of other types of polyelectrolyte complex (PEC) microcapsules. PECs are the association complexes formed between oppositely charged particles. They are formed due to electrostatic interaction between oppositely charged polyions. In the absence of chemical crosslinking agents, the possibility of toxicity and other undesirable effects of the reagents are reduced (Lankalapalli and Kolapalli 2009). Some of the polyelectrolytes and their ionic nature have been given by Meka et al. (2017).

One of the commonly employed PEC systems is sodium cellulose sulphate (NaCS) / poly [dimethyl(diallyl)ammonium chloride] (PDMDAAC). The physical properties of NaCS-PDMDAAC polymeric carrier, such as mechanical strength, opacity, pore diameter and mass transfer rate, can be adjusted by varying synthesis variables (Zeng et al. 2012).

In the very beginning of the reaction between oppositely charged polyelectrolytes at the interface between their aqueous solutions, a semipermeable primary membrane is formed at the boundary. Further membrane growth of PEC is governed by this primary membrane via its diffusion resistance. The osmotic pressure differences caused by the difference between counterion concentrations inside and outside the capsule also affect the membrane formation process (Dautzenberg et al. 1996).

For the application as an encapsulating material, NaCS which is derived from sulfation of insoluble cellulose, is produced by the process with alcohol/sulfuric acid. A kinetic model for cellulose sulfation was established by Yao (1999) which enabled the determination of conversion ratios of cellulose sulfation and the yield of NaCS. Large

amount of reaction solution is usually exhausted as waste after sulfation especially during the scale-up of NaCS production, leading to high production costs and heavy load for the environment. To overcome this problem, Yao (2000) demonstrated that the reaction solution can be regenerated by adding fuming H_2SO_4 (oleum) and/or normal H_2SO_4, and the resulting NaCS exhibited the same qualities as that obtained with fresh reaction solution.

2.9.1 Characteristics of NaCS-PDMDAAC capsules

NaCS-PDMDAAC polymeric capsule has a relatively compact and low molecular weight cut-off (MWCO) membrane, which would limit applications to high density cell culture or macromolecules such as extracellular enzyme, hormone and DNA. Therefore, Zhang et al. (2005) formulated the inclusion of a pore forming agent starch to produce macroporous NaCS-PDMDAAC capsules. Pores were formed after the starch initially immobilized in the membrane of the capsules was degraded by amylase. The MWCO of the macroporous capsules was 70 kDa which was 5 times higher than the standard capsules. The macroporous capsules also had better mass transfer behavior while maintaining other characteristics such as mechanical strength, size and thickness of the membrane. It was also reported that maximum cell density in the macroporous capsules was 20% higher than the standard ones because the enlarged pore size of the membrane greatly enhanced the rate of oxygen transfer across the membrane. A novel homogeneous micro-sized hollow PDMDAAC-NaCS microcapsules with MWCO > 50 kDa was developed through layer-by-layer technique. After depositing four bilayers of PDMDAAC and NaCS polymer films on the spherical $CaCO_3$ particles, the coated $CaCO_3$ particles were exposed to EDTA-Na solution to obtain the hollow capsules (Tan et al. 2011).

The presence of inorganic salts in the sulfonation process can also affect PEC capsule formation. Zhang et al. (2006) revealed that increasing salt concentration resulted in increase of membrane thickness and MWCO but decrease in density and permeability of the membrane. The mechanical strength of the capsules increased at lower salt concentrations and followed the ion order of $Mg^{2+} > Ca^{2+} > Na^{+} > K^{+}$ for cations and $Cl^{-} > SO_4^{2-}$ for anions. On the other hand, Chen et al. (2013) reported a similar research finding as Zhang et al. (2006), whereby the addition of Na_2SO_4 increased the molecular weight of the product through minimizing the hydrolysis of cellulose chain. They also

noticed that the viscosity of the cellulose sulphate solution increased remarkably with increase in the salt concentration, but the addition of salt only had minor effect on sulfonating. Besides Na_2SO_4, their study also demonstrated the effects of reaction time, temperature, the sulphuric acid/alcohol ratio and liquid/solid ratio on the properties of cellulose sulphate.

The characteristics of NaCS-PDMDAAC capsules can also be altered by adjusting the concentrations of polyelectrolytes and/or reaction conditions. Addition of carboxymethyl cellulose (CMC) as polyanion in the preparation of NaCS-PDMDAAC capsules caused the capsules formed to become opaque. Increase in either CMC or PDMDAAC concentrations resulted in increased membrane thickness and mechanical strength of the capsules. The diameter of the capsules was greatly reduced by increase in reaction time, but not membrane thickness and mechanical strength of capsules. The influence of temperature on the performance of capsules was minimal, but higher temperature caused earlier shrinking of the capsules (Chen et al. 2005). The diffusion coefficients of low molecular weight substances such as glucose, glycerol, tyrosine and Vitamin B_{12} in NaCS-CMC/PDMDAAC capsule membrane were 10-40% of the corresponding diffusivity in pure water (Chen et al. 2005). According to Yao et al. (2006), the diffusion coefficients of low molecular weight substrates in the NaCS-PDMDAAC capsules decreased with increasing PDMDAAC molecular weight but increased with increasing PDMDAAC concentration. The values of diffusion coefficients in the membrane were about 2-10% of those in pure water.

2.9.2 Applications of NaCS-PDMDAAC system

NaCS-PDMDAAC matrix system has found applications in different areas such as medical, cell cultures and separation. Stadlbauer et al. (2006) demonstrated that microencapsulation of pancreatic β-cells in NaCS-PDMDAAC did not influence cell proliferation, insulin secretion and glucose uptake, indicating that NaCS-PDMDAAC was suitable for microencapsulation of pancreatic β-cells. Entrapment of recombinant *Dictyostelium discoideum* in NaCS-PDMDAAC capsules for the biosynthesis of the heterologous protein, soluble human Fas ligand (hFasL) was conducted by Zheng et al. (2015). The maximum cell density and hFasL concentration in the vitreous airlift bioreactor were lower than those obtained in the shake flasks, due to longer lag phase of cells and the presence of compressed air in the bioreactor which caused lower

glucose consumption. Nonetheless, the immobilized cells enabled easy and continuous cultivation, while maintaining cell density and productivity at high lever over a long period of time. The system of NaCS-PDMDAAC has also been tested in tissue engineering / gene transfer in medical systems (Sittinger et al. 1996; Lohr et al. 2002; Saller et al. 2002).

Förster et al. (1996) in their work using *Serratia marcescens* B345 (IMET 11312) as a model organism to convert gluconic acid to 2-ketogluconic acid, elucidated that NaCS-PDMDAAC had high stability towards 2-ketogluconic acid, and the encapsulated cells were used for 1200 hours in a continuous biotransformation process. Encapsulated *Saccharomyces cerevisiae* demonstrated same growth trends as its free cell culture, with highest cell density of 2.64 x 10^{10} cells/mL and ethanol concentration of 47.0 g/L in the capsules. The encapsulated *S. cerevisiae* cells were fermented sequentially for 16 batches (Mei and Yao 2002). Cultivation of encapsulated *Monascus purpureus* for natural pigment production was carried out in a bubble column, resulting in 14.8 g/L cell density and negligible cell leakage for 14 batches. Pigment yield obtained by encapsulated cells was 2 times higher than free cells, while the fermentation period of each batch in the column was shortened by 15% than that in free cells (Liu et al. 2010).

Application of NaCS-PDMDAAC system to microalgae immobilization was conducted by Zeng and co-workers. Besides physicochemically characterizing the NaCS-PDMDAAC capsules, they also found that microalgae cell growth under immobilized cultivation was slower than suspended cultivation due to mass transfer limitation (Zeng, Danquah, Potumarthi, et al. 2013). In addition, they also noticed that immobilized microalgae cells had substantial changes in cell size, surface charge, lipid/chlorophyll content and composition, protein content and molecular compositions as compared to suspended cultivated cells (Zeng, Danquah, Halim, et al. 2013). The biocompatibility between NaCS-PDMDAAC and the microalgae cells *Chlorella* sp. resulted in biomass enrichment within the capsules as well as high substrate concentration tolerance. NaCS-PDMDAAC *Chlorella* sp. capsules demonstrated a removal rate of 12.56 and 10.24 mg/g biomass per day for T-N and PO_4^{3-} respectively (Zeng et al. 2012).

A single-layer PEC membrane was prepared by Li and Yao (2009) through simultaneous interfacial reaction between NaCS and PDMDAAC. Their study demonstrated that molecular weight of PDMDAAC and reaction time affected the permeability of the membrane. Membrane produced at the optimum conditions exhibited steady state water flux and showed potential in salt rejection process by affording higher rejections of divalent ions (SO_4^{2-}) to that of monovalent ions (Cl^-).

2.10 CONTINUOUS PHENOL REMOVAL IN COLUMNS

Enzyme immobilization helps to circumvent the non-reusability problem faced by free enzymes. However, majority of the previous studies on phenol removal using immobilized peroxidases were limited to batch studies. Since industrial effluents are usually emitted in bulk quantity from the processes, it is thus more economical and practical to treat wastewater continuously using the appropriate reactor configurations. Some of the benefits of continuous degradation of toxic pollutants over a batch process include ease of automation and control which leads to lower operational cost, and an increase in throughput at consistent treatment rate (Sheeja and Murugesan 2002). Following sections will discuss two of the most commonly used reactor configurations for continuous phenol removal via biological, adsorption, AOPs as well as peroxidase-based enzymatic processes.

2.10.1 Packed bed reactor

Packed bed reactor (PBR) is a contacting device in which wastewater containing pollutants is passed through a column packed with immobilized biocatalysts for biochemical reaction or porous adsorbent for adsorption of pollutants. Longitudinal mixing is minimal or negligible when the fluid particles pass through the reactor, and they exit from the reactor in the same order as they entered. Some of the advantages of a continuous packed bed process are high yield operations and easy scale-up from a laboratory set up. With a definite quantity of immobilized cells, PBR can treat large volume of wastewater continuously (Tepe and Dursun 2008). For biological purposes, upflow PBR not only prevents the suspended biomass from wash out, but also reduces clogging problem which is frequently encountered in downflow PBR. However, gas channeling may occur in a PBR operating in upflow mode with oxygen being supplied from the bottom of the reactor, causing development of liquid-rich and gas-rich regions rather than uniform distribution of oxygen and nutrients throughout the reactor bed

(Sahoo et al. 2011). For phenol oxidation process using immobilized peroxidase, insoluble products formed during the process may lead to clogging phenomena and an increase in pressure drop in a PBR (Gómez et al. 2007).

Sheeja and Murugesan (2002) investigated the biodegradation of phenols in upflow packed bed reactors using three types of immobilization systems, namely *Pseudomonas pictorum*-alginate, activated carbon-*P. pictorum*-alginate and celite-*P. pictorum*-alginate beads. Mass transfer correlation of the type $J_D = K(Re')^{n-1}$ was developed from the study, and K values for *P. pictorum*-alginate, activated carbon-*P. pictorum*-alginate and celite-*P. pictorum*-alginate were 1.56, 2.26 and 1.56 respectively, with n value equalled to 0.72. When *P. pictorum*-alginate and activated carbon-*P. pictorum*-alginate beads were applied to petrochemical, leather and polymer industry effluents, the K values were determined as 1.59, 1.07 and 1.42 using *P. pictorum*-alginate and 2.26, 1.75 and 1.92 using activated carbon-*P. pictorum*-alginate respectively (Murugesan and Sheeja 2005). For both immobilization systems, the value of n was found to be 0.72. Phenol removal from petrochemical, leather and polymer effluents were 89.72, 90.18 and 91.95% respectively using *P. pictorum*-alginate beads, whereas the removal efficiency using activated carbon-*P. pictorum*-alginate beads were 97.43, 97.75 and 94.06% in the same order. Tepe and Dursun (2008) reported a K and n values of 1.34 and 0.65 respectively when using *Ralstonia eutropha* encapsulated in calcium alginate beads for phenol treatment.

Using indigenous bacteria from olive pulp, Tziotzios et al. (2007) examined the effect of specific surface area of the support material and operating mode on phenol removal. Under draw-fill operation, the maximum phenol removal rates achieved with gravel and plastic tubes support materials were 25.3 and 14.03 g/d respectively. The time needed for complete phenol degradation using gravel was about half of that required for plastic tubes. This was attributed to the higher specific surface area of the gravel as compared to plastic tubes. However, having low porosity, gravel required backwashing from time to time as it frequently suffered from pore clogging due to excessive biomass growth. Under draw-fill mode with recirculation, the packed bed reactor loaded with plastic tubes attained maximum phenol removal rate of 29.9 g/d because homogeneity was achieved in the reactor, resulting in better exploitation of the column volume.

Biodegradation of *p*-nitrophenol was conducted in a novel upflow packed bed reactor with multiple numbers of ports for cross flow aeration using *Arthrobacter chlorophenolicus* A6 grown on polyurethane foams (PUF). Complete removal of *p*-nitrophenol was achieved for loading rate as high as 2787 mg/L/d (Sahoo et al. 2011).

Activated carbons prepared from oil palm shell were used to remove phenol (Lua and Jia 2009) and 2,4,6-trichlorophenol (Tan et al. 2009) in a fixed bed column. Both studies demonstrated that increased inlet substrate concentration, increased flow rate and decreased bed height resulted in steeper breakthrough curves with shorter breakthrough times. Their findings were later supported by Alhamed (2009) who used activated carbon from dates' stones for absorptive removal of phenol from packed bed column. In addition, reported that activated carbon in smaller particle size improved the performance of the adsorptive column but caused high pressure drop in the column.

Soybean seed coats were ground to powder and encapsulated in calcium alginate beads for phenol removal from refinery wastewater in a packed bed bioreactor. CCD study revealed that temperature and flow rate had significant effect on the phenol removal efficacy. However, phenol conversion decreased to half of its initial value of 96-97% after 2 h of continuous run, probably due to the results of long-term exposure to high temperature at 56 ^{o}C. Numerical results of the reaction behaviour obtained from computational fluid dynamics (CFD) simulation was also found to be in good agreement with the experimental results (Rezvani et al. 2015).

2.10.2 Fluidized bed reactor

Fluidized bed reactor (FBR) can be regarded as a packed bed through which fluid flows (upward or downward) at a sufficient velocity to expand the bed and the particle-fluid mixture behaves like a fluid (Burghate and Ingole 2013; Tisa et al. 2014). The concept of fluidization is applied in FBR's operation, and both gas and liquid flow can be used to fluidize a bed of particles (Tisa et al. 2014). In wastewater treatment, fluidization is provided by the flow of wastewater through the catalyst or biomass bed. The size and density of particle as well as the upflow velocity of the fluid and its viscosity determine the degree of the bed expansion (Bello et al. 2017). Upon fluidization in a FBR, it is possible to attain phase homogeneity and enhancement of solid-fluid contact interfacial area which enables handling of high volumetric loading (Girish and Ramachandra Murty 2013). FBR offers some excellent features such as low operating

cost, high resistance to system upsets, high mass transfer rates, uniform particle mixing and uniform temperature distribution (Bello et al. 2017). Moreover, the pressure drop is smaller, and the formation of preferential channels is minimized because the flow distribution through the reactor radial section is more uniform (Gómez et al. 2007).

FBR has been widely used in wastewater treatment particularly in biological processes (González et al. 2001; Ochieng et al. 2003). *P. putida* immobilized on plastic beads was used to degrade synthetic wastewater containing phenol in a draft tube FBR. It was estimated that the mass transfer coefficient of phenol transfer from bulk phase to the surface of the biofilm on the solid particle be in the range of 0.0726-0.2012 ($\times 10^{-5}$) m/s. Increase in feed concentration, air flow rate and feed flow rate increased the mass transfer coefficient (Vinod and Reddy 2006). *Candida tropicalis* yeast immobilized onto granular activated carbon (GAC) particles was able to remove > 99% of phenol at volumetric loading rate of 60 mg/L/d in a FBR. For a mixture feed of phenol and 4-chlorophenol, the removal efficiency was > 98% at 4.1 and 55 mg/L/d for 4-chlorophenol and phenol respectively (Galíndez-Mayer et al. 2008). Haribabu and Sivasubramanian (2016) evaluated the biodegradation of organic content in domestic wastewater using FBR and attained a maximum COD removal of 96.7%. COD reduction increased with the increase in superficial gas velocity but decreased with the decrease in initial concentration.

In terms of phenol adsorption in FBR, Mohanty et al. (2008) demonstrated that nearly 95% removal of phenol was achieved at shorter reaction time and lower activated carbon loading as compared to batch adsorption system. Zhou et al. (2015) designed an integrated flocculation-adsorption fluidized bed for the treatment of synthetic influent consisting of 150 mg/L kaolin clay and 100 mg/L phenol, by using polymer aluminium chloride as flocculant and GAC as adsorbent. A flocculation efficiency of 96% and an adsorption efficiency of 80% were achieved with a reaction time as short as 25 and 12 s, respectively. Moreover, utilization of FBR in adsorption process aids in overcoming the common challenges faced by packed-bed column adsorption such as clogging, temperature gradient, channeling and dead zones (Bello et al. 2017).

The performance of FBR-integrated AOPs in phenol treatment has also been shown to be better than the conventional AOPs due to the combining advantages of FBR and the effectiveness of AOPs (Muangthai et al. 2010; Mokhtar et al. 2011). A photo-FBR

was designed by Huang and Huang (2009) for mineralisation of phenol using immobilized iron oxide in the presence of H_2O_2. Approximately 98% mineralisation of phenol was obtained in the photo-FBR, leading to fewer iron species being leached from the immobilized iron oxide. Moreover, a reduction of > 40% in H_2O_2 dosage was also observed. Shet and Vidya (2016) pointed out that the performance of immobilized Ag@TiO_2 nonoparticles in solar photocatalysis of phenol depended on catalyst loading, active catalyst sites and light penetration limitations.

Even though the research studies on FBR for wastewater treatment are enumerable, incorporation of peroxidase-based enzymatic approach onto this continuous system is limited. Trivedi et al. (2006a) demonstrated a 54% phenol conversion when SBP entrapped in silica sol-gel/alginate particles were applied to a liquid-solid circulating fluidized bed where reaction and regeneration were carried out simultaneously and continuously. The performance of the system was improved when a 10% inventory was replaced by fresh biocatalysts before each new cycle run, and > 70% phenol removal efficiency was observed after eight operation runs by applying this practice. SBP covalently bound to glass supports with different surface areas were examined for their viability in phenol removal in a FBR, and it was found that 80% removal was achieved using immobilized SBP on support with the highest surface area. Maximum phenol conversion increased with increasing bed height and specific surface area, but was independent of initial phenol concentration (Gómez et al. 2007).

As can been seen, most of the continuous phenol degradation processes in either packed bed or fluidized bed reactors employed conventional treatment methods such as microbial degradation and adsorption processes. Incorporation of AOPs in these types of reactors is gaining attention in the recent years. However, the report on peroxidase-based enzymatic treatment method in continuous process is still sketchy and lacking. The viability of peroxidase for large-scale wastewater treatment application relies on its performance in the continuous operation mode. Therefore, it is of great importance to evaluate the efficacy of immobilized peroxidases in this particular area.

In short, it can be concluded from this chapter that phenols present in wastewater of various industries with concentration ranging from <10 to >6000 mg/L depending on the processes. In view of current technologies for phenol treatment which suffer from

some recurrent drawbacks, peroxidase-based enzymatic method is regarded as alternative approach due to perceived advantages including low energy requirements, more flexible operation conditions, and minimal environmental impacts. However, free enzymes are usually challenged by susceptibility to inactivation, lack of long-term stability, difficulty in recovery, and non-reusability. In addition, most of the reported studies on peroxidases for phenol degradation are limited to batch operation mode (either in free or immobilized state). Therefore, this research project proposed the extraction of newly sourced plant peroxidases from local agricultural wastes, namely Luffa and JP peroxidases, and immobilization of peroxidase onto NaCS-PDMDAAC polymeric capsules for phenol removal under batch and continuous processes.

CHAPTER 3: RESEARCH METHODOLOGY

3.1 LIST OF MATERIALS, CHEMICALS AND REAGENTS

Table 3.1: List of materials, chemicals and reagents used in the research project.

Material	Description	Supplier
LP skin peel	Non-edible agricultural waste	Local restaurant, Miri
JP skin peel	Non-edible agricultural waste	Local restaurant, Miri
Cotton linter	Raw material for the synthesis of sodium cellulose sulphate (NaCS)	Xiamen University, China
Acetic acid	Glacial 100%	Merck (Darmstadt, Germany)
Boric acid		Merck (Darmstadt, Germany)
Citric acid		Fisher Scientific (Loughborough, UK)
Hydrochloric acid		Merck (Darmstadt, Germany)
Sulphuric acid		Merck (Darmstadt, Germany)
Sodium acetate		Merck (Darmstadt, Germany)
Sodium tetraborate		Acros Organics (New Jersey, USA)
Tri-sodium citrate		Fisher Scientific (Loughborough, UK)
Sodium dihydrogen phosphate		Merck (Darmstadt, Germany)
di-sodium hydrogen orthophosphate		Fisher Scientific (Loughborough, UK)
Sodium hydrogen carbonate		Fisher Scientific (Loughborough, UK)
Sodium hydroxide		Merck (Darmstadt, Germany)
4-aminoantipyrene (4-AAP)		Acros Organics (New Jersey, USA)
Absolute ethanol	99.4%	Fisher Scientific (Loughborough, UK)
Hydrogen peroxide	30% w/v	Merck (Darmstadt, Germany)
Phenol detached crystal		Fisher Scientific (Loughborough, UK)
Potassium ferricyanide		Acros Organics (New Jersey, USA)

Poly-dimethyl (diallyl) ammonium chloride (PDMDAAC)	Molecular weight 200,000 – 350,000 g/mol, 20 wt. % in H_2O	Sigma-Aldrich (USA)
Polyethylene glycol (PEG)	Molecular weight 6,000 g/mol	Fisher Scientific (Loughborough, UK)
Polyvinylpyrrolidone (PVP)	Molecular weight 40,000 g/mol	Sigma-Aldrich (USA)
Bradford reagent		Thermo Fisher Scientific (Loughborough, UK)
Bovine serum albumin (BSA)	Molecular weight ~66,000 Da (≥ 98% by agarose electrophoresis)	Santa Cruz, USA
Phosphate buffered saline (PBS) tablets	One tablet dissolved in 200 mL deionized water at 25ºC yields 0.01 M phosphate buffer, 0.0027 M potassium chloride, 0.137 M sodium chloride, and pH 7.4	Sigma-Aldrich (Malaysia)

3.2 EXTRACTION OF LP / JP

LP / JP skin peels as plant-based agricultural wastes for enzyme extraction were obtained from a local restaurant in Sarawak, Malaysia. The skin peels were thoroughly washed with distilled water and air-dried. Coarsely chopped LP / JP skin peels were blended with 0.1 M buffer solution of specific pH value at specific plant sample-to-buffer percentage (w/v) for 1 min, and then homogenized with constant stirring using magnetic stirrer. Several parameters including pH of buffer solution, plant sample-to-buffer percentage (w/v), temperature, presence of additives, and extraction time were manipulated in order to study their effects on extraction process via one-factor-at-a-time (OFAT) approach. The extraction conditions of each factor test were discussed in the subsequent sections. After extraction, the extract was filtered through four layers of cheesecloth before subjecting to centrifugation (Universal 320R, Hettich, UK) at 4000 rpm, 4 ºC for 20 min. The supernatant (crude extract) collected was sonicated and stored at 4 ºC until further use.

3.2.1 Peroxidase activity assay

Enzyme activities of LP and JP were measured using a colorimetric assay containing phenol, 4-aminoantipyrene (4-AAP) and H_2O_2. Absorbance measurements were performed using a UV-Vis spectrophotometer (Lambda 25 UV/Vis Double Beam,

Perkin Elmer). This assay is adopted from Wu et al. (1993) in which the assay mixture consists of 250 μL of 9.6 mM 4-AAP, 100 μL of 100 mM phenol, 100 μL of 2 mM hydrogen peroxide, 450-500 μL of 100 mM phosphate buffer pH 7.4 and 50-100 μL of enzyme solution. A slight modification was made to the assay by changing the buffer to pH 6 because pH 6 was found to be the optimum pH for LP and JP activity. Enzyme activity is proportional to the rate of formation of a coloured complex which absorbs light at a peak wavelength of 510 nm with an extinction coefficient of 7100 L/mol.cm based on the conversion of H_2O_2. The initial linear increase of absorbance was monitored for 1.5 min, and the enzyme activity of sample was calculated based on Equations 3.1 and 3.2. One unit of activity is defined as the number of micromoles of H_2O_2 consumed per minute at pH 6.0 and 25ºC.

$$\text{Activity in cuvette}\,(\text{U/mL}) = \frac{\Delta\text{A}\,@\,510\text{nm/s} \times \frac{60\text{s}}{\text{min}}}{7100\text{M}^{-1}\text{cm}^{-1}} \times 10^6\ \frac{\mu\text{mol}}{\text{mol}} \times \frac{1\text{L}}{1000\text{mL}} \qquad (3.1)$$

$$\text{Activity in sample}\,(\text{U/mL}) = \text{Activity in cuvette}\,(\text{U/mL}) \times \frac{1000\,\mu\text{L}}{\text{sample volume}\,(\mu\text{L})} \qquad (3.2)$$

3.2.2 Effect of pH on extraction process

The effect of pH on peroxidase extraction from LP and JP skin peels was conducted by varying the buffer solutions used during blending/homogenization. 0.1 M buffer solutions of various pH values were prepared using citric/citrate (pH 3), acetic/acetate (pH 4-5), monobasic/dibasic phosphate (pH 6-7) and boric/borate (pH 8-9). Plant sample-to-buffer solution percentage was fixed at 10% (w/v, g/mL). Homogenization was carried out at room temperature (25 ºC) for 30 min.

3.2.3 Effect of plant sample-to-buffer ratio on peroxidase extraction

Various amounts of coarsely chopped LP and JP skin peels were blended separately with buffer solution at optimum pH as determined in Section 3.2.2. Three different sample-to-buffer ratios (w/v %) were evaluated, including 10%, 30% and 50%. The maximum ratio was determined based on the requirement that blending and homogenization process be done properly. Other conditions of homogenization were maintained at 25 ºC for 30 min.

3.2.4 Effect of temperature on peroxidase extraction

The coarsely chopped LP and JP skin peels was blended in buffer solution at optimum pH and optimum sample-to-buffer ratio as determined previously. Homogenization of the blended mixture was then carried out at various temperatures ranging from 25 to 65 ^{o}C. For elevated temperatures (35-65 ^{o}C), the extraction process was thermally controlled using a water bath. The temperatures of the water bath remained constant throughout the 30 min of extraction process. Aliquots of 100 μL enzyme solution were withdrawn every 5 min and centrifuged (Eppendorf Refrigerated Centrifuge 5415 R) at 4000 rpm, 4 ^{o}C for 1 min. The supernatant was assayed for peroxidase activity as described in Section 3.2.1.

3.2.5 Effect of additives on peroxidase extraction

Polyethylene glycol (PEG) and polyvinylpyrrolidone (PVP) were evaluated for their effects on peroxidase extraction by dissolving the chemicals separately in buffer solution at optimal pH. The amount of PEG and PVP evaluated was 1% and 3% w/v for each additive. Buffer solutions with dissolved additives were then used to blend coarsely chopped plant samples at optimum sample-to-buffer ratio. Homogenization was carried out at optimum temperature as determined in Section 3.2.4 for 30 min. Aliquots of 100 μL enzyme solution were withdrawn every 5 min and centrifuged (Eppendorf Refrigerated Centrifuge 5415 R) at 4000 rpm, 4 ^{o}C for 1 min. The supernatant was assayed for peroxidase activity as described in Section 3.2.1.

3.2.6 Effect of peroxidase extraction time

The time required for optimum yield of peroxidase activity was investigated by conducting the extraction process at their optimum extraction conditions as determined previously in Sections 3.2.2 – 3.2.5, and analyzing samples for peroxidase activity at various time intervals. Aliquots of 100 μL enzyme solution were withdrawn every 5 min and centrifuged (Eppendorf Refrigerated Centrifuge 5415 R) at 4000 rpm, 4 ^{o}C for 1 min. The supernatant was assayed for peroxidase activity as described in Section 3.2.1.

3.3 CHARACTERIZATION OF LP / JP

Crude enzyme extracts of LP and JP obtained at optimum extraction conditions were

characterized from various aspects as follows.

3.3.1 Optimum pH and temperature for peroxidase activity

The optimum pH for LP and JP activities was determined by assaying the enzyme activity at different pH levels. This was achieved by varying the buffer solutions in the enzyme assay. The pH conditions of the buffer solutions used ranged from 3-10, and were prepared using citric/citrate (pH 3), acetic/acetate (pH 4 to 5), monobasic/dibasic phosphate (pH 6 to 7), boric/borate (pH 8 to 9) and sodium hydrogen carbonate/sodium carbonate (pH 10). The concentrations of all buffer solutions were maintained at 100 mM. The pH activity profiles for both plant peroxidases were generated by keeping all other conditions in enzyme assay constant as described in Section 2.2.

The effect of temperature on LP and JP activities was determined by assaying enzyme activities at optimum pH but at different temperatures, ranging from 25 ^{o}C to 65 ^{o}C. Assay mixture except enzyme was pre-mixed in cuvette and incubated in a thermostatic water bath equilibrated to desired temperature for 5 min. After that, enzyme was quickly added to the reaction mixture and the activity measured instantly.

3.3.2 pH and thermal stability of enzymes

5 mL of LP and JP solutions was individually placed into different test tubes and the pH was adjusted using 1 M HCl or 1 M NaOH to yield a series of samples at pH ranging from 2 to 11. The enzyme extracts were kept in these pH conditions for 30 min at 25 ^{o}C. At the end of the experimental test, the pH of the enzyme solutions in each test tube was adjusted back to pH 7. The remaining activities of the enzymes were assayed at optimum pH, and the pH stability of these enzymes was determined.

For thermal stability experiments, crude enzyme extracts (2 mL) were put in separate test tubes and kept at various temperatures (25-80 ^{o}C) in thermostatic water bath for 60 min. Aliquots of 50 μL were withdrawn at 10-min intervals and carefully immersed in ice water. Remaining activities of the enzymes were assayed according to Section 3.2.1. Residual peroxidase activity was calculated based on percentage of the original activity of the unheated enzyme solution.

3.3.3 Hydrodynamic size and zeta potential of enzymes

The hydrodynamic sizes and zeta potentials of soluble LP and JP were examined under varying pH conditions using Malvern Zetasizer Nano-ZS, Model ZEN3600, UK. 10 mL of crude enzyme extracts was put in separate test tubes and the pH of the enzyme solutions was adjusted using HCl (1 M) or NaOH (1 M) to give a pH range of 1.5 – 10. The pH-adjusted enzyme solutions were then centrifuged (Universal 320R, Hettich, UK) at 4000 rpm and 25 ºC for 5 min. After centrifugation, the supernatants were collected and sonicated for 3 min. 1 mL of supernatant was injected into folded capillary zeta cell DTS-1070 and analyzed for hydrodynamic size. After size measurement, the same sample was analyzed again for zeta potential. Three measurements of size and zeta potential were taken for each sample and the average was calculated.

3.3.4 Determination of enzymatic kinetic parameters

The kinetic characterization of LP and JP was performed by measuring the initial rates of phenol oxidation at 25 ºC in 100 mM phosphate buffer pH 6 for 1.5 mins, at varying phenol (10-100 mM) and H_2O_2 (1-4 mM) concentrations. H_2O_2 concentration was kept constant at 2 mM while phenol concentration was varied from 10 to 100 mM to evaluate Michaelis-Menten constants for phenol. Likewise, Michaelis-Menten constant for H_2O_2 was determined by keeping phenol concentration constant at 100 mM and varying H_2O_2 concentration from 1 to 4mM. The apparent K_m and V_{max} values for both phenol and H_2O_2 were determined from Lineweaver-Burk plots at optimum pH and temperature conditions. Plots of $1/V_o$ versus 1/S were constructed according to Equation 3.3:

$$\frac{1}{V_o} = \frac{K_m}{V_{max}} \frac{1}{[S]} + \frac{1}{V_{max}} \tag{3. 3}$$

Where [S] is the concentration of the substrate and V_o is the initial reaction rate ($UmL^{-1}min^{-1}$), V_{max} is the maximum rate, and K_m is the Michaelis-Menten constant (mM).

3.3.5 Determination of protein content

Protein concentration of the crude enzyme extracts was determined according to Bradford method using bovine serum albumin as standard (Bradford 1976). All

samples for analysis were diluted 50 times using phosphate buffered saline (PBS) solution. 100 µL of diluted sample was then taken and mixed with 1 mL of Bradford reagent. The mixture was let rest for 1 min before its absorbance taken at 595 nm against water. Protein concentration of the sample was compared with the standard curve prepared using bovine serum albumin (BSA). BSA solutions of various concentrations were prepared through serial dilution using PBS. The standard curve of protein concentrations was shown in Appendix A.

3.3.6 Molecular mass detection by SDS-PAGE

The molecular weight of peroxidase was estimated by sodium dodecyl sulphate (SDS) polyacrylamide gel electrophoresis (PAGE) procedure as described by Laemmli (1970). Enzyme samples were loaded to SDS-PAGE using 15% resolving gel and 6% stacking gel. Electrophoresis was carried out in vertical slab gels and the runs were performed at constant current intensity of 15 mA/plate in the stacking and 30 mA/plate in the running gels. Protein bands were stained using Coomassie Brilliant Blue R-250. The protein ladders used were phophorylase b (97 kDa), bovine serum albumin (66 kDa), ovalbumin (45 kDa), carbonic anhydrase (30 kDa), trypsin inhibitor (20.1 kDa) and α-Lactalbumin (14.4 kDa).

3.4 BATCH TREATMENT OF AQUEOUS PHENOL SOLUTION USING CRUDE LP / JP

LP / JP – catalyzed treatment of phenol was conducted in conical flasks. The conical flask contained a total of 10 mL mixture of 1 mL phenol (10 mM), 1.5-4.5 mL LP or JP solution, 0.2 mL H_2O_2 and 4.3-7.3 mL buffer solution (0.1 M). The initial concentration of phenol in the mixture was 1 mM. The enzymatic reaction was initiated by the addition of H_2O_2 to the reaction mixture, and the mixture was incubated (Programmable Incubator Shaker, SISTEC) for 24 h with constant shaking to ensure homogeneity. 1 mL of sample was withdrawn after the reaction and centrifuged to remove sedimentation from the reaction mixture, before analyzing for final phenol concentration.

Several operating parameters affecting the rate of phenol removal were investigated. These include pH, H_2O_2 concentration, enzyme loading, temperature, and reaction time. A single factor approach was applied in each case where only the operating

parameter under investigation was varied. The operating parameter settings for each effect were presented in Table 3.2. For the study of reaction time, aliquots of 100 µL were withdrawn at various time intervals to determine phenol content in the mixture.

Table 3.2: Operating parameter settings for batch treatment of aqueous phenol solution using free enzyme.

Experimental parameters	**pH**	**H_2O_2 concentration (mM)**	**Enzyme loading (mL)**	**Temperature (°C)**
Effect of pH	4 – 9	1	1.5	25
Effect of H_2O_2 concentration	Optimum pH	1 – 12	1.5	25
Effect of enzyme loading	Optimum pH	Optimum concentration	0.5 – 4.5	25
Effect of temperature	Optimum pH	Optimum concentration	Optimum loading	25 – 70
Effect of reaction time	Optimum conditions of pH, H_2O_2, enzyme loading, and temperature			

3.4.1 Determination of phenol concentration

Phenol concentrations were determined colorimetrically using 4-AAP and potassium ferricyanide in an alkaline buffer medium with a UV-Vis spectrophotometer (Lambda 25 UV/Vis Double Beam, Perkin Elmer). The assay contains 100 µL of potassium ferricyanide (83.4 mM in 0.25 M sodium hydrogen carbonate), 100 µL of 4-AAP (20.8 mM in 0.25 M sodium hydrogen carbonate) and 800 µL of sample or sample diluted with distilled water (Feng et al. 2013). Under alkaline conditions, phenolic compounds react with 4-AAP to form an intermediate molecule which is then oxidized by potassium ferricyanide to form a quinone-type dye which absorbs light at 510 nm. The colour intensity is linear with respect to phenol concentration. The cuvette mixture is prepared in the sequence of sample, 4-AAP followed by potassium ferricyanide, and absorbance reading taken after 5 min.

A standard curve of phenol concentrations is prepared by measuring the absorbance readings of aqueous phenol solutions of different concentrations. Each phenol sample was diluted 11 times to ensure that the maximum absorbance reading did not exceed 1. All the experimental samples in this study followed the same dilution factor, and the respective phenol concentrations of the samples were determined from the phenol

standard curve (Appendix A). Phenol removal efficiency is calculated based on Equation 3.4:

$$\text{Phenol removal (\%)} = \frac{\text{Initial concentrat ion} - \text{final concentrat ion}}{\text{Initial concentrat ion}} \times 100\% \quad (3.4)$$

3.5 OPTIMIZATION VIA EXPERIMENTAL DESIGN

A two-level (2^k) full factorial design was performed using Design Expert software (STAT-EASE Inc., Minneapolis USA) to determine the relationship between key process variables and phenol removal efficiency as the response (Y). Process variables investigated were (i) x_1, pH (ii) x_2, H_2O_2 concentration and (iii) x_3, enzyme loading. The ranges of each variable was based on previously determined experimental analyses. The variables were coded (-1, 1) to indicate low and high levels respectively (Table 3.3).

Three center points were also included in the 2^k factorial design to check for curvature in the response pattern. The total number of experimental runs as determined by the statistical software was 11. The sequence of experimental runs was randomized to minimize stochasticity. Each run was carried out for 24 h in an incubator (Programmable Incubator Shaker, SISTEC). The presence of a significant curvature in the first-order modelling would result in data augmentation to RSM central composite design (CCD) in order to predict a quadratic or higher-level process model. The empirical model developed correlated the response (phenol removal efficiency) to the process variables examined (pH, H_2O_2 concentration and enzyme loading).

Table 3.3. Variables coded for 2^k factorial design

Variables	Factors	Low Level (-1)	High Level (1)
x_1	pH	5	8
x_2	H_2O_2 concentration (mM)	1	8
x_3	Enzyme loading (mL)	1.5	4.5

3.5.1 Statistical analysis

Analysis of variance (ANOVA) was used for regression analysis of the experimental data and to investigate statistical significance of the model developed.

3.6 SYNTHESIS OF SODIUM CELLULOSE SULPHATE (NACS)

NaCS was prepared according to previously published procedures by Zeng, Danquah, Potumarthi, et al. (2013). Briefly, cold absolute ethanol was added slowly to cold concentrated sulfuric acid on ice at a volume ratio of 1:1.51. The solution was gently stirred to ensure complete mixing. Cotton linter was immersed in the reaction mixture at 1:50 w/v and kept at 0±1.0 ºC for 1 h. The remaining solid was then removed, squeezed dry and washed with cold absolute ethanol three times to remove the residual sulfuric acid. The solid was then added to distilled water (same volume as reaction mixture) and stirred vigorously for 10 min. The insoluble cotton linter residue was separated by centrifugation at 4000 rpm for 10 min. The pH of the supernatant collected (NaCS solution) was adjusted to 9.0 – 9.3 using 2 M sodium hydroxide (NaOH) solution. Cold absolute ethanol at 1-1.5 times the volume of the supernatant was added to drive sedimentation. The NaCS sediment was collected and freeze-dried for 24 h.

3.7 FORMATION OF NACS-PDMDAAC POLYMERIC CAPSULES

The solid NaCS synthesized in the preceding section was dissolved in distilled water at various concentrations (2, 2.5 and 3% w/v) and constantly stirred until homogeneously mixed. NaCS solution was then dropped into PDMDAAC solution of different concentrations (4, 6 and 8% diluted from 20% (w/v) PDMDAAC) by using a silicone dropper with constant gently stirring. Formation of polymeric capsules at varying concentrations of NaCS and PDMDAAC was carried out at room temperature (~25 ºC). The capsules formed were separated from the solution after 10 min and washed with distilled water several times. The capsules were then stored in 0.9% sodium chloride (NaCl) solution until use.

For the study of effect of reaction temperature, both NaCS and PDMDAAC solutions were cooled in ice water (10 ºC) or heated in water bath (35 ºC). After reaching the respective temperatures, NaCS-PDMDAAC capsules were formed according to the procedures above.

3.7.1 Biophysical characterizations of NaCS-PDMDAAC polymeric capsules

The mechanical strength of capsules was determined by placing 5 capsules on an electronic scale, and a thin microscope slide was placed on top of the capsules. The

force exerted on the slide which caused the rupture of the capsules was recorded as a function of the weight displayed on the scale.

Shrinking time was determined by taking the time when the capsules formed begin to shrink. Shrinking is considered to occur when the crumples are seen on the capsule membrane. Capsule diameter was measured using a digimatic caliper (Absolute Digimatic Caliper, Mitutoyo Corporation).

3.8 ENCAPSULATION OF PEROXIDASE ONTO NACS-PDMDAAC CAPSULES

Encapsulation of JP onto NaCS-PDMDAAC polymeric capsules follows the procedure mentioned in Section 3.7 with the exception that dry NaCS was dissolved in JP enzyme extract (prepared from Section 3.2) at a concentration of 2% w/v. NaCS-peroxidase solution was dropped into 6% PDMDAAC solution using silicone dropper to form peroxidase-immobilized polymeric capsules at 25 ^{o}C. After washed with distilled water several times, the immobilized biocatalysts were stored in 0.9% sodium chloride (NaCl) solution until use.

3.8.1 Encapsulation efficiency of JP unto NaCS-PDMDAAC capsules

Encapsulation efficiency of JP unto NaCS-PDMDAAC capsules was determined by placing 15 enzyme-immobilized polymeric capsules in 5 mL phosphate buffer pH 7.4. The capsules were cut into half and left in buffer solution for 24 h. Encapsulated JP was released into buffer solution after the capsules were cut into half. Protein content in the phosphate buffer solution after 24 h can therefore be assumed as the amount of JP being encapsulated. Protein content of JP solution initially applied for encapsulation was determined by mixing 1 mL JP solution with 5 mL phosphate buffer pH 7.4. This volume of JP solution was based on the estimation that 1 mL JP solution with 2% NaCS can produce ~15 capsules. Protein content was measured according to Section 3.3.5. Encapsulation efficiency is calculated based on the following equation:

$$\text{Encapsulation efficiency (\%)} = \frac{\text{Protein content of encapsulated JP}}{\text{Protein content of JP applied}} \times 100\% \qquad (3.5)$$

3.8.2 pH and thermal stability of immobilized JP

2 mL of phosphate buffer pH 7 was placed separately in different test tubes and the pH adjusted using 1 M HCl or 1 M NaOH to yield a pH range of 3 to 11. Approximately 10 JP-immobilized capsules were put in each test tube for 30 min at 25 ^{o}C. After 30 min, the capsules were taken out from the buffer solution and ruptured to obtain the encapsulated enzyme. The enzyme activities of the immobilized JP were assayed according to Section 3.2.1 to determine its residual peroxidase activity.

Thermal stability of immobilized JP was conducted by placing enzyme-immobilized capsules in test tube, and the test tube was immersed in thermostatic water bath at a specific temperature. The temperature range being studied was from 30 to 80 ^{o}C. For one specific temperature setting, 6 test tubes containing 10 capsules each were prepared. One test tube will be withdrawn from the water bath at 10-min intervals and briefly immersed in ice water for cooling purpose. After that, the capsules were ruptured and aliquots of immobilized enzyme taken for peroxidase activity assay. Residual peroxidase activity was calculated based on percentage of the original activity of the unheated immobilized JP at 25 ^{o}C.

3.8.3 Hydrodynamic size and zeta potential of immobilized JP

The hydrodynamic sizes and zeta potentials of immobilized JP were examined under varying pH conditions using Malvern Zetasizer Nano-ZS, Model ZEN3600, UK. 2 mL of phosphate buffer pH 7 was put in separate test tubes and the pH of the buffer solution was adjusted using HCl (1 M) or NaOH (1 M) to give a pH range of 2 – 10. Approximately 10 JP-immobilized capsules were put in each test tube and then ruptured to release the encapsulated enzyme. The mixture in the test tube was vortexed and then centrifuged (Universal 320R, Hettich, UK) at 4000 rpm and 25 ^{o}C for 5 min. After centrifugation, the supernatants were collected and sonicated for 3 min. 1 mL of supernatant was injected into folded capillary zeta cell DTS-1070 and analyzed for hydrodynamic size. After size measurement, the same sample was analyzed again for zeta potential. Three measurements of size and zeta potential were taken for each sample and the average was calculated.

3.8.4 Scanning electron microscopy (SEM) analysis

NaCS-PDMDAAC polymeric capsules were cut into half and let to dry overnight at room temperature. The capsules were then placed accordingly on SEM specimen stubs with double-sided adhesive tape to show inner and outer surfaces, followed by coating with a 10 nm gold layer. The inner and outer surface morphology of capsules were investigated with field-emission scanning electron microscopy (SEM) (JEOL JSM-6390LA, Japan).

3.8.5 Fourier transform infrared spectroscopy (FTIR) analysis

Fourier transform infrared spectroscopy (Agilent Technologies Cary 630 FTIR) was used to identify various functional groups and chemical bonds in cotton linter (cellulose), NaCS, PDMDAAC, and NaCS-PDMDAAC matrix in order to identify any potential modifications in the initial compositional structures during the synthesis process. The principle of FTIR is based on relative spectral vibration of molecules in a sample on exposure to infrared (IF) within a specific range of wave number or frequency. The IR spectra of cellulose (cotton linter), NaCS, PDMDAAC, and NaCS-PDMDAAC capsule were obtained in the frequency range of 600-4000 cm^{-1} with step size of 7.45 cm^{-1}.

3.9 BATCH TREATMENT OF AQUEOUS PHENOL SOLUTION USING IMMOBILIZED JP

For phenol degradation using immobilized JP, reaction mixture consisting of 8.8 mL buffer solution (0.1 M), 1.0 mL phenol solution (10 mM) and some JP-encapsulated biopolymer capsules was prepared in conical flask. The enzymatic reaction was initiated by the addition of 0.2 mL H_2O_2 into the reaction mixture, and the mixture incubated (Programmable Incubator Shaker, SISTEC) for 24 h with constant shaking to ensure proper mixing and maximum phenol removal. The initial phenol concentration in each reaction medium was 1 mM, and the total volume of the reaction mixture was 10 mL. The efficiency of JP in phenol degradation between free and immobilized conditions was compared under varying operating conditions such as pH, H_2O_2 concentration, enzyme loading and temperature to establish optimum conditions. The compositions of the reaction mixtures under varying operating conditions were summarized in Table 3.4. The kinetic behaviour and rate constants were also

investigated by conducting the reaction under the optimum operating conditions. The extent of immobilized JP reusability was evaluated by recycling the capsules with fresh reaction mixture. The percentage of phenol removal was calculated based on Equation 3.4.

Table 3.4: Operating parameter settings for batch treatment of aqueous phenol solution using immobilized enzyme.

Experimental parameters	**pH**	**H_2O_2 concentration (mM)**	**Enzyme loading (U/mL)**	**Temperature (°C)**
Effect of pH	5 – 8	1	0.23	25
Effect of H_2O_2 concentration	Optimum pH	1 – 12	0.23	25
Effect of enzyme loading	Optimum pH	Optimum concentration	0.16 – 0.70	25
Effect of temperature	Optimum pH	Optimum concentration	Optimum concentration	25 – 50
Kinetic behaviour	Optimum conditions of pH, H_2O_2 and enzyme concentrations, and temperature			
Reusability	Optimum conditions of pH, H_2O_2 concentration, and temperature			

3.10 DESIGN OF FLUIDIZED BED COLUMN

The fluidized bed column used in this research project was custom made by Jaya Chemical Sdn Bhd. As shown in Figure 3.1(a), the column consists of two parts, an outer column which has a dimension of 200 mm x 30 mm, and an inner column with a dimension of 120 mm x 25 mm. There are two side openings located near the top and bottom of the outer column respectively which act as sampling points. Enzyme-immobilized biopolymer capsules are filled into the outer column from the top opening. A glass sieve is located 2.5 cm from the bottom of the outer column to retain the biopolymer capsules in place in the column. The inner column has a total of 3 small holes scattering around the column to ensure the flow of solution from outer column to inner column and subsequently out of the column for recycling purpose.

(a)

(b)

Figure 3.1: Customized fluidized bed column: (a) separate outer and inner column; (b) interlocked outer and inner column.

Figure 3.1(b) shows the fluidized bed column when the inner column is locked into the outer column. When the inner column is tightly screwed and locked to the outer column, the available space for the placement and/or fluidization of biopolymer capsules is 10 cm in height. The inner column also prevents the capsules from escaping through the top of the column especially during fluidization.

The schematic diagram of the fluidized bed column with JP-immobilized polymeric capsules for continuous phenol removal from aqueous solution is illustrated in Figure 3.2. As can be seen, both top and bottom of the column are connected with tubing. A peristaltic pump is used to supply phenol solution from beaker into the column in an upward flow. The peristaltic pump has a flow rate knob with different settings, ranging from 0 to 10 which correspond to 0-206.4 mL/min. Phenol solution leaving the column from the top is recycled to the beaker before being fed into the column again via the pump.

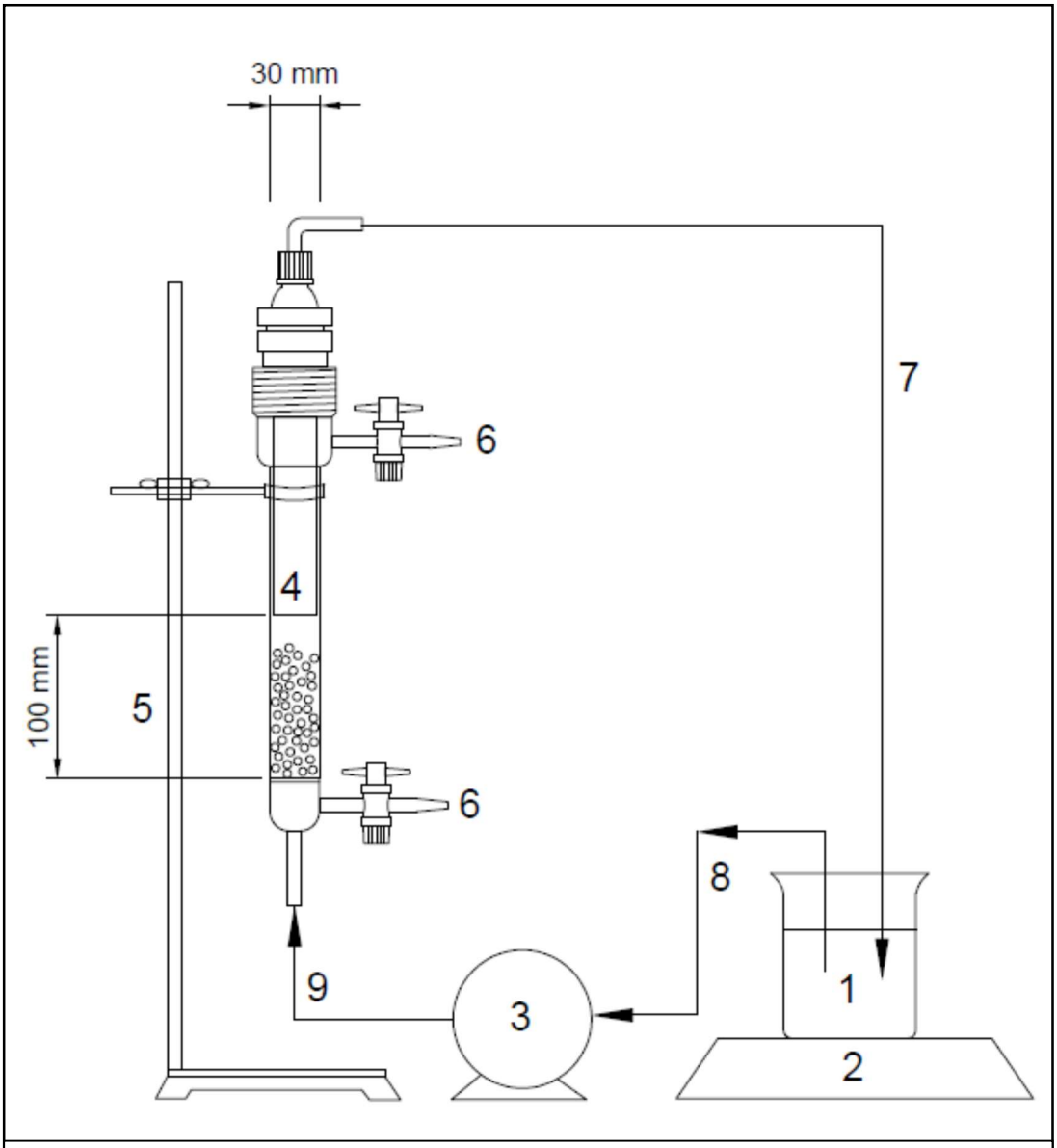

1 – Beaker
2 – Magnetic hot plate stirrer
3 – Peristaltic pump
4 – Customized fluidized bed column
5 – Retort stand
6 – Sampling points
7, 8 & 9 – Connecting tubing

Figure 3.2: Schematic diagram of fluidized bed column with JP-immobilized polymeric capsules for continuous phenol degradation.

3.11 CONTINUOUS PHENOL DEGRADATION IN FLUIDIZED BED COLUMN USING JP-IMMOBILIZED BIOPOLYMER CAPSULES

In order to examine the viability of JP-immobilized NaCS-PDMDAAC polymeric capsules for continuous phenol degradation, a fluidized bed column set up as depicted in Figure 3.2 was used. Before start up, both side openings of the column were closed. The beaker was filled with 200 mL of 0.1 M sodium phosphate buffer solution of pH 6. 2 mL of 0.1 M phenol solution was then added into the beaker and thoroughly mixed with buffer solution through continuous stirring on a magnetic plate to ensure homogeneity. Phenol solution was pumped into the column until half-filled before biopolymer capsules encapsulated with JP were placed inside the column. The inner column was then attached and locked properly to the outer column. Phenol removal reaction was initiated by the addition of 1 mL of 0.2 M H_2O_2 solution into the beaker with constant stirring followed by the start-up of peristaltic pump to supply reaction mixture from the beaker to the column. The beaker was covered with parafilm to avoid the release of phenol molecules through evaporation. 100 µL of phenol aqueous solution was withdrawn from beaker before the addition of H_2O_2 to determine initial phenol concentration. For phenol concentration at different time intervals, aliquots were withdrawn from the top sampling point and analysed according to Section 3.4.1.

3.11.1 Effect of flow rate on phenol removal in fluidized bed column

The effect of flow rate on phenol removal efficiency in the fluidized bed column was investigated by adjusting the flow rate knob setting to 4, 6 and 7 separately. The actual flow rates corresponded to these settings were 1.167, 1.827 and 2.146 mL/s respectively. The amount of biopolymer capsules used in this study was kept relatively constant by producing the capsules from 20 mL of JP solution containing 2% (w/v) of NaCS. Other operating parameters were as given in Section 3.11.

3.11.2 Effect of enzyme loading on phenol removal in fluidized bed column

The optimal flow rate determined from Section 3.3.1 was used throughout the study of the effect of enzyme loading on phenol removal in fluidized bed column. JP-immobilized polymeric capsules were prepared from three different starting volumes of JP solutions containing 2% (w/v) NaCS, which were 10, 20 and 30 mL respectively. Other operating parameters were kept constant as given in Section 3.11.

3.11.3 Reusability of immobilized biocatalysts in fluidized bed column

The reusability of JP-immobilized polymeric capsules in the fluidized bed column was conducted at the optimal flow rate and enzyme loading as determined from Sections 3.3.1 and 3.3.2. After each cycle, all the reaction solution in the column and tubing was drained whilst the capsules were retained in the column. Fresh phenol solution was prepared in a clean beaker according to Section 3.3. Reaction was initiated by the addition of 1 mL of 200 mM H_2O_2 solution into the beaker with constant stirring followed by the start-up of peristaltic pump at optimal flow rate to supply reaction mixture from the beaker to the column. Each cycle was carried out for 18 h and final phenol concentration was analysed by following the procedures in Section 3.4.1. Reusability test was continued until the phenol removal efficiency decreased to 50%.

CHAPTER 4: RESULTS AND DISCUSSION

4.1 EXTRACTION OF PEROXIDASES

Extraction of peroxidases from the non-edible plant skin peels has been successfully carried out based on the method discussed in Chapter 3. Figure 4.1 shows the homogenization step during peroxidase extraction process as well as the crude enzyme extracts obtained after centrifugation and sonication for LP and JP respectively.

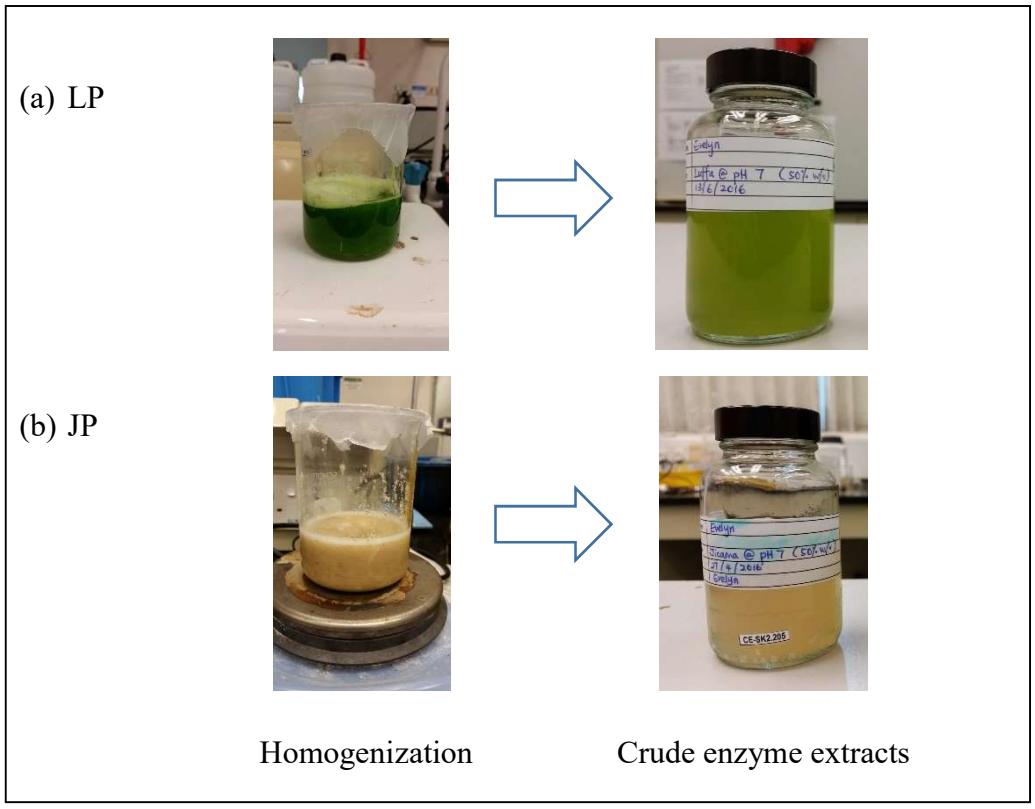

Figure 4.1: Homogenization step in peroxidase extraction process and the final products of crude enzyme extracts; (a) LP, (b) JP.

4.1.1 Effect of pH on peroxidase extraction

Figure 4.2 shows the relative activities of LP and JP as a function of extracting buffer pH. Relative activity is defined as the rate of H_2O_2 consumption at a particular pH normalized with respect to the highest rate (Ghaemmaghami et al. 2010). The pH condition of the extracting buffer medium plays an important role in the enzyme extraction process as it affects the ionization state of the enzyme amino acids side chains. Using a plant sample-to-buffer solution percentage of 10% (w/v), both plant

peroxidases exhibited similar trend over the pH range being studied, with low yield activities at highly acidic and basic conditions. Low enzymatic activities at extreme pH conditions are due to the detachment of haem prosthetic groups from the poly-peptide chain of the enzymes (Vámos-Vigyázó and Haard 1981), which caused the enzymes to lose their catalytic functionalities. Optimum extraction pH was observed at pH 7 for both peroxidases. The enzymatic activities of LP and JP were 0.34±0.02 U/mL and 0.36±0.01 U/mL respectively.

It is also noticed from Figure 4.2 that the effect of extracting buffer pH on extraction yield activity was more profound on LP. In general, LP extracted using buffer solutions with pH other than 7 yielded much lower enzymatic activities than JP. This shows that the secretion of LP from skin peels is more pH dependent, because such extracting buffer solutions did not support effective and complete chemo-diffusion of the enzymes from the plant possibly due to their low solvation potential and equilibrium limits. Therefore, it is important to extract peroxidase at its optimum pH to promote maximal yield activity.

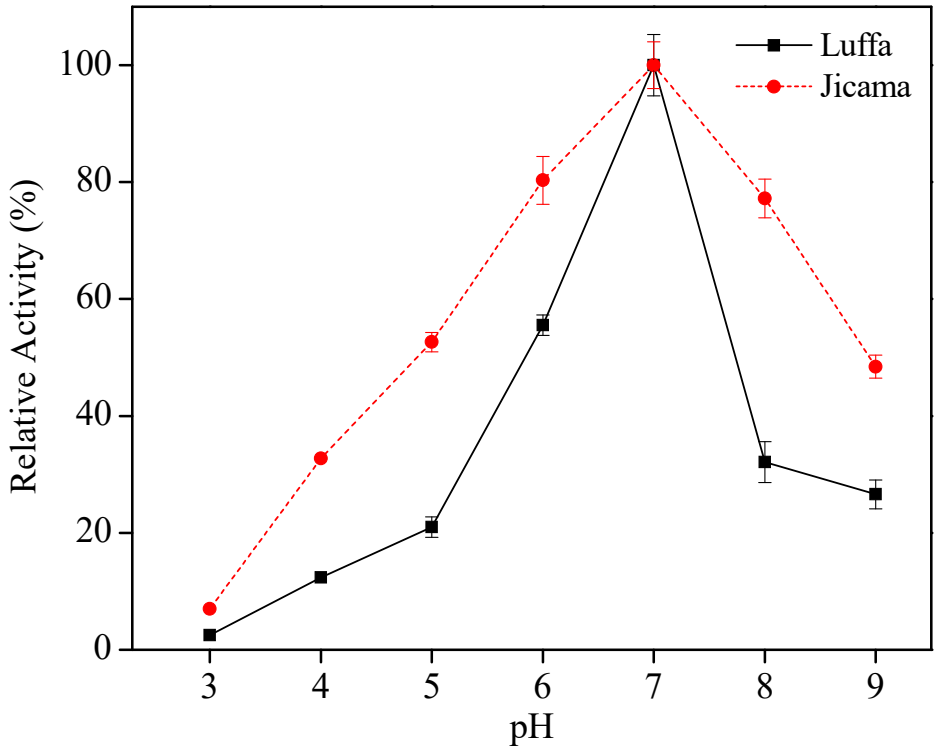

Figure 4.2: Relative activity yield as a function of extracting buffer pH. Experiments were carried out using plant sample-to-buffer ratio of 1:10 and homogenization at 25 ºC for 30 min.

4.1.2 Effect of feedstock-to-buffer solution percentage on peroxidase extraction

The activity yield during extraction process was improved by increasing the feedstock-to-buffer percentage. Using a constant volume of buffer solution at optimum pH, the ratio can be varied by manipulating the amount of plant skin peels added to the buffer medium. Three different percentages (10, 30 and 50% (w/v)) were studied. As depicted in Figure 4.3, when the amounts of LP / JP increased in the homogenization medium, the enzyme activity obtained also increased. Increasing the quantity of feedstock increases the mass of peroxidases available for extraction per unit volume of buffer. At 50%, LP extract showed an enzymatic activity of 1.37±0.03 U/mL, which was 4-fold of its activity at 10%. JP extract, on the other hand, demonstrated an activity of 1.51±0.06 U/mL at 50% ratio, with an increment of more than 4-fold of its activity at 10%. The highest plant sample-to-buffer ratio achieved with LP and JP was both 50%. Beyond this ratio, the proper blending of plant skin peels with buffer solution could not be performed and extraction mixture becomes very viscous for effective homogenization. This would increase the economics of the extraction process especially for large-scale preparations. However, it is expected that, with further increase, the equilibrium amount of peroxidase extracted will be lower than the amount of peroxidases existing in the plant. Under this condition, more peroxidases can be extracted by distorting the existing equilibrium pattern through temperature variation, buffer chemo-diffusion parameters and/or homogenization rate.

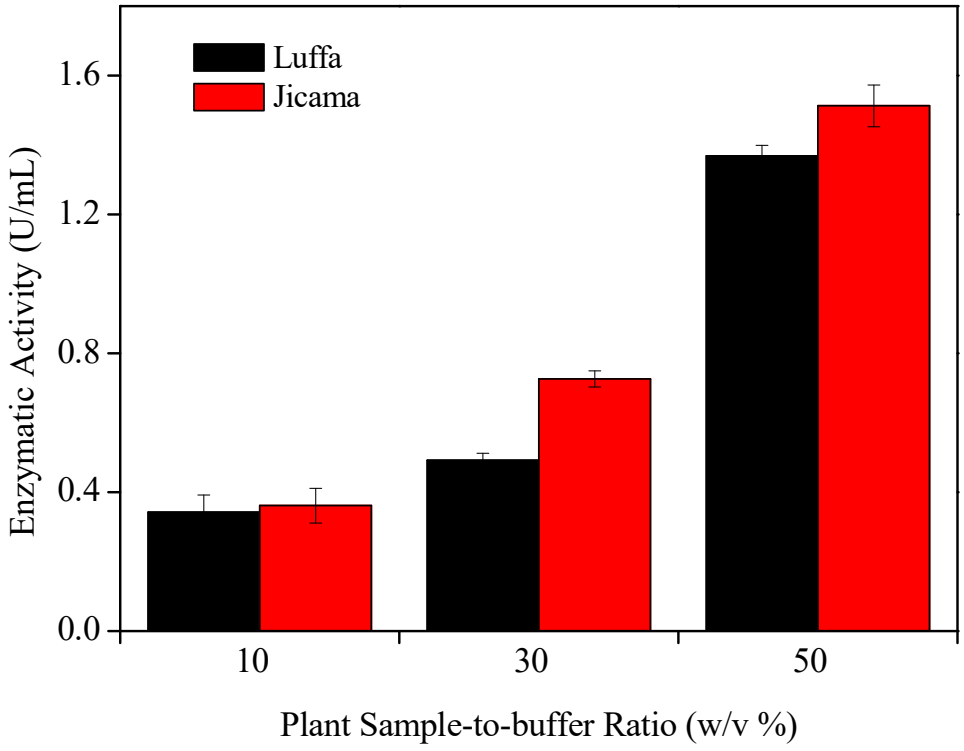

Figure 4.3: Peroxidase extraction activity yield as a function of plant sample-to-buffer ratio (w/v %). Ratios of 10%, 30% and 50% were evaluated using a constant volume buffer pH 7; homogenization at 25 ºC for 30 min.

4.1.3 Effect of temperature on peroxidase extraction

In order to evaluate the influence of temperature on the extraction process, homogenization was carried out at various temperatures ranging from 25 to 65 ºC after blending of plant skin peels with buffer pH 7 at sample-to-buffer ratio of 50% (w/v). The temperature profiles of LP and JP in terms of relative enzymatic activity are presented in Figure 4.4(a) and (b) respectively. For LP, the optimum extraction temperature was observed at 25 ºC with an enzymatic activity of 1.39±0.02 U/mL. Other elevated temperatures (35-65ºC) did not enhance the extraction process but also adversely affected the activity yield. Extraction of LP at 35 ºC yielded only 70% of its optimal activity at 25 ºC. The enzymatic activity yield continued to decrease when extraction processes were carried out at even higher temperatures. At 65 ºC, the activity of LP obtained was less than 40% of its optimal value.

As for JP, extraction processes at temperature range of 25- 45 ºC gave an optimum enzymatic activity of 1.55±0.02 U/mL after 25-30 min homogenization. It is also

noticed that the rate of extraction for these three temperatures was in the order of 45 ºC > 35 ºC > 25 ºC. Extraction at 45 ºC gave high yield of enzymatic activity of 92% of optimal after only 5 min of homogenization. Higher temperatures provided more kinetic energy to the system and thus enhanced the secretion of enzyme molecules into the buffer medium. When the temperature was further increased to 55 ºC, the activity yield obtained was slightly lower than the optimum. At 65 ºC, the extracted JP showed an activity of ~60% of its optimal.

Lower yield of enzymatic activity at high temperatures could be attributed to thermal denaturation which results in either loss of enzyme active sites or molecular seclusion of active sites from substrate molecules due to structural deformation. The results from Figure 4.4 also showed that LP is more sensitive to heat and slight thermal change of the environment could cause loss of enzyme activity during extraction. Therefore, the extraction of LP should be performed at 25 ºC. Extraction of JP, though enhanced at slightly elevated temperatures, a compromise between extraction time and operational cost (heating) should be taken into consideration. For ease of extraction process as well as from an economic standpoint, the extraction of JP will also be conducted at 25 ºC in the present work.

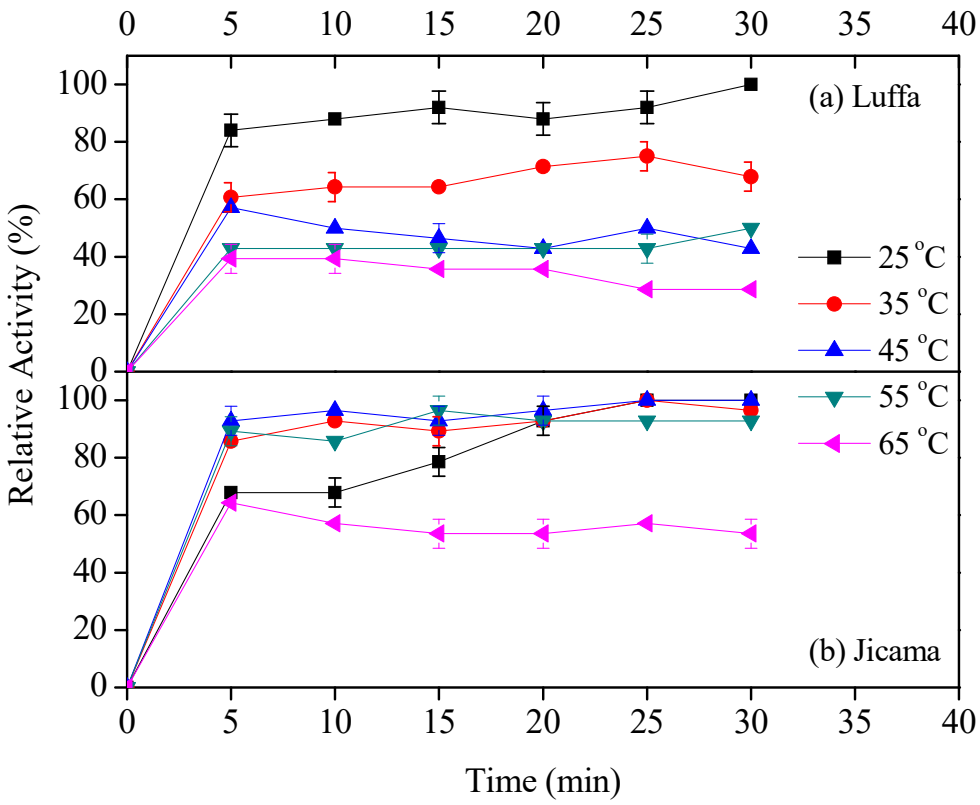

Figure 4.4: Temperature profile of peroxidase extraction: (a) LP; (b) JP. Both plants were extracted using buffer pH 7 with sample-to-buffer ratio of 50% (w/v), and homogenization at various temperatures (25-65 °C).

4.1.4 Effect of additives on peroxidase extraction

Polyethylene glycol (PEG) and polyvinylpyrrolidone (PVP) are often used as phenolic scavengers during enzyme extraction process. In order to determine the effect of these additives on enzymatic activity yield, pre-weighed PEG and PVP at 1% and 3% (w/v) was separately dissolved in buffer solution pH 7, and the solutions were then used to extract LP and JP. Extraction using solely buffer pH 7 without any additive served as control for comparison purpose. The extraction profiles of different dosages of additives were presented in Figure 4.5. For LP, neither PEG nor PVP enhanced the extraction process (Figure 4.5(a)). An optimum enzymatic activity of 1.39±0.01 U/mL was obtained when LP was extracted without any additive. With the presence of additives in the extracting buffer medium, the extracted LP exhibited lower activities than the optimal. The higher the concentration of additives in the buffer medium, the lower the enzymatic activities. This was demonstrated by 1% and 3% PEG with average relative activities of 77% and 58% respectively, as well as 1% and 3% PVP

with average relative activities of 53% and 37% respectively. Comparatively, PVP caused lower enzymatic activity yield in LP extraction than PEG. This can be attributed to the presence of electronegative N and O groups available on the PVP molecule which project a nucleophilic attack on the extracted peroxidase. This weakens the peptide forming units of the peroxidase structure, causing denaturation of the peroxidase protein. In addition, the presence of the electronegative O and N groups can also contribute more negative zeta potential compared to PEG. This reduces the degree of permeation into the plant matrix for the extraction of peroxidases since the cell membrane structure of the plant matrix is electronegative. Therefore, there is increasing repulsion in the presence of PVP.

However, the impact of additives on the extraction of JP was not as unfavorably as that of LP (Figure 4.5(b)). The optimum enzymatic activity yield was obtained in the absence of additives, with an average of 1.55±0.02 U/mL. Increasing the amount of PEG in the extracting buffer solutions from 1% to 3% did not affect the enzymatic activity yield significantly. The relative activities shown by these conditions were rather close, with 85% and 87% for 1% PEG and 3% PEG respectively. Extraction with 1% PVP showed comparable enzymatic activity yield as control, but lower activity yield was observed when the concentration was increased to 3%. The effect of surfactant structure in peroxidase extraction could be attributed to the balance of hydrophobic and hydrophilic forces in extracting these molecules because of the divers range of various inter-molecular interactions role in extraction phenomena (Hosseinzadeh et al. 2013).

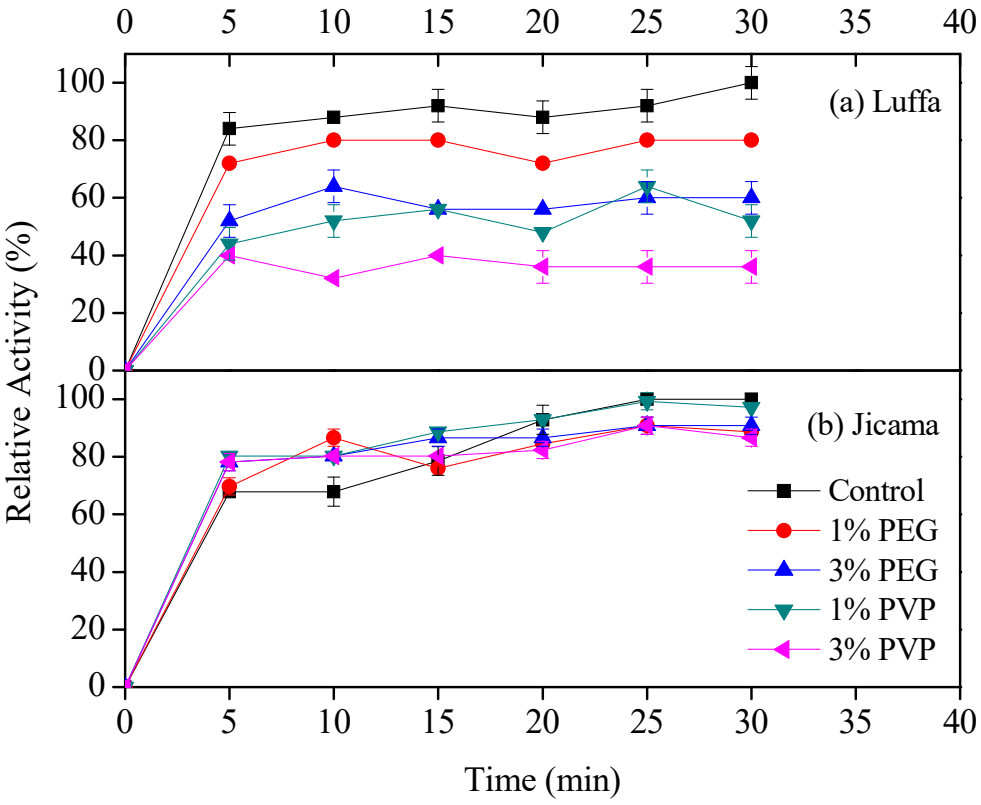

Figure 4.5: Effect of additives on extraction process: (a) LP; (b) JP. Peroxidase extraction was performed using buffer pH 7 at sample-to-buffer ratio of 50% w/v at 25 ºC, with 1% or 3% (w/v) of PEG / PVP dissolved in buffer solution.

4.1.5 Effect of peroxidase extraction time

The minimum time required to acquire optimal enzymatic activity yield was determined by conducting the extraction process for both plant peroxidases at their optimum extraction conditions. As determined in the preceding sections, the optimum extraction conditions were found to be buffer pH 7, sample-to-buffer ratio of 50%, 25 ºC and in the absence of additive. Under these conditions, aliquots of samples were withdrawn at various time intervals and analyzed for enzyme activity. The extraction profiles were as illustrated in Figure 4.6.

Extraction of peroxidases from LP and JP skin peels happened rather rapidly. The fast initial rate of enzyme extraction is due to the existing driving force relating to the difference in peroxidase concentrations within the plant sample and the extracting buffer. After 5 min of homogenization, LP demonstrated a relative activity of 84% whilst JP only 67%. The initial rate of extraction of LP was higher than JP. This could be due to the differences in the molecular diffusivity of the enzyme molecules and

solubilisation energies of the peroxidases in the extracting buffer, resulting from the molecular formation and bonding structures of the peroxidases. The enzymatic activity continued to increase as the time progressed, showing that more peroxidase molecules were being secreted into the medium. Extraction of both peroxidases achieved equilibrium within 30 min, though JP demonstrating a slightly shorter time of 25 min. After 30 min, the rate of extraction stabilized with no significant increase in the differential rate of extraction per unit time. The maximal enzymatic activities demonstrated by LP and JP were 1.38±0.03 and 1.57±0.02 U/mL respectively. With that, the minimum time required for extraction of both plant peroxidases to reach equilibrium was 30 min under optimum extraction conditions.

The optimum conditions for LP and JP extraction are summarized in Table 4.1.

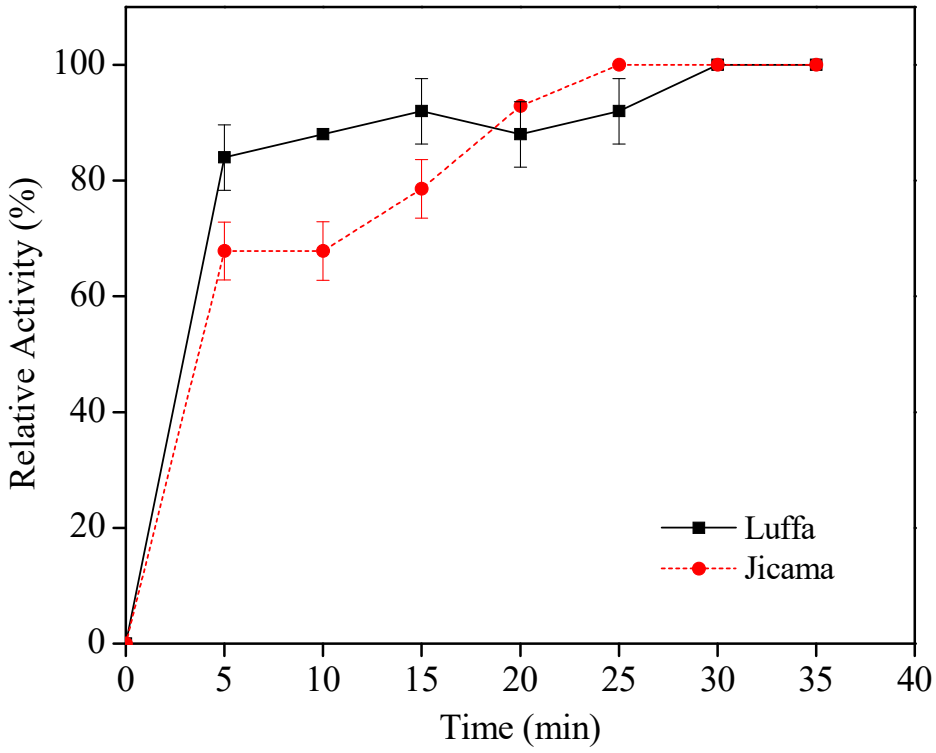

Figure 4.6: Peroxidase extraction as a function of time. Extraction was conducted at optimum conditions of buffer pH 7, plant sample-to-buffer ratio of 50% w/v at 25 ºC.

Table 4.1: Optimum conditions for LP and JP extraction.

Experimental parameters	LP	JP
pH	7	7
Feedstock-to-buffer solution percentage (w/v)	50%	50%
Temperature	25 ºC	25 ºC
Additives	Without additive	Without additive
Extraction time	30 min	30 min
Enzymatic activity	1.38±0.03 U/mL	1.57±0.02 U/mL

4.2 CHARACTERIZATION OF LP / JP

4.2.1 Optimum pH and temperature for peroxidase activity

Crude enzyme extracts of LP and JP obtained under optimum extraction conditions were characterized for their respective optimum pH and temperature for peroxidase assay. The pH dependence of peroxidase enzymatic activity measured at 510 nm is depicted in Figure 4.7. For both enzymes, the optimum pH value was found to be 6. The optimum pH of 6 either promotes the molecular active state of the substrate and enhances the kinetics of initiation or favours the 3D structure of the enzyme to enable easy access to its active sites. Both peroxidases showed similar activity profiles, with decreasing enzyme activity under the conditions of high acidity and alkalinity. Reduced enzyme activity under extreme pH conditions could be attributed to reasons including instability of the coloured complex product under extreme pH conditions, reactive or conformational changes of the coloured complex new products, and enzyme inactivation via charge saturation (Wright and Nicell 1999). Optimum pH of enzyme activity for other peroxidases have been reported to be within a similar range, from pH 5 to 7. The optimum pH values of those reported peroxidases are summarized in Table 4.2. These results suggest that the relationship between enzyme activity and pH depends on the assay chromogens and the type of peroxidase enzyme.

The optimum temperatures of LP and JP activity were evaluated by assaying the enzymatic activity at optimum pH 6 under various temperatures, ranging from 25 to 65 ºC. The relative activities at different temperatures with regards to the optimal were shown in Figure 4.8. The optimum temperature for both peroxidases was observed at 35 ºC. In fact, JP remained active at 25 ºC, 45 ºC and 55 ºC with relative activities of over 90%. Elevated temperatures did not favour the enzymatic assay of LP, showing

an average relative activity of 60% at 45 ºC and above. Nevertheless, the optimum temperature demonstrated by LP and JP was in keeping with other plant peroxidases in the range of 30-40 ºC (see Table 4.2).

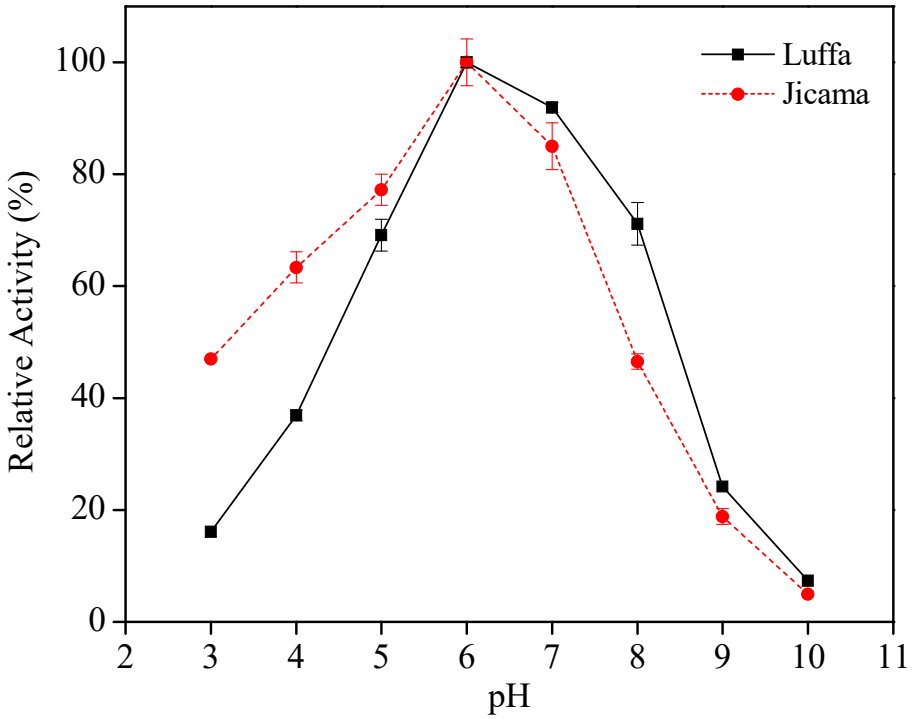

Figure 4.7: Optimum pH of LP and JP.

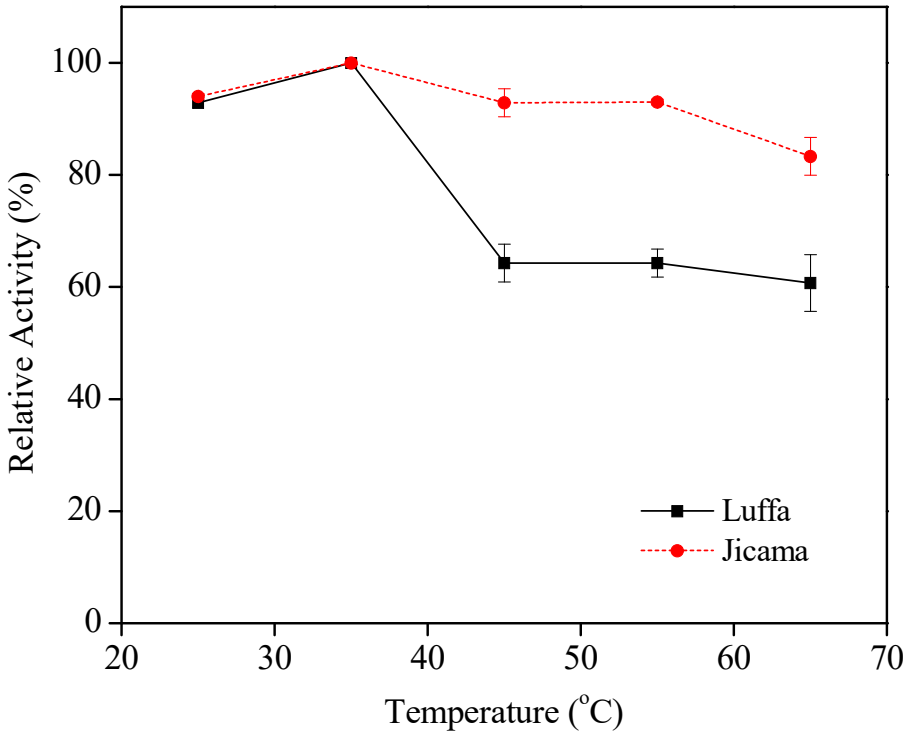

Figure 4.8: Optimum temperature of LP and JP.

Table 4.2: Comparison of optimum pH and temperature of various peroxidases.

Source of peroxidase	Optimum pH	Optimum temperature	References
LP	6	35 ºC	Present work
JP	6	35 ºC	Present work
Haricot bean	5	40 ºC	(Köktepe et al. 2017)
Royal palm leaves	5 – 5.5		(Sakharov et al. 2001)
Bitter gourd	5.6	40 ºC	(Fatima and Husain 2008)
Rosemary leaves	6	40 ºC	(Aghelan and Shariat 2015)
Turkish blackradish	6.5	30 ºC	(Kalin et al. 2014)
Turnip roots	6.5 4.0	30 ºC 35 ºC	(Kalin et al. 2014) (Motamed et al. 2009)
Korean radish seeds	7	n.a.	(Kim and Lee 2005)

*n.a. – data not available

4.2.2 pH stability of peroxidase

The stability of enzyme under varying pH conditions is crucial because it bearings the potential and feasibility of enzyme application for various processes and/or large-scale

operations. Figure 4.9 shows the stability of LP and JP after incubating at varying pH conditions for 30 min.

Overall, LP showed better pH stability than JP over the pH range studied. Over 90% of its enzyme activity was retained at pH conditions 6.4 to 8.2, and more than 80% thereafter up to pH 10.4. At pH below 5, the retained enzyme activity of LP was less than 70%, and further loss of enzymatic activity was observed when the acidity of the buffering medium increased. As for JP, more than 80% of its activity was preserved after incubation at pH conditions of 6.4 to 8.2. JP suffered a sharp decline in stability and lose about 50% of its activity when the pH was lower than 6. Increase in alkalinity also caused JP to lose its enzyme activity progressively. Ionization state of side chain of enzyme amino acids is highly pH dependent. Considering that heme group is essential for peroxidase activity, the instability of heme binding to the enzyme or ionic changes in the heme group at extreme pH conditions cause enzymes to suffer loss of activity (Al-Senaidy and Ismael 2011; Pina et al. 2001).

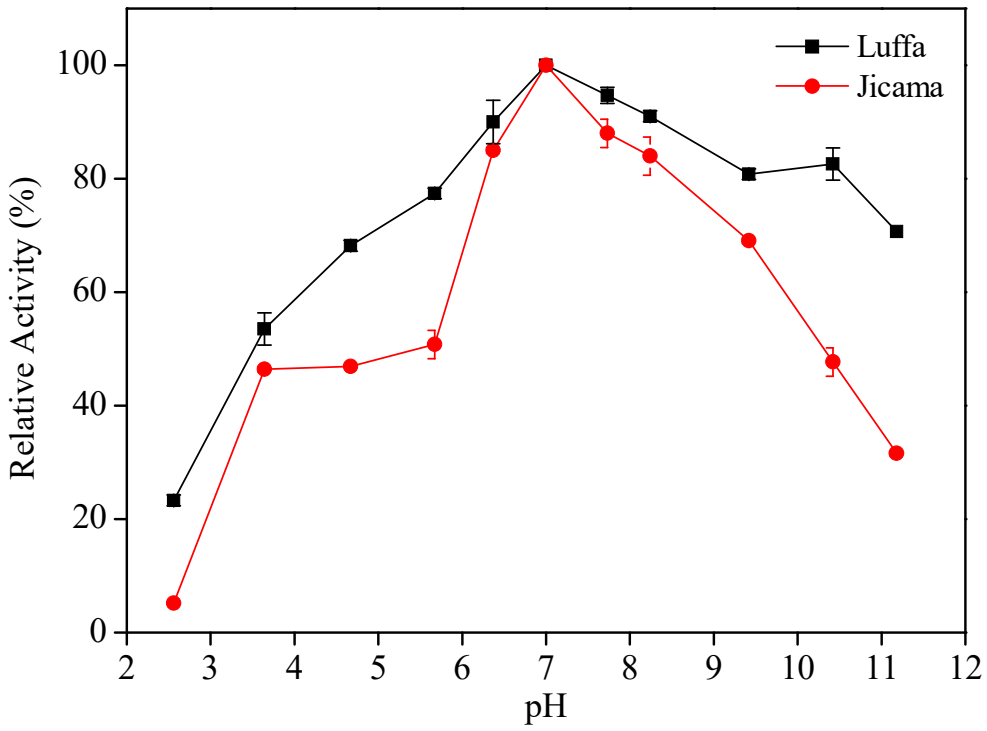

Figure 4.9: Stability of LP and JP over pH range of 2.5 – 11.2 for 30 min.

4.2.3 Thermal stability of peroxidase

Crude extracts of LP and JP were incubated at various temperatures ranging from 25 to 80 ºC and the residual enzyme activities were analyzed at various time intervals in order to determine their thermal stability. The results are presented in Figure 4.10(a) and (b) for LP and JP respectively.

The enzymatic activities of LP and JP were well preserved over 90% at temperatures close to ambient temperature (25-30 ºC). At 40 ºC, both peroxidases retained ~80% of their respective activities. Incubation at elevated temperature of 50 ºC caused decline in enzymatic activities for both peroxidases, with LP and JP losing about 40% and 30% of their respective activities. As the incubation temperature further increased, the loss of enzymatic activity became greater, showing a loss of about 50% for both peroxidases at 60 ºC. Comparatively, JP suffered a more significant decline in enzymatic activity at extremely high temperatures, demonstrating a residual activity of less than 10% at 70 ºC and losing all of its activity at 80 ºC. LP experienced gradual loss of activity at 70 ºC over the period of 1 h, from 40% at 10 min to 20% after 60 min.

Low enzymatic activity of peroxidases at high temperatures was due to thermal denaturation. Under elevated temperatures, the heme prosthetic group which governs the thermal stability of peroxidases is released, and a less stable apoenzyme is formed. This transient enzyme is more susceptible to thermal inactivation as compared to the native enzyme (McEldoon and Dordick 1996). Due to structural deformation of enzyme molecules at high temperatures, the binding capacity of enzyme active sites onto substrate molecules is limited, thus causing the low enzymatic activity.

In comparison, the thermal stability of LP and JP was not as high as commercially available HRP and SBP. SBP has been proven to show higher thermal stability than HRP owing to its higher heme affinity which increased the heme-apo-protein interaction (Kamal and Behere 2008). The inactivation temperature of SBP was reported to be 90.5 ºC, while that of HRP is 81.5 ºC (McEldoon and Dordick 1996). Other plant peroxidases such as oil palm leaf peroxidase also demonstrated high resistance to heat by retaining majority of its enzymatic activity up to 70 ºC. The high thermostability is due to the presence of a large number of cysteine residues in the polypeptide chain (Deepa and Arumughan 2002).

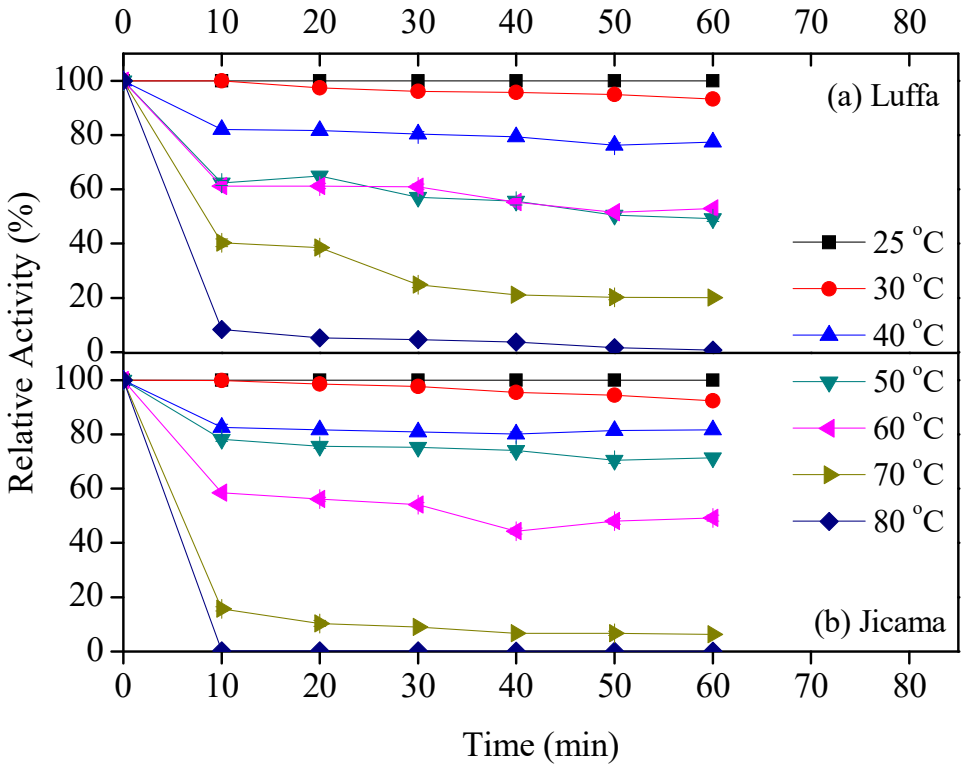

Figure 4.10: Temperature stability of (a) LP and (b) JP at various temperatures ranging from 25 to 80 ºC over a period of 60 min.

4.2.4 Hydrodynamic size and zeta potential of enzymes

The hydrodynamic sizes of LP and JP under varying pH conditions were studied to probe their diffusion rates and correlate effects on enzyme activity yield. The results are illustrated in Figure 4.11(a) and (b) for LP and JP respectively. The hydrodynamic sizes of both peroxidases are pH dependent. For LP, the molecules were in stable configurations with sizes ranging from 111-154 nm throughout the pH range being studied except at pH between 2.47 and 4.01. In between pH 2.47 and 4.01, the size of LP molecules peaked to 1200-1700 nm. The average hydrodynamic size of LP was 127 nm. On the other hand, the hydrodynamic size of JP ranged from 305-427 nm at pH 1.73-2.91 and 5.91-10.16, with an average of 365 nm. The hydrodynamic size of JP peaked at pH 3.75 and 4.88, corresponded to 997 and 1001 nm respectively.

The pH effect on hydrodynamic size distribution is caused by surface electrical charge accumulation and stability in response to protonation and deprotonation of the protein molecule. Surface electrical charge of protein molecules is measured as zeta potential. A higher inter-chain aggregation occurs at isoelectric point (pI) because the inter-chain

electrostatic repulsive forces and excess charge density of the molecule are reduced to zero. At pI, the protein structure is less stable and more hydrophobic owing to it possessing a net charge of zero with minimal intermolecular repulsive forces. Because of that, aggregation and precipitation of protein molecules tend to occur (Salgin et al. 2012). Both LP and JP were observed to aggregate and agglomerate in acidic condition at close proximity of its pI, resulting in drastic increase in hydrodynamic size. The isoelectric points of LP and JP were ~4.4 and ~4.9 respectively. Both LP and JP were anionic peroxidases under the conditions of extraction pH since their isoelectric points were at pH <7.

Previously, other anionic peroxidases have been identified, with isoelectric points of 3.5 in sweet potato (Leon et al. 2002), 3.8 in oil palm leaves (Sakharov et al. 2000) and 4.1 in soybean seed coat (Gillikin and Graham 1991). Lee and Kim (1994) demonstrated that six isoperoxidases co-existed in Korean radish root, with four anionic (pI 3.0-4.0) and two cationic isoperoxidases (pI 8.6-9.0).

Comparatively, the average hydrodynamic size of JP molecules is more than doubled the size of LP. The smaller size of LP offers a higher molecular diffusivity compared to JP, and this allows rapid dissolution of the enzyme in the extracting buffer. This effect can be seen in Figure 4.6 under Section 4.1.5 where the initial activity yield of LP was higher than JP. Nevertheless, JP achieved comparable final activity yield given sufficient extraction time to reach equilibrium.

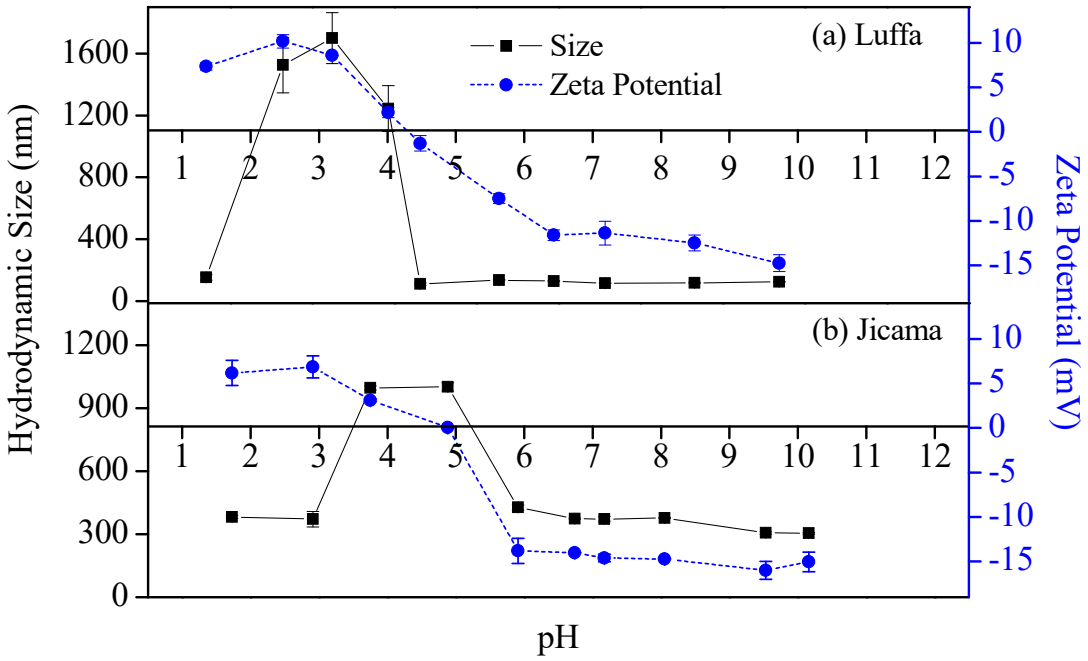

Figure 4.11: Hydrodynamic sizes and zeta potentials of peroxidases under varying pH conditions; (a) LP, (b) JP.

4.2.5 Determination of enzymatic kinetic parameters

Substrate specificity of LP and JP was evaluated by assaying the enzyme extracts at varying phenol and H_2O_2 concentrations. Phenol substrate saturation curves were constructed by interpolating the enzyme activities against various substrate concentrations while keeping H_2O_2 concentration constant at 2 mM. The results for LP and JP are shown in Figures 4.12 and 4.13 respectively. It is noticed that both peroxidases showed typical Michaelis-Menten kinetics for phenol substrate. Michaelis-Menten constants (K_m) of LP and JP towards phenol as substrate were determined from Lineweaver-Burk double reciprocal plots as shown in the insets of Figures 4.12 and 4.13 respectively. LP and JP had K_m values of 60.7 and 22.8 mM for phenol, and V_{max} of 1.92 and 1.81 mL/U respectively. Lower K_m value of JP suggests that it has a higher apparent affinity toward phenol than LP.

The K_m values of enzymes for H_2O_2 substrates were determined from Lineweaver-Burk plot in Figure 4.14. The calculated K_m values for LP and JP were comparable, being 0.64 and 0.68 mM respectively. This indicates that both peroxidases have similar affinity towards H_2O_2. This is important as H_2O_2 is an essential component in

peroxidase activation into catalytically active forms for various bioprocesses. The V_{max} values were also determined, with 1.84 mL/U for LP and 2.40 mL/U for JP.

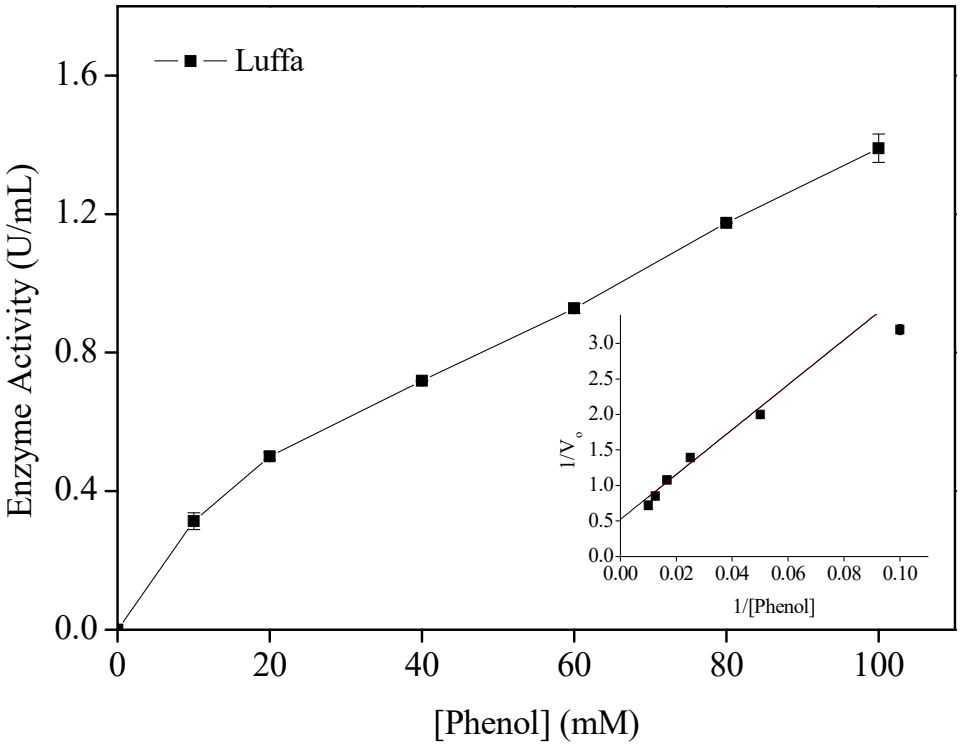

Figure 4.12: Substrate saturation curves and Lineweaver-Burk plots of LP towards varying phenol concentrations at 2 mM H_2O_2.

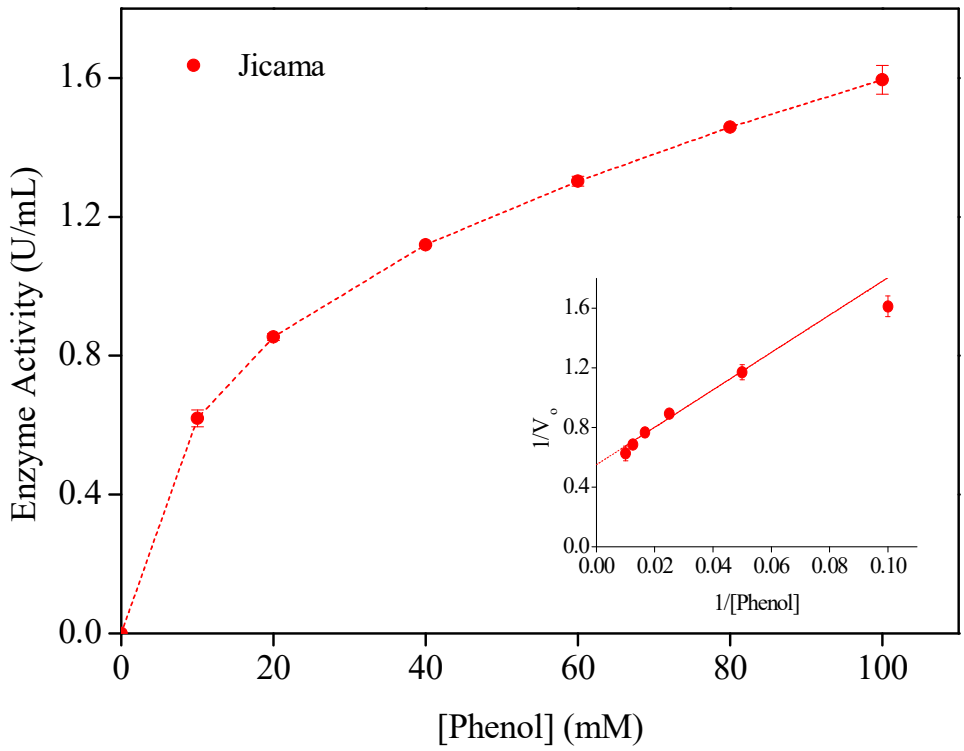

Figure 4.13: Substrate saturation curves and Lineweaver-Burk plots of JP towards varying phenol concentrations at 2 mM H_2O_2.

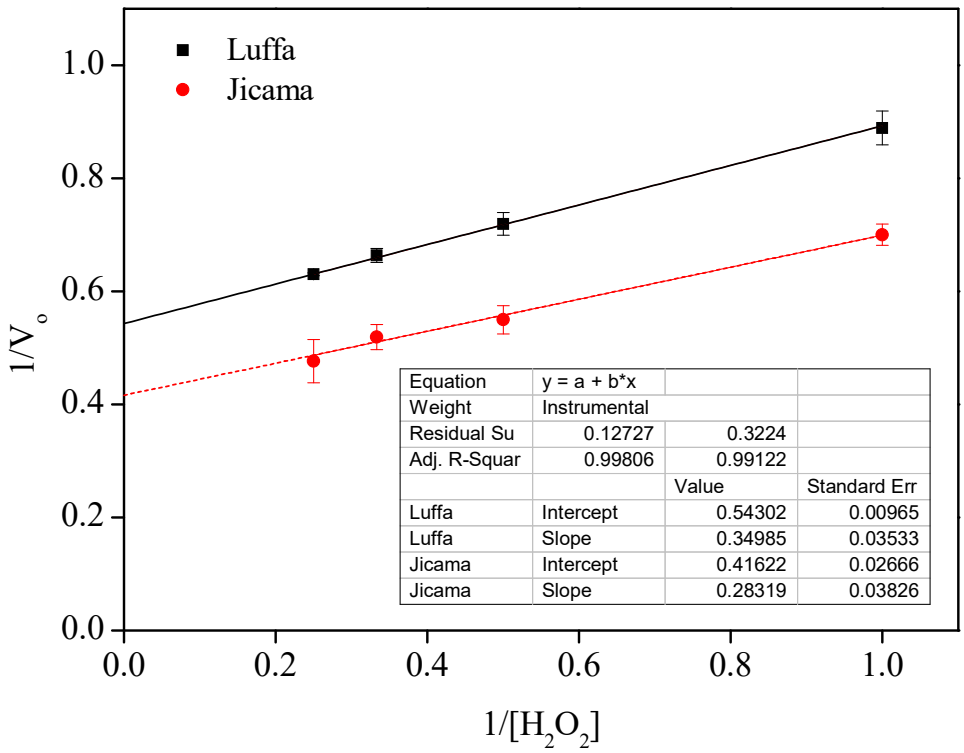

Figure 4.14: Lineweaver-Burk plot of LP and JP towards varying concentrations of H_2O_2 at 100 mM phenol.

4.2.6 Determination of protein content in enzyme solutions

Protein concentration in each enzyme extract was analyzed according to Bradford method. Specific activity of respective enzyme was calculated by dividing the total activity to total protein. The results are presented in Table 4.3. It is noticed that the protein concentration in LP extract was lower than JP extract. As a result, the calculated specific activity of LP was higher than JP.

Table 4.3: Protein content of crude enzyme extracts of LP and JP.

Enzyme	Volume (mL)	Total activity (U)	Total protein (mg)	Specific activity (U/mg protein)
Crude LP extract*	100	140	63	2.22
Crude JP extract*	100	160	364	0.44

*Calculation was based on preparation of 100 mL enzyme solution from 50 g starting material of chopped LP/JP skin peels.

4.2.7 Molecular weight of peroxidases

The results of molecular weight estimation by SDS-PAGE are illustrated in Figure 4.15. JP showed a distinct band between 20.1 and 30 kDa standard protein markers, and the molecular weight was estimated to be 26 kDa. SDS-PAGE revealed a fairly faint band for LP peroxidase possibly due to its low protein concentration. Nonetheless, the band corresponded to a molecular weight of 25 kDa. In comparison to molecular weights of other plant peroxidases such as horseradish at 44 kDa (Pina et al. 2001), soybean at 37 kDa (Gillikin and Graham 1991), artichoke at 38 kDa (Cardinali et al. 2011), bitter gourd at 43 kDa (Fatima and Husain 2008) and oil palm leaves at 48 kDa (Deepa and Arumughan 2002), the molecular weights of LP and JP were lower. The difference in molecular weights of different plant peroxidases could be due to differences in amino acid sequence or the degree of glycosylation.

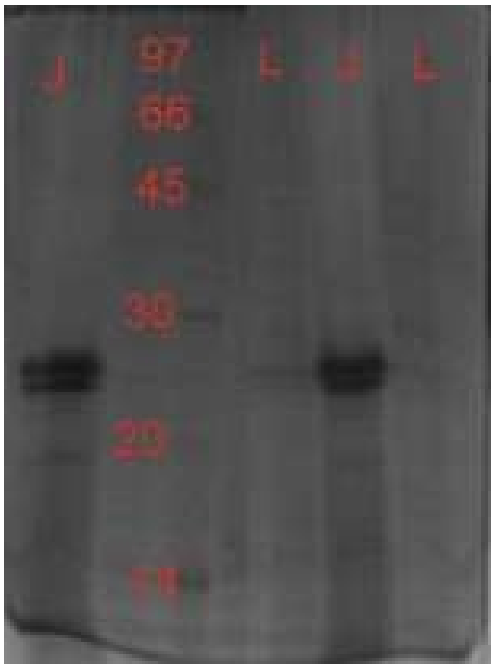

Figure 4.15: SDS-PAGE result of LP and JP. Lane L: LP peroxidase, lane J: JP.

4.3 BATCH TREATMENT OF AQUEOUS PHENOL SOLUTION USING FREE LP / JP

Crude LP and JP extracts prepared at the optimum conditions of extraction process were investigated for their efficiency in the treatment of aqueous phenol solution under free enzyme state. The average enzymatic activities exhibited by crude LP and JP were comparable, with 1.39±0.03 and 1.55±0.02 U/mL respectively. The crude enzyme extracts were used as produced without any further purification. The effects of various operating parameters which included pH, H_2O_2 concentration, enzyme loading, temperature, and reaction time on the performance of LP and JP in phenol degradation were studied and compared.

4.3.1 Effect of pH on phenol degradation using free LP / JP

Enzymes are generally known to be highly pH dependent as they are only functional when certain ionizable side chains are in specific forms. Therefore, the effect of pH on LP and JP was investigated to determine their optimum pH ranges. The initial compositions of other reagents in the reaction mixture were 1 mM phenol, 1 mM H_2O_2, and 1.5 mL enzyme solutions. Figure 4.16 presents the effect of pH on the phenol removal efficiency of LP and JP. The optimal phenol removal demonstrated by LP was 27% and 31% at pH 6 and pH 7 respectively. JP demonstrated > 90% removal under

identical pH conditions. Though LP and JP exhibited comparable enzyme activities over the same pH range, the difference in phenol removal performance suggested that LP might require higher concentrations of H_2O_2 to drive oxidation into catalytically active forms capable of reacting with phenolic compounds (Hamid and Rehman 2009).

At pH below 5 and above 8, LP resulted in low phenol removal, averaging around 12.4%. JP showed lower phenol removal performances under these pH conditions. The lower removal efficiency below pH 5 and above pH 8 is due to variations in the enzyme protein structure under extreme pH conditions. Enzyme molecules undergo structural modifications due to protonation and hydroxylation effects. These modifications could potentially obscure relevant active sites before causing denaturation and permanent loss of functionality. In addition, the decrease in removal efficiency at pH above 8 could also be attributed to the formation of phenol conjugated base since the pK_a of phenol at 25 ^oC is 10. This conjugated basic form prevents phenolic compounds from acting as hydrogen donors (Duarte-Vázquez et al. 2003), thus hindering their binding onto the surface of the enzyme active sites.

Previous studies on phenol removal catalyzed by HRP demonstrated efficient removal over the pH range of 6 to 9, with the optimum at pH 8, which is slightly basic (Nicell, Bewtra, Biswas, St. Pierre, et al. 1993). Another work by Wright and Nicell (Wright and Nicell 1999) showed that almost complete phenol removal was achieved with soybean peroxidase (SBP) over a pH range of 5 to 9, with the maximum removal at pH 6 under high SBP dosage. At least 85% removal of phenolic compounds was achieved with turnip peroxidase over a broad range of pH 4 – 8, with the maximum removal within pH 5 to 7 (Duarte-Vázquez et al. 2003). The optimum operating pH range exhibited by JP is in keeping with some of the aforementioned peroxidases though JP displayed a tighter pH range, suggesting the JP is more pH sensitive. Based on the finding in Figure 4.16, all subsequent enzymatic reactions were performed at pH 7.

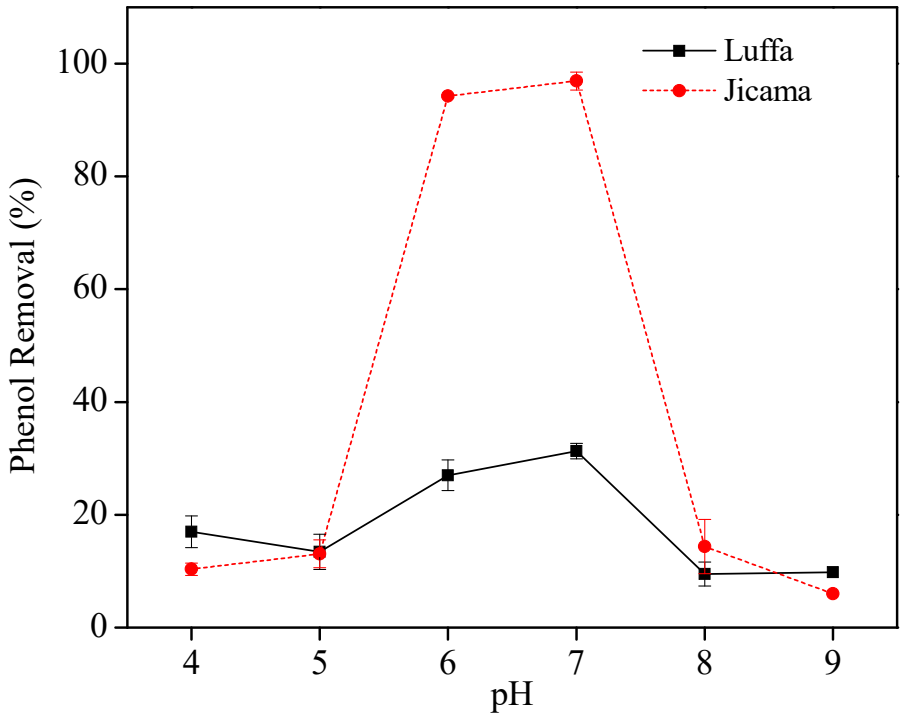

Figure 4.16: Effect of buffer pH on the phenol removal efficiency of JP and LP. The range of pH tested is 4 to 9. Other experimental conditions: 1 mM H_2O_2, 1.5 mL enzyme solutions, 25 ºC and 24 h incubation.

4.3.2 Effect of H_2O_2 concentration on phenol degradation using free LP / JP

H_2O_2 is an essential component of peroxidase-catalyzed reactions as it activates the peroxidase enzyme molecules (E) into active forms labeled as Compound I (E_i) which can oxidize aromatic phenolic compounds. Nonetheless, H_2O_2 concentration requires rigorous control for specific peroxidases as excess H_2O_2 has been reported to cause peroxidase inactivation.

As illustrated in Figure 4.17, LP showed phenol removal of ~30% phenol at 1 mM H_2O_2. When the concentration of H_2O_2 in the reaction mixture was increased, the percentage of phenol removal also increased until it reached the optimum of >95% at 6 mM. This demonstrates that LP requires a higher initial dosage of H_2O_2 for the oxidation of enzyme molecules as hypothesized earlier. The requirement for high H_2O_2 loading could be due to the characteristics of LP molecular active site induction which is driven by H_2O_2 concentrations higher than the optimal rate limiting concentration. Subsequent increments in H_2O_2 concentration did not further enhance phenol removal efficiency. However, a drop in phenol removal percentage was observed when the

H_2O_2 concentration was higher than 8 mM. High concentrations of H_2O_2 inhibit peroxidase catalytic activity by irreversibly oxidizing the enzyme ferriheme group which is vital for peroxidase catalysis (Duarte-Vázquez et al. 2003). Reaction with excess H_2O_2 can also cause peroxidase to be converted into inactive verdohaemoprotein called P-670 (Arnao et al. 1990).

JP, on the other hand, functions well over a broad range of H_2O_2 concentrations and demonstrated an average of 94.5% phenol removal from 1-9 mM H_2O_2. Above 9 mM, the efficiency starts to decrease due to enzyme inactivation. Figure 4.17 also shows that ratios of 6:1 and 1:1 mole H_2O_2 per mole of phenol are required by LP and JP respectively to achieve enhanced treatment of phenol. The value 1:1 ratio determined for JP is in keeping with the stoichiometry reported by other researcher for HRP (Wagner and Nicell 2001a; Nicell et al. 1992). Subsequent experimental embodiments of this work were conducted at 6 mM and 1 mM H_2O_2 for LP and JP respectively, at optimal operating pH of 7.

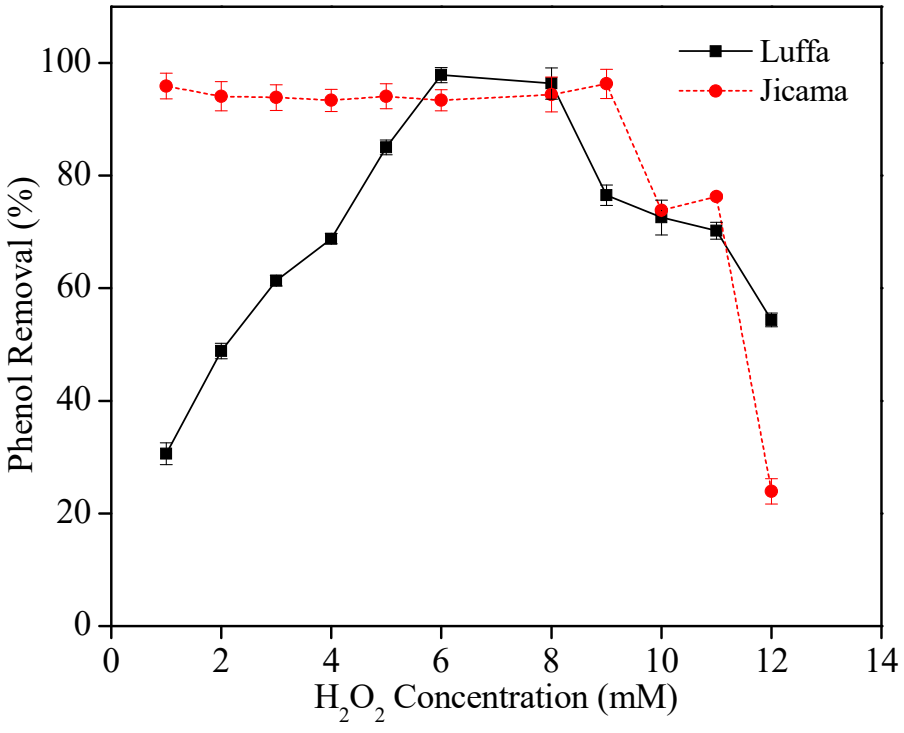

Figure 4.17: Effect of H_2O_2 concentration on the phenol removal efficiency of JP and LP. The range of H_2O_2 concentrations tested was 1 – 12 mM. Other experimental conditions: pH 7, 1.5 mL enzyme solutions, 25 ^oC and 24 h incubation.

4.3.3 Effect of enzyme loading on phenol degradation using free LP / JP

Enzyme concentration plays an important role in the removal of phenolic compounds not only in terms of removal efficiency but also on the process economics. Extracted LP and JP enzymes used in this work are crude with no concentration step hence variation in loading is achieved on volumetric basis. The volume of enzyme added to the reaction mixture was varied to adjust the total amount of enzyme molecules in the mixture. At 0.5, 1.0, 1.5, 3 and 4.5 mL of enzyme loadings, the enzymatic activities of LP in the reaction medium were 0.07, 0.14, 0.21, 0.42 and 0.63 U/mL respectively. For the same volumes of enzyme loading, the enzymatic activities of JP were 0.08, 0.16, 0.23, 0.47 and 0.70 U/mL respectively. The volume of buffer solution (pH 7) was also adjusted accordingly to ensure that the final volume of reaction mixture was maintained at 10 mL.

At 0.5 mL enzyme loading, LP demonstrated a low removal of 44% as shown in Figure 4.18. Its removal efficiency improved to 76% at 1.0 mL enzyme volume, and eventually achieving an optimal value of >95% at 1.5 mL. JP showed a relatively more effective phenol removal of 85% even at 0.5 mL enzyme loading, and demonstrated an increasing trend with increasing enzyme loading until 1.5 mL. Increasing enzyme loading introduces increasing amount of peroxidase molecules in the solution, and consequently increasing the number of active sites for phenol binding.

Further increase beyond 1.5 mL loading did not significantly increase the removal efficiency. The removal efficiency was mostly constant at 98% and 96% for LP and JP respectively. Under high enzyme loading, more H_2O_2 is required to initiate the catalytic conversion reaction. The potential depletion and/or the presence of insufficient H_2O_2 under increasing concentration of enzyme explains the stagnation in removal efficiency after 1.5 mL loading. The heme prosthetic group of the peroxidase reacts with H_2O_2 in the first step of the catalytic cycle, hence low H_2O_2 concentrations can affect enzyme activation. With increasing enzyme loading and H_2O_2 concentration, higher removal efficiencies can be obtained even for a more concentrated phenolic feedstock.

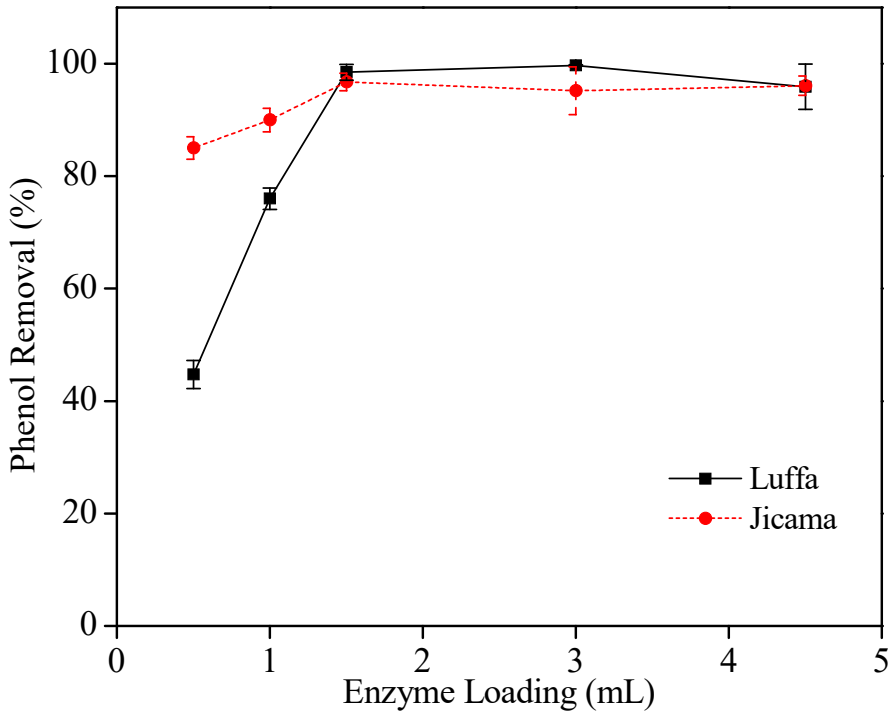

Figure 4.18: Effect of enzyme volume on the phenol removal efficiency of JP and LP. The range of enzyme loading tested is 0.5 – 4.5 mL. Other experimental conditions: pH 7, 6 and 1 mM H_2O_2 for LP and JP respectively, 25 ºC and 24 h incubation.

4.3.4 Effect of temperature on phenol degradation using free LP / JP

Using buffer pH 7, 1.5 mL enzyme solution, as well as 6 and 1 mM H_2O_2 for LP and JP respectively, the effect of temperature on phenol degradation was studied. As shown in Figure 4.19, both LP and JP demonstrated high phenol removal efficiencies of >95% when the peroxidase-catalyzed enzymatic reaction was carried out at 25 ºC and 30 ºC. The efficiency of LP decreased from 95% to 73% when the reaction temperature was increased from 30 to 40 ºC. From 40 to 50 ºC, the removal percentage remained constant at an average of 74%. The efficiency decreased to 44% when the temperature was further increased to 60 ºC and above. JP retained its catalytic conversion efficiency up to 40 ºC with a nearly constant removal efficiency of 95%. Above 40 ºC, the conversion efficiency of JP decreased drastically to 50%, about half of the optimal value. The efficiency continued to decrease with increasing temperature, reaching < 10% above 60 ºC.

In comparison, LP was slightly more sensitive to temperature change, with a narrower optimal operating range than JP. JP is more stable over a wider temperature range than

LP though its catalytic efficiency decreases significantly at elevated temperatures conditions above 40 ºC. The optimal operating ranges shown by LP and JP were consistent with the work published by other researchers. Commercial HRP and SBP achieved maximum phenol removal at temperatures ranging from 25 ºC and 40 ºC (Bódalo, Gómez, Gómez, Bastida, et al. 2006). Masuda and co-workers (Masuda et al. 2001) also reported that nearly a complete phenol removal was obtained over a wide range of temperatures (0-60 ºC) under excess peroxidase provision.

The decline in removal efficiencies shown by LP and JP with increasing temperature could be attributed to thermal denaturation. Protein denaturation occurs under elevated temperature conditions and leads to either loss of its active sites or molecular seclusion of active sites from substrate molecules due to structural deformation. The haem prosthetic group of peroxidases governs the thermal stability of peroxidases, but it is released under elevated temperatures to form apoenzyme. Having lower thermal stability, apoenzyme is more susceptible to thermal inactivation as compared to the native enzyme (McEldoon and Dordick 1996). Enzyme structure is distorted under elevated temperature conditions, thus limits its active sites to bind with substrate molecules. Therefore, the optimum operating temperature for both LP and JP was selected at 25 ºC, in order to preserve peroxidase activities and save operating cost. This optimum temperature (25 ºC) is beneficial to enzymatic treatment of phenol as no additional cooling or heating process is required.

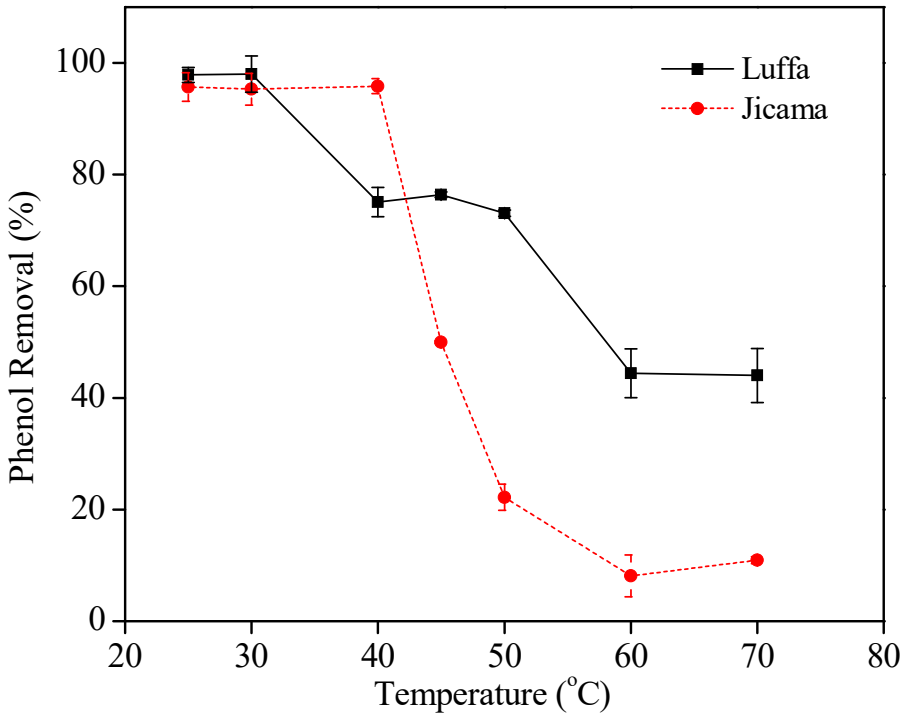

Figure 4.19: Effect of temperature on the phenol removal efficiency of JP and LP. The range of temperature tested was 25 – 70 °C. Other experimental conditions: pH 7, 6 and 1 mM H_2O_2 for LP and JP respectively, 1.5 mL enzyme solutions and 24 h incubation.

4.3.5 Effect of reaction time on phenol degradation using free LP / JP

Using the optimum conditions determined for pH, H_2O_2 concentration, enzyme loading and temperature, the kinetic behaviour of peroxidase-catalyzed phenol removal process was investigated over an extended period of 23 h. Figure 4.20 shows the profiles for LP and JP phenol degradation as a function of time.

LP removed approximately 32% of phenol within 15 min of reaction. The removal efficiency increased steadily over the next 45 min until it was almost doubled. The maximum phenol removal efficiency demonstrated by LP was about 96% after 16 h of reaction. JP showed a different kinetic profile from LP. The phenol removal efficiency of JP remained almost constant, averaging around 20% during the first 11 h of reaction. The efficiency increased to 55% after 12 h, eventually reaching 93% after 13 h of reaction. Further increase in the reaction time beyond this point only resulted in a 2% increment. This is potential due to saturation of available enzyme active sites, resulting

in insignificant differential changes in the concentration of enzyme-substrate complex accumulation, and/or depletion of substrate in the reaction medium.

Figure 4.20 also indicates that LP required a longer period of time before achieving maximum removal even though its initial phenol removal efficiency was higher than JP. The first order kinetic rate constants for LP and JP during the exponential phase of phenol removal were determined as 1.18 h^{-1} and 1.21 h^{-1}, respectively.

In comparison with other plant peroxidases, LP and JP required a much longer reaction time to achieve optimal phenol removal. This could potentially be due to difficulty in oxidizing LP and JP into active catalytic forms to attack phenolic species. The presence of impurities associated with LP and JP as crude enzyme extracts could interfere with H_2O_2 oxidation mechanism and inhibit catalytic activity. Wagner and Nicell (Wagner and Nicell 2002) reported a reaction time of 3 h for optimal phenol conversion by HRP. Another reported work by (Vasudevan and Li 1996) demonstrated 97% phenol removal within 10 min of reaction using highly purified HRP. A low-purity SBP with high enzymatic activity was reported to achieve a maximum phenol conversion of 95% within a period of 100 min (Wilberg et al. 2002).

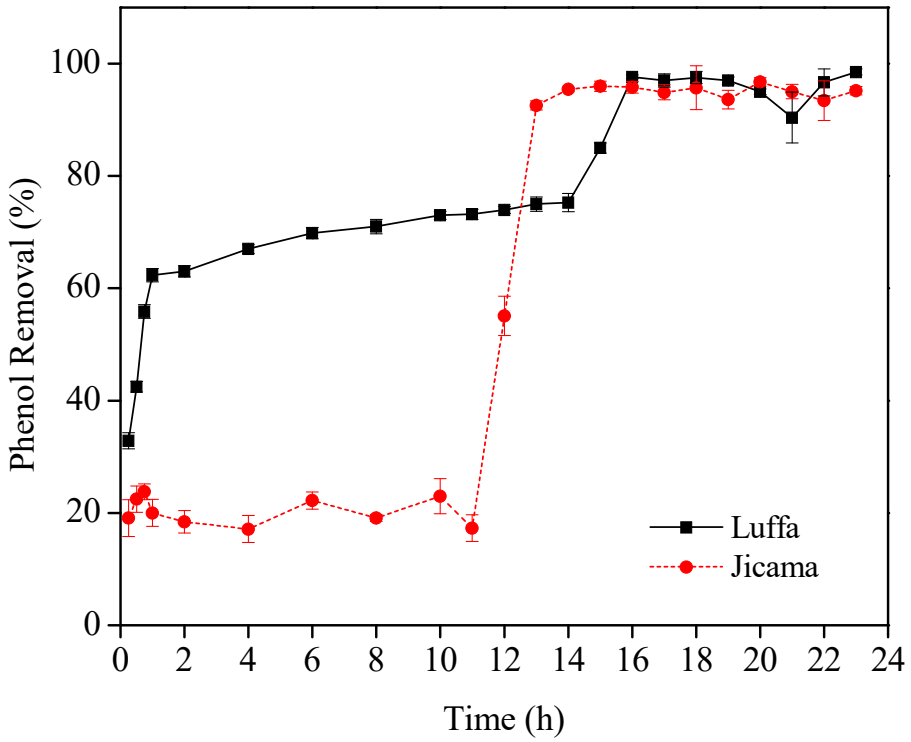

Figure 4.20: Effect of reaction time on the phenol removal efficiency of JP and LP. Other experimental conditions: pH 7, 6 and 1 mM H_2O_2 for LP and JP respectively, 1.5 mL enzyme solutions and 25 ºC.

4.3.6 Storage stability of crude LP / JP

The relationship between peroxidase storage stability and its removal efficiency was investigated by analyzing the enzyme activities of crude LP and JP solutions stored at 4 ºC and subjecting them to phenol removal tests for an extended period of 42 days. This test is necessary to determine the life span of crude LP and JP whilst they retain their phenol degradation capability. This type of stability analysis is limited in the literature. One of the few reports investigated the preservation of SBP activity during storage, and determined low temperatures prevent soybean seed hulls from inactivation, and loss of activity is observed with aged hulls (Wilberg et al. 2002).

As illustrated in Figure 4.21, LP was well preserved over the storage time as there was no marked fluctuation in its enzyme activity. The average enzyme activity was 1.29 U/mL throughout the first 7 days of storage. However, the phenol removal efficiency started decreasing from day 4 onwards, and was 72% after 1 week. The enzyme activity of JP was also well preserved over the same period of storage with an average of 1.35 U/mL. The phenol removal efficiency of JP, on the contrary, was not affected

by storage time and remained at its optimum value of 96%. When its stability was evaluated for an extended period of 42 days (Figure 4.22), JP retained its efficiency 5-fold longer in storage time even though its enzyme activity started decreasing gradually after 14 days. When the enzyme activity of JP dropped to about 40% of its initial value, a more significant decrease in phenol removal efficiency was observed (on day 42).

The findings presented here indicate that comparatively, JP demonstrated a more stable performance in treating phenol. LP is more susceptible to biological and physicochemical changes associated with prolong storage and hence freshly prepared LP has better efficacy.

Optimum operating conditions for batch treatment of aqueous phenol solution using free LP and JP are also summarized in Table 4.4.

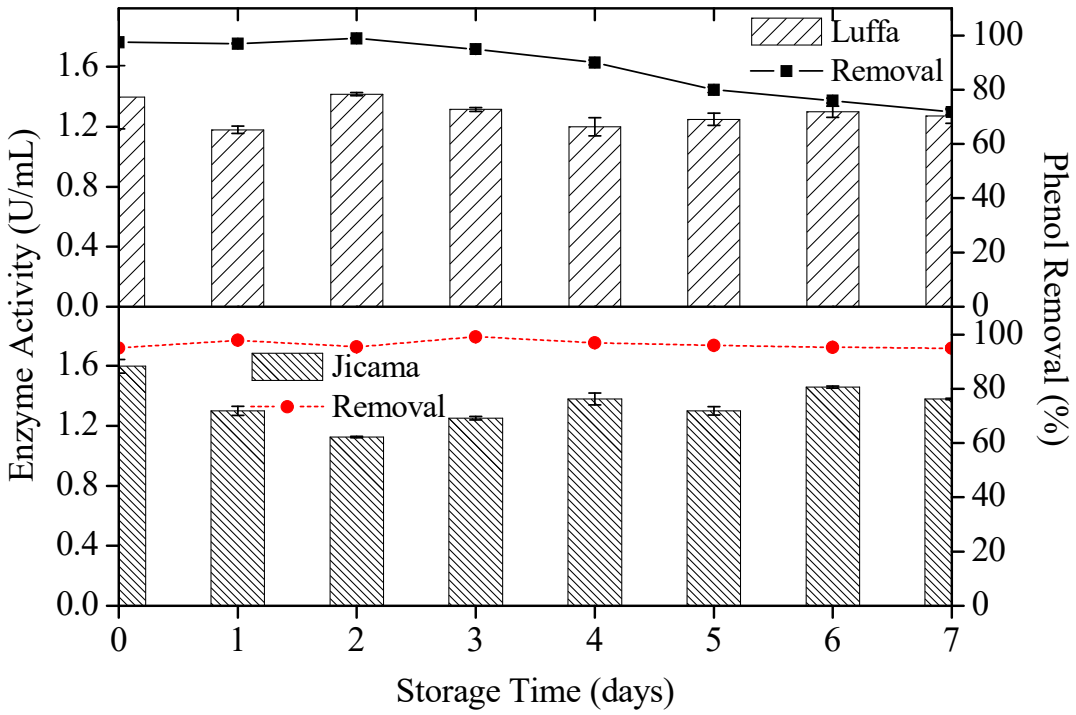

Figure 4.21: Relationship between storage stability and phenol removal efficiency by LP and JP respectively over 7 days.

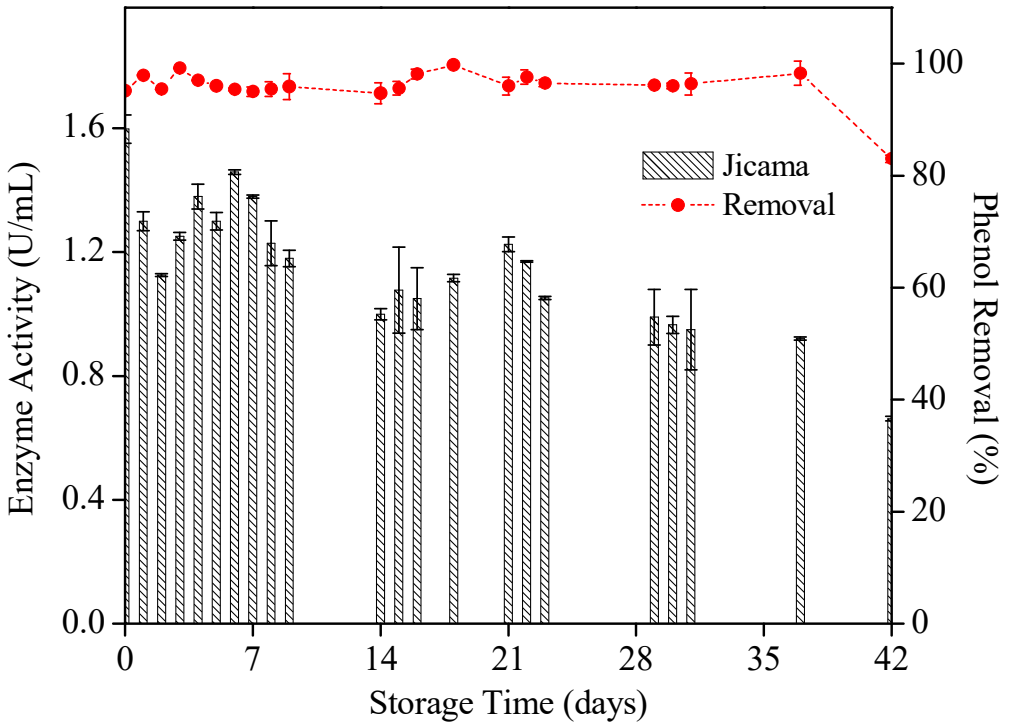

Figure 4.22: Storage stability and phenol removal efficiency of JP over 42 days.

Table 4.4: Optimum operating conditions for batch treatment of aqueous phenol solution using free LP and JP.

Experimental parameters	**LP**	**JP**
pH of solution	7	7
H_2O_2 concentration	6 mM	1 mM
Enzyme loading	0.21 U/mL	0.23 U/mL
Temperature	25 ºC	25 ºC
Reaction time	16 h	13 h
Phenol removal efficiency	96%	93%

4.4 OPTIMIZATION OF PHENOL REMOVAL PROCESS VIA EXPERIMENTAL DESIGN

Although both LP and JP were able to accomplish high phenol degradation, the results shown in the previous Section indicate that JP is more favourable than LP from the perspectives of lower H_2O_2 concentration requirement, wider optimal temperature range, shorter reaction time and better storage stability. Hence, the following step of this research was to statistically optimize the peroxidase-based phenol removal process

by using crude JP via experimental design. The process variables being studied were pH, H_2O_2 concentration, and enzyme loading, with phenol removal efficiency being the response. Temperature was excluded from the optimization study because 25 ºC has been shown to give maximum phenol removal efficiency for JP (Figure 4.19). Moreover, the operation of phenol degradation at 25 ºC ensures ease of process control thermally and is also beneficial from the perspective of cost savings.

4.4.1 Factorial design experiment

With three variables and three center points, the total number of experimental runs as determined by the statistical software was 11. The design matrix of the 11 experimental runs along with the response values of phenol removal efficiency is presented in Table 4.5.

Table 4.5: Experimental design matrix and results.

Run	Levels			Phenol removal process variables			Removal efficiency, Y (%)
				pH, x_1	H_2O_2 concentration, x_2 (mM)	Enzyme loading, x_3 (mL)	
1	-1	-1	-1	5	1	1.5	30.35
2	1	-1	-1	8	1	1.5	14.52
3	-1	1	-1	5	8	1.5	67.96
4	1	1	-1	8	8	1.5	34.56
5	-1	-1	1	5	1	4.5	19.96
6	1	-1	1	8	1	4.5	16.73
7	-1	1	1	5	8	4.5	65.78
8	1	1	1	8	8	4.5	48.51
9	0	0	0	6.5	4.5	3	90.17
10	0	0	0	6.5	4.5	3	90.05
11	0	0	0	6.5	4.5	3	94.96

Analysis of variance (ANOVA) performed on phenol removal efficiency indicated that the model was significant with a curvature. This is shown in Table 4.6 where the p-values for the model and curvature were 0.0017 and <0.0001 respectively. To further prove the presence of curvature, Figure 4.23(a-c) shows that the responses obtained at center points (filled oval dots) fall outside the linear line connecting the low and high levels of each process variable. This means that the characteristic equation of the enzymatic process cannot be represented by a linear function model, and therefore a higher degree polynomial model must be used.

Table 4.6: ANOVA analysis for phenol removal efficiency indicating the presence of a curvature.

Source	Sun of squares	Degree of freedom	Mean square	F value	p-value	
Model	2895.99	3	965.33	19.60	0.0017	Significant
x_1	607.78	1	607.78	12.34	0.0126	
x_2	2286.58	1	2286.58	46.43	0.0005	
x_3	1.62	1	1.62	0.033	0.8619	
Curvature	6463.29	1	6463.29	131.24	<0.0001	Significant
Residual	295.49	6	49.25			
Lack of Fit	279.36	4	69.84	8.66	0.1061	Not significant
Pure error	16.12	2	8.06			
Cor total	9654.76	10				

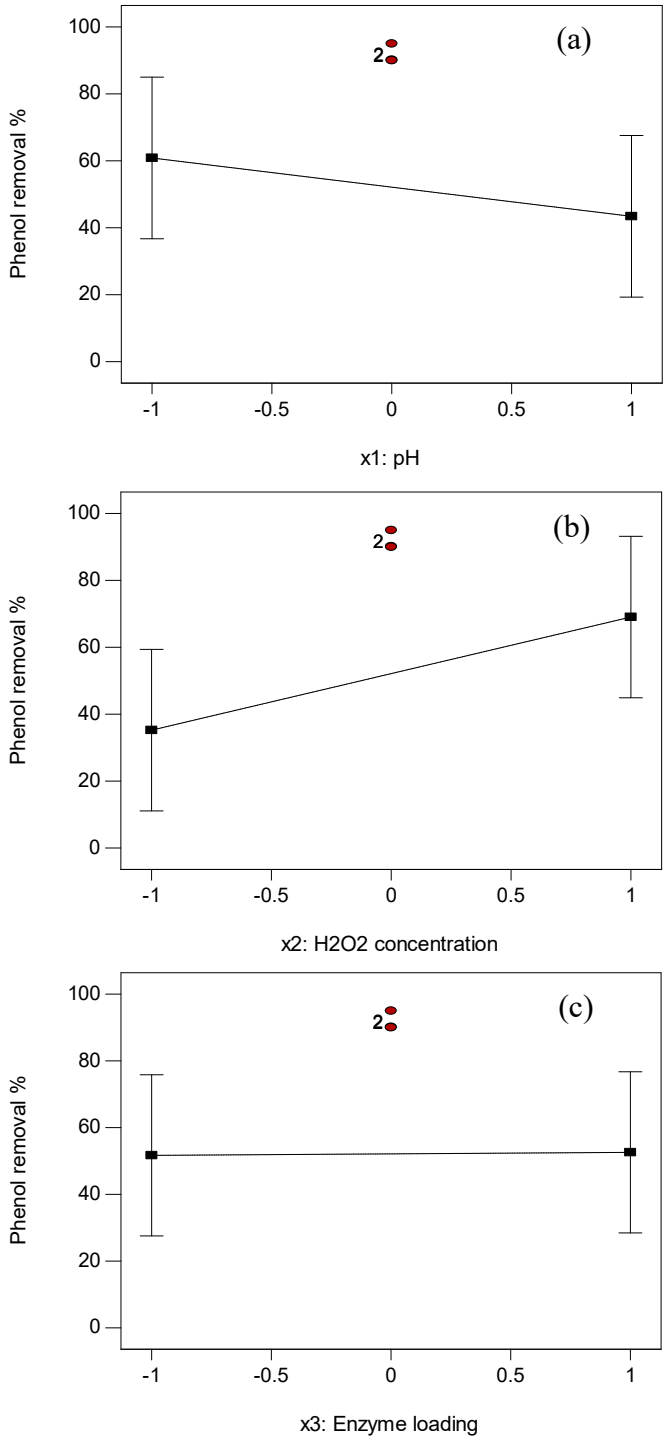

Figure 4.23: One factor plots for phenol removal efficiency; (a) effect of pH, (b) effect of H_2O_2 concentration, and (c) effect of enzyme loading.

4.4.2 Augmentation to central composite design

Since a significant curvature existed within the model, the previous design was augmented to central composite design (CCD) to improve the degree of agreement by fitting into a second order model. Six axial point runs were added to the original design with alpha (α) equals to 0.5. Table 4.7 shows the extended experimental runs 12-17 with the responses obtained.

Table 4.7: Extended experimental design matrix (augmented to CCD) and corresponding results.

Run	Levels			Phenol removal process variables			Removal efficiency, Y (%)
				pH, x_1	H_2O_2 concentration, x_2 (mM)	Enzyme loading, x_3 (mL)	
12	-0.5	0	0	5.75	4.5	3	94.37
13	0.5	0	0	7.25	4.5	3	94.12
14	0	-0.5	0	6.5	2.75	3	93.77
15	0	0.5	0	6.5	6.25	3	94.52
16	0	0	-0.5	6.5	4.5	2.25	95.26
17	0	0	0.5	6.5	4.5	3.75	93.34

The results obtained from the 17 runs were analyzed by ANOVA. Based on sequential model sum of squares, lack of fit tests, and model summary statistics, a quadratic model better described the characteristics of the phenol removal efficiency profile. A summary of the various models is presented in Table 4.8. The final empirical model in terms of coded factors for phenol removal efficiency is represented by Equation 4.1. The quality of the model developed was evaluated based on the correlation coefficient R^2 and standard deviation. The R^2 value of the model was 0.9817, indicating that 98.17% of the variations is in agreement with data generated from the independent variables within the range of study. The R^2 value was also in good agreement with the adjusted R^2 value (0.9542). The standard deviation of the model was 5.4, which is within the limit of 5% generally required for a process. The close-to-unity R^2 value and relatively small standard deviation value suggested that the model developed was sufficiently adequate in representing phenol degradation process using JP.

Table 4.8: Summary of various models for characterizing phenol degradation.

Source	Sequential p-value	Lack of fit p-value	Adjusted R-squared	Predicted R-squared	
Linear	0.2448	0.0116	0.1045	-0.3018	
2FI	0.9426	0.0085	-0.1460	-5.2120	
Quadratic	<0.0001	0.1740	0.9542	0.8738	Suggested
Cubic	0.1740		0.9875		Aliased

$$\text{Removal} = 95.24 - 8.22x_1 + 15.96x_2 + 0.31x_3 - 3.95x_1x_2 + 3.59x_1x_3 + 2.50x_2x_3 - 18.07x_1^2 - 18.49x_2^2 - 17.86x_3^2 \quad (4.1)$$

Figure 4.24 investigates the relationship between the predicted and experimental values of phenol removal efficiency. The two data sets show significant agreement, implying that the model was successful in predicting response variables based on process variables.

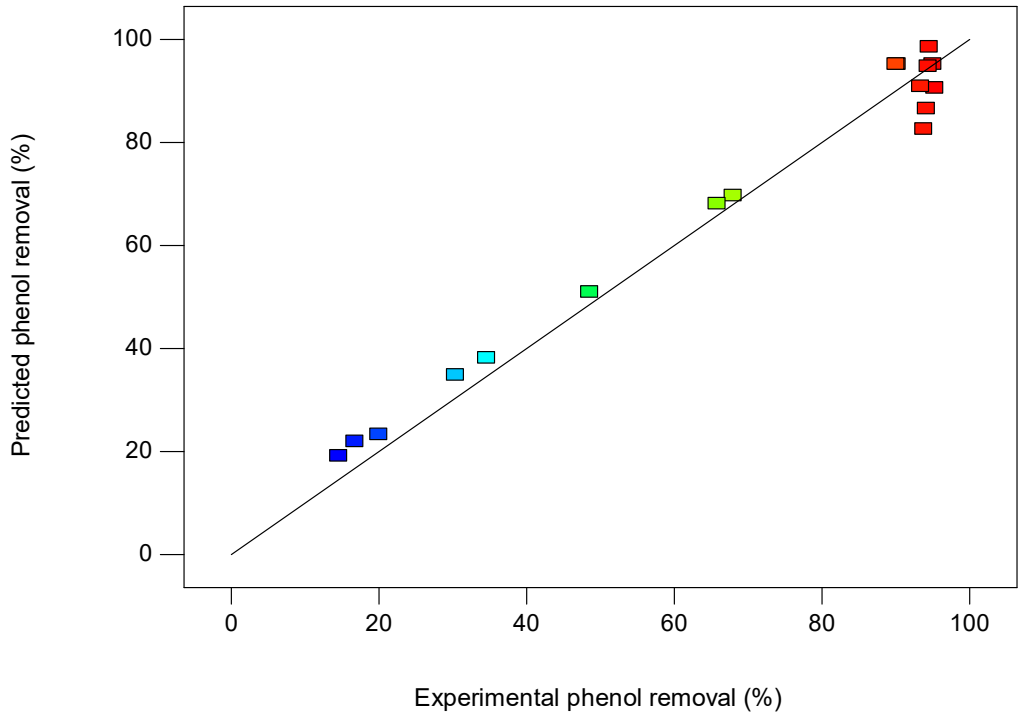

Figure 4.24: Relationship between predicted response from the model and experimental phenol removal data. Data shows significant agreement between the two variables.

Table 4.9 summarizes the ANOVA results for the model. The model had a significant p-value of 0.0002. Amongst all the factors, H_2O_2 concentration (x_2) showed the lowest p-value, indicating that it imposed the most significant effect on phenol removal. The effect of pH (x_1) on phenol removal was also significant, as demonstrated by its low p-value of 0.0045. However, enzyme loading (x_3) comparatively did not show a significant effect on phenol removal efficiency. All other model terms (x_1^2, x_2^2 and x_3^2) including interactions between different variables (x_1x_2, x_1x_3 and x_2x_3) were found to be insignificant and their effects on phenol degradation were negligible. The insignificant lack-of-fit indicated that the model fits well.

Table 4.9: ANOVA analysis of response surface quadratic model for phenol removal efficiency.

Source	Sun of squares	Degree of freedom	Mean square	F value	p-value	
Model	9480.06	9	1053.34	35.73	0.0002	Significant
x_1	574.09	1	574.09	19.47	0.0045	
x_2	2164.04	1	2164.04	73.40	0.0001	
x_3	0.82	1	0.82	0.028	0.8730	
x_1x_2	124.87	1	124.87	4.24	0.0853	
x_1x_3	103.12	1	103.12	3.50	0.1107	
x_2x_3	49.81	1	49.81	1.69	0.2414	
x_1^2	60.68	1	60.68	2.06	0.2014	
x_2^2	63.52	1	63.52	2.15	0.1925	
x_3^2	59.23	1	59.23	2.01	0.2061	
Residual	176.90	6	29.48			
Lack of Fit	160.78	4	40.19	4.99	0.1740	Not significant
Pure error	16.12	2	8.06			
Cor total	16534.46	16				

A three-dimensional surface plot was constructed to illustrate the effects of pH and H_2O_2 concentration on phenol removal by JP (Figure 4.25). Enzyme loading was kept constant. Phenol removal efficiency was low under acidic and basic conditions. Higher removal efficiencies were observed at pH values close to neutral. The reduced phenol removal efficiency under acidic and/or basic conditions was attributed to significant variations in the enzyme molecular structure. Enzymes are generally known to be highly pH dependent as they are only functional when certain ionizable side chains and active groups are in specific molecular forms. As a result of protonation and hydroxylation effects, the enzyme molecules undergo structural modifications,

potentially obscuring relevant active sites before denaturation and permanent loss of functionality. Wright and Nicell (1999) reported a nearly complete phenol removal with SBP over a pH range of 5-9, with the maximum at pH 6 under high enzyme dosage. Turnip peroxidase achieved 85% of phenolic compounds over a broad range of pH 4-8, with the maximum removal within pH 5-7 (Duarte-Vázquez et al. 2003). The optimum operating pH range achieved in the present work by JP is in keeping with the aforementioned peroxidases. JP however demonstrated a tighter pH range, suggesting that JP is more pH sensitive than other peroxidases.

Phenol removal efficiency increased with increasing H_2O_2 concentration before plateauing over an optimum range and eventually decreasing beyond the optimum range, as shown by Figure 4.25. Functioning as an essential component in peroxidase-catalyzed reactions, H_2O_2 oxidizes the peroxidase enzyme molecules (E) into active forms which carry out phenolic oxidation reactions. In the absence of H_2O_2, activated peroxidase molecular forms are not generated to polymerize phenolic compounds enzymatically. At low concentrations of H_2O_2, a reduced phenol removal efficiency is observed due to low concentrations of activated peroxidase required to drive the enzymatic process. On the other hand, extremely high concentration of H_2O_2 resulted in peroxidase inactivation. The effect of H_2O_2 is observed in the 3D surface plot where phenol removal efficiency decreased below the optimum range under high and low concentrations of H_2O_2. High concentrations of H_2O_2 inhibit peroxidase catalytic activity by irreversibly oxidizing the ferriheme group of the enzyme. The ferriheme group is vital for peroxidase catalysis (Duarte-Vázquez et al. 2003). Reaction with excess H_2O_2 can also convert the peroxidase into inactive verdohaemoprotein called P-670 (Arnao et al. 1990).

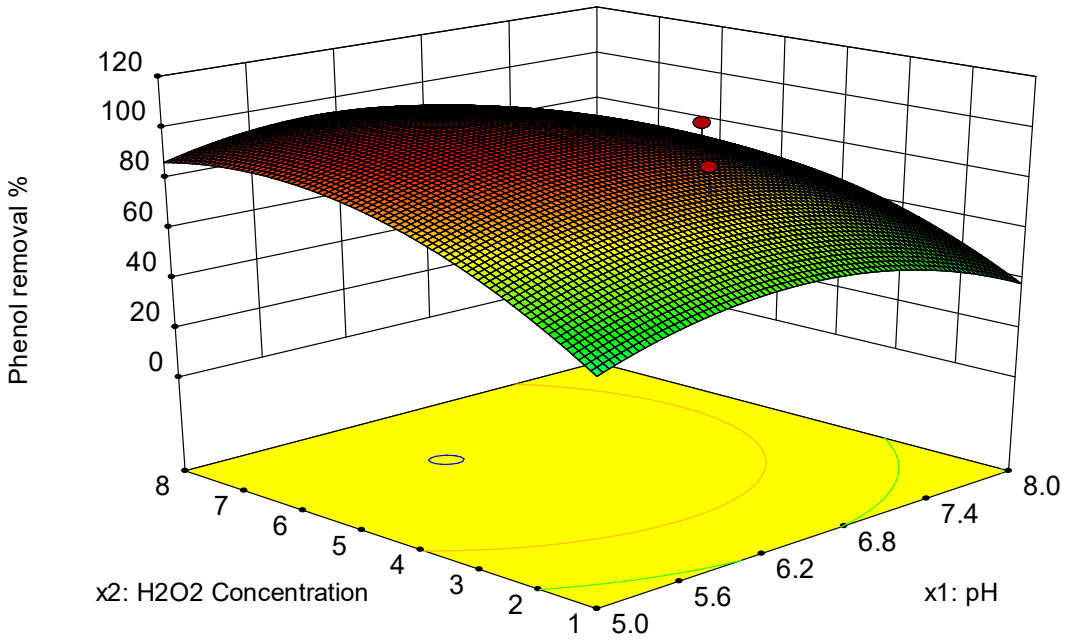

Figure 4.25: 3D surface plot of phenol removal by JP (enzyme loading, x_3=3 mL). The data demonstrates the effect of H_2O_2 concentration and pH on phenol removal.

4.4.3 Process optimization and model validation

The empirical model developed statistically was validated at the experimental conditions that yielded a phenol removal efficiency of > 95%. An overlay plot, as shown in Figure 4.26 was developed to determine the operating conditions required to obtain targeted phenol removal efficiency. In comparison to numerical optimization where definite conditions of process variables are chosen for optimal response, overlay plot enhances the flexibility and robustness of a specific process as operating conditions are varied within the optimum region. In Figure 4.26, the yellow region indicates pH and H_2O_2 concentration range where 95% phenol removal efficiency by JP can be achieved. This optimum region corresponds to an enzyme loading of 3 mL. The simulated optimum conditions for > 95% phenol removal efficiency were pH ranging from 5.3 to 7 and H_2O_2 concentrations ranging from 4.3 to 7.9 mM. Several points within the region were selected for validation. The experimental conditions as well as predicted and actual values of phenol removal efficiencies were summarized in Table 4.10. The predicted values were calculated according to the model Equation 4.1. It was demonstrated that the experimental values of removal efficiency were in good agreement with the predicted values from the model. The errors between the

predicted and experimental values were considerably small, ranging from 0.04% to 3%.

The performance of JP for phenol biodegradation is quite promising, showing a treatment efficiency as high as 95% at optimum operating conditions. This enzymatic process is considered economically feasible because the peroxidase used was obtained from agricultural waste via a simple extraction method. Though not subjected to any purification, the crude enzyme extracts demonstrated high phenol removal efficiencies. In addition, the enzymatic treatment was performed at 25 °C, thus avoiding additional process cost due to cooling and heating requirements.

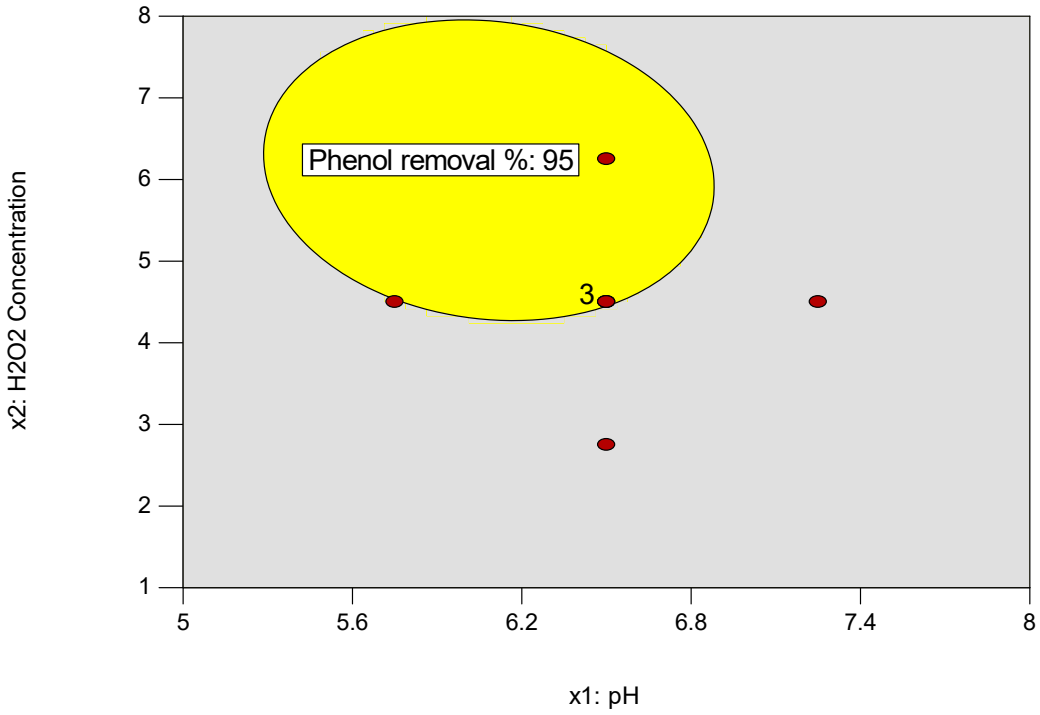

Figure 4.26: Overlay plot of phenol removal by JP for efficiency > 95% (enzyme loading, x_3=3 mL).

Table 4.10: Model validation at optimized conditions of phenol removal efficiency.

pH, x_1	H_2O_2 concentration, x_2 (mM)	Phenol removal efficiency (%)	
		Predicted	Experimental
5.3	6.1	95.13	94.26
6	4.3	94.92	94.88
6	6.1	100	96.79
6	7.8	95.82	94.72
7	5.8	93.38	94.98

4.5 SYNTHESIS OF SODIUM CELLULOSE SULPHATE (NACS)

NaCS is prepared from cellulose sulphation reaction between cotton linter and cold concentrated H_2SO_4 in the presence of cold absolute ethanol on ice. The temperature is strictly controlled at 0±1 ºC for 1 h by immersing the beaker containing the reaction mixture in icy water full of ice cubes. In this study, NaCS was produced in batch mode with starting materials of 5 g cotton linter, 151 mL cold H_2SO_4 and 100 mL cold absolute ethanol. Since the reaction of ethanol and H_2SO_4 is an exothermic process, the reaction solution is cooled down on ice before the addition of cotton linter. Figure 4.27 illustrates the steps in the synthesis of NaCS. After cellulose sulphation, it was noticed that both cotton linter and reaction solution turned brown in colour. Vigorous mixing of washed cotton linter in distilled water resulted in viscous mixture as shown in Figure 4.27(f). The supernatant collected after centrifugation of the mixture was a yellowish solution with slight viscosity. This yellowish supernatant has high acidity with pH ~1.45. After pH adjustment to 9.0-9.3 using 2M NaOH, cold absolute ethanol was added to the supernatant to form sedimentation as in Figure 4.27(i), and the sediment obtained was shown in Figure 4.27(j). Dried NaCS (Figure 4.27(k)) was obtained after freeze-drying the sediment. Synthesis of NaCS via cellulose sulphation reaction is as shown in Figure 4.28.

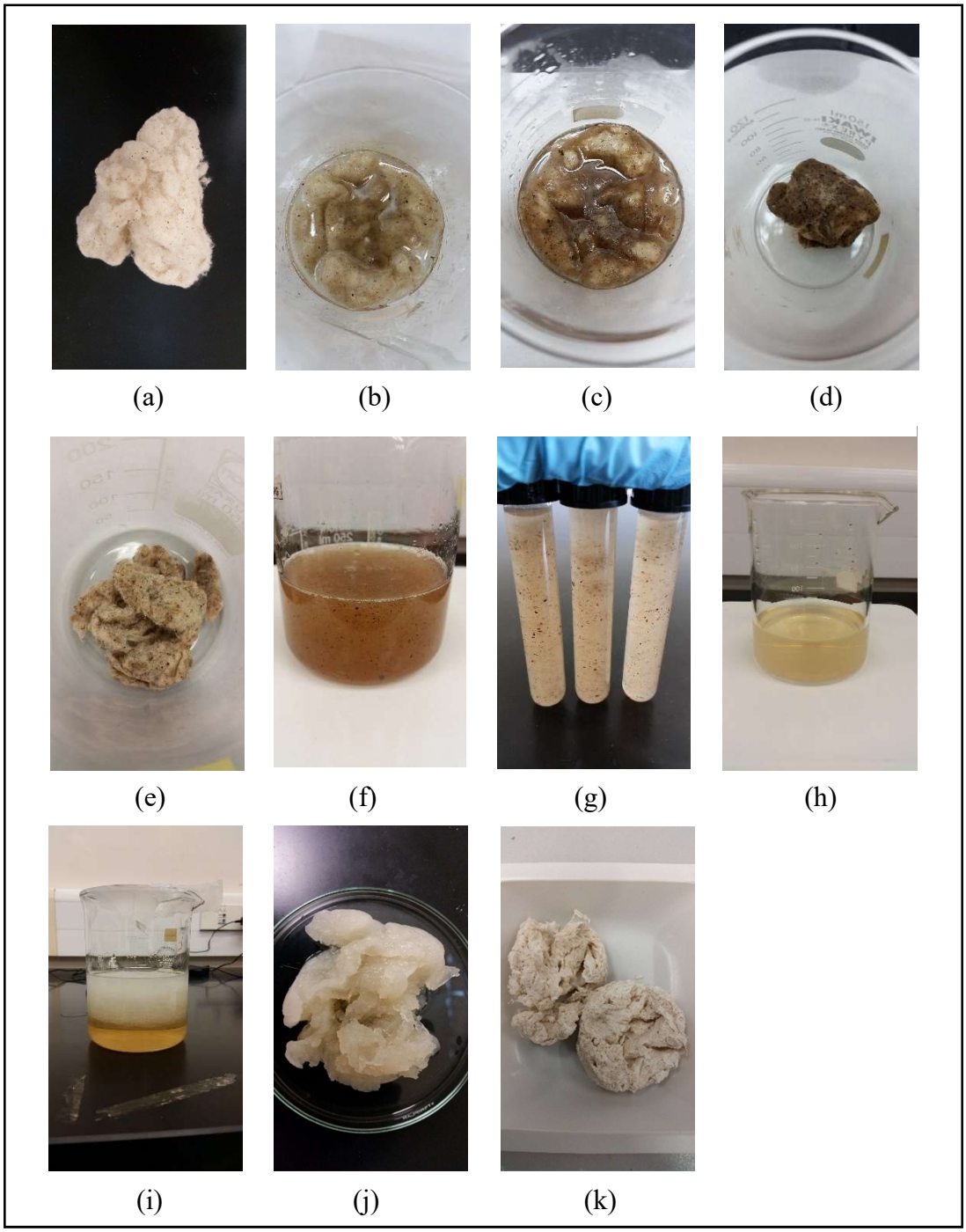

Figure 4.27: Various steps in the synthesis of NaCS; (a) cotton linter, (b) reaction of cotton linter in the mixture of H_2SO_4 and ethanol, (c) cotton linter in reaction solution after 1 h reaction, (d) squeeze-dried cotton linter, (e) cotton linter after several washes with cold absolute ethanol, (f) suspension of residual cotton linter in distilled water after vigorous mixing, (g) residual cotton linter suspension for centrifugation, (h) supernatant after centrifugation, (i) formation of sedimentation after the addition of cold absolute ethanol, (j) NaCS sediment, and (k) dried NaCS after freeze-drying.

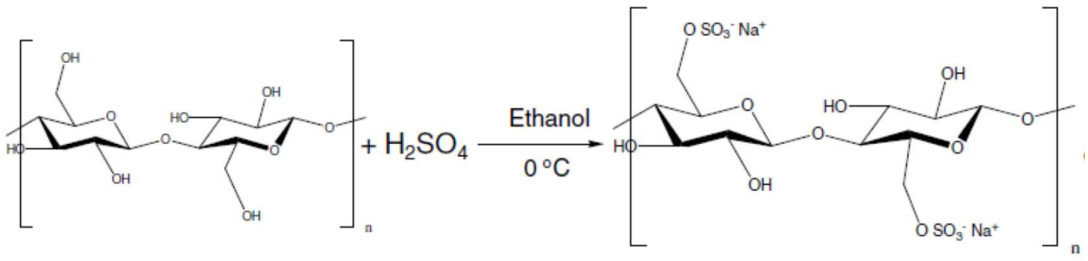

Figure 4.28: Synthesis of NaCS via cellulose sulphation reaction (Zeng, Danquah, Potumarthi, et al. 2013).

4.6 PREPARATION OF NACS-PDMDAAC POLYMERIC CAPSULES

NaCS-PDMDAAC polymeric capsules were formed by dropping NaCS solution into PDMDAAC solution under gentle stirring. When NaCS droplets were introduced into PDMDAAC solution, capsules consisting of a liquid core surrounded by a semipermeable capsule wall were formed immediately. After the formation of the outer primary layer, the PDMDAAC in solution and the NaCS in the capsule slowly diffused towards the capsule membrane and react to form the porous layer at the inner surface (Zeng, Danquah, Potumarthi, et al. 2013). Cellulose sulphate ionized from NaCS crosslinks with diallyldimethyl ammonium group via active interactions between the oppositely charged units, but not through covalent linkage with the sulpho group of the cellulose sulphate. Figure 4.29 depicts the reaction between NaCS and PDMDAAC.

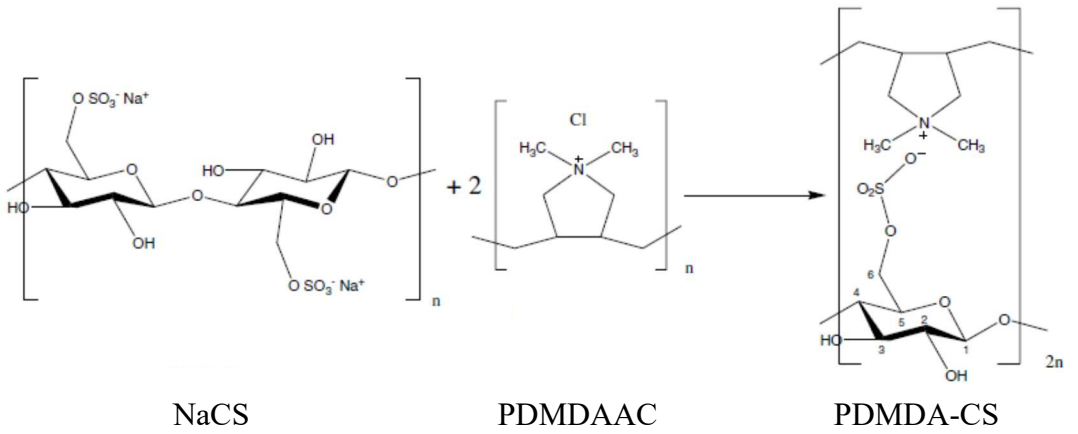

Figure 4.29: Reaction between NaCS and PDMDAAC (Zeng, Danquah, Potumarthi, et al. 2013).

In order to produce NaCS-PDMDAAC polymeric capsules with optimum characteristics, the microcapsules were prepared in varying concentrations of NaCS (2, 2.5 and 3% w/v) and PDMDAAC (4, 6 and 8% w/v). The degree of sphericity, shrinking time and mechanical strength of the microcapsules formed at various concentrations of polyions are presented in Table 4.11.

Table 4.11: Influence of polyanion and polycation concentrations on capsule properties.

	Concentration of PDMDAAC (w/v) = 4% Concentration of NaCS (w/v)		
	2%	**2.5%**	**3%**
Sphericity	Poor	Good, uniform	Good, uniform
Shrinking time (min)	15	13	14
Strength (N)	0.20±0.03	0.21±0.03	0.05±0.01
	Concentration of PDMDAAC (w/v) = 6% Concentration of NaCS (w/v)		
	2%	**2.5%**	**3%**
Sphericity	Good, uniform	Good, uniform	Good, uniform
Shrinking time (min)	10	10	15.5
Strength (N)	1.12±0.35	1.10±0.13	1.60±0.06
	Concentration of PDMDAAC (w/v) = 8% Concentration of NaCS (w/v)		
	2%	**2.5%**	**3%**
Sphericity	Poor	Poor	Poor
Shrinking time (min)	7	8	14.5
Strength (N)	2.01±0.43	2.60±0.06	3.43±0.37

At 2% NaCS and 4% PDMDAAC, microcapsules with poor sphericity were formed. This was because the PDMDAAC solution was dilute and could not form proper spherical capsules when in contact with NaCS droplets even after gentle stirring. At PDMDAAC concentrations of 6 and 8%, the microcapsules formed were generally spherical and uniform. The boundary of the capsules also looked solid. NaCS solution prepared at 2.5% concentration had higher viscosity than that prepared at 2%. Using 2.5% NaCS solution, the microcapsules formed were spherical, uniform and solid at all three different concentrations of PDMDAAC solutions. However, when the concentration of NaCS was further increased to 3%, the microcapsules formed had poor sphericity. It was noticed that the viscosity of the 3% NaCS solution was much higher than those obtained at 2 and 2.5%, resulting in difficulty in the formation of proper NaCS droplets. Drag tail tended to happen when viscous NaCS solution was

dropped into PDMDAAC solution, causing irregular shapes of the capsules formed. Capsules formed at various concentrations of NaCS and PDMDAAC are shown in Figure 4.30.

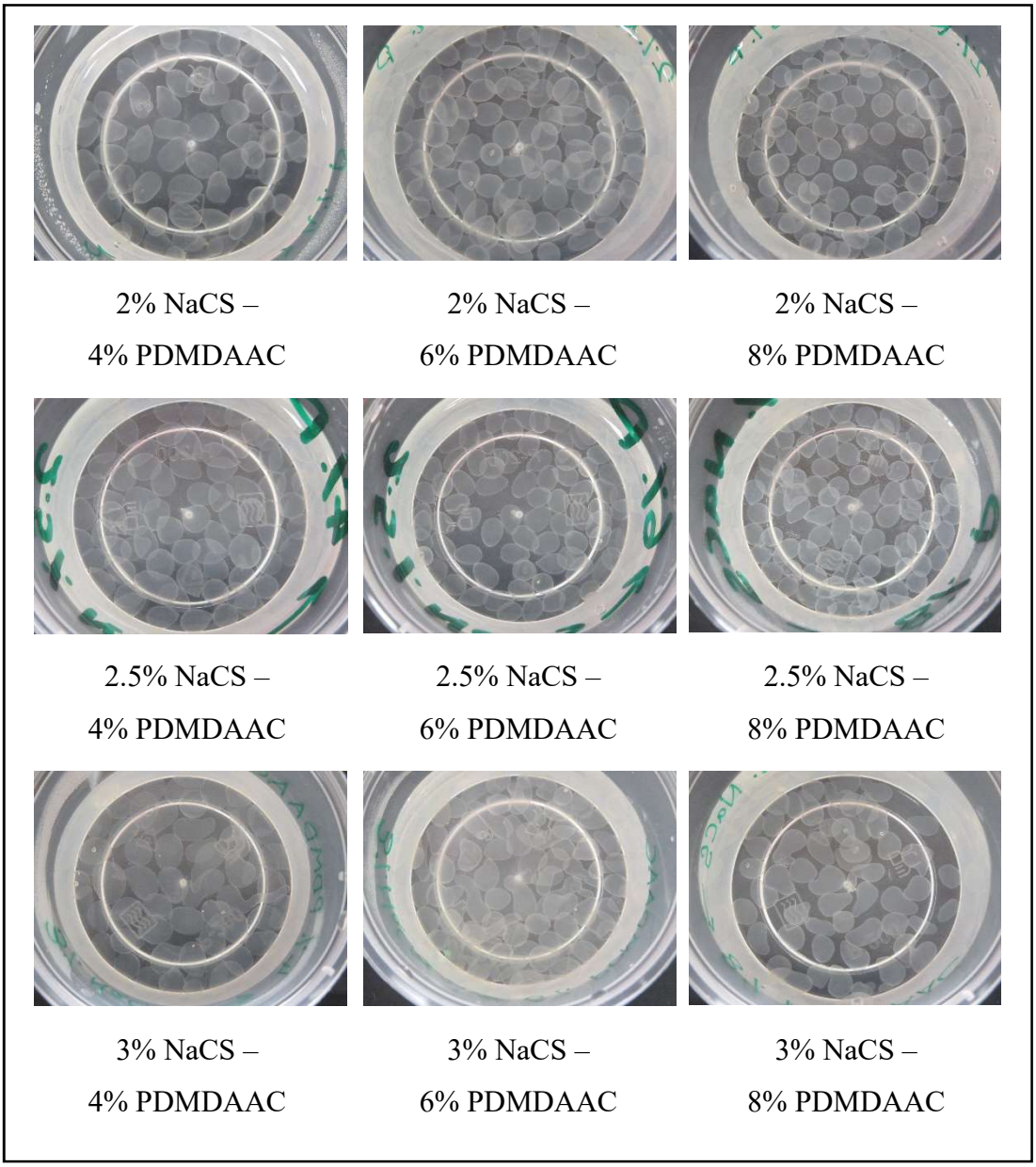

Figure 4.30: Images of capsules formed at various concentrations of NaCS and PDMDAAC.

It can also be noticed from Table 4.9 that the concentration of PDMDAAC had an impact on the shrinking time of the capsules. For 2 and 2.5% NaCS, the shrinking time was shortened when PDMDAAC concentration increased. Shrinkage of capsules is a result of osmotic stress exerted by high concentration of PDMDAAC (Chen et al. 2005). The osmotic stress is caused by the difference in concentrations between the

inner and outer sides of the capsules. For a fixed concentration of NaCS, the higher the concentration of PDMDAAC solution, the greater the concentration gradient between the two sides of the capsule membrane. Greater concentration gradient results in greater osmotic stress causing greater driving force for the diffusion of water molecules out of the liquid core of the capsules. Hence, microcapsules formed in high concentration of PDMDAAC solution shrunk faster than those in lower concentrations. As for 3% NaCS, the influence of PDMDAAC concentration on the microcapsules shrinkage time is not profound. The increment of PDMDAAC concentration did not result in significant changes in the shrinkage time. The reason could be due to the higher concentration of NaCS in the center of the capsules which form more ions. Strong bonding such as hydrogen and ionic bonds between the ions and water molecules could have restricted the diffusion of water molecules out of the capsules. Capsules shrinkage were only observed 14 – 15 min after capsule formation. Apart from PDMDAAC, capsules shrinking time was also affected by the concentration of NaCS. Except for 4% PDMDAAC which could be low to show any significant effect, shrinking time of capsules increased with increase in NaCS concentrations for 6 and 8% PDMDAAC. With the increase in NaCS concentration, the osmotic stress exerted by PDMDAAC onto the microcapsules became less because the concentration gradient between the inner and outer sides of the capsules had decreased. The effects of polyions on the shrinking time of capsules were in keeping with those reported by Chen et al. (2005).

The mechanical strength of the capsules prepared at various concentrations of NaCS and PDMDAAC is shown in Figure 4.31. It can be seen that mechanical strength increased when the PDMDAAC concentration was increased. Not only that, increase in NaCS concentration also resulted in higher mechanical strength of the capsules. This observation is in agreement with the findings demonstrated by Chen et al. (2005).

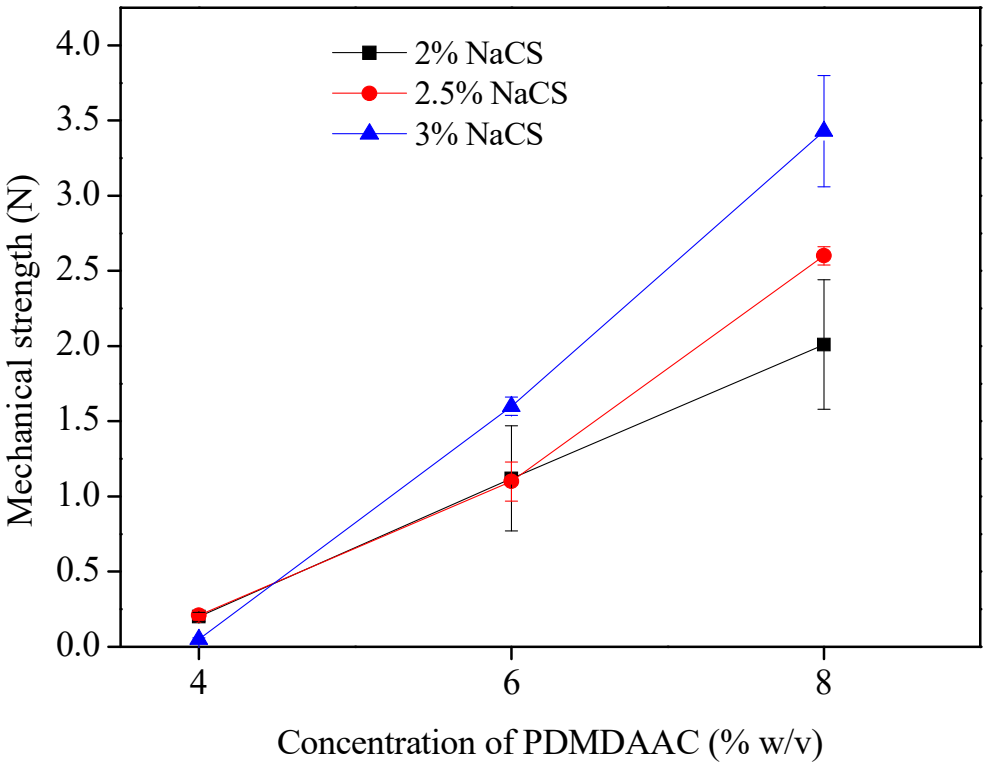

Figure 4.31: Mechanical strength of capsules prepared at various concentrations of NaCS and PDMDAAC.

From the results tabulated in Table 4.9, it is clear that the properties of NaCS-PDMDAAC capsules are influenced by the varying concentrations of polyanion and polycation, hence can be engineered to meet the requirement of various processes accordingly. From the concentration range of PDMDAAC being examined in this study, PDMDAAC concentration at 8% is not appropriate because the capsules formed have poor degree of sphericity, whilst 4% PDMDAAC is also avoided because the mechanical strength of the capsules formed is low. At 6% PDMDAAC, the capsules formed at different NaCS concentrations demonstrated good and uniform sphericity, and the mechanical strength was in the range of 1.1 – 1.6 N. In view that NaCS is synthesized through cellulose sulphation reaction, it is more economical to prepare capsules using 2% NaCS since the properties established are acceptable. NaCS-PDMDAAC capsules for immobilization of *Chlorella* sp. (Zeng, Danquah, Halim, et al. 2013) and *D. discoideum* (Zheng et al. 2015) were also prepared using 2% NaCS and 6% PDMDAAC. On the other hand, Chen et al. (2005) reported that the optimum conditions for preparing capsules were 35-40 g/L NaCS and 60 g/L PDMDAAC (equivalent to 3.5-4% and 6% for NaCS and PDMDAAC respectively) in the presence

of 6-8 g/L carboxymethyl cellulose (CMC). From this research work, it was found that capsules made from 2-3% NaCS and 6% PDMDAAC exhibited good capsule properties, with uniform sphericity, 10-15.5 min shrinking time and 1.12-1.60N strength.

After determining the optimum concentrations of polyions for the synthesis of NaCS-PDMDAAC capsules, subsequent test was to investigate the effect of reaction temperature on capsule properties. Capsules formation was carried out at 10, 25 and 35 ^{o}C by cooling or heating both NaCS and PDMDAAC solutions to the respective temperatures. Temperature did not significantly influence the performance of capsules in terms of degree of sphericity and mechanical strength. However, higher temperature resulted in earlier shrinking time. Since sufficient reaction time is essential for proper formation of capsule membrane (Chen et al. 2005), therefore capsules prepared at 35 ^{o}C is unfavourable because the capsule shrinking time is early. For ease of capsule preparation without any temperature control, optimal temperature for the synthesis of capsule in this study is determined as 25 ^{o}C.

Table 4.12: Influence of reaction temperature on capsule properties.

	Temperature (^{o}C)		
	10	**25**	**35**
Sphericity	Good, uniform	Good, uniform	Good, uniform
Shrinking time (min)	13	10	6.5
Strength (N)	1.59±0.05	1.40±0.03	1.61±0.03

4.7 ENCAPSULATION OF JP IN NACS-PDMDAAC CAPSULES

For encapsulation of JP within NaCS-PDMDAAC polymeric capsules, 2% NaCS was dissolved in crude JP solution. Addition of NaCS to JP extract also resulted in a slight viscous NaCS-JP solution, a similar observation as to dissolution of NaCS in distilled water. Uniform spherical capsules with light brown colour were produced when NaCS-JP droplets were added to 6% PDMDAAC solution. The brownish colour was originated from the crude JP extracts. Figure 4.32 shows the image of the capsular biopolymeric system immobilized with JP. About 15 capsules were generated from 1 mL of NaCS-JP solution, with the capsules having an average size of 5.05 mm±0.16 mm measured using Mitutoyo Absolute Digimatic Caliper. The thickness of the membrane from capsule cross-section was ~31 μm using microscope (Figure 4.33).

Encapsulation efficiency of JP within NaCS-PDMDAAC polymeric capsules was determined to be 87.4%. This result was in keeping with reported encapsulation efficiencies using other encapsulation matrixes such as calcium alginate in the range of 70-95% (Alemzadeh and Nejati 2009) and phospholipid-templated titania at 70.5% (Jiang et al. 2014).

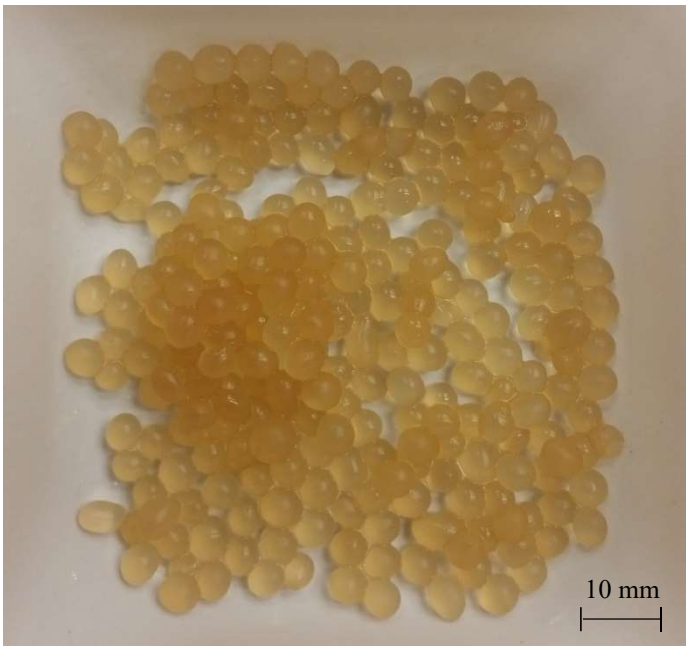

Figure 4.32: Image of NaCS-PDMDAAC capsules with encapsulated JP.

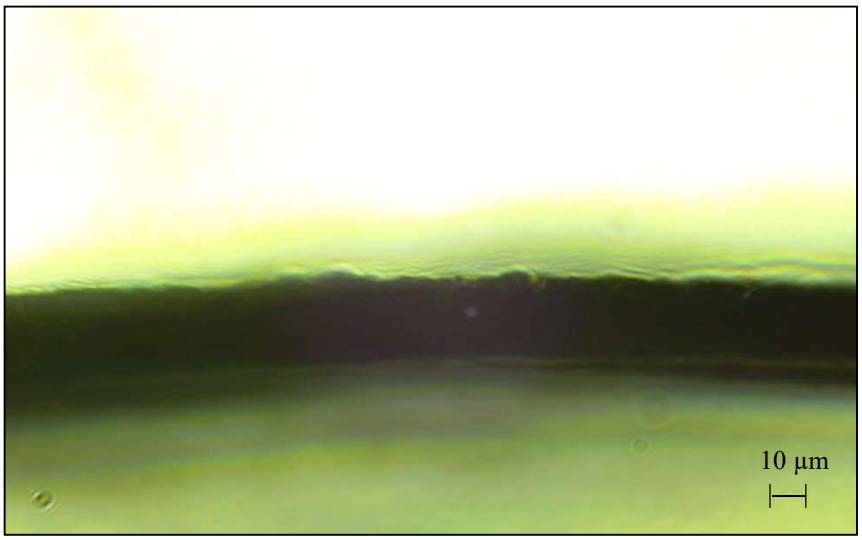

Figure 4.33: Cross-section of capsule membrane under microscope.

4.7.1 Morphology analysis of JP-immobilized capsules

Figure 4.34 shows the capsule outer and inner surface morphologies of JP-immobilized capsules using field emission scanning electron microscopy. The inner surface of the capsule is much rougher, indicating the reactive surface distribution from the interaction between NaCS and PDMDAAC. After forming an outer layer of capsule when NaCS droplets (or NaCS-JP solution) interacts with PDMDAAC solution, the PDMDAAC in solution and the NaCS in the capsule diffuse slowly towards the capsule membrane and react to form the porous layer at the inner surface. This porous layer causes the roughness at the inner surface of the capsule. The porous layer could possibly act as the polymeric support matrix for the immobilized JP molecules within the capsules (Dautzenberg et al. 1996). A schematic diagram of NaCS-PDMDAAC immobilized JP capsules is illustrated in Figure 4.35.

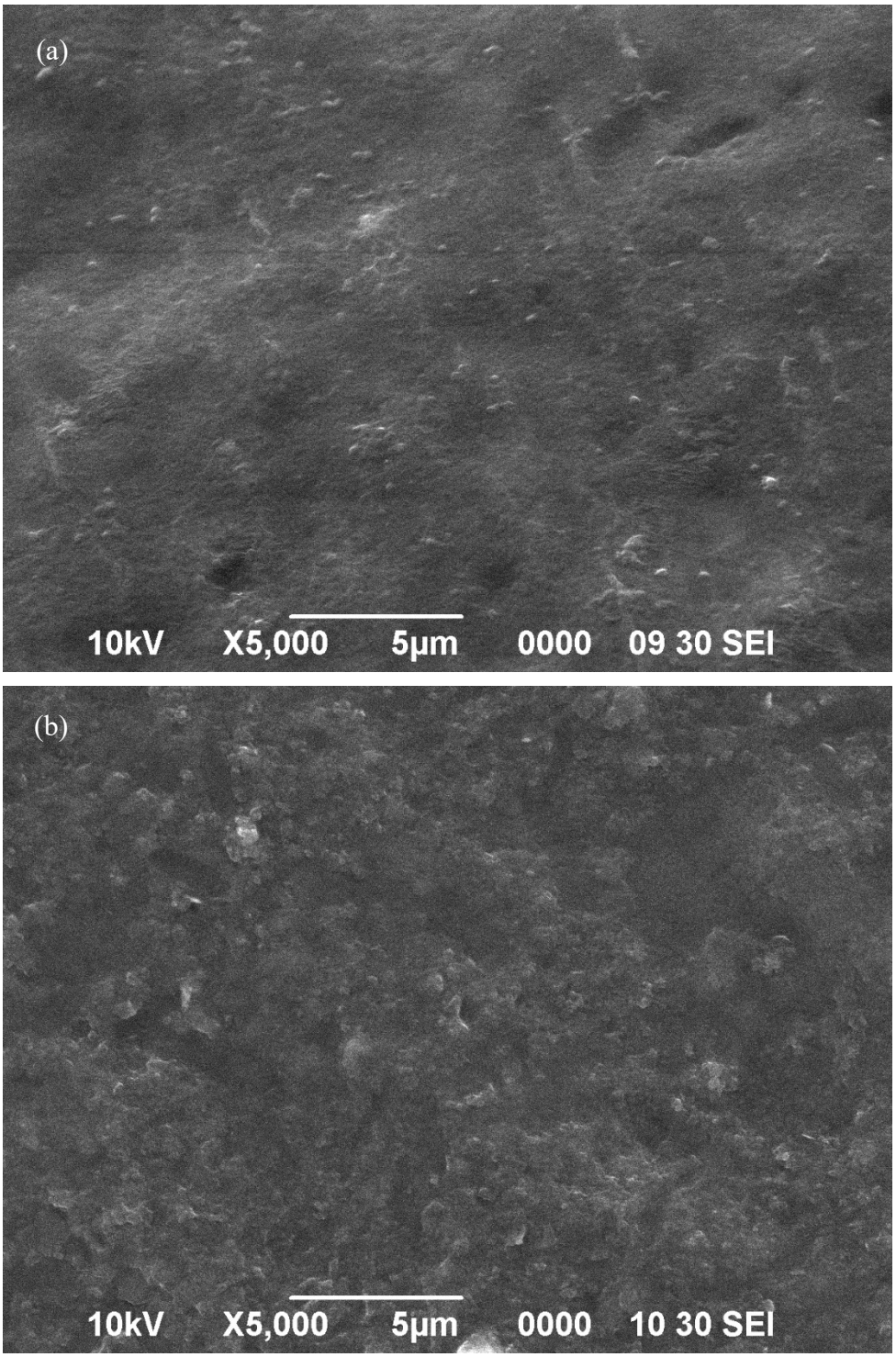

Figure 4.34: Field emission SEM images of NaCS-PDMDAAC polymeric capsules; (a) outer surface, (b) inner surface.

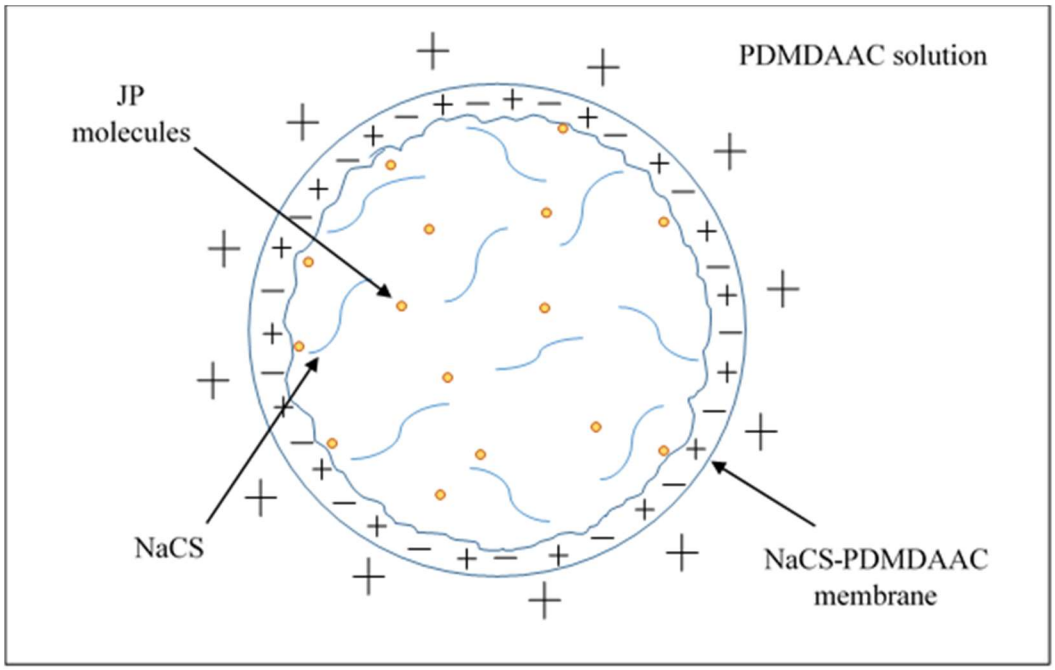

Figure 4.35: Schematic diagram of NaCS-PDMDAAC immobilized JP capsule.

4.7.2 FTIR analysis

FTIR analysis was used to investigate the structural characteristics, chemical composition and functional groups present in the synthesized NaCS and NaCS-PDMDAAC polymeric capsules. The IR spectra of the capsule as well as the native cotton linter (cellulose) and PDMDAAC are shown in Figure 4.36. The spectra of cotton linter (cellulose) and PDMDAAC are in keeping with previously reported studies (Nazi et al. 2012; Zeng, Danquah, Potumarthi, et al. 2013). Cellulose and NaCS showed similar vibration bands at ~3400 cm^{-1} and ~2900 cm^{-1}, corresponding to H-bonded O–H stretching and C–H stretching, respectively. This shows the presence of alcohols and alkanes respectively. The structure of cellulose also demonstrated a peak at 1633 cm^{-1} which attributes to the absorbed water by fibers (fibers–OH) (Morán et al. 2008), and this peak was also observed in NaCS. The C–O stretching at C_3, C–C stretching and C–O stretching at C_6 are between 1073 and 1058 cm^{-1}. The presence of absorption bands within these wavenumbers in NaCS confirms that the capsule is a derivative of cellulose via a sulphonating process (Chen et al. 2013). The peaks at 1240 and 820 cm^{-1} in NaCS corresponded to O–SO_3^- and C_6–OSO_3^- vibrations respectively, confirming that sulpho groups were successfully bonded to the cellulose alcohol group, and that the cellulose was successfully sulphated (Zeng, Danquah, Potumarthi, et al. 2013). The spectra of the polymeric capsule was comparable to that of NaCS since the

capsule is formed via crosslinking between the charged sulpho groups of cellulose sulphate and diallyldimethyl ammonium group of PDMDAAC (refer Figure 4.29 under Section 4.6). A summary of active functional groups of native cotton linter, NaCS and polymeric capsule is listed in Table 4.13.

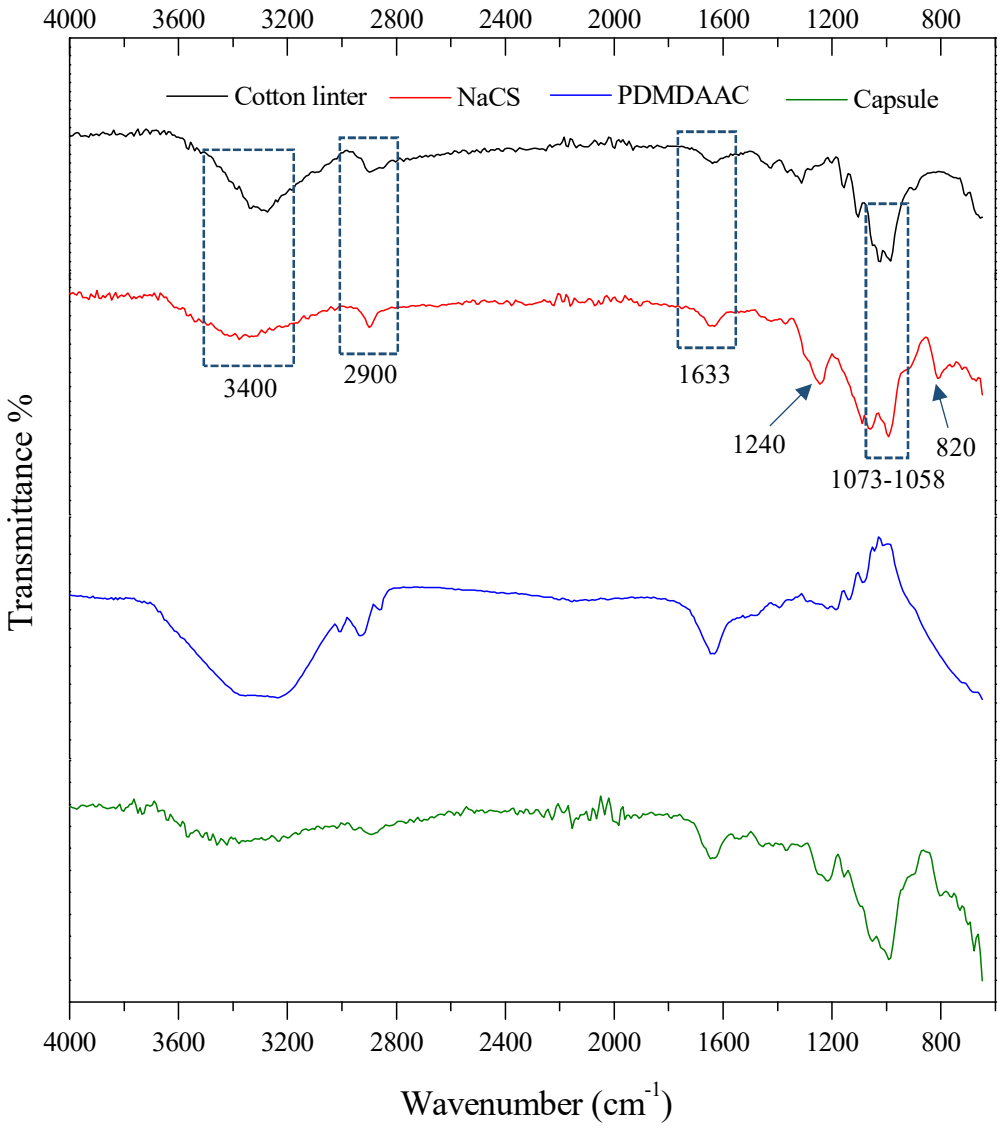

Figure 4.36: FTIR spectra of cotton linter (cellulose), NaCS, PDMDAAC (6%), and NaCS-PDMDAAC polymeric capsule.

Table 4.13: Summary of active functional groups of native cotton linter, NaCS and polymeric capsule.

Wavenumber (cm^{-1})	Active functional groups		
	Native cotton linter	**NaCS**	**Polymeric capsule**
~3400	H-bonded O–H stretching (alcohol)		
~2900	C–H stretching (alkane)		
1633	Fibers-OH		
1073 – 1058	C–O stretching at C_3, C–C stretching, C–O stretching at C_6		
1240	nil	$O–SO_3^-$	
820	nil	$C_6–OSO_3^-$	

4.7.3 pH stability of immobilized JP

One of the advantages of enzyme immobilization is the improvement of enzyme stability towards harsh environments such as extreme pH conditions. Both free and immobilized JP were kept in varying pH conditions for 30 min, and their respective enzyme activities at different pH conditions were compared. Figure 4.37 shows that immobilized JP demonstrated higher enzyme activity than free JP over a broad pH range. Immobilized JP activity was over 85% even at high acidity and alkalinity conditions. Comparatively, free JP demonstrated over 85% enzyme activity over a narrower pH range, from 6.4 to 8.2. From pH 3.6 to 5.7, the relative enzyme activities of immobilized JP were largely constant with an average of 87.5%. These activities were ~40% higher than those exhibited by free JP at the same pH values. Enzyme activities for immobilized JP were >90% at pH values in between 6.4 and 10.4, with an optimum at pH 7. Encapsulation of JP unto NaCS-PDMDAAC polymeric capsules did not alter the optimal pH of the peroxidase. The enzyme activities of immobilized JP at extreme pH of <2.5 and >11.1 were 15% and 61% respectively. The decrease in enzyme activities at these extreme pH conditions was attributed to the instability of heme binding to the enzyme or ionic changes in the heme group, which is pH dependent and essential for peroxidase activity (Al-Senaidy and Ismael 2011; Pina et al. 2001).

pH stability of immobilized JP was enhanced because peroxidase molecules bound within the NaCS-PDMDAAC capsules were protected from the harsh environment of

the reaction solutions by the capsule membranes. This enables the peroxidase molecules to retain their enzymatic activities at extreme pH conditions to achieve significant phenol removal. The enhanced pH stability observed by immobilized JP is in keeping with other immobilized peroxidases in literature, such as BGP immobilized on Con A-adsorbed Sephadex (Akhtar et al. 2005), HRP immobilized on modified chitosan beads (Monier et al. 2010), and HRP immobilized on chitosan-halloysite hybrid-nanotubes (Zhai et al. 2013).

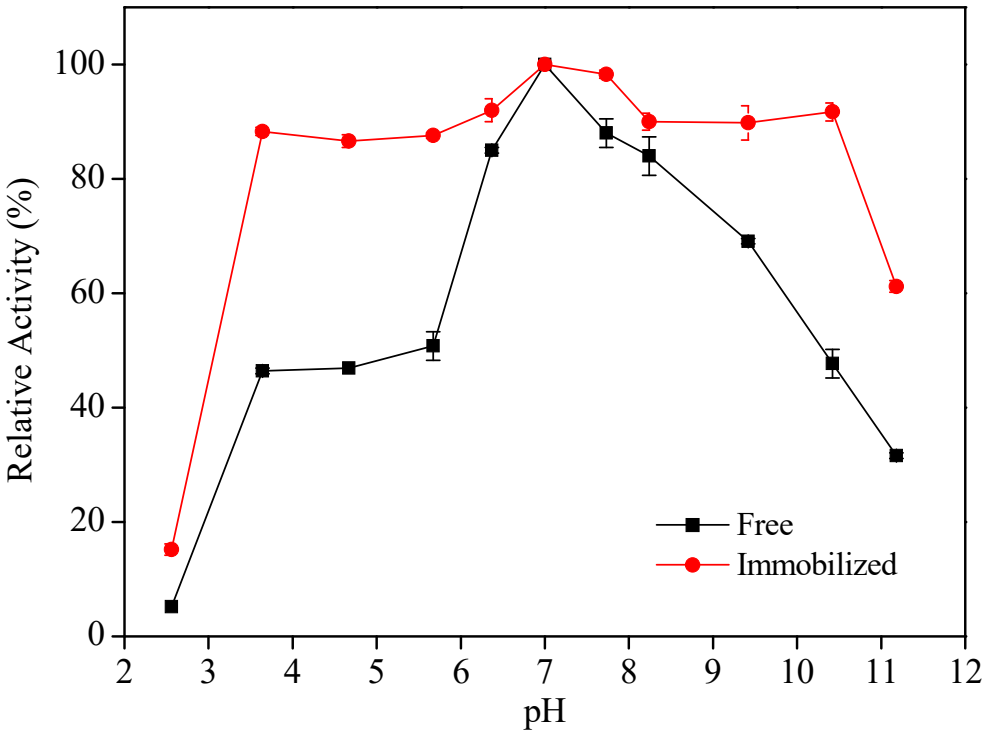

Figure 4.37: Comparison of pH stability between free and immobilized JP over varying pH conditions for 30 mins.

4.7.4 Thermal stability of immobilized JP

The temperature stability profiles of free and immobilized JP after incubation at various temperatures for different time intervals are illustrated in Figure 4.38. Thermal stability profiles for free and immobilized JP were comparable for incubation up to 50 ^{o}C. Free JP retained average enzyme activities of 96, 81 and 74% after 1 h incubation at 30, 40 and 50 ^{o}C respectively. For the same temperatures, the average enzyme activities retained by immobilized JP after incubation were 90, 84, and 75% respectively. Thermal stability of immobilized JP at elevated temperatures was better

than free JP. At 60 ºC, the enzyme activities retained by immobilized and free JP were 62.5 and 52% respectively. At temperature of 70 ºC, JP suffered from thermal inactivation regardless of its enzyme state, though immobilized JP retained 25% of its initial enzyme activity as compared to 9% exhibited by free JP. Both free and immobilized JP lost their enzyme activities after incubation at 80 ºC due to inactivation. The better thermal stability shown by immobilized JP is due to the protective effect of polymeric capsules. Enzyme molecules entrapped within the capsules were not directly exposed to heat denaturation at elevated temperatures due to the presence of NaCS-PDMDAAC membrane. Other peroxidases have also demonstrated improvement in thermal stability upon immobilization. For instance, immobilized BGP exhibited 85% of the original enzyme activity after 2 h incubation at 60 ºC while soluble BGP retained half of its initial enzyme activity (Akhtar et al. 2005). HRP covalently coupled onto AAm-HEMA copolymers also showed better thermal stability than free enzyme at 35-55 ºC (Shukla and Devi 2005). Besides, alginate-entrapped and covalently immobilized TP were also found to be thermally more stable than free TP (Quintanilla-Guerrero, Duarte-Vázquez, García-Almendarez, et al. 2008).

It can also be noticed from Figure 4.38 that the temperature profiles demonstrated by free JP were generally stable and consistent throughout the incubation period. Enzyme inactivation was observed at temperatures 40 ºC and above after incubation for 10 min, but prolong incubation did not significantly decreased the enzyme activity further. On the other hand, enzyme activities exhibited by immobilized JP were slightly more fluctuating than free JP especially at 30, 40 and 50 ºC. Upon dissolution of NaCS in JP solution, crosslinking between cellulose sulphate and peroxidase molecules took place. When capsule membrane was formed due to the reaction between NaCS and PDMDAAC, some peroxidase molecules were thus entrapped among the matrix attachment of the capsule membrane. Such crosslinking and/or entrapment could possibly hinder the release of JP molecules upon rupture of capsules for analysis, causing low enzyme activity at earlier time intervals. Further incubation at elevated temperatures may have weakened the bonds, since enzyme molecules possessed higher energy to break themselves free. This resulted in higher enzyme activities at time intervals of 50 min for 30 ºC, and 40 min for 40 and 50 ºC respectively.

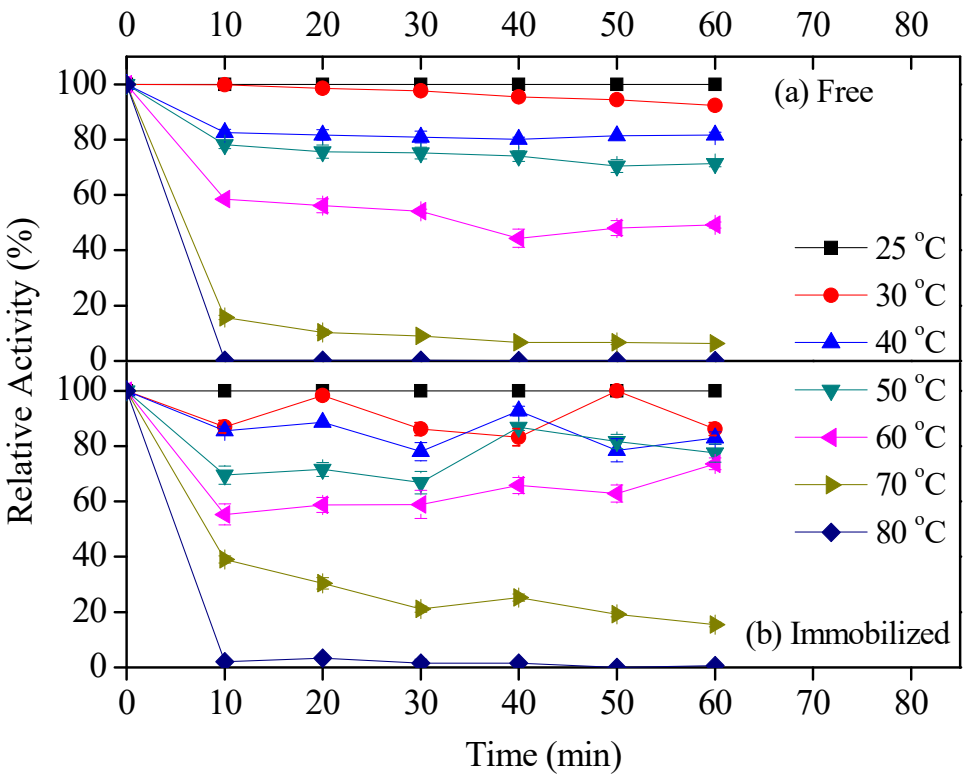

Figure 4.38: Comparison of thermal stability between free and immobilized JP over temperature range of 25 – 80 °C.

4.7.5 Hydrodynamic size and zeta potential of immobilized JP

The effect of immobilization on hydrodynamic size and zeta potential of JP was evaluated at various pH conditions ranging from 2.5 to 10.1 as shown in Figure 4.39(b). The results were compared with free JP in Figure 4.39(a). As mentioned previously in Section 4.2.4, the increase in hydrodynamic size of free JP at pH 3.75-4.88 with an average of 999 nm was due to higher inter-chain aggregation which occurred near isoelectric point (pI). The average hydrodynamic size of free JP was 365 nm. After immobilization, the average size of JP became smaller than that of free enzyme. The average size of immobilized JP was 341 nm, which was about 7% smaller than free JP. Similar observation has also been reported in the immobilization of microalgae using NaCS-PDMDAAC (Zeng, Danquah, Halim, et al. 2013), and was believed to be attributed to higher inner pressures. The entrapment of JP molecules among the polymeric matrix of NaCS as well as NaCS-PDMDAAC near the boundary of capsule membrane could have squeezed the enzyme molecules, resulting in smaller size of immobilized JP molecules. At high alkalinity conditions of pH 10.1, immobilized JP

underwent structural conformation, resulting in decrease of hydrodynamic size to 287 nm.

In terms of zeta potential, immobilized JP demonstrated consistent zeta potential of -14 mV over the pH range being studied. Unlike crude free JP, the isoelectric point (pI) of immobilized JP was unable to be determined. This is mainly due to the co-existence of cellulose sulphate ions and JP molecules in the liquid core of polymeric capsules. Both cellulose sulphate ions and JP molecules are negatively charged. The total surface electrical charges of these two components were greater than the positive charge shown by hydrogen ions (H^+). Therefore, zeta potential collected at acidic conditions was no different from neutral or alkaline conditions. The consistent surface electrical charge also means that aggregation of enzyme molecules is unlikely to take place inside the capsules, hence preventing the drawback of protein agglomeration which would possibly affect the enzyme efficiency in phenol removal process.

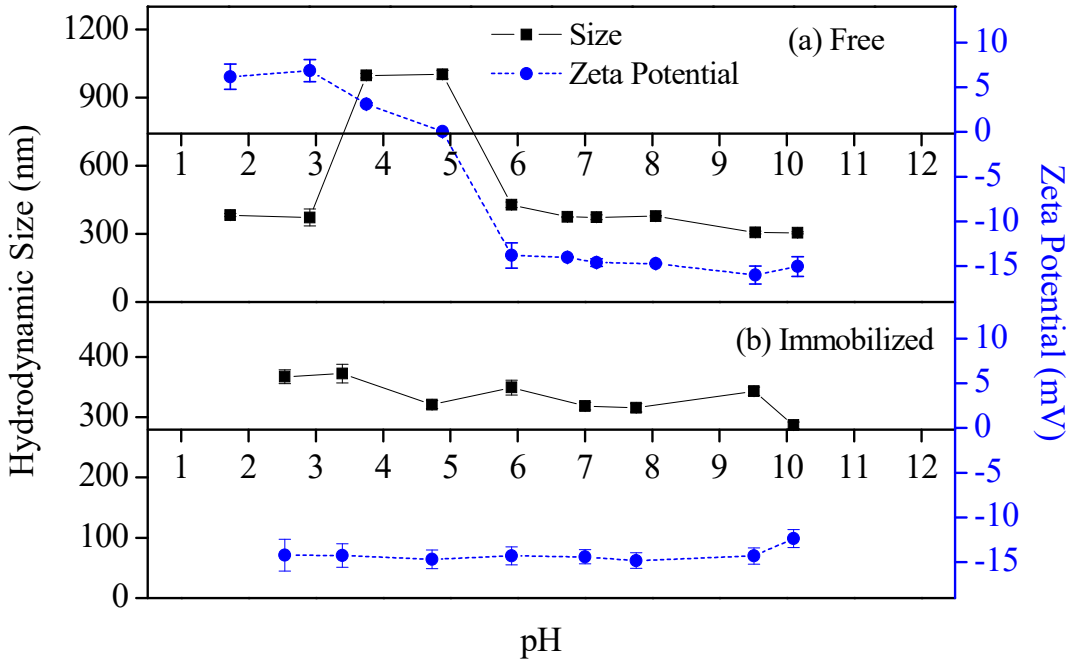

Figure 4.39: Comparison of hydrodynamic size and zeta potential between free and immobilized JP over varying pH conditions; (a) free JP, (b) immobilized JP.

4.8 COMPARISON OF PHENOL DEGRADATION EFFICIENCY BETWEEN FREE AND IMMOBILIZED JP

The performance of immobilized JP prepared using 2% NaCS and 6% PDMDAAC was compared with free JP under varying operating parameters including pH, H_2O_2 concentration, enzyme loading, temperature, and reaction time. The reusability of immobilized JP was also evaluated.

4.8.1 Effect of pH on phenol degradation using immobilized JP

The influence of pH on the performance of free and immobilized JP for phenol removal was carried out by varying the pH defined buffer solutions used as the reaction medium. The buffer solutions used were acetic / acetate (pH 5), monobasic / dibasic sodium phosphate (pH 6-7) and boric / borate (pH 8). The concentration of JP in the reaction mixture was maintained at 0.23 U/mL for both free and immobilized conditions. H_2O_2 concentration in the mixture was kept at 1 mM for both enzyme conditions, and the removal process was conducted at 25 ºC. From Figure 4.40, free and immobilized JP exhibited similar trends within the range of pH investigated. A high phenol removal efficiency of > 95% was observed at pH between 6 and 7.

At pH 5 and 8, both free and immobilized JP demonstrated lower phenol removal efficiencies, though the immobilized peroxidase was higher than that of free peroxidase. This could be attributed to the protective effect of the capsule membrane towards the encapsulated peroxidase molecules. The loss in phenol removal efficiency due to increasing acidity and alkalinity is driven by molecular variations in the protein structure of the enzymes and active sites availability for effective target binding and removal. The modification of protein structure due to protonation and hydroxylation effects leads to obscurant of its active sites before eventually causing permanent loss of functionality.

Encapsulation of JP in the NaCS-PDMDAAC capsular matrix did not affect the pH range for optimal phenol degradation. HRP immobilized on chitosan-halloysite hybrid-nanotubes exhibited an optimum working pH of 7 and achieved a removal efficiency of 94.3% for 1 mM phenol (Zhai et al. 2013). HRP immobilized on magnetic poly(glycidylmethacrylate-co-methylmethacrylate) via covalent bonding also showed an optimum pH of 7, similar to that of free HRP (Bayramoğlu and Arıca 2008). Whilst

our present finding on the effect of pH on phenol removal for free and immobilized JP is in keeping with the aforementioned reported work, a different observation was reported by Cheng et al. (2006) in their study on HRP immobilization on aluminum-pillared interlayered clay (Al-PILC). After immobilization, the optimal operating pH range shifted to 4.5 and 9.3, a broader range compared to that of free enzyme (6 to 9). In the presence of protonated, unreacted Si-OH on the surface of Al-PILC, protons from the vicinity of the surface are repelled and this creates a higher pH at the boundary layer between the support and the bulk solution, leading to lowering of the apparent optimal pH. This demonstrates that the nature of the immobilization support can affect the interactions between the support and the enzyme molecules as well as the optimum operating pH of the phenol treatment process.

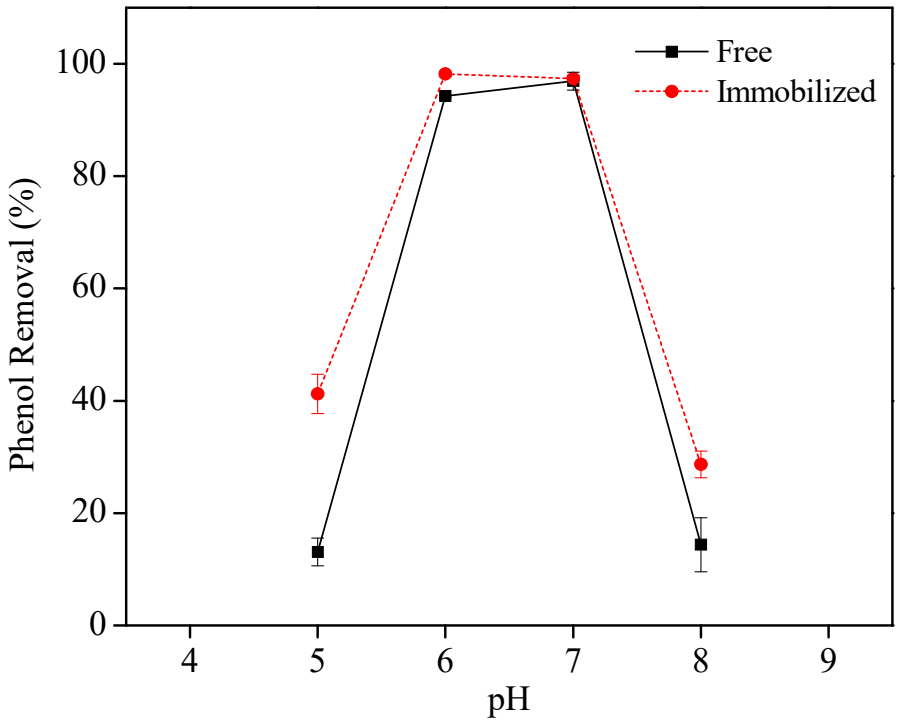

Figure 4.40: Effect of pH on phenol removal efficiency for free and immobilized JP. Other experimental conditions: 1 mM H_2O_2, 0.23 U/mL enzymes (both free and immobilized), 25 ^oC and 24 h incubation.

4.8.2 Effect of H_2O_2 concentration on phenol degradation using immobilized JP

Phenol removal efficiency as a function of H_2O_2 dosage was investigated at a constant reaction medium pH of 6. The result is as shown in Figure 4.41. The phenol removal

efficiencies demonstrated by free and immobilized enzymes were comparable from 1 to 8 mM, with an average of 94% and 97% respectively. When H_2O_2 concentration in the reaction mixture was increased to 9 mM, free JP maintained its phenol removal efficiency. However, the removal efficiency decreased to ~88% for immobilized JP. Phenol removal efficiency by free JP dropped to 78% when H_2O_2 concentration increased to 9.5 mM, remaining constant up to 11 mM at an average of 76%. The removal efficiency of free JP dropped to <25% at 12mM. Comparatively, immobilized JP suffered a greater decrease in efficiency under high concentrations of H_2O_2. At 9.5mM, immobilized JP demonstrated 60% phenol removal. The efficiency decreased to <50% at H_2O_2 concentrations of 10 mM and above.

In general, both free and immobilized JP were active over a broad range of H_2O_2 concentrations. H_2O_2 concentration as low as 1 mM, JP showed high phenol removal efficiency under both free and immobilized conditions. The low H_2O_2 concentration of 1 mM was sufficient to oxidize peroxidase molecules into active forms for further oxidation of phenol compounds. High concentrations of H_2O_2 (> 9.5 mM) can induce inhibitory effects to the peroxidase catalytic activity by irreversibly oxidizing the enzyme ferriheme group which is vital for peroxidase catalysis (Duarte-Vázquez et al. 2003). Excess H_2O_2 can also promote the conversion of peroxidase into inactive verdohaemoprotein called P-670 (Arnao et al. 1990). Therefore, the concentration of H_2O_2 in phenol degradation process is critical to prevent enzyme inactivation. It should also be noted that peroxidase-catalyzed polymerization of phenol relies on the molecular activation functionality of H_2O_2 to create active forms for phenolic oxidation hence no activity was observed at 0 mM H_2O_2.

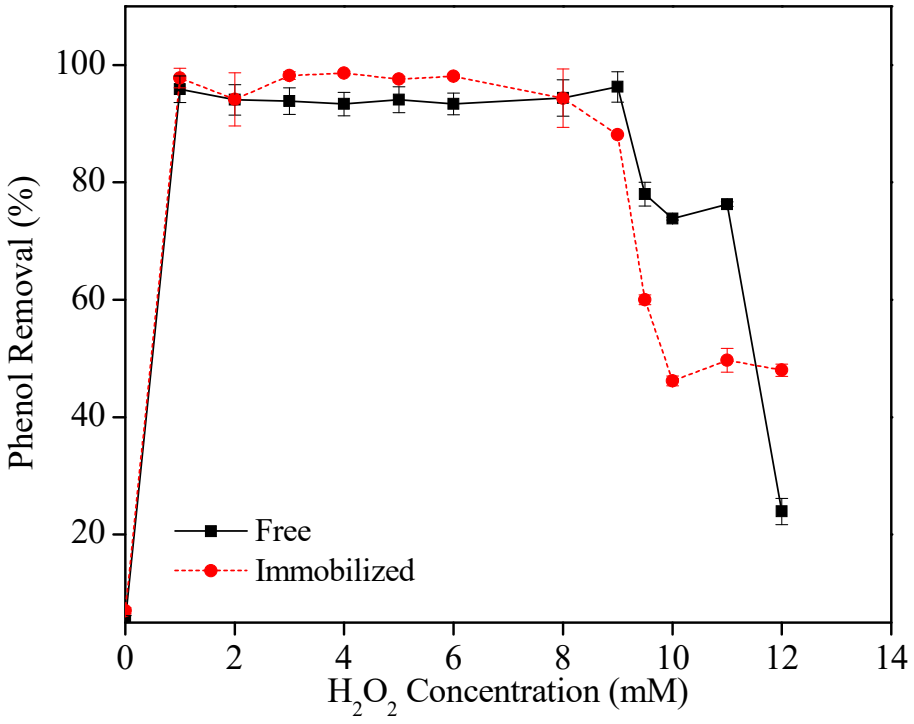

Figure 4.41: Effect of H_2O_2 concentration on phenol removal efficiency for free and immobilized JP. Other experimental conditions: pH 7 and 6 for free and immobilized JP respectively, 0.23 U/mL for both enzymes, 25 ºC and 24 h incubation.

4.8.3 Effect of enzyme loading on phenol degradation using immobilized JP

Four different enzyme loadings (0.16, 0.23, 0.47 and 0.70 U/mL) were used to investigate the phenol removal efficiencies of free and immobilized JP. No removal of phenolic molecules were observed in the absence of the enzyme. Application of H_2O_2 alone does not result in the oxidation of phenolic compounds, though some removal of phenols have been reported under extremely high peroxide concentrations (Cooper and Nicell 1996).

As shown in Figure 4.42, under low enzyme concentrations (0.16 U/mL), free JP demonstrated a high phenol removal efficiency of 90% whilst immobilized JP attained 43%. The low phenol conversion of immobilized JP at low enzyme loadings could be attributed to the presence of mass transfer barrier posed by the polymeric capsule, slowing the diffusive rate of phenolic and H_2O_2 molecules for adsorption at the limited enzyme sites. Since the peroxidase molecules are encapsulated, the degree of accessibility of H_2O_2 molecules to peroxidase and also the phenolic compounds to active sites of the enzyme is reduced in comparison to the free enzyme. This diffusive

limitation delays the oxidation of peroxidase molecules, which in turn delays the polymerization of phenol compounds. As a result, given the same reaction time (24 h), the efficiency of 0.16 U/mL immobilized JP was only half of that demonstrated by free JP.

At optimal enzyme loading of about 0.23 U/mL, both free and immobilized JP exhibited > 95% removal efficiency. The increase in phenol removal efficiency was more significant for immobilized JP as the efficiency was found double of the free enzyme. Increasing the concentration of immobilized enzyme within the capsule may result in some degree of adsorption at the capsule surface with the limited intra-capsular volume per unit capsule size, and this minimizes the capsule barrier effect. The presence of higher concentrations of enzyme molecules in the reaction mixture increases the availability of enzyme active sites and hence promotes the binding of phenol molecules to these sites for oxidation.

A further increase in enzyme loading (0.47 and 0.70 U/mL) did not enhance removal efficiency due to substrate limitation. In order to fully utilize the available enzyme sites, the initial phenol concentration can be increased alongside H_2O_2 concentration. From Figure 4.42, it can also be noticed that free and immobilized JP demonstrated similar phenol removal trends from 0.23-0.70 U/mL. This is because the results were obtained at steady state where the removal process has reached completion. A reaction time study (differential removal) will be able to reveal the phenol removal attained at various time intervals between free and immobilized JP. Such study has been conducted at optimum operating conditions and will be presented in Section 4.8.5.

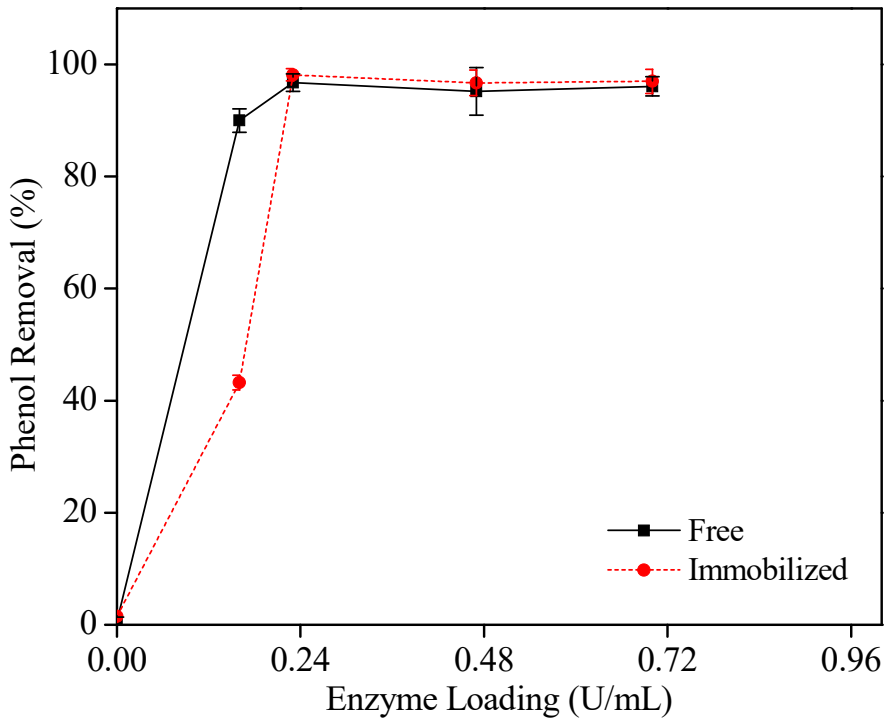

Figure 4.42: Effect of enzyme loading on phenol removal efficiency for free and immobilized JP. Other experimental conditions: pH 7 and 6 for free and immobilized JP respectively, 1 mM H_2O_2, 25 ºC and 24 h incubation.

4.8.4 Effect of temperature on phenol degradation using immobilized JP

Enzymatic activities are known to be temperature dependent as extreme temperatures restrict the catalytic functionality of the enzyme by distorting the 3D structure of the enzyme, reducing the binding accessibility and capacity of its active sites. The effect of temperature on free and immobilized JP was evaluated by incubating the reaction mixture under various temperature conditions ranging from 25 ºC to 50 ºC for 24 h. Incubation of 24 h ensures completion of phenol removal by both enzyme states. As shown in Figure 4.43, from 25 ºC to 40 ºC, both free and immobilized JP demonstrated high phenol removal efficiencies, with averages of 95.6% and 98% respectively. Above 40 ºC, the removal efficiencies decreased to <50% for free JP and <30% for immobilized JP, reaching ~20% at 50 ºC for both JPs.

The decline in removal efficiencies shown by free and immobilized JP at elevated temperatures is attributed to thermal denaturation which results in either loss of active sites or molecular seclusion of active sites from substrate molecules due to structural deformation. The haem prosthetic group, which governs the thermal stability of

peroxidases, is released under high temperatures to form apoenzyme. Apoenzyme is more susceptible to thermal inactivation as compared to the native enzyme (McEldoon and Dordick 1996). Enzyme structure is distorted at elevated temperature conditions, thus limiting its binding capacity with substrate molecules. The effect of thermal denaturation coupled with the diffusional limitation of the polymeric capsule membrane caused the removal efficiency demonstrated by immobilized JP to be lower by 20% as compared to free JP at 45 ^{o}C.

Similar trends have been reported for other types of peroxidases immobilized on different supports. HRP immobilized on magnetic beads demonstrated an optimum temperature between 25 ^{o}C to 35 ^{o}C (Bayramoğlu and Arıca 2008). Con A-Sephadex-bound bitter gourd peroxidase exhibited a phenol removal efficiency of 92% at 40 ^{o}C (Akhtar and Husain 2006). Shukla and Devi (2005) reported an optimum temperature of 45 ^{o}C with an efficiency of > 80%. The results from these studies revealed that thermal denaturation occurred at elevated temperatures, and phenol removal efficiencies of immobilized peroxidases decreased beyond their optimum ranges. Moreover, the optimal capability of JP (free and immobilized) in treating phenol under mild temperature conditions is attractive from process economics standpoint.

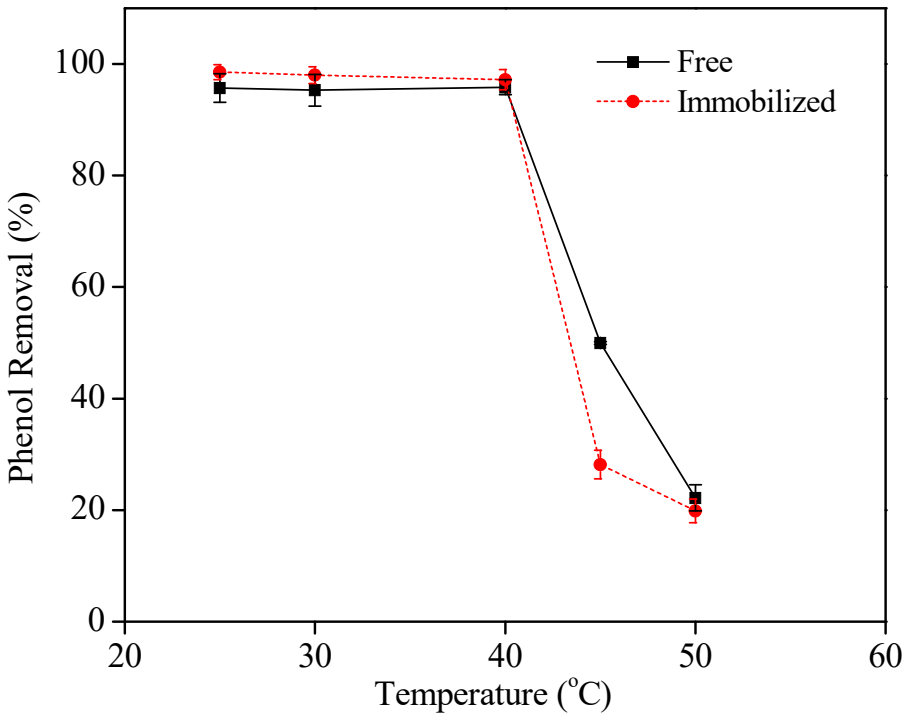

Figure 4.43: Effect of temperature on phenol removal efficiency for free and immobilized JP. Other experimental conditions: pH 7 and 6 for free and immobilized JP respectively, 1 mM H_2O_2, 0.23 U/mL for both enzymes, and 24 h incubation.

4.8.5 Effect of reaction time on phenol degradation using immobilized JP

The rate of phenol degradation has a significant impact on the process economics. The rates at which free and immobilized JP attain optimum phenol removal were investigated by analyzing the phenol content in the reaction mixture at various time intervals. As shown in Figure 4.44, free JP demonstrated a rather constant removal rate for the first 11 h of reaction, with an average of 20%. The rate then increased at 12 h to 55%, before finally achieving >90% after 13 h of reaction. The removal efficiency stabilized afterwards to an average of 95%. Immobilized JP, on the other hand, showed gradual increment in removal efficiency for the first 4 h before stabilizing after additional 6 h. Its efficiency increased again after 10 h, reaching 95% after 15 h. Extending the reaction time thereafter, did not result in any improvement in phenol removal efficiency. This is potentially due to saturation of available enzyme active sites, resulting in insignificant differential changes in the concentration of enzyme-substrate complex accumulation, and/or depletion of substrate in the reaction medium.

Low phenol removal rates at the beginning could be due to the steady state requirements of oxidizing JP into active catalytic forms to attack phenolic species. The presence of impurities associated with JP as crude enzyme extract interfere with H_2O_2 oxidation mechanism and inhibit catalytic activity. Substrate inhibition from phenol could also contribute to the low removal efficiency at the initial stages. Relatively, phenol inhibition on immobilized JP was less significant than free JP, owing to the protective effect from the polymeric capsules. The decrease in phenol concentration after 11 h reduced the substrate inhibition effect on the enzymes. Coupling with the availability of JP molecules in active forms, the phenol removal efficiency increased after 2-4 h, with free JP demonstrating a more profound increment.

In comparison, free JP required a shorter reaction time (13 h) than immobilized JP (15 h) to achieve maximum phenol removal. This is due to the effect of diffusional limitation in polymeric capsules. Phenol molecules interact with enzyme active sites readily for free JP. However, for immobilized JP, the mass transfer of phenol molecules first takes place from the bulk solution to the external surface of the capsules. Phenol molecules then diffuse from the external surface into and through the pores within the capsule membrane, before reaching peroxidases enzyme active sites for oxidation. It should also be noted that the pores in capsule membrane are not straight and cylindrical but rather a series of tortuous, interconnecting paths of pore bodies and pore throats with varying cross-sectional areas. This resulted in the delay of transport and reaction between phenol molecules and enzyme active sites. Moreover, the release of reaction products through the membrane may also hinder the entry of unreacted phenol molecules.

The first order kinetic rate constants for free and immobilized JP during the exponential phase of phenol removal were determined as 1.21 h^{-1} and 1.02 h^{-1}, respectively.

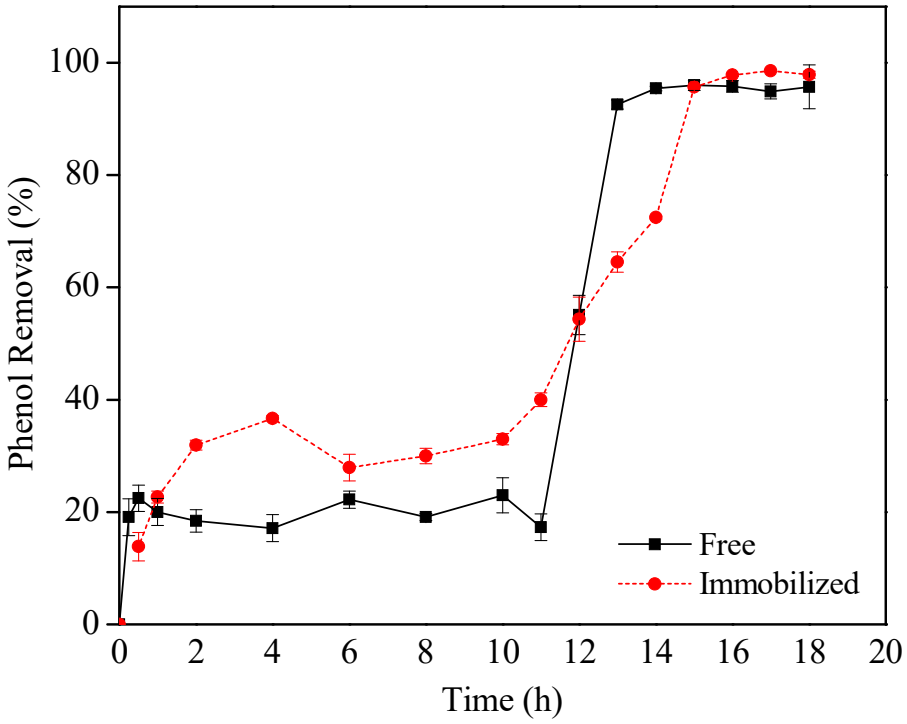

Figure 4.44: Effect of reaction time on phenol removal efficiency for free and immobilized JP. Other experimental conditions: pH 7 and 6 for free and immobilized JP respectively, 1 mM H_2O_2, 0.23 U/mL for both enzymes, and 25 ºC.

4.8.6 Reusability of immobilized JP

A major advantage of enzyme immobilization that drives its widespread application is unique reusability characteristic. Immobilized enzyme can be easily recovered from process medium and regenerated for use. The capacity of JP capsules for repeated cycles of phenol removal was investigated by separating the capsules from the reaction mixture after each cycle, and subjecting the capsules to fresh aqueous phenol solution. The operating conditions of each cycle remained unchanged at pH 6 and 25 ºC. Each new cycle of phenol removal was initiated by the addition of H_2O_2 and allowed to proceed for 24 h. Two different enzyme loadings were investigated: 0.23 and 0.70 U/mL. As shown in Figure 4.45, immobilized JP capsules demonstrated reusability up to at least 3 cycles depending on the enzyme loading with maintained phenol removal efficiency. Both enzyme loadings achieved >95% removal efficiency for 3 cycles. During the 4^{th} cycle, the higher enzyme loaded JP capsules (0.70 U/mL) maintained 95% phenol removal whilst the lower enzyme loaded JP capsules (0.23 U/mL) resulted

in a drop in efficiency to <40%. A further reuse of the 0.70 U/mL JP capsules in a 5th cycle resulted in a removal efficiency of 60%, followed by 33% in the 6th cycle.

The decrease in phenol removal efficiency after several process cycles resulted from the loss of activities of the enzyme or potential enzyme leaching from the capsules after multiple reuse. Another possible reason could be the accumulation of reactive products synthesized during the enzymatic process. Insoluble polymers from the enzymatic process could attach and cover the capsule surface, hindering effective mass transfer across the capsule membrane to the enzyme active sites and out of the intra-capsular environment.

High loading of immobilized JP (0.70 U/mL) demonstrated a longer cyclic duration of reusability due to higher concentrations of the peroxidase molecules in the reaction medium. Some of the enzyme molecules retained their activities after several cycles as they are not fully utilized during the phenol degradation process. It may be inferred that an optimal dosage of enzyme loading is required to promote repeated use of immobilized enzymes.

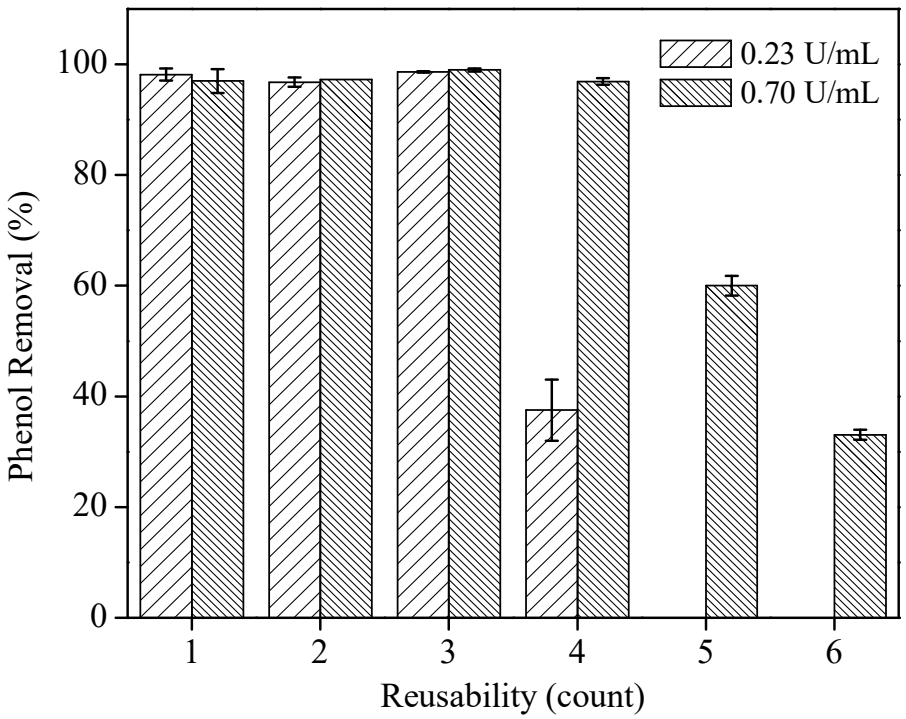

Figure 4.45: Reusability of immobilized JP at two different enzyme loadings – 0.23 U/mL and 0.70 U/mL. Other experimental conditions: pH 6, 1 mM H_2O_2, 25 ^oC, and 24 h incubation for each cycle.

Comparison of optimum operating parameters between free and immobilized JP for batch phenol degradation is summarized in Table 4.14.

Table 4.14: Optimum operating conditions for batch treatment of aqueous phenol solution using free and immobilized JP.

Experimental parameters	Free JP	Immobilized JP
pH of solution	7	6
H_2O_2 concentration	1 mM	1 mM
Enzyme loading	0.23 U/mL	0.23 U/mL
Temperature	25 ºC	25 ºC
Reaction time	13 h	15 h
Phenol removal efficiency	95%	95%

4.9 CONTINUOUS PHENOL REMOVAL IN FLUIDIZED BED COLUMN USING IMMOBILIZED JP

The comparison between free and immobilized JP for phenol degradation in the previous section was conducted under batch process. The feasibility of immobilized JP in treating larger amount of wastewater is of crucial importance from scale-up and economic standpoints. Therefore, JP-encapsulated NaCS-PDMDAAC polymeric capsules were investigated for its efficacy in continuous phenol removal process in a customized fluidized bed column with upward flow.

The total volume of buffered phenol solution for each cycle in fluidized bed was 202 mL. The initial phenol concentration in the reaction mixture was ~1 mM, obtained by adding 2 mL of 0.1 M phenol stock solution into 200 mL of 0.1 M sodium phosphate buffer solution pH 6. The concentration of H_2O_2 in the reaction mixture in the beaker was also ~1 mM. After the addition of 1 mL H_2O_2 solution (0.2 M), phenol concentration in the beaker decreased slightly to 0.985 mM, which corresponded to 0.5% and thus can be assumed negligible. Detailed calculation of phenol and H_2O_2 concentrations is presented in Appendix B.

4.9.1 Effect of flow rate on phenol removal in fluidized bed column

Three different flow rate settings – 4, 6, and 7 which corresponded to 70.0, 109.6 and 128.8 mL/min respectively, were chosen in the study of the effect of flow rate on phenol removal in fluidized bed column. Flow rate settings were chosen from the range

of 4 to 7 because proper fluidization took place in this range. Flow rates lower than setting 4 (< 1.167 mL/s) did not generate significant expansion of biopolymer capsules, whereas flow rates greater than setting 7 (> 1.827 mL/s) caused rigorous fluidization which resulted in some rupture of capsules. Enzyme loading for this study was kept relatively constant at ~300 capsules, produced from 20 mL JP solution containing 2% NaCS. The average weight of these ~300 capsules was 18.49±0.07 g. The total enzyme activity was 27.1 U, and the average enzyme activity for the treatment of 202 mL phenol solution was 0.13 U/mL.

Figure 4.46 shows the fluidization conditions in the column at flow rates 70.0, 109.6 and 128.8 mL/min respectively. As can be seen, the capsules bed expansions caused by flow rates 70.0 and 109.6 mL/min did not occupy the entire 10 cm height given for the working of fluidization. Flow rate 128.8 mL/min resulted in greater expansion of capsule bed which occupied the entire space of 10 cm height. The heights of fluidization resulted from these flow rates were 5.83, 7.75 and 10 cm respectively.

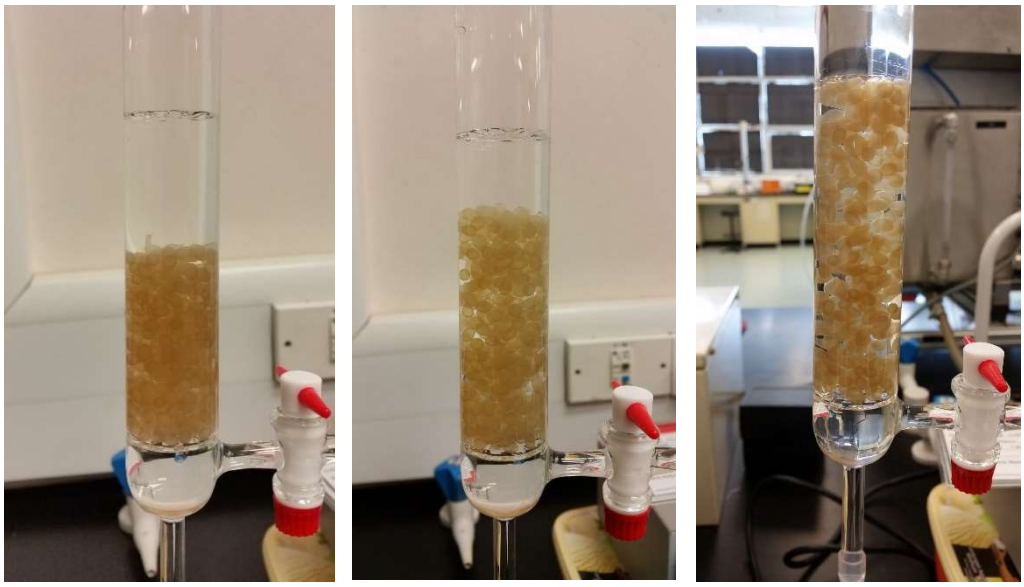

(a) (b) (c)

Figure 4.46: Fluidization in the column at three different flowrates; (a) setting 4 – 70.0 mL/min, (b) setting 6 – 109.6 mL/min, and (c) setting 7 – 128.8 mL/min.

Phenol degradation profile in the fluidized bed column under the influence of flow rate is presented in Figure 4.47. For all three flow rates, the conversion of phenol increased

gradually over the course of reaction. Flow rate 109.6 mL/min achieved 96% phenol removal after 8 h of reaction, while flow rates 70.0 and 128.8 mL/min achieved 90.5 and 92% after 11 and 19 h. Flow rate 109.6 mL/min is considered the optimum because the time required to attain > 90% phenol removal efficiency was the shortest amongst the flow rates being studied. Fluidization promotes the collision between phenol molecules and polymeric capsules encapsulated with JP molecules. Phenol molecules being transported to the boundary of the capsules are attached to the capsule membrane and diffused into the capsules for oxidation and polymerization process. The reaction products are being carried away from the polymeric capsules by the upward flow of fluidization. This reduces the chances of reaction products attached to the enzyme active sites and subsequently blocked the access of fresh phenol molecules to the active sites.

Different flow rates affect the retention time of phenol molecules along the fluidization height where capsules are expanded in the column. For high flow rate at 128.8 mL/min, the passing of phenol solution through the expansion of biopolymer capsules was fast and the retention time may not be sufficient for diffusion and oxidation of phenol molecules, thus resulting in lower removal rate. When the reaction was allowed to continue for a longer period of time, the phenol removal efficiency eventually reached 92% after 19 h. On the other hand, fluidization at flow rate 70.0 mL/min showed smooth laminar compared to the optimum flow rate at 109.6 mL/min. The height of expansion as well as the movement/rotation of polymeric capsules were less than those observed under optimal flow rate. Low particle velocity at low flow rate resulted in less collision between phenol molecules and immobilized biocatalysts for effective phenol oxidation. The transportation of reaction products away from the capsules may also be slower, hindering the access of unreacted phenol molecules to the boundary of the capsules.

The first order reaction rate constant for flow rate 109.6 mL/min was the highest among all, with a value of 0.349 h^{-1}. This is followed by 0.237 and 0.122 h^{-1} given by flow rates 70.0 and 128.8 mL/min respectively.

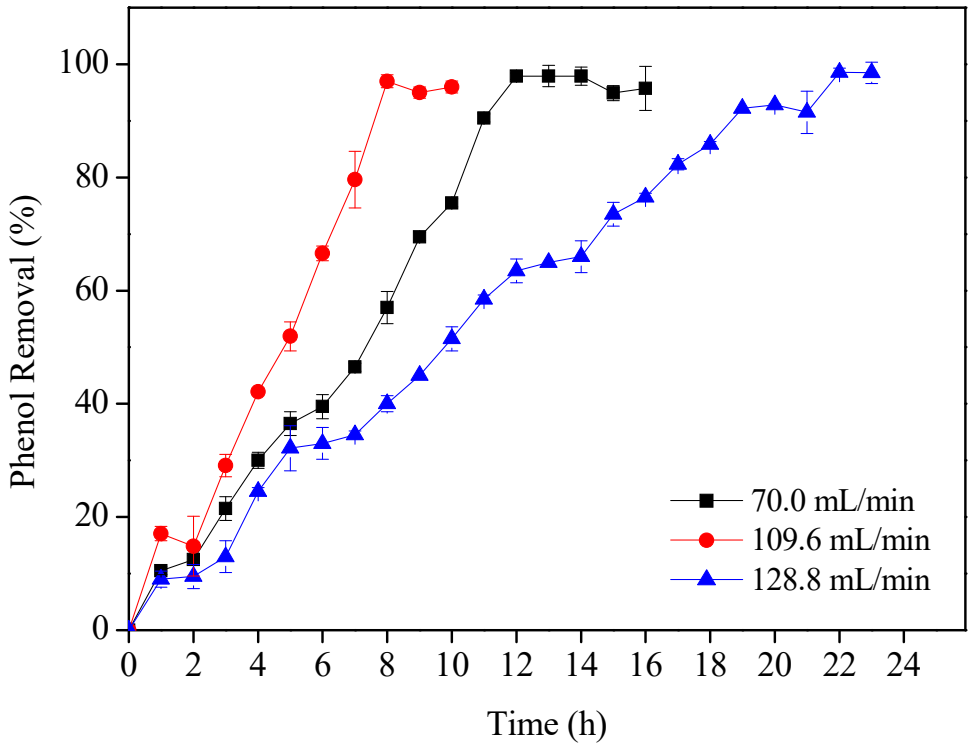

Figure 4.47: Effect of different flow rates on phenol removal in a fluidized bed column. Other experimental conditions: pH 6, 1 mM H_2O_2, 0.13 U/mL immobilized JP, and 25 ^oC.

4.9.2 Effect of enzyme loading on phenol removal in fluidized bed column

At optimal flow rate of 109.6 mL/min, three different enzyme loadings (low, medium and high) were investigated for their effects on phenol removal efficiency in fluidized bed column. The enzyme loadings being investigated were produced from three different volumes of JP solutions containing 2% NaCS, which were 10, 20 and 30 mL. For low enzyme loading, 10 mL JP solution produced ~150 capsules with an average weight of 8.64±0.21 g. Approximately 300 capsules (medium enzyme loading) with an average weight of 18.49±0.07 g were obtained from 20 mL JP solution, while 30 mL JP solutions produced ~450 capsules (high enzyme loading) with an average weight of 24.14±0.10 g. The total enzyme activities of these loadings were 13.6, 27.1, and 40.7 U, whilst the average enzyme activities for the treatment of 202 mL phenol solution were 0.07, 0.13, and 0.20 U/mL respectively. The fluidization conditions shown by various enzyme loadings are illustrated in Figure 4.48. The fluidization heights shown by 10 and 20 mL immobilized JP at flow rate 109.6 mL/min were 4.38 and 7.75 cm respectively. For high enzyme loading of 30 mL, it can be noticed that

the entire space allocated for expansion was full of capsules. The arrangement of capsules in Figure 4.48(c) was more packed than in Figure 4.46(c).

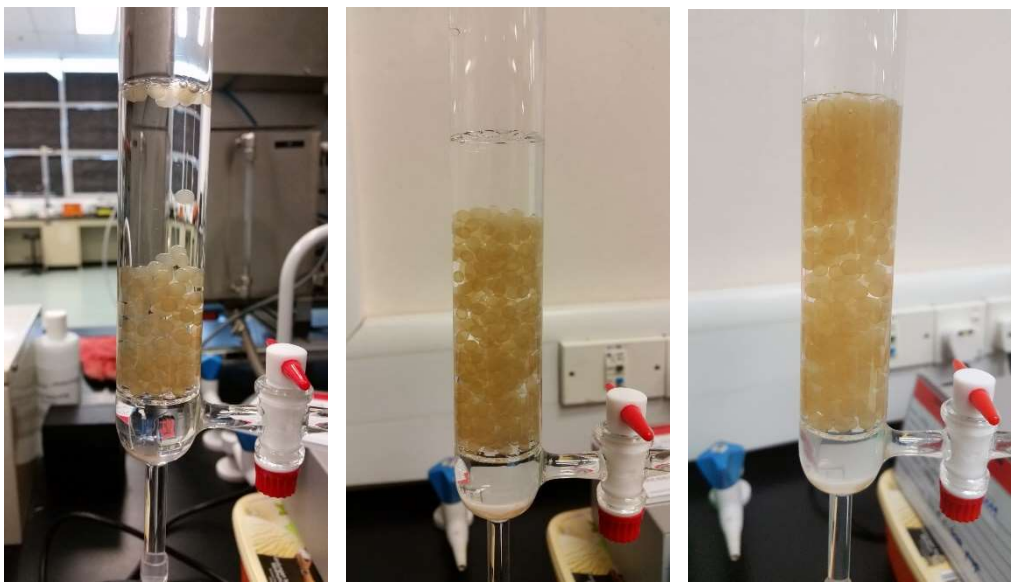

(a) (b) (c)

Figure 4.48: Fluidization in the column at three different enzyme loadings; (a) 10 mL (0.07 U/mL), (b) 20 mL (0.13 U/mL), and (c) 30 mL (0.20 U/mL).

Figure 4.49 shows the effect of enzyme loading on phenol removal process in fluidized bed column under a constant flow rate of 109.6 mL/min. A gradual increase in phenol removal efficacy was demonstrated by low enzyme loading throughout the course of reaction, eventually reaching maximum removal after 24 h with an average of 95.6%. Medium enzyme loading demonstrated an average of 18.3% phenol removal efficiency for the first 2 h, but took on a steady increment for the following 6 h and finally achieved maximal removal of 95.9%. On the other hand, phenol removal efficiency for high enzyme loading increased gradually for the initial 4 h, followed by a drastic increase of 30% for the next 1 h, and subsequently ~20% increase before eventually reaching 95.8% after 7 h.

Phenol conversion demonstrated by low enzyme loading was lower than medium and high enzyme loadings at all times in this study. Enzyme concentration of 0.07 U/mL was approximately 3-fold lower than those used in free and immobilized states under batch conditions (Figure 4.42). This amount of peroxidase was insufficient for high phenol oxidation in short period of time. Longer reaction time was required for removal efficiency >95% because of the limited availability of enzyme molecules and

enzyme active sites. When the enzyme concentration in the column was doubled, significant reduction in reaction time from 24 to 8 h for maximal removal was observed. Higher enzyme loading in the column ensures sufficient availability of enzyme active sites to accept phenol molecules. Further increase of enzyme concentration to 0.20 U/mL resulted in slight improvement in reaction time, from 8 to 7 h. This might be due to the decrease in quantity of unreacted phenol molecules available in the column when most of the phenol molecules had been oxidized. Nevertheless, Figure 4.49 clearly indicated that high enzyme loading enhances the performance of phenol conversion in the fluidized bed column by shortening the time needed for high removal efficiency.

The calculated first order reaction rate constants with respect to low, medium and high enzyme loadings were 0.109, 0.349 and 0.639 h^{-1} respectively. Various enzyme loading conditions for phenol degradation in fluidized bed column at optimal flow rate of 109.6 mL/min are also summarized in Table 4.15.

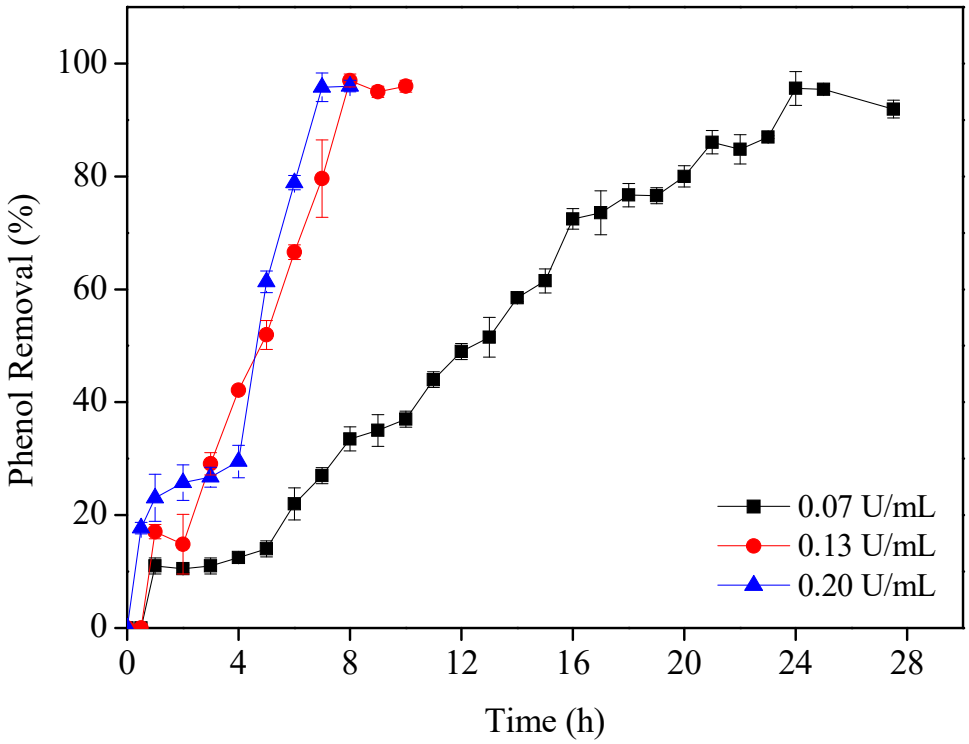

Figure 4.49: Effect of enzyme loadings on phenol removal in a fluidized bed column.

Table 4.15: Various enzyme loading conditions for phenol degradation in fluidized bed column at optimal flow rate of 109.6 mL/min.

Enzyme loadings	Low	Medium	High
Number of capsules	~150	~300	~450
Average weight	8.64±0.21 g	18.49±0.07 g	24.14±0.10 g
Total enzyme activities	13.6 U	27.1 U	40.7 U
Average enzyme activities	0.07 U/mL	0.13 U/mL	0.20 U/mL
Fluidization height	4.38 cm	7.75 cm	10.0 cm
Reaction time	24 h	8 h	7 h
Phenol removal efficiency	95.6%	95.9%	95.8%

4.9.3 Reusability of immobilized biocatalysts in fluidized bed column

One of the advantages of fluidized bed/packed bed column is the capacity for continuous treatment process. NaCS-PDMDAAC polymeric capsules encapsulated with JP have been proven previously that it can be reused up to 4 cycles with phenol removal efficiency >90% under batch operation condition (Figure 4.45). By incorporating these two benefits, the reusability of immobilized biocatalysts in fluidized bed column for continuous treatment of phenol solution was studied. Reusability test was carried out at optimum conditions of 109.6 mL/min and 0.20 U/mL enzyme loading, and other operating conditions were kept constant. Figure 4.50 shows that JP immobilized biopolymer capsules can be reused up to 8 cycles with phenol removal efficacy averaging at 95%. The removal efficiency decreased to 77% in 9^{th} cycle and 57% in 10^{th} cycle. This could be attributed to enzyme inactivation after several operational runs. Besides, breakage of polymeric capsules was also observed after several cycles resulting in loss of enzyme activity, probably due to repeated draining and filling of phenol solutions from every cycle.

It is worth mentioning that the immobilized biocatalysts in this study was not subjected to any solvent regeneration. The biocatalysts were reused directly after draining the treated phenol solution. This enables the continuous usage of biocatalysts without halting the treatment process from time to time for enzyme regeneration. According to Trivedi et al. (2006a), no significant phenol conversion was observed using immobilized SBP in silica sol-gel/alginate even in 2^{nd} cycle without any regeneration of the biocatalysts. With continuous regeneration using 5% (v/v) ethanol, phenol

removal efficiency did not decrease drastically, but under a gradual decreasing profile until <40% after 8 cycles. The performance of the system was further improved by continuous regeneration and 10% replacement of biocatalysts with the fresh ones every new cycle. Phenol removal efficiency was improved to >70% after 8 runs of operation.

Except first cycle, all subsequent cycles in this study were run for 18 h. This was because high phenol removal efficiency of >90% could not be achieved within 7 h after first cycle, probably due to some enzyme inactivation and/or clogging of the capsule membranes. Apart from that, precipitates were also noticed at the curvy areas of the fluidized bed set up, such as in the tubing connected to the top outlet of the column as well as at the curvy bottom of the column. The precipitates are the insoluble reaction products generated from the enzymatic process. The insoluble reaction products are phenolic polymers with molecular weights of several thousands (Kim et al. 2007; Kim et al. 2008). This problem can be overcome by placing sieves before and after the fluidization bed to collect the precipitates. However, due to constraint in the design of the column in this study, the placement of sieves could not be done properly. Tubing were changed and column was thoroughly cleaned to remove the precipitates at the end of one full set of experimental work.

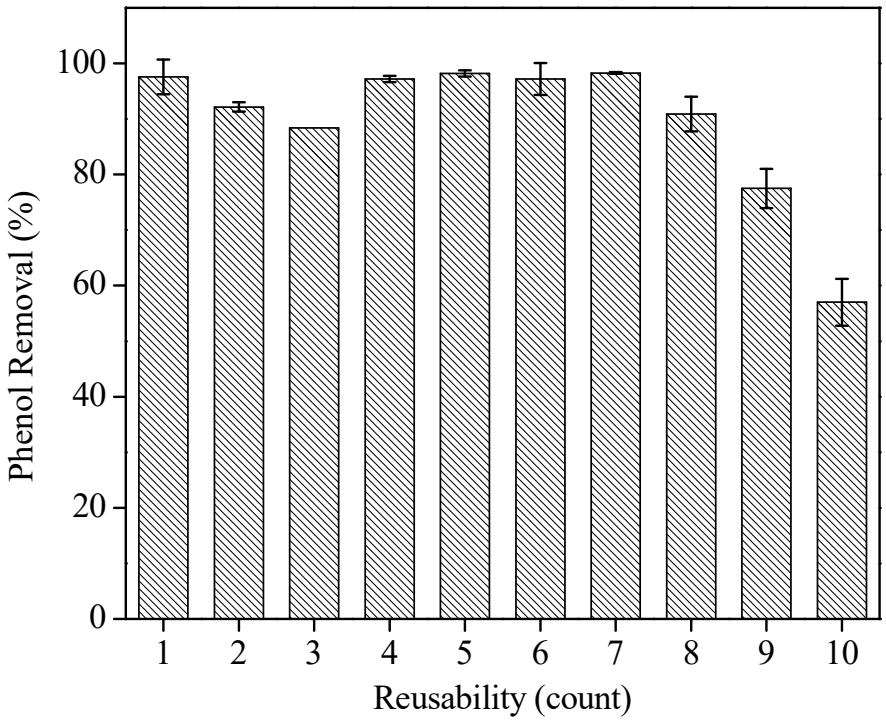

Figure 4.50: Reusability of JP-encapsulated polymeric capsules for phenol removal in a fluidized bed column.

CHAPTER 5: CONCLUSIONS AND RECOMMENDATIONS

5.1 CONCLUSIONS

For decades, the problems associated with phenol-containing wastewater generated from various industrial activities remain a great threat to human beings and other living organisms, particularly due to its toxicity even at low concentrations as well as other health implications. Focus and attention are continuously geared towards identification of new technology and/or improvement of existing ones for enhanced efficacy in phenol removal processes. For this reason, peroxidase-catalyzed enzymatic approach has emerged as alternative to conventional technologies in the treatment of phenol solutions, owing to the beneficial characteristics of peroxidases in targeting and oxidizing phenolic compounds. Although successful studies of various peroxidases in phenol degradation are largely available, some challenges related to this approach still remain which need addressing, such as susceptibility of enzymes to inactivation, lack of long-term stability, non-reusability of free enzymes resulting in high cost of peroxidase, and limited work on continuous phenol treatment. Therefore, this research project seeks to design and synthesize an enzyme-immobilized polymeric capsules for continuous treatment of phenol solution by answering to several research questions. Firstly, can newly-sourced crude peroxidase extracts from local agricultural wastes be used for biodegradation of phenol from aqueous solutions via enzymatic approach? Secondly, can such peroxidase be successfully immobilized onto NaCS-PDMDAAC polymeric capsules? And lastly, can peroxidase-immobilized NaCS-PDMDAAC polymeric capsules be an alternative for phenol removal under batch and/or continuous process?

Objective 1 of this research project was achieved by successfully extracting peroxidase enzymes from local agricultural wastes and characterised in order to explore optimal applications in phenol treatment under varying physicochemical conditions. Luffa and Jicama were selected for evaluation in the present study. The first body of work of Objective 1 focused on extracting peroxidases from the agricultural wastes (skin peels) of Luffa and Jicama, and investigating the biophysical and biochemical characteristics of the extracted peroxidases. Experimental results showed that extraction at pH 7

demonstrated the highest peroxidase yields for both LP and JP, with maximum enzymatic activities occurring at pH 6. Plant sample-to-buffer percentage of 50% (w/v) was found to be optimal for the extraction of both peroxidases. Enzyme homogenization was achieved in 30 min at 25 ^{o}C. Additives such as PEG and PVP did not significantly improve the extraction yield. The enzyme activity yield of LP and JP extracted under optimum extraction conditions were found to be 1.38±0.03 and 1.57±0.02 U/mL respectively. The optimum pH and temperature conditions for enzymatic activities were found to be pH 6 and 35 ^{o}C for both peroxidases. Both peroxidases showed fair stability under varying pH and temperatures. The hydrodynamic sizes of both peroxidases are pH dependent. Under stable configurations, LP molecules demonstrated an average size of 127 nm while JP molecules averaged at 365 nm. The isoelectric points of LP and JP were ~4.4 and ~4.9 respectively. Both LP and JP were anionic peroxidases under the conditions of extraction pH since their isoelectric points were at pH <7. Kinetic analysis showed that the K_m and V_{max} values of LP and JP towards phenol substrate were 60.7 mM and 1.92 mL/U, and 22.8 mM and 1.81 mL/U respectively. JP has a higher apparent affinity toward phenol than LP due to its lower K_m value. Towards H_2O_2 substrate, both peroxidases demonstrated similar affinity as the calculated K_m values were comparable, being 0.64 mM for LP and 0.68 mM for JP respectively. The V_{max} values were determined to be 1.84 mL/U for LP and 2.40 mL/U for JP. The molecular weights of LP and JP were 25 and 26 kDa respectively based on SDS-PAGE results. The second body of work of Objective 1 was on the investigation of the rate of phenol removal from a synthetic aqueous medium using the extracted crude enzymes under varying conditions of pH, H_2O_2 concentrations, enzyme loading, temperature, and reaction time. LP demonstrated a maximum phenol removal of >95% under H_2O_2 concentrations of 6-8 mM and pH 7. JP showed an optimum phenol removal efficiency of 94.5% at pH 7 with no significant effect resulting from variations in H_2O_2 concentrations. Both LP and JP achieved maximum removal efficiencies at 1.5 mL enzyme loading, and further increments in enzyme dosage did not improve the removal efficiency. LP maintained effective removal at 25-30 ^{o}C whereas JP showed extended functionality up to 40 ^{o}C. The optimal retention times required to achieve maximum removal was 16 and 13 h for LP and JP respectively. First order enzyme kinetic analysis of LP and JP activities resulted in reaction rate constants 1.18 and 1.21h^{-1} respectively. JP also exhibited better storage stability than LP by demonstrating a more

stable performance in phenol degradation. Freshly prepared LP has better efficacy as LP is more susceptible to biological and physicochemical changes associated with prolong storage. With that, JP was selected as the peroxidase for further studies of optimization and immobilization. For optimization of phenol removal process using JP, three key process variables (pH, H_2O_2 concentration and enzyme loading) were evaluated for their effects on phenol removal efficiency via factorial and central composite designs. A characteristic second order model, validated with ANOVA at R^2 and R^2_{adj} values of 0.9817 and 0.9542 respectively, was generated to represent phenol removal efficiency. The most influential factors were determined as H_2O_2 concentration and pH. Accordingly, the optimal operating conditions for JP-catalyzed phenol removal were pH ~ 5.3-7, H_2O_2 concentrations ~ 4.3-7.9 mM, and an enzyme loading of 3 mL. These optimal conditions resulted in a phenol removal efficiency of 95%.

For Objective 2, NaCS-PDMDAAC polymeric capsules were synthesized and biophysically characterized for effective peroxidase binding and enhanced mass transport. NaCS was successfully synthesized through cellulose sulphation process which utilize cotton linter as source of cellulose. It was found out that 2% NaCS and 6% PDMDAAC gave uniform spherical capsules with mechanical strength of 1.12±0.35 N. The synthesis of capsules was carried out at 25 ^oC for ease of process control as well as cost saving. With regard to second research question of whether such peroxidase can be successfully immobilized onto NaCS-PDMDAAC polymeric capsules, it was demonstrated that the encapsulation efficiency of JP within this biopolymers was 87.4%. The JP beaded capsules had an average diameter of 5.05±0.16 mm and a membrane thickness of ~31 μm. SEM analysis showed that the inner surface of the capsule is much rougher than its outer surface, indicating the reactive surface distribution from the interaction between NaCS and PDMDAAC. Immobilization also markedly improved the pH stability of JP. Temperature stability of immobilized JP was comparable to free enzyme. Upon immobilization, the hydrodynamic size of JP molecules decreased slightly by ~24 nm while zeta potential were constant at -14 mV.

After immobilization, the performance of peroxidase-immobilized polymeric capsules for batch and continuous biodegradation of phenol was experimentally studied, and this addressed Objective 3 of the research project. Phenol biodegradation analysis showed that the free and immobilized JP capsules demonstrated optimum working pH

values of 7 and 6 respectively, and both systems maintained JP catalytic functionalities over a broad range of H_2O_2 concentration before H_2O_2 inhibition. The optimal temperature range for phenol removal was from 25-40 ^oC for both free and immobilized JP. Immobilized JP capsules required a longer reaction time of 15 h for optimal phenol removal efficiency of >95%, whilst free JP achieved the same efficiency in 13 h. The first order kinetic rate constants for free and immobilized JP capsules were determined to be 1.21 h^{-1} and 1.02 h^{-1}, respectively. JP capsules maintained reusability up to 4 cycles at the highest removal efficiency of >95% with no regeneration. For continuous biodegradation of phenol, a fluidized bed column was designed and custom-made. The performance of JP-immobilized NaCS-PDMDAAC capsules in the customized fluidized bed column was evaluated under the effects of flow rate and enzyme loading. From the three flow rates being studied, maximal phenol removal efficiency of 96% was achieved at flow rate 109.6 mL/min after 8 h of reaction by using 20 mL immobilized JP with an average enzymatic activity of 0.13 U/mL. The first order reaction rate constant at this flow rate was 0.349 h^{-1}. Phenol removal efficiency of 95.8% was achieved by 30 mL immobilized JP in 7 h. The enzymatic activity and first order reaction rate constant at this condition were 0.20 U/mL and 0.639 h^{-1} respectively. Under continuous phenol removal process, JP immobilized biopolymer capsules can be reused up to 8 cycles with a removal efficacy averaging at 95%. Comparatively, immobilized JP demonstrated better performance under continuous treatment of phenol in fluidized bed column than batch process as the reaction time was reduced from 15 to 7 h for >95% removal efficiency. Moreover, the reusability of immobilized JP under continuous mode was also greater than batch process. Nonetheless, it was clearly demonstrated that immobilized JP in NaCS-PDMDAAC capsules holds great potential to be alternative for phenol treatment under batch and continuous processes.

5.2 RECOMMENDATIONS

For future work, immobilized JP can be applied to actual wastewater to evaluate their efficiencies in treating phenolic compounds. Nonetheless, the wastewater needs to be pre-treated to remove the suspended solids as a conventional primary treatment approach. The effects of other soluble compounds present in wastewater on the performance of JP can also be studied.

The accuracy of current work can also be improved by using a high pressure liquid chromatography (HPLC) to analyse phenol concentration. A high pressure liquid chromatography-mass spectrometry (HPLC-MS) can also be used to identify and quantify any intermediate products and/or by-products from phenol oxidation and polymerisation process.

In addition, since the continuous treatment process is more practical in wastewater management, the work on enzyme-immobilized polymeric capsules in a column can be further improved. The customized column can be turned into a packed bed column, and its efficacy in phenol degradation be compared to the results from the fluidized bed technology developed in the current project. Simulation and mass transfer modelling can also be considered in order to better understand the transport mechanisms associated with the removal process. This work is necessary for establishing the application of enzyme-immobilized NaCS-PDMDAAC capsules for large-scale wastewater treatment in the future.

REFERENCES

Agarry, S., B. Solomon, and S. Layokun. 2008a. "Kinetics of Batch Microbial Degradation of Phenols by Indigenous Binary Mixed Culture of Pseudomonas Aeruginosa and Pseudomonas Fluorescence." *African Journal of Biotechnology* 7 (14).

Agarry, S., B. Solomon, and S. K. Layokun. 2008b. *Optimization of Process Variables for the Microbial Degradation of Phenol by Pseudomonas Aeruginosa Using Response Surface Methodology*. Vol. 7.

Aghelan, Z., and S. Z. S. Shariat. 2015. "Partial Purification and Biochemical Characterization of Peroxidase from Rosemary (Rosmarinus Officinalis L.) Leaves." *Advanced Biomedical Research* 4: 159.

Agostini, E., J. Hernandez-Ruiz, M. B. Arnao, S. R. Milrad, H. A. Tigier, and M. Acosta. 2002. "A Peroxidase Isoenzyme Secreted by Turnip (Brassica Napus) Hairy-Root Cultures: Inactivation by Hydrogen Peroxide and Application in Diagnostic Kits." *Biotechnology and Applied Biochemistry* 35 (Pt 1): 1-7.

Aitken, M. D. 1993. "Waste Treatment Applications of Enzymes: Opportunities and Obstacles." *The Chemical Engineering Journal* 52 (2): B49-B58.

Aitken, M. D., R. Venkatadri, and R. L. Irvine. 1989. "Oxidation of Phenolic Pollutants by a Lignin Degrading Enzyme from the White-Rot Fungus Phanerochaete Chrysosporium." *Water Research* 23 (4): 443-450.

Akhtar, S., A. Ali Khan, and Q. Husain. 2005. "Simultaneous Purification and Immobilization of Bitter Gourd (Momordica Charantia) Peroxidases on Bioaffinity Support." *Journal of Chemical Technology & Biotechnology* 80 (2): 198-205.

Akhtar, S., and Q. Husain. 2006. "Potential Applications of Immobilized Bitter Gourd (Momordica Charantia) Peroxidase in the Removal of Phenols from Polluted Water." *Chemosphere* 65 (7): 1228-1235.

Al-Kassim, L., K. E. Taylor, J. K. Bewtra, and N. Biswas. 1994. "Optimization of Phenol Removal by a Fungal Peroxidase from Coprinus Macrorhizus Using Batch, Continuous, and Discontinuous Semibatch Reactors." *Enzyme and Microbial Technology* 16 (2): 120-124.

al-Kassim, L., K. E. Taylor, J. A. Nicell, J. K. Bewtra, and N. Biswas. 1994. "Enzymatic Removal of Selected Aromatic Contaminants from Wastewater by a Fungal Peroxidase from Coprinus Macrorhizus in Batch Reactors." *J Chem Technol Biotechnol* 61 (2): 179-82.

Al-Senaidy, A. M., and M. A. Ismael. 2011. "Purification and Characterization of Membrane-Bound Peroxidase from Date Palm Leaves (Phoenix Dactylifera L.)." *Saudi Journal of Biological Sciences* 18 (3): 293-298.

Alam, M. Z., E. S. Ameem, S. A. Muyibi, and N. A. Kabbashi. 2009. "The Factors Affecting the Performance of Activated Carbon Prepared from Oil Palm Empty Fruit Bunches for Adsorption of Phenol." *Chemical Engineering Journal* 155 (1–2): 191-198.

Alemzadeh, I., and S. Nejati. 2009. "Phenols Removal by Immobilized Horseradish Peroxidase." *Journal of Hazardous materials* 166 (2–3): 1082-1086.

Alhamed, Y. A. 2009. "Adsorption Kinetics and Performance of Packed Bed Adsorber for Phenol Removal Using Activated Carbon from Dates' Stones." *Journal of Hazardous materials* 170 (2): 763-770.

Anderson, M. J., and P. J. Whitcomb. 2010. "Design of Experiments." In *Kirk-Othmer Encyclopedia of Chemical Technology*. John Wiley & Sons, Inc.

Andreescu, S., B. Bucur, and J.-L. Marty. 2006. "Affinity Immobilization of Tagged Enzymes." In *Immobilization of Enzymes and Cells*, ed. Jose M. Guisan, 97-106. Totowa, NJ: Humana Press.

Annadurai, G., L. Y. Ling, and J.-F. Lee. 2008. "Statistical Optimization of Medium Components and Growth Conditions by Response Surface Methodology to Enhance Phenol Degradation by Pseudomonas Putida." *Journal of Hazardous materials* 151 (1): 171-178.

Antonopoulos, V. T., M. Hernandez, M. E. Arias, E. Mavrakos, and A. S. Ball. 2001. "The Use of Extracellular Enzymes from Streptomyces Albus Atcc 3005 for the Bleaching of Eucalyptus Kraft Pulp." *Applied Microbiology and Biotechnology* 57 (1-2): 92-7.

Aranda, E., I. Sampedro, J. A. Ocampo, and I. García-Romera. 2006. "Phenolic Removal of Olive-Mill Dry Residues by Laccase Activity of White-Rot Fungi and Its Impact on Tomato Plant Growth." *International Biodeterioration & Biodegradation* 58 (3): 176-179.

Archana, V., K. M. Meera S. Begum, and N. Anantharaman. "Studies on Removal of Phenol Using Ionic Liquid Immobilized Polymeric Micro-Capsules." *Arabian Journal of Chemistry*.

Arnao, M. B., M. Acosta, J. A. del Rio, R. Varón, and F. García-Cánovas. 1990. "A Kinetic Study on the Suicide Inactivation of Peroxidase by Hydrogen Peroxide." *Biochimica et Biophysica Acta (BBA) - Protein Structure and Molecular Enzymology* 1041 (1): 43-47.

Asadgol, Z., H. Forootanfar, S. Rezaei, A. H. Mahvi, and M. A. Faramarzi. 2014. "Removal of Phenol and Bisphenol-a Catalyzed by Laccase in Aqueous Solution." *Journal of Environmental Health Science and Engineering* 12 (1): 93.

Ashraf, H., and Q. Husain. 2010. "Studies on Bitter Gourd Peroxidase Catalyzed Removal of P-Bromophenol from Wastewater." *Desalination* 262 (1–3): 267-272.

Babuponnusami, A., and K. Muthukumar. 2012. "Advanced Oxidation of Phenol: A Comparison between Fenton, Electro-Fenton, Sono-Electro-Fenton and Photo-Electro-Fenton Processes." *Chemical Engineering Journal* 183 (0): 1-9.

Banci, L., S. Ciofi-Baffoni, and M. Tien. 1999. "Lignin and Mn Peroxidase-Catalyzed Oxidation of Phenolic Lignin Oligomers." *Biochemistry* 38 (10): 3205-10.

Barbosa, E. F., F. J. Molina, F. M. Lopes, P. A. García-Ruíz, S. S. Caramori, and K. F. Fernandes. 2012. "Immobilization of Peroxidase onto Magnetite Modified Polyaniline." *The Scientific World Journal* 2012: 5.

Bayramoglu, G., A. Akbulut, and M. Yakup Arica. 2013. "Immobilization of Tyrosinase on Modified Diatom Biosilica: Enzymatic Removal of Phenolic Compounds from Aqueous Solution." *Journal of Hazardous materials* 244-245: 528-536.

Bayramoğlu, G., and M. Y. Arıca. 2008. "Enzymatic Removal of Phenol and P-Chlorophenol in Enzyme Reactor: Horseradish Peroxidase Immobilized on Magnetic Beads." *Journal of Hazardous materials* 156 (1–3): 148-155.

Bello, M. M., A. A. Abdul Raman, and M. Purushothaman. 2017. "Applications of Fluidized Bed Reactors in Wastewater Treatment – a Review of the Major Design and Operational Parameters." *Journal of Cleaner Production* 141: 1492-1514.

Bernards, M. A., W. D. Fleming, D. B. Llewellyn, R. Priefer, X. Yang, A. Sabatino, and G. L. Plourde. 1999. "Biochemical Characterization of the Suberization-Associated Anionic Peroxidase of Potato." *Plant Physiology* 121 (1): 135-146.

Besharati Vineh, M., A. A. Saboury, A. A. Poostchi, A. M. Rashidi, and K. Parivar. 2018. "Stability and Activity Improvement of Horseradish Peroxidase by Covalent Immobilization on Functionalized Reduced Graphene Oxide and Biodegradation of High Phenol Concentration." *International Journal of Biological Macromolecules* 106: 1314-1322.

Bezerra, M. A., R. E. Santelli, E. P. Oliveira, L. S. Villar, and L. A. Escaleira. 2008. "Response Surface Methodology (Rsm) as a Tool for Optimization in Analytical Chemistry." *Talanta* 76 (5): 965-977.

Bindhu, L. V., and E. T. Abraham. 2003. "Immobilization of Horseradish Peroxidase on Chitosan for Use in Nonaqueous Media." *Journal of Applied Polymer Science* 88 (6): 1456-1464.

Bódalo, A., J. Bastida, M. F. Máximo, M. C. Montiel, M. Gómez, and M. D. Murcia. 2008. "A Comparative Study of Free and Immobilized Soybean and Horseradish Peroxidases for 4-Chlorophenol Removal: Protective Effects of Immobilization." *Bioprocess and Biosystems Engineering* 31 (6): 587-593.

Bódalo, A., J. L. Gómez, E. Gómez, J. Bastida, and M. F. Máximo. 2006. "Comparison of Commercial Peroxidases for Removing Phenol from Water Solutions." *Chemosphere* 63 (4): 626-632.

Bódalo, A., J. L. Gómez, E. Gómez, A. M. Hidalgo, M. Gómez, and A. M. Yelo. 2006. "Removal of 4-Chlorophenol by Soybean Peroxidase and Hydrogen Peroxide in a Discontinuous Tank Reactor." *Desalination* 195 (1–3): 51-59.

Box, G. E. P., and K. B. Wilson. 1951. "On the Experimental Attainment of Optimum Conditions." *Journal of the Royal Statistical Society. Series B (Methodological)* 13 (1): 1-45.

Bradford, M. M. 1976. "A Rapid and Sensitive Method for the Quantitation of Microgram Quantities of Protein Utilizing the Principle of Protein-Dye Binding." *Analytical Biochemistry* 72 (1–2): 248-254.

Brena, B., and F. Batista-Viera. 2006. "Immobilization of Enzymes." In *Immobilization of Enzymes and Cells*, ed. JoseM Guisan, 15-30. Humana Press.

Burghate, S. P., and N. W. Ingole. 2013. *"Fluidized Bed Biofilm Reactor- a Novel Wastewater Treatment Reactor" (2013)*. Vol. 3.

Busca, G., S. Berardinelli, C. Resini, and L. Arrighi. 2008. "Technologies for the Removal of Phenol from Fluid Streams: A Short Review of Recent Developments." *Journal of Hazardous materials* 160 (2–3): 265-288.

Caetano, M., C. Valderrama, A. Farran, and J. L. Cortina. 2009. "Phenol Removal from Aqueous Solution by Adsorption and Ion Exchange Mechanisms onto Polymeric Resins." *Journal of Colloid and Interface Science* 338 (2): 402-9.

Caramori, S. S., and K. F. Fernandes. 2004. "Covalent Immobilisation of Horseradish Peroxidase onto Poly(Ethylene Terephthalate)–Poly(Aniline) Composite." *Process Biochemistry* 39 (7): 883-888.

Cardinali, A., N. Tursi, A. Ligorio, M. G. Giuffrida, L. Napolitano, R. Caliandro, L. Sergio, D. Di Venere, V. Lattanzio, and G. Sonnante. 2011. "Purification, Biochemical Characterization and Cloning of a New Cationic Peroxidase Isoenzyme from Artichoke." *Plant Physiology and Biochemistry* 49 (4): 395-403.

Casella, L., S. Poli, M. Gullotti, C. Selvaggini, T. Beringhelli, and A. Marchesini. 1994. "The Chloroperoxidase-Catalyzed Oxidation of Phenols. Mechanism,

Selectivity, and Characterization of Enzyme-Substrate Complexes." *Biochemistry* 33 (21): 6377-86.

Castillo, J., S. Gaspar, I. Sakharov, and E. Csoregi. 2003. "Bienzyme Biosensors for Glucose, Ethanol and Putrescine Built on Oxidase and Sweet Potato Peroxidase." *Biosensors and Bioelectronics* 18 (5-6): 705-14.

Caza, N., J. K. Bewtra, N. Biswas, and K. E. Taylor. 1999. "Removal of Phenolic Compounds from Synthetic Wastewater Using Soybean Peroxidase." *Water Research* 33 (13): 3012-3018.

Chagas, P. M. B., J. A. Torres, M. C. Silva, and A. D. Corrêa. 2015. "Immobilized Soybean Hull Peroxidase for the Oxidation of Phenolic Compounds in Coffee Processing Wastewater." *International Journal of Biological Macromolecules* 81: 568-575.

Chai, Y., L. H. Mei, G. L. Wu, D. Q. Lin, and S. J. Yao. 2004. "Gelation Conditions and Transport Properties of Hollow Calcium Alginate Capsules." *Biotechnology and Bioengineering* 87 (2): 228-33.

Chakraborty, S., T. Bhattacharya, T. N. Patel, and K. K. Tiwari. 2010. "Biodegradation of Phenol by Native Microorganisms Isolated from Coke Processing Wastewater." *Journal of Environment Biology* 31 (3): 293-6.

Chaudhary, N., and C. Balomajumder. 2014. "Optimization Study of Adsorption Parameters for Removal of Phenol on Aluminum Impregnated Fly Ash Using Response Surface Methodology." *Journal of the Taiwan Institute of Chemical Engineers* 45 (3): 852-859.

Chen, G., S.-j. Yao, Y.-x. Guan, and D.-q. Lin. 2005. "Preparation and Characterization of Nacs–Cmc/Pdmdaac Capsules." *Colloids and Surfaces B: Biointerfaces* 45 (3–4): 136-143.

Chen, G., B. Zhang, J. Zhao, and H. Chen. 2013. "Improved Process for the Production of Cellulose Sulfate Using Sulfuric Acid/Ethanol Solution." *Carbohydrate Polymers* 95 (1): 332-337.

Cheng, J., S. Ming Yu, and P. Zuo. 2006. "Horseradish Peroxidase Immobilized on Aluminum-Pillared Interlayered Clay for the Catalytic Oxidation of Phenolic Wastewater." *Water Research* 40 (2): 283-290.

Cho, S.-H., J. Shim, S.-H. Yun, and S.-H. Moon. 2008. "Enzyme-Catalyzed Conversion of Phenol by Using Immobilized Horseradish Peroxidase (Hrp) in a Membraneless Electrochemical Reactor." *Applied Catalysis A: General* 337 (1): 66-72.

Choquette-Labbé, M., W. Shewa, J. Lalman, and S. Shanmugam. 2014. *Photocatalytic Degradation of Phenol and Phenol Derivatives Using a Nano-Tio2 Catalyst: Integrating Quantitative and Qualitative Factors Using Response Surface Methodology*. Vol. 6.

Chu, L., J. Wang, J. Dong, H. Liu, and X. Sun. 2012. "Treatment of Coking Wastewater by an Advanced Fenton Oxidation Process Using Iron Powder and Hydrogen Peroxide." *Chemosphere* 86 (4): 409-414.

Civello, P. M., G. A. Martinez, A. R. Chaves, and M. C. Anon. 1995. "Peroxidase from Strawberry Fruit (Fragaria Ananassa Duch.): Partial Purification and Determination of Some Properties." *Journal of Agricultural and Food Chemistry* 43 (10): 2596-2601.

Cohen, S., P. A. Belinky, Y. Hadar, and C. G. Dosoretz. 2009. "Characterization of Catechol Derivative Removal by Lignin Peroxidase in Aqueous Mixture." *Bioresource Technology* 100 (7): 2247-2253.

Cooper, V. A., and J. A. Nicell. 1996. "Removal of Phenols from a Foundry Wastewater Using Horseradish Peroxidase." *Water Research* 30 (4): 954-964.

Costa, S., H. Azevedo, and R. L. Reis. 2005. *Enzyme Immobilization in Biodegradable Polymers for Biomedical Applications*.

Cruz-Silva, R., J. Romero-García, J. L. Angulo-Sánchez, A. Ledezma-Pérez, E. Arias-Marín, I. Moggio, and E. Flores-Loyola. 2005. "Template-Free Enzymatic Synthesis of Electrically Conducting Polyaniline Using Soybean Peroxidase." *European Polymer Journal* 41 (5): 1129-1135.

Dalal, S., and M. N. Gupta. 2007a. "Treatment of Phenolic Wastewater by Horseradish Peroxidase Immobilized by Bioaffinity Layering." *Chemosphere* 67 (4): 741-7.

Dalal, S., and M. N. Gupta. 2007b. "Treatment of Phenolic Wastewater by Horseradish Peroxidase Immobilized by Bioaffinity Layering." *Chemosphere* 67 (4): 741-747.

Datta, S., L. R. Christena, and Y. R. S. Rajaram. 2013. "Enzyme Immobilization: An Overview on Techniques and Support Materials." *3 Biotech* 3 (1): 1-9.

Dautzenberg, H., G. Arnold, B. Lukanoff, U. Eckert, and B. Tiersch. 1996. "Polyelectrolyte Complex Formation at the Interface of Solutions." In *Interfaces, Surfactants and Colloids in Engineering*, 149-156. Springer.

de Souza-Cruz, P. B., J. Freer, M. Siika-Aho, and A. Ferraz. 2004. "Extraction and Determination of Enzymes Produced by Ceriporiopsis Subvermispora During Biopulping of Pinus Taeda Wood Chips." *Enzyme and Microbial Technology* 34 (3): 228-234.

Dec, J., and J.-M. Bollag. 1994. "Use of Plant Material for the Decontamination of Water Polluted with Phenols." *Biotechnology and Bioengineering* 44 (9): 1132-1139.

Deepa, S. S., and C. Arumughan. 2002. "Purification and Characterization of Soluble Peroxidase from Oil Palm (Elaeis Guineensis Jacq.) Leaf." *Phytochemistry* 61 (5): 503-511.

Deva, A. N., C. Arun, G. Arthanareeswaran, and P. Sivashanmugam. 2014. "Extraction of Peroxidase from Waste Brassica Oleracea Used for the Treatment of Aqueous Phenol in Synthetic Waste Water." *Journal of Environmental Chemical Engineering* 2 (2): 1148-1154.

Duarte-Vázquez, M. A., B. E. García-Almendárez, C. Regalado, and J. R. Whitaker. 2001. "Purification and Properties of a Neutral Peroxidase Isozyme from Turnip (Brassica Napus L. Var. Purple Top White Globe) Roots." *Journal of Agricultural and Food Chemistry* 49 (9): 4450-4456.

Duarte-Vázquez, M. A., M. A. Ortega-Tovar, B. E. García-Almendarez, and C. Regalado. 2003. "Removal of Aqueous Phenolic Compounds from a Model System by Oxidative Polymerization with Turnip (Brassica Napus L Var Purple Top White Globe) Peroxidase." *Journal of Chemical Technology and Biotechnology* 78 (1): 42-47.

Duarte-Vázquez, M. A., M. A. Ortega-Tovar, B. E. García-Almendarez, and C. Regalado. 2003. "Removal of Aqueous Phenolic Compounds from a Model System by Oxidative Polymerization with Turnip (Brassica Napus L Var Purple Top White Globe) Peroxidase." *Journal of Chemical Technology and Biotechnology* 78 (1): 42-47.

Durán, N., and E. Esposito. 2000. "Potential Applications of Oxidative Enzymes and Phenoloxidase-Like Compounds in Wastewater and Soil Treatment: A Review." *Applied Catalysis B: Environmental* 28 (2): 83-99.

Eş, I., J. D. G. Vieira, and A. C. Amaral. 2015. "Principles, Techniques, and Applications of Biocatalyst Immobilization for Industrial Application." *Applied Microbiology and Biotechnology* 99 (5): 2065-2082.

Fatima, A., and Q. Husain. 2008. "Purification and Characterization of a Novel Peroxidase from Bitter Gourd (Momordica Charantia)." *Protein Pept Lett* 15 (4): 377-84.

Feng, W., K. E. Taylor, N. Biswas, and J. K. Bewtra. 2013. "Soybean Peroxidase Trapped in Product Precipitate During Phenol Polymerization Retains Activity and May Be Recycled." *Journal of Chemical Technology & Biotechnology* 88 (8): 1429-1435.

Ferreira, S. L. C., V. A. Lemos, V. S. de Carvalho, E. G. P. da Silva, A. F. S. Queiroz, C. S. A. Felix, D. L. F. da Silva, G. B. Dourado, and R. V. Oliveira. 2018. "Multivariate Optimization Techniques in Analytical Chemistry - an Overview." *Microchemical Journal*.

Firozjaee, T. T., G. D. Najafpour, A. Asgari, and M. Khavarpour. 2012. "Biological Treatment of Phenolic Wastewater in an Anaerobic Continuous Stirred Tank Reactor." *Chemical Industry & Chemical Engineering Quarterly* 19 (2): 173-179.

Fornera, S., T. E. Balmer, B. Zhang, A. D. Schlüter, and P. Walde. 2011. "Immobilization of Peroxidase on Sio2 Surfaces with the Help of a Dendronized Polymer and the Avidin-Biotin System." *Macromolecular Bioscience* 11 (8): 1052-1067.

Förster, M., J. Mansfeld, H. Dautzenberg, and A. Schellenberger. 1996. "Immobilization in Polyelectrolyte Complex Capsules: Encapsulation of a Gluconate-Oxidizing Serratia Marcescens Strain." *Enzyme and Microbial Technology* 19 (8): 572-577.

Galíndez-Mayer, J., J. Ramón-Gallegos, N. Ruiz-Ordaz, C. Juárez-Ramírez, A. Salmerón-Alcocer, and H. M. Poggi-Varaldo. 2008. "Phenol and 4-Chlorophenol Biodegradation by Yeast Candida Tropicalis in a Fluidized Bed Reactor." *Biochemical Engineering Journal* 38 (2): 147-157.

Gernjak, W., T. Krutzler, A. Glaser, S. Malato, J. Caceres, R. Bauer, and A. R. Fernández-Alba. 2003. "Photo-Fenton Treatment of Water Containing Natural Phenolic Pollutants." *Chemosphere* 50 (1): 71-78.

Ghaemmaghami, F., I. Alemzadeh, and S. Motamed. 2010. "Seed Coat Soybean Peroxidase: Extraction and Biocatalytic Properties Determination." *Iranian Journal of Chemical Engineering(IJChE)* 7 (2): 28-38.

Ghasempur, S., S.-F. Torabi, S.-O. Ranaei-Siadat, M. Jalali-Heravi, N. Ghaemi, and K. Khajeh. 2007. "Optimization of Peroxidase-Catalyzed Oxidative Coupling Process for Phenol Removal from Wastewater Using Response Surface Methodology." *Environmental Science & Technology* 41 (20): 7073-7079.

Ghioureliotis, M., and J. A. Nicell. 1999. "Assessment of Soluble Products of Peroxidase-Catalyzed Polymerization of Aqueous Phenol." *Enzyme and Microbial Technology* 25 (3–5): 185-193.

Gholami-Borujeni, F., A. H. Mahvi, S. Naseri, M. A. Faramarzi, R. Nabizadeh, and M. Alimohammadi. 2011. "Application of Immobilized Horseradish Peroxidase for Removal and Detoxification of Azo Dye from Aqueous Solution." *Res J Chem Environ* 15 (2): 217-222.

Gillikin, J. W., and J. S. Graham. 1991. "Purification and Developmental Analysis of the Major Anionic Peroxidase from the Seed Coat of Glycine Max." *Plant Physiology* 96 (1): 214-220.

Girish, C., and V. Ramachandra Murty. 2013. "Removal of Phenol from Wastewater in Packed Bed and Fluidized Bed Columns: A Review‖." *International Research Journal of Environment Sciences* 2 (10): 96-100.

Gómez, J. L., A. Bódalo, E. Gómez, J. Bastida, A. M. Hidalgo, and M. Gómez. 2006. "Immobilization of Peroxidases on Glass Beads: An Improved Alternative for Phenol Removal." *Enzyme and Microbial Technology* 39 (5): 1016-1022.

Gómez, J. L., A. Bódalo, E. Gómez, A. M. Hidalgo, M. Gómez, and M. D. Murcia. 2007. "Experimental Behaviour and Design Model of a Fluidized Bed Reactor with Immobilized Peroxidase for Phenol Removal." *Chemical Engineering Journal* 127 (1–3): 47-57.

Gómez, J. L., E. Gómez, J. Bastida, A. M. Hidalgo, M. Gómez, and M. D. Murcia. 2008. "Experimental Behaviour and Design Model of a Continuous Tank Reactor for Removing 4-Chlorophenol with Soybean Peroxidase." *Chemical Engineering and Processing: Process Intensification* 47 (9–10): 1786-1792.

Gomez, M., G. Matafonova, J. L. Gomez, V. Batoev, and N. Christofi. 2009. "Comparison of Alternative Treatments for 4-Chlorophenol Removal from Aqueous Solutions: Use of Free and Immobilized Soybean Peroxidase and Krcl Excilamp." *Journal of Hazardous materials* 169 (1–3): 46-51.

Gómez, M., M. D. Murcia, R. Dams, N. Christofi, E. Gómez, and J. L. Gómez. 2011. "Removal Efficiency and Toxicity Reduction of 4-Chlorophenol with Physical, Chemical and Biochemical Methods." *Environmental Technology* 33 (9): 1055-1064.

González, G., M. G. Herrera, M. T. García, and M. M. Peña. 2001. "Biodegradation of Phenol in a Continuous Process: Comparative Study of Stirred Tank and Fluidized-Bed Bioreactors." *Bioresource Technology* 76 (3): 245-251.

González, P. S., E. Agostini, and S. R. Milrad. 2008. "Comparison of the Removal of 2,4-Dichlorophenol and Phenol from Polluted Water, by Peroxidases from Tomato Hairy Roots, and Protective Effect of Polyethylene Glycol." *Chemosphere* 70 (6): 982-989.

González, P. S., C. E. Capozucca, H. A. Tigier, S. R. Milrad, and E. Agostini. 2006. "Phytoremediation of Phenol from Wastewater, by Peroxidases of Tomato Hairy Root Cultures." *Enzyme and Microbial Technology* 39 (4): 647-653.

Grabski, A. C., H. J. Grimek, and R. R. Burgess. 1998. "Immobilization of Manganese Peroxidase from Lentinula Edodes and Its Biocatalytic Generation of Mniii-Chelate as a Chemical Oxidant of Chlorophenols." *Biotechnology and Bioengineering* 60 (2): 204-15.

Halaouli, S., M. Asther, J. C. Sigoillot, M. Hamdi, and A. Lomascolo. 2006. "Fungal Tyrosinases: New Prospects in Molecular Characteristics, Bioengineering and Biotechnological Applications." *J Appl Microbiol* 100 (2): 219-32.

Hameed, B. H., and A. A. Rahman. 2008. "Removal of Phenol from Aqueous Solutions by Adsorption onto Activated Carbon Prepared from Biomass Material." *Journal of Hazardous materials* 160 (2–3): 576-581.

Hameed, B. H., I. A. W. Tan, and A. L. Ahmad. 2009. "Preparation of Oil Palm Empty Fruit Bunch-Based Activated Carbon for Removal of 2,4,6-Trichlorophenol: Optimization Using Response Surface Methodology." *Journal of Hazardous materials* 164 (2): 1316-1324.

Hamid, M., and K. u. Rehman. 2009. "Potential Applications of Peroxidases." *Food Chemistry* 115 (4): 1177-1186.

Haribabu, K., and V. Sivasubramanian. 2016. "Biodegradation of Organic Content in Wastewater in Fluidized Bed Bioreactor Using Low-Density Biosupport." *Desalination and Water Treatment* 57 (10): 4322-4327.

Henriksen, A., A. T. Smith, and M. Gajhede. 1999. "The Structures of the Horseradish Peroxidase C-Ferulic Acid Complex and the Ternary Complex with Cyanide Suggest How Peroxidases Oxidize Small Phenolic Substrates." *Journal of Biological Chemistry* 274 (49): 35005-11.

Hiraga, S., K. Sasaki, H. Ito, Y. Ohashi, and H. Matsui. 2001. "A Large Family of Class Iii Plant Peroxidases." *Plant Cell Physiol* 42 (5): 462-8.

Hosseinzadeh, R., K. Khorsandi, and S. Hemmaty. 2013. "Study of the Effect of Surfactants on Extraction and Determination of Polyphenolic Compounds and Antioxidant Capacity of Fruits Extracts." *PLoS One* 8 (3): e57353.

Huang, C.-P., and Y.-H. Huang. 2009. "Application of an Active Immobilized Iron Oxide with Catalytic H2o2 for the Mineralization of Phenol in a Batch Photo-Fluidized Bed Reactor." *Applied Catalysis A: General* 357 (2): 135-141.

Husain, Q., and R. Ulber. 2011. *Immobilized Peroxidase as a Valuable Tool in the Remediation of Aromatic Pollutants and Xenobiotic Compounds: A Review*. Vol. 41.

Ikehata, K., I. D. Buchanan, M. A. Pickard, and D. W. Smith. 2005. "Purification, Characterization and Evaluation of Extracellular Peroxidase from Two Coprinus Species for Aqueous Phenol Treatment." *Bioresource Technology* 96 (16): 1758-1770.

Ikehata, K., and J. A. Nicell. 2000. "Characterization of Tyrosinase for the Treatment of Aqueous Phenols." *Bioresource Technology* 74 (3): 191-199.

Ito, H., N. Hiraoka, A. Ohbayashi, and Y. Ohashi. 1991. "Purification and Characterization of Rice Peroxidases." *Agric Biol Chem* 55 (10): 2445-54.

Jafarzadeh, N. K., S. Sharifnia, S. N. Hosseini, and F. Rahimpour. 2011. "Statistical Optimization of Process Conditions for Photocatalytic Degradation of Phenol with Immobilization of Nano Tio2 on Perlite Granules." *Korean Journal of Chemical Engineering* 28 (2): 531-538.

Jia, J., B. Wang, A. Wu, G. Cheng, Z. Li, and S. Dong. 2002. "A Method to Construct a Third-Generation Horseradish Peroxidase Biosensor: Self-Assembling Gold Nanoparticles to Three-Dimensional Sol−Gel Network." *Analytical Chemistry* 74 (9): 2217-2223.

Jiang, Y., W. Tang, J. Gao, L. Zhou, and Y. He. 2014. "Immobilization of Horseradish Peroxidase in Phospholipid-Templated Titania and Its Applications in Phenolic Compounds and Dye Removal." *Enzyme and Microbial Technology* 55: 1-6.

Kalaiarasan, E., and T. Palvannan. 2014. "Removal of Phenols from Acidic Environment by Horseradish Peroxidase (Hrp): Aqueous Thermostabilization of Hrp by Polysaccharide Additives." *Journal of the Taiwan Institute of Chemical Engineers* 45 (2): 625-634.

Kalin, R., A. Atasever, and H. Ozdemir. 2014. "Single-Step Purification of Peroxidase by 4-Aminobenzohydrazide from Turkish Blackradish and Turnip Roots." *Food Chemistry* 150: 335-40.

Kallel, M., C. Belaid, R. Boussahel, M. Ksibi, A. Montiel, and B. Elleuch. 2009. "Olive Mill Wastewater Degradation by Fenton Oxidation with Zero-Valent Iron and Hydrogen Peroxide." *Journal of Hazardous materials* 163 (2): 550-554.

Kamal, J. K. A., and D. V. Behere. 2008. "Kinetic Stabilities of Soybean and Horseradish Peroxidases." *Biochemical Engineering Journal* 38 (1): 110-114.

Kang, G., and D. Stevens. 1994. *Degradation of Pentachlorophenol in Bench Scale Bioreactors Using the White Rot Fungus Phanerochaete Chrysosporium*. Vol. 11.

Karam, J., and J. A. Nicell. 1997. "Potential Applications of Enzymes in Waste Treatment." *Journal of Chemical Technology & Biotechnology* 69 (2): 141-153.

Kariminiaae-Hamedaani, H.-R., A. Sakurai, and M. Sakakibara. 2007. "Decolorization of Synthetic Dyes by a New Manganese Peroxidase-Producing White Rot Fungus." *Dyes and Pigments* 72 (2): 157-162.

Kauffmann, C., B. R. Petersen, and M. J. Bjerrum. 1999. "Enzymatic Removal of Phenols from Aqueous Solutions by Coprinus Cinereus Peroxidase and Hydrogen Peroxide." *Journal of Biotechnology* 73 (1): 71-4.

Kawatsu, K., Y. Hamano, A. Sugiyama, K. Hashizume, and T. Noguchi. 2002. "Development and Application of an Enzyme Immunoassay Based on a Monoclonal Antibody against Gonyautoxin Components of Paralytic Shellfish Poisoning Toxins." *Journal of Food Protection* 65 (8): 1304-8.

Kennedy, K., K. Alemany, and M. Warith. 2002. "Optimisation of Soybean Peroxidase Treatment of 2, 4-Dichlorophenol." *Water SA* 28 (2): 149-158.

Khuri, A. I. 2006. *Response Surface Methodology and Related Topics*: World scientific.

Kim, S. S., and D. J. Lee. 2005. "Purification and Characterization of a Cationic Peroxidase Cs in Raphanus Sativus." *J Plant Physiol* 162 (6): 609-17.

Kim, Y.-J., K. Shibata, H. Uyama, and S. Kobayashi. 2008. "Synthesis of Ultrahigh Molecular Weight Phenolic Polymers by Enzymatic Polymerization in the Presence of Amphiphilic Triblock Copolymer in Water." *Polymer* 49 (22): 4791-4795.

Kim, Y. H., E. S. An, S. Y. Park, J.-O. Lee, J. H. Kim, and B. K. Song. 2007. "Polymerization of Bisphenol a Using Coprinus Cinereus Peroxidase (Cip) and Its Application as a Photoresist Resin." *Journal of Molecular Catalysis B: Enzymatic* 44 (3): 149-154.

Kim, Y. H., E. S. An, B. K. Song, D. S. Kim, and R. Chelikani. 2003. "Polymerization of Cardanol Using Soybean Peroxidase and Its Potential Application as Anti-Biofilm Coating Material." *Biotechnology Letters* 25 (18): 1521-4.

Kinsley, C., and J. A. Nicell. 2000. "Treatment of Aqueous Phenol with Soybean Peroxidase in the Presence of Polyethylene Glycol." *Bioresource Technology* 73 (2): 139-146.

Klibanov, A. M., B. N. Alberti, E. D. Morris, and L. M. Felshin. 1980. "Enzymatic Removal of Toxic Phenols and Anilines from Waste Waters." *Journal of Applied Biochemistry* 2: 414-421.

Klibanov, A. M., and E. D. Morris. 1981. "Horseradish Peroxidase for the Removal of Carcinogenic Aromatic Amines from Water." *Enzyme and Microbial Technology* 3 (2): 119-122.

Klibanov, A. M., T. M. Tu, and K. P. Scott. 1983. "Peroxidase-Catalyzed Removal of Phenols from Coal-Conversion Waste Waters." *Science* 221 (4607): 259-61.

Köktepe, T., S. Altın, H. Tohma, İ. Gülçin, and E. Köksal. 2017. "Purification, Characterization and Selected Inhibition Properties of Peroxidase from Haricot Bean (Phaseolus Vulgaris L.)." *International Journal of Food Properties*: 1-10.

Krastanov, A., Z. Alexieva, and H. Yemendzhiev. 2013. "Microbial Degradation of Phenol and Phenolic Derivatives." *Engineering in Life Sciences* 13 (1): 76-87.

Kulshrestha, Y., and Q. Husain. 2006a. "Bioaffinity-Based an Inexpensive and High Yield Procedure for the Immobilization of Turnip (Brassica Rapa) Peroxidase." *Biomolecular Engineering* 23 (6): 291-297.

———. 2006b. "Direct Immobilization of Peroxidase on Deae Cellulose from Ammonium Sulphate Fractionated Proteins of Bitter Gourd (Momordica Charantia)." *Enzyme and Microbial Technology* 38 (3): 470-477.

La Rotta Hernández, C. E., E. D'Elia, and E. P. S. Bon. 2007. *Chloroperoxidase Mediated Oxidation of Chlorinated Phenols Using Electrogenerated Hydrogen Peroxide* [biodegradation, bioelectrochemistry, Caldariomyces fumago, chlorinated phenols, chloroperoxidase, hydrogen peroxide electrogeneration], *2007*.

Laemmli, U. K. 1970. "Cleavage of Structural Proteins During the Assembly of the Head of Bacteriophage T4." *Nature* 227: 680.

Lai, Y.-C., and S.-C. Lin. 2005. "Application of Immobilized Horseradish Peroxidase for the Removal of P-Chlorophenol from Aqueous Solution." *Process Biochemistry* 40 (3–4): 1167-1174.

Lankalapalli, S., and V. R. M. Kolapalli. 2009. "Polyelectrolyte Complexes: A Review of Their Applicability in Drug Delivery Technology." *Indian Journal of Pharmaceutical Sciences* 71 (5): 481-487.

Lee, M. Y., and S. S. Kim. 1994. "Characteristics of Six Isoperoxidases from Korean Radish Root." *Phytochemistry* 35 (2): 287-290.

Lee, W. J., M. K. Shin, S. B. Cha, and H. S. Yoo. 2013. "Development of a Novel Enzyme-Linked Immunosorbent Assay to Detect Anti-Igg against Swine Hepatitis E Virus." *Journal of Veterinary Science* 14 (4): 467-472.

Leon, J. C., I. S. Alpeeva, T. A. Chubar, I. Y. Galaev, E. Csoregi, and I. Y. Sakharov. 2002. "Purification and Substrate Specificity of Peroxidase from Sweet Potato Tubers." *Plant Science* 163 (5): 1011-1019.

Li, M.-M., and S.-J. Yao. 2009. "Preparation of Polyelectrolyte Complex Membranes Based on Sodium Cellulose Sulfate and Poly(Dimethyldiallylammonium Chloride) and Its Permeability Properties." *Journal of Applied Polymer Science* 112 (1): 402-409.

Lin, S.-H., and R.-S. Juang. 2009. "Adsorption of Phenol and Its Derivatives from Water Using Synthetic Resins and Low-Cost Natural Adsorbents: A Review." *Journal of Environmental Management* 90 (3): 1336-1349.

Liu, J., Y. Ren, and S. Yao. 2010. "Repeated-Batch Cultivation of Encapsulated Monascus Purpureus by Polyelectrolyte Complex for Natural Pigment Production." *Chinese Journal of Chemical Engineering* 18 (6): 1013-1017.

Liu, N., G. Liang, X. Dong, X. Qi, J. Kim, and Y. Piao. 2016. "Stabilized Magnetic Enzyme Aggregates on Graphene Oxide for High Performance Phenol and Bisphenol a Removal." *Chemical Engineering Journal* 306: 1026-1034.

Liu, Y., Z. Zeng, G. Zeng, L. Tang, Y. Pang, Z. Li, C. Liu, X. Lei, M. Wu, P. Ren, Z. Liu, M. Chen, and G. Xie. 2012. "Immobilization of Laccase on Magnetic Bimodal Mesoporous Carbon and the Application in the Removal of Phenolic Compounds." *Bioresource Technology* 115: 21-26.

Liu, Z., W. Xie, D. Li, Y. Peng, Z. Li, and S. Liu. 2016. "Biodegradation of Phenol by Bacteria Strain Acinetobacter Calcoaceticus Pa Isolated from Phenolic Wastewater." *International Journal of Environmental Research and Public Health* 13 (3): 300.

Liu, Z. F., G. M. Zeng, H. Zhong, X. Z. Yuan, H. Y. Fu, M. F. Zhou, X. L. Ma, H. Li, and J. B. Li. 2012. "Effect of Dirhamnolipid on the Removal of Phenol

Catalyzed by Laccase in Aqueous Solution." *World Journal of Microbiology and Biotechnology* 28 (1): 175-81.

Lohr, M., F. Hummel, G. Faulmann, J. Ringel, R. Saller, J. Hain, W. H. Gunzburg, and B. Salmons. 2002. "Microencapsulated, Cyp2b1-Transfected Cells Activating Ifosfamide at the Site of the Tumor: The Magic Bullets of the 21st Century." *Cancer Chemother Pharmacol* 49 Suppl 1: S21-4.

Lua, A. C., and Q. Jia. 2009. "Adsorption of Phenol by Oil–Palm-Shell Activated Carbons in a Fixed Bed." *Chemical Engineering Journal* 150 (2–3): 455-461.

Lundstedt, T., E. Seifert, L. Abramo, B. Thelin, Å. Nyström, J. Pettersen, and R. Bergman. 1998. "Experimental Design and Optimization." *Chemometrics and intelligent laboratory systems* 42 (1-2): 3-40.

Majeau, J.-A., S. K. Brar, and R. D. Tyagi. 2010. "Laccases for Removal of Recalcitrant and Emerging Pollutants." *Bioresource Technology* 101 (7): 2331-2350.

Manimekalai, R., and T. Swaminathan. 2000. "Removal of Hazardous Compounds by Lignin Peroxidase from Phanerochaete Chrysosporium." *Bioprocess Engineering* 22 (1): 29-33.

Mao, L., S. Luo, Q. Huang, and J. Lu. 2013. "Horseradish Peroxidase Inactivation: Heme Destruction and Influence of Polyethylene Glycol." *Scientific Reports* 3: 3126.

Marangoni, A. G., E. D. Brown, D. W. Stanley, and R. Y. Yada. 1989. "Tomato Peroxidase: Rapid Isolation and Partial Characterization." *Journal of Food Science* 54 (5): 1269-1271.

Marrot, B., A. Barrios-Martinez, P. Moulin, and N. Roche. 2006. "Biodegradation of High Phenol Concentration by Activated Sludge in an Immersed Membrane Bioreactor." *Biochemical Engineering Journal* 30 (2): 174-183.

Martin, C. R., and P. Kohli. 2003. "The Emerging Field of Nanotube Biotechnology." *Nat Rev Drug Discov* 2 (1): 29-37.

Martínková, L., and M. Chmátal. 2016. "The Integration of Cyanide Hydratase and Tyrosinase Catalysts Enables Effective Degradation of Cyanide and Phenol in Coking Wastewaters." *Water Research* 102: 90-95.

Masuda, M., A. Sakurai, and M. Sakakibara. 2001. "Effect of Reaction Conditions on Phenol Removal by Polymerization and Precipitation Using Coprinus Cinereus Peroxidase." *Enzyme and Microbial Technology* 28 (4-5): 295-300.

Masuda, M., A. Sakurai, and M. Sakakibara. 2002. *Effect of Temperature and Ph on Phenol Removal Using Purified Coprinus Cinereus Peroxidase*. Vol. 18.

Mateo, C., J. M. Palomo, G. Fernandez-Lorente, J. M. Guisan, and R. Fernandez-Lafuente. 2007. "Improvement of Enzyme Activity, Stability and Selectivity Via Immobilization Techniques." *Enzyme and Microbial Technology* 40 (6): 1451-1463.

Mathews, P. G. 2005. *Design of Experiments with Minitab*: ASQ Quality Press.

Matto, M., and Q. Husain. 2009. "Calcium Alginate–Starch Hybrid Support for Both Surface Immobilization and Entrapment of Bitter Gourd (Momordica Charantia) Peroxidase." *Journal of Molecular Catalysis B: Enzymatic* 57 (1): 164-170.

McEldoon, J. P., and J. S. Dordick. 1996. "Unusual Thermal Stability of Soybean Peroxidase." *Biotechnology Progress* 12 (4): 555-558.

Mei, L. H., and S. J. Yao. 2002. "Cultivation and Modelling of Encapsulated Saccharomyces Cerevisiae in Nacs-Pdmdaac Polyelectrolyte Complexes." *J Microencapsul* 19 (4): 397-405.

Meka, V. S., M. K. G. Sing, M. R. Pichika, S. R. Nali, V. R. M. Kolapalli, and P. Kesharwani. 2017. "A Comprehensive Review on Polyelectrolyte Complexes." *Drug Discovery Today* 22 (11): 1697-1706.

Michałowicz, J., and W. Duda. 2007. "Phenols--Sources and Toxicity." *Polish Journal of Environmental Studies* 16 (3).

Mohamad, N. R., N. H. C. Marzuki, N. A. Buang, F. Huyop, and R. A. Wahab. 2015. "An Overview of Technologies for Immobilization of Enzymes and Surface Analysis Techniques for Immobilized Enzymes." *Biotechnology, Biotechnological Equipment* 29 (2): 205-220.

Mohamed, S. A., A. A. Darwish, and R. M. El-Shishtawy. 2013. "Immobilization of Horseradish Peroxidase on Activated Wool." *Process Biochemistry* 48 (4): 649-655.

Mohanty, K., D. Das, and M. N. Biswas. 2008. "Treatment of Phenolic Wastewater in a Novel Multi-Stage External Loop Airlift Reactor Using Activated Carbon." *Separation and Purification Technology* 58 (3): 311-319.

Mokhtar, Z., N. A. H. Hairul, H. M. R. Akmal, and M. Abdul Rahman. 2011. *Photocatalytic Degradation of Phenol in a Fluidized Bed Reactor Utilizing Immobilized Tio2 Photocatalyst: Characterization and Process Studies*. Vol. 11.

Monier, M., D. M. Ayad, Y. Wei, and A. A. Sarhan. 2010. "Immobilization of Horseradish Peroxidase on Modified Chitosan Beads." *International Journal of Biological Macromolecules* 46 (3): 324-330.

Montgomery, D. C. 2017. *Design and Analysis of Experiments*: John wiley & sons.

Morán, J. I., V. A. Alvarez, V. P. Cyras, and A. Vázquez. 2008. "Extraction of Cellulose and Preparation of Nanocellulose from Sisal Fibers." 15 (1): 149-159.

Motamed, S., F. Ghaemmaghami, and I. Alemzadeh. 2009. "Turnip (Brassica Rapa) Peroxidase: Purification and Characterization." *Industrial & Engineering Chemistry Research* 48 (23): 10614-10618.

Muangthai, I., C. Ratanatamskul, and M.-C. Lu. 2010. *Removal of 2,4-Dichlorophenol by Fluidized-Bed Fenton Process*. Vol. 20.

Murugesan, T., and R. Y. Sheeja. 2005. "A Correlation for the Mass Transfer Coefficients During the Biodegradation of Phenolic Effluents in a Packed Bed Reactor." *Separation and Purification Technology* 42 (2): 103-110.

MWA. 1994. *Malaysian Water Association: Design Guidelines for Water Supply Systems*. Kuala Lumpur, Malaysia: Malaysian Water Association.

Nakamoto, S., and N. Machida. 1992. "Phenol Removal from Aqueous Solutions by Peroxidase-Catalyzed Reaction Using Additives." *Water Research* 26 (1): 49-54.

Nazi, M., R. M. A. Malek, and R. Kotek. 2012. "Modification of B-Cyclodextrin with Itaconic Acid and Application of the New Derivative to Cotton Fabrics." *Carbohydrate Polymers* 88 (3): 950-958.

Nicell, J. A. 1994. "Kinetics of Horseradish Peroxidase-Catalysed Polymerization and Precipitation of Aqueous 4-Chlorophenol." *Journal of Chemical Technology and Biotechnology* 60 (2): 203-215.

Nicell, J. A., L. Al-Kassim, J. Bewtra, and K. Taylor. 1993. "Wastewater Treatment by Enzyme Catalysed Polymerization and Precipitation" *Biodeterioration Abstracts*,

Nicell, J. A., J. Bewtra, K. Taylor, N. Biswas, and C. StPierre. 1992. "Enzyme Catalyzed Polymerization and Precipitation of Aromatic Compounds from Wastewater." *Water Science & Technology* 25 (3): 157-164.

Nicell, J. A., J. K. Bewtra, N. Biswas, C. C. St. Pierre, and K. E. Taylor. 1993. "Enzyme Catalyzed Polymerization and Precipitation of Aromatic Compounds from Aqueous Solution." *Canadian Journal of Civil Engineering* 20 (5): 725-735.

Nicell, J. A., J. K. Bewtra, N. Biswas, and E. Taylor. 1993. "Reactor Development for Peroxidase Catalyzed Polymerization and Precipitation of Phenols from Wastewater." *Water Research* 27 (11): 1629-1639.

Nicell, J. A., K. W. Saadi, and I. D. Buchanan. 1995. "Phenol Polymerization and Precipitation by Horseradish Peroxidase Enzyme and an Additive." *Bioresource Technology* 54 (1): 5-16.

Nickheslat, A., M. M. Amin, H. Izanloo, A. Fatehizadeh, and S. M. Mousavi. 2013. "Phenol Photocatalytic Degradation by Advanced Oxidation Process under Ultraviolet Radiation Using Titanium Dioxide." *Journal of Environmental and Public Health* 2013: 815310.

Niladevi, K. N., and P. Prema. 2008. "Immobilization of Laccase from Streptomyces Psammoticus and Its Application in Phenol Removal Using Packed Bed Reactor." *World Journal of Microbiology and Biotechnology* 24 (7): 1215-1222.

Nisha, S., A. Karthick, and N. Gobi. 2012. "A Review on Methods, Application and Properties of Immobilized Enzyme." *Chemical Science Review and Letters* 1 (3): 148-155.

Ochieng, A., J. O. Odiyo, and M. Mutsago. 2003. "Biological Treatment of Mixed Industrial Wastewaters in a Fluidised Bed Reactor." *Journal of Hazardous materials* 96 (1): 79-90.

OSHA. 2018. Occupational Safety and Health Administration: Osha Annotated Table Z-1. Accessed 6 August, https://www.osha.gov/dsg/annotated-pels/tablez-1.html#annotated_table_Z-1.

Passardi, F., C. Cosio, C. Penel, and C. Dunand. 2005. "Peroxidases Have More Functions Than a Swiss Army Knife." *Plant Cell Rep* 24 (5): 255-65.

Peings, V., J. Frayret, and T. Pigot. 2015. "Mechanism for the Oxidation of Phenol by Sulfatoferrate(Vi): Comparison with Various Oxidants." *Journal of Environment Management* 157: 287-96.

Pezzotti, F., K. Okrasa, and M. Therisod. 2004. "Oxidation of Chlorophenols Catalyzed by Coprinus Cinereus Peroxidase with in Situ Production of Hydrogen Peroxide." *Biotechnol Prog* 20 (6): 1868-71.

Pigatto, G., A. Lodi, B. Aliakbarian, A. Converti, R. M. G. da Silva, and M. S. A. Palma. 2013. "Phenol Oxidation by Mushroom Waste Extracts: A Kinetic and Thermodynamic Study." *Bioresource Technology* 143: 678-681.

Pina, D. G., A. V. Shnyrova, F. Gavilanes, A. Rodríguez, F. Leal, M. G. Roig, I. Y. Sakharov, G. G. Zhadan, E. Villar, and V. L. Shnyrov. 2001. "Thermally Induced Conformational Changes in Horseradish Peroxidase." *European Journal of Biochemistry* 268 (1): 120-126.

Pradeep, N. V., S. Anupama, K. Navya, H. N. Shalini, M. Idris, and U. S. Hampannavar. 2015. "Biological Removal of Phenol from Wastewaters: A Mini Review." *Applied Water Science* 5 (2): 105-112.

Prashanthakumar, T. K. M., S. K. Ashok Kumar, and S. K. Sahoo. 2018. "A Quick Removal of Toxic Phenolic Compounds Using Porous Carbon Prepared from

Renewable Biomass Coconut Spathe and Exploration of New Source for Porous Carbon Materials." *Journal of Environmental Chemical Engineering* 6 (1): 1434-1442.

Quintanilla-Guerrero, F., M. A. Duarte-Vázquez, B. E. García-Almendarez, R. Tinoco, R. Vazquez-Duhalt, and C. Regalado. 2008. "Polyethylene Glycol Improves Phenol Removal by Immobilized Turnip Peroxidase." *Bioresource Technology* 99 (18): 8605-8611.

Quintanilla-Guerrero, F., M. A. Duarte-Vázquez, R. Tinoco, M. Gomez-Suarez, B. E. Garcia-Almendarez, R. Vazquez-Duhalt, and C. Regalado. 2008. "Chemical Modification of Turnip Peroxidase with Methoxypolyethylene Glycol Enhances Activity and Stability for Phenol Removal Using the Immobilized Enzyme." *Journal of Agricultural and Food Chemistry* 56 (17): 8058-65.

Rathinam, A., J. R. Rao, and B. U. Nair. 2011. "Adsorption of Phenol onto Activated Carbon from Seaweed: Determination of the Optimal Experimental Parameters Using Factorial Design." *Journal of the Taiwan Institute of Chemical Engineers* 42 (6): 952-956.

Regalado, C., B. García-Almendárez, and M. Duarte-Vázquez. 2004. "Biotechnological Applications of Peroxidases." *Phytochemistry Reviews* 3 (1-2): 243-256.

Rezvani, F., H. Azargoshasb, O. Jamialahmadi, S. Hashemi-Najafabadi, S. M. Mousavi, and S. A. Shojaosadati. 2015. "Experimental Study and Cfd Simulation of Phenol Removal by Immobilization of Soybean Seed Coat in a Packed-Bed Bioreactor." *Biochemical Engineering Journal* 101: 32-43.

Rezvani, F., S. Hashemi-Najafabadi, S. M. Mousavi, S. A. Shojaosadati, and S. Saharkhiz. 2012. "Optimization of the Removal of Phenol by Soybean Seed Coats Using Response Surface Methodology." *Water Sci Technol* 66 (10): 2229-36.

Rodríguez Couto, S., and J. L. Toca Herrera. 2006. "Industrial and Biotechnological Applications of Laccases: A Review." *Biotechnology Advances* 24 (5): 500-513.

Ruttimann-Johnson, C., and R. T. Lamar. 1996. "Polymerization of Pentachlorophenol and Ferulic Acid by Fungal Extracellular Lignin-Degrading Enzymes." *Applied and Environment Microbiology* 62 (10): 3890-3.

Ryan, D., W. Leukes, and S. Burton. 2007. "Improving the Bioremediation of Phenolic Wastewaters by Trametes Versicolor." *Bioresource Technology* 98 (3): 579-587.

Sahare, P., M. Ayala, R. Vazquez-Duhalt, and V. Agrawal. 2014. "Immobilization of Peroxidase Enzyme onto the Porous Silicon Structure for Enhancing Its Activity and Stability." *Nanoscale Research Letters* 9 (1): 409-409.

Sahoo, N. K., K. Pakshirajan, and P. K. Ghosh. 2011. "Biodegradation of P-Nitrophenol Using Arthrobacter Chlorophenolicus A6 in a Novel Upflow Packed Bed Reactor." *Journal of Hazardous materials* 190 (1–3): 729-737.

Said, M., A. Ahmad, and A. W. Mohammad. 2013. "Removal of Phenol During Ultrafiltration of Palm Oil Mill Effluent (Pome): Effect of Ph, Ionic Strength, Pressure and Temperature." *Der Pharma Chemica* 5 (3): 190-196.

Sakharov, I. Y., J. L. Castillo, J. C. Areza, and I. Y. Galaev. 2000. "Purification and Stability of Peroxidase of African Oil Palm Elaies Guineensis." *Bioseparation* 9 (3): 125-132.

Sakharov, I. Y., M. K. Vesgac B, I. Y. Galaev, I. V. Sakharova, and O. Y. Pletjushkina. 2001. "Peroxidase from Leaves of Royal Palm Tree Roystonea Regia: Purification and Some Properties." *Plant Science* 161 (5): 853-860.

Salgin, S., U. Salgin, and S. Bahadir. 2012. "Zeta Potentials and Isoelectric Points of Biomolecules: The Effects of Ion Types and Ionic Strengths." *Int. J. Electrochem. Sci* 7 (12): 12404-12414.

Saller, R. M., S. Indraccolo, V. Coppola, G. Esposito, J. Stange, S. Mitzner, A. Amadori, B. Salmons, and W. H. Gunzburg. 2002. "Encapsulated Cells Producing Retroviral Vectors for in Vivo Gene Transfer." *J Gene Med* 4 (2): 150-60.

Sardar, M., I. Roy, and M. N. Gupta. 2000. "Simultaneous Purification and Immobilization of Aspergillus Niger Xylanase on the Reversibly Soluble Polymer Eudragit Tm L-100." *Enzyme and Microbial Technology* 27 (9): 672-679.

Sharma, S., N. Sehgal, and A. Kumar. 2002. "A Quick and Simple Biostrip Technique for Detection of Lactose." *Biotechnology Letters* 24 (20): 1737-1739.

Sheeja, R. Y., and T. Murugesan. 2002. "Mass Transfer Studies on the Biodegradation of Phenols in up-Flow Packed Bed Reactors." *Journal of Hazardous materials* 89 (2–3): 287-301.

Sheldon, R. A. 2007. "Enzyme Immobilization: The Quest for Optimum Performance." *Advanced Synthesis & Catalysis* 349 (8-9): 1289-1307.

Shen, Q., R. Yang, X. Hua, F. Ye, W. Zhang, and W. Zhao. 2011. "Gelatin-Templated Biomimetic Calcification for B-Galactosidase Immobilization." *Process Biochemistry* 46 (8): 1565-1571.

Shet, A., and S. K. Vidya. 2016. "Solar Light Mediated Photocatalytic Degradation of Phenol Using Ag Core – Tio2 Shell (Ag@Tio2) Nanoparticles in Batch and Fluidized Bed Reactor." *Solar Energy* 127: 67-78.

Shourian, M., K. A. Noghabi, H. S. Zahiri, T. Bagheri, R. Karbalaei, M. Mollaei, I. Rad, S. Ahadi, J. Raheb, and H. Abbasi. 2009. "Efficient Phenol Degradation by a Newly Characterized Pseudomonas Sp. Sa01 Isolated from Pharmaceutical Wastewaters." *Desalination* 246 (1): 577-594.

Shukla, S. P., and S. Devi. 2005. "Covalent Coupling of Peroxidase to a Copolymer of Acrylamide (Aam)-2-Hydroxyethyl Methaacrylate (Hema) and Its Use in Phenol Oxidation." *Process Biochemistry* 40 (1): 147-154.

Shukla, S. P., K. Modi, P. K. Ghosh, and S. Devi. 2004. "Immobilization of Horseradish Peroxidase by Entrapment in Natural Polysaccharide." *Journal of Applied Polymer Science* 91 (4): 2063-2071.

Singh, N., and J. Singh. 2002. "An Enzymatic Method for Removal of Phenol from Industrial Effluent." *Preparative Biochemistry and Biotechnology* 32 (2): 127-33.

Sittinger, M., B. Lukanoff, G. R. Burmester, and H. Dautzenberg. 1996. "Encapsulation of Artificial Tissues in Polyelectrolyte Complexes: Preliminary Studies." *Biomaterials* 17 (10): 1049-1051.

Sobiesiak, M., and B. Podkoscielna. 2010. "Preparation and Characterization of Porous Dvb Copolymers and Their Applicability for Adsorption (Solid-Phase Extraction) of Phenol Compounds." *Applied Surface Science* 257 (4): 1222-1227.

Song, Y., J. Jiang, J. Ma, S. Y. Pang, Y. Z. Liu, Y. Yang, C. W. Luo, J. Q. Zhang, J. Gu, and W. Qin. 2015. "Abts as an Electron Shuttle to Enhance the Oxidation

Kinetics of Substituted Phenols by Aqueous Permanganate." *Environmental Science and Technology* 49 (19): 11764-71.

Soravia, S., and A. Orth. 2009. "Design of Experiments." In *Ullmann's Encyclopedia of Industrial Chemistry*. Wiley-VCH Verlag GmbH & Co. KGaA.

Sosa Alderete, L. G., M. A. Talano, S. G. Ibanez, S. Purro, E. Agostini, S. R. Milrad, and M. I. Medina. 2009. "Establishment of Transgenic Tobacco Hairy Roots Expressing Basic Peroxidases and Its Application for Phenol Removal." *Journal of Biotechnology* 139 (4): 273-9.

Spiker, J. K., D. L. Crawford, and E. C. Thiel. 1992. "Oxidation of Phenolic and Non-Phenolic Substrates by the Lignin Peroxidase of Streptomyces Viridosporus T7a." *Applied Microbiology and Biotechnology* 37 (4): 518-523.

Stadlbauer, V., P. B. Stiegler, S. Schaffellner, O. Hauser, G. Halwachs, F. Iberer, K. H. Tscheliessnigg, and C. Lackner. 2006. "Morphological and Functional Characterization of a Pancreatic Beta-Cell Line Microencapsulated in Sodium Cellulose Sulfate/Poly(Diallyldimethylammonium Chloride)." *Xenotransplantation* 13 (4): 337-44.

Steevensz, A., S. Madur, W. Feng, K. E. Taylor, J. K. Bewtra, and N. Biswas. 2014. "Crude Soybean Hull Peroxidase Treatment of Phenol in Synthetic and Real Wastewater: Enzyme Economy Enhanced by Triton X-100." *Enzyme and Microbial Technology* 55 (0): 65-71.

Suzuki, H., S. Araki, and H. Yamamoto. 2015. "Evaluation of Advanced Oxidation Processes (Aop) Using O3, Uv, and Tio2 for the Degradation of Phenol in Water." *Journal of Water Process Engineering* 7: 54-60.

Tan, I. A. W., A. L. Ahmad, and B. H. Hameed. 2008. "Preparation of Activated Carbon from Coconut Husk: Optimization Study on Removal of 2,4,6-Trichlorophenol Using Response Surface Methodology." *Journal of Hazardous Materials* 153 (1): 709-717.

———. 2009. "Fixed-Bed Adsorption Performance of Oil Palm Shell-Based Activated Carbon for Removal of 2,4,6-Trichlorophenol." *Bioresource Technology* 100 (3): 1494-1496.

Tan, J.-Y., Y.-R. Ren, and S.-J. Yao. 2011. "Preparation of Micro-Scaled Multilayer Capsules of Poly-Dimethyl-Diallyl-Ammonium Chloride and Sodium Cellulose Sulfate by Layer-by-Layer Self-Assembly Technique." *Carbohydrate Polymers* 84 (1): 351-357.

Tatsumi, K., S. Wada, and H. Ichikawa. 1996. "Removal of Chlorophenols from Wastewater by Immobilized Horseradish Peroxidase." *Biotechnology and Bioengineering* 51 (1): 126-130.

Tepe, O., and A. Y. Dursun. 2008. "Combined Effects of External Mass Transfer and Biodegradation Rates on Removal of Phenol by Immobilized Ralstonia Eutropha in a Packed Bed Reactor." *Journal of Hazardous materials* 151 (1): 9-16.

Thue, P. S., E. C. Lima, J. M. Sieliechi, C. Saucier, S. L. P. Dias, J. C. P. Vaghetti, F. S. Rodembusch, and F. A. Pavan. 2017. "Effects of First-Row Transition Metals and Impregnation Ratios on the Physicochemical Properties of Microwave-Assisted Activated Carbons from Wood Biomass." *Journal of Colloid and Interface Science* 486: 163-175.

Tien, M., and T. K. Kirk. 1983. "Lignin-Degrading Enzyme from the Hymenomycete Phanerochaete Chrysosporium Burds." *Science* 221 (4611): 661-3.

Tisa, F., A. A. Abdul Raman, and W. M. A. Wan Daud. 2014. "Applicability of Fluidized Bed Reactor in Recalcitrant Compound Degradation through

Advanced Oxidation Processes: A Review." *Journal of Environmental Management* 146: 260-275.

Triplett, B. A., and J. E. Mellon. 1992. "Purification and Characterization of Anionic Peroxidases from Cotton (Gossypium Hirsutum L.)." *Plant Science* 81 (2): 147-154.

Trivedi, U., A. Bassi, and J.-X. Zhu. 2006a. "Continuous Enzymatic Polymerization of Phenol in a Liquid–Solid Circulating Fluidized Bed." *Powder Technology* 169 (2): 61-70.

Trivedi, U. J., A. S. Bassi, and J. Zhu. 2006b. "Investigation of Phenol Removal Using Sol-Gel/Alginate Immobilized Soybean Seed Hull Peroxidase." *The Canadian Journal of Chemical Engineering* 84 (2): 239-247.

Tziotzios, G., C. N. Economou, G. Lyberatos, and D. V. Vayenas. 2007. "Effect of the Specific Surface Area and Operating Mode on Biological Phenol Removal Using Packed Bed Reactors." *Desalination* 211 (1–3): 128-137.

Valderrama, B., M. Ayala, and R. Vazquez-Duhalt. 2002. "Suicide Inactivation of Peroxidases and the Challenge of Engineering More Robust Enzymes." *Chem Biol* 9 (5): 555-65.

Valli, K., and M. H. Gold. 1991. "Degradation of 2,4-Dichlorophenol by the Lignin-Degrading Fungus Phanerochaete Chrysosporium." *Journal of Bacteriology* 173 (1): 345-352.

Vámos-Vigyázó, L., and N. F. Haard. 1981. "Polyphenol Oxidases and Peroxidases in Fruits and Vegetables." *C R C Critical Reviews in Food Science and Nutrition* 15 (1): 49-127.

Vasileva, N., T. Godjevargova, D. Ivanova, and K. Gabrovska. 2009. "Application of Immobilized Horseradish Peroxidase onto Modified Acrylonitrile Copolymer Membrane in Removing of Phenol from Water." *International Journal of Biological Macromolecules* 44 (2): 190-194.

Vasudevan, P., and L. Li. 1996. "Peroxidase Catalyzed Polymerization of Phenol." *Applied Biochemistry and Biotechnology* 60 (1): 73-82.

Vera Candioti, L., M. M. De Zan, M. S. Cámara, and H. C. Goicoechea. 2014. "Experimental Design and Multiple Response Optimization. Using the Desirability Function in Analytical Methods Development." *Talanta* 124: 123-138.

Villegas, L. G. C., N. Mashhadi, M. Chen, D. Mukherjee, K. E. Taylor, and N. Biswas. 2016. "A Short Review of Techniques for Phenol Removal from Wastewater." *Current Pollution Reports* 2 (3): 157-167.

Vinod, A. V., and G. V. Reddy. 2006. "Mass Transfer Correlation for Phenol Biodegradation in a Fluidized Bed Bioreactor." *Journal of Hazardous materials* 136 (3): 727-734.

Wada, S., H. Ichikawa, and K. Tastsumi. 1995. "Removal of Phenols and Aromatic Amines from Wastewater by a Combination Treatment with Tyrosinase and a Coagulant." *Biotechnology and Bioengineering* 45 (4): 304-9.

Wagner, M., and J. A. Nicell. 2001a. "Peroxidase-Catalyzed Removal of Phenols from a Petroleum Refinery Wastewater." *Water Sci Technol* 43 (2): 253-60.

Wagner, M., and J. A. Nicell. 2001b. "Treatment of a Foul Condensate from Kraft Pulping with Horseradish Peroxidase and Hydrogen Peroxide." *Water Research* 35 (2): 485-495.

———. 2002. "Detoxification of Phenolic Solutions with Horseradish Peroxidase and Hydrogen Peroxide." *Water Research* 36 (16): 4041-4052.

Wang, S., H. Fang, Y. Wen, M. Cai, W. Liu, S. He, and X. Xu. 2015. "Applications of Hrp-Immobilized Catalytic Beads to the Removal of 2,4-Dichlorophenol from Wastewater." *RSC Advances* 5 (71): 57286-57292.

Wang, S., H. Fang, X. Yi, Z. Xu, X. Xie, Q. Tang, M. Ou, and X. Xu. 2016. "Oxidative Removal of Phenol by Hrp-Immobilized Beads and Its Environmental Toxicology Assessment." *Ecotoxicology and Environmental Safety* 130: 234-239.

Wang, S., W. Liu, J. Zheng, and X. Xu. 2016. "Immobilization of Horseradish Peroxidase on Modified Pan-Based Membranes for the Removal of Phenol from Buffer Solutions." *The Canadian Journal of Chemical Engineering* 94 (5): 865-871.

Welinder, K. G. 1992. "Superfamily of Plant, Fungal and Bacterial Peroxidases." *Current Opinion in Structural Biology* 2 (3): 388-393.

WHO. 2011. "Guidelines for Drinking-Water Quality." *WHO chronicle* 38 (4): 104-8.

Wilberg, K., C. Assenhaimer, and J. Rubio. 2002. "Removal of Aqueous Phenol Catalysed by a Low Purity Soybean Peroxidase." *Journal of Chemical Technology & Biotechnology* 77 (7): 851-857.

Wilberg, K. Q., D. G. Nunes, and J. Rubio. 2000. "Removal of Phenol by Enzymatic Oxidation and Flotation." *Brazilian Journal of Chemical Engineering* 17: 907-914.

Wong, S., N. Ngadi, I. M. Inuwa, and O. Hassan. 2018. "Recent Advances in Applications of Activated Carbon from Biowaste for Wastewater Treatment: A Short Review." *Journal of Cleaner Production* 175: 361-375.

Wright, H., and J. A. Nicell. 1999. "Characterization of Soybean Peroxidase for the Treatment of Aqueous Phenols." *Bioresource Technology* 70 (1): 69-79.

Wu, J., J. K. Bewtra, N. Biswas, and K. E. Taylor. 1994. "Effect of H2o2 Addition Mode on Enzymatic Removal of Phenol from Wastewater in the Presence of Polyethylene Glycol." *The Canadian Journal of Chemical Engineering* 72 (5): 881-886.

Wu, J., K. E. Taylor, J. K. Bewtra, and N. Biswas. 1993. "Optimization of the Reaction Conditions for Enzymatic Removal of Phenol from Wastewater in the Presence of Polyethylene Glycol." *Water Research* 27 (12): 1701-1706.

Wu, Y., K. E. Taylor, N. Biswas, and J. K. Bewtra. 1997. "Comparison of Additives in the Removal of Phenolic Compounds by Peroxidase-Catalyzed Polymerization." *Water Research* 31 (11): 2699-2704.

———. 1998. "A Model for the Protective Effect of Additives on the Activity of Horseradish Peroxidase in the Removal of Phenol." *Enzyme and Microbial Technology* 22 (5): 315-322.

Xu, D.-Y., and Z. Yang. 2013. "Cross-Linked Tyrosinase Aggregates for Elimination of Phenolic Compounds from Wastewater." *Chemosphere* 92 (4): 391-398.

Yahiaoui, I., F. Aissani-Benissad, F. Fourcade, and A. Amrane. 2012. "Response Surface Methodology for the Optimization of the Electrochemical Degradation of Phenol on Pb/Pbo2 Electrode." *Environmental Progress & Sustainable Energy* 31 (4): 515-523.

Yao, S.-J., Y.-X. Guan, and D.-Q. Lin. 2006. "Mass Transfer Behavior of Solutes in Nacs−Pdmdaac Capsules." *Industrial & Engineering Chemistry Research* 45 (5): 1811-1816.

Yao, S. 1999. *Sulfation Kinetics in the Preparation of Cellulose Sulfate*. Vol. 7.

———. 2000. "An Improved Process for the Preparation of Sodium Cellulose Sulphate." *Chemical Engineering Journal* 78 (2–3): 199-204.

Younis, S. A., W. I. El-Azab, N. S. El-Gendy, S. Q. Aziz, Y. M. Moustafa, H. A. Aziz, and S. S. A. Amr. 2014. "Application of Response Surface Methodology to Enhance Phenol Removal from Refinery Wastewater by Microwave Process." *International Journal of Microwave Science and Technology* 2014: 12.

Yu, J., K. E. Taylor, H. Zou, N. Biswas, and J. K. Bewtra. 1994. "Phenol Conversion and Dimeric Intermediates in Horseradish Peroxidase-Catalyzed Phenol Removal from Water." *Environmental Science & Technology* 28 (12): 2154-2160.

Zeng, X., M. K. Danquah, R. Halim, S. Yang, X. D. Chen, and Y. Lu. 2013. "Comparative Physicochemical Analysis of Suspended and Immobilized Cultivation of Chlorella Sp." *Journal of Chemical Technology & Biotechnology* 88 (2): 247-254.

Zeng, X., M. K. Danquah, R. Potumarthi, J. Cao, X. D. Chen, and Y. Lu. 2013. "Characterization of Sodium Cellulose Sulphate/Poly-Dimethyl-Diallyl-Ammonium Chloride Biological Capsules for Immobilized Cultivation of Microalgae." *Journal of Chemical Technology & Biotechnology* 88 (4): 599-605.

Zeng, X., M. K. Danquah, C. Zheng, R. Potumarthi, X. D. Chen, and Y. Lu. 2012. "Nacs–Pdmdaac Immobilized Autotrophic Cultivation of Chlorella Sp. For Wastewater Nitrogen and Phosphate Removal." *Chemical Engineering Journal* 187 (0): 185-192.

Zhai, R., B. Zhang, Y. Wan, C. Li, J. Wang, and J. Liu. 2013. "Chitosan–Halloysite Hybrid-Nanotubes: Horseradish Peroxidase Immobilization and Applications in Phenol Removal." *Chemical Engineering Journal* 214: 304-309.

Zhang, F., B. Zheng, J. Zhang, X. Huang, H. Liu, S. Guo, and J. Zhang. 2010. "Horseradish Peroxidase Immobilized on Graphene Oxide: Physical Properties and Applications in Phenolic Compound Removal." *The Journal of Physical Chemistry C* 114 (18): 8469-8473.

Zhang, J., Y.-X. Guan, Z. Ji, and S.-J. Yao. 2006. "Effects on Membrane Properties of Nacs–Pdmdaac Capsules by Adding Inorganic Salts." *Journal of Membrane Science* 277 (1): 270-276.

Zhang, J., S.-J. Yao, and Y.-X. Guan. 2005. "Preparation of Macroporous Sodium Cellulose Sulphate/Poly(Dimethyldiallylammonium Chloride) Capsules and Their Characteristics." *Journal of Membrane Science* 255 (1–2): 89-98.

Zhang, J., P. Ye, S. Chen, and W. Wang. 2007. "Removal of Pentachlorophenol by Immobilized Horseradish Peroxidase." *International Biodeterioration & Biodegradation* 59 (4): 307-314.

Zhang, Y., P. He, and N. Hu. 2004. "Horseradish Peroxidase Immobilized in Tio2 Nanoparticle Films on Pyrolytic Graphite Electrodes: Direct Electrochemistry and Bioelectrocatalysis." *Electrochimica Acta* 49 (12): 1981-1988.

Zhang, Y., Z. Zeng, G. Zeng, X. Liu, Z. Liu, M. Chen, L. Liu, J. Li, and G. Xie. 2012. "Effect of Triton X-100 on the Removal of Aqueous Phenol by Laccase Analyzed with a Combined Approach of Experiments and Molecular Docking." *Colloids and Surfaces B: Biointerfaces* 97: 7-12.

Zhao, Y.-N., G. Chen, and S.-J. Yao. 2006. "Microbial Production of 1,3-Propanediol from Glycerol by Encapsulated Klebsiella Pneumoniae." *Biochemical Engineering Journal* 32 (2): 93-99.

Zhao, Z., Q. Chen, and J.-i. Anzai. 2009. "Horseradish Peroxidase Microcapsules Based on Layer-by-Layer Polyelectrolyte Deposition." *Journal of Environmental Sciences* 21: S135-S138.

Zheng, C., X. Zeng, M. K. Danquah, and Y. Lu. 2015. "Nacs-Pdmdaac Immobilized Cultivation of Recombinant Dictyostelium Discoideum for Soluble Human Fas Ligand Production." *Biotechnology Progress* 31 (2): 424-430.

Zheng, H., and X. Jiang. 2014. *Immobilization of Soybean Hulls Peroxidase on Activated Carbon*. Vol. 26.

Zhou, D., Z. Xu, Y. Wang, J. Wang, D. Hou, and S. Dong. 2015. "Simultaneous Removal of Multi-Pollutants in an Intimate Integrated Flocculation-Adsorption Fluidized Bed." *Environ Sci Pollut Res Int* 22 (5): 3794-802.

Zhou, J., X. Yu, C. Ding, Z. Wang, Q. Zhou, H. Pao, and W. Cai. 2011. "Optimization of Phenol Degradation by Candida Tropicalis Z-04 Using Plackett-Burman Design and Response Surface Methodology." *J Environ Sci (China)* 23 (1): 22-30.

Zhou, M.-F., X.-Z. Yuan, H. Zhong, Z.-F. Liu, H. Li, L.-L. Jiang, and G.-M. Zeng. 2011. "Effect of Biosurfactants on Laccase Production and Phenol Biodegradation in Solid-State Fermentation." *Applied Biochemistry and Biotechnology* 164 (1): 103-114.

Zhuang, H., Y. Cui, and W. Zhu. 2001. *[Development of a Diagnostic Kit of Enzyme-Linked Immunoassay for Detecting Serum Anti-Hepatitis E Virus Igg]*. Vol. 35.

APPENDICES

APPENDIX A

1) Standard curve of phenol concentrations:

Table A. 1: Raw data for phenol concentration standard curve.

Phenol concentration, mg/mL	Absorbance, A_{510nm}
0.00	0
0.01	0.0621
0.02	0.1320
0.03	0.2160
0.04	0.3063
0.05	0.3838
0.06	0.4576
0.07	0.5608
0.08	0.6448
0.09	0.7268
0.10	0.8114

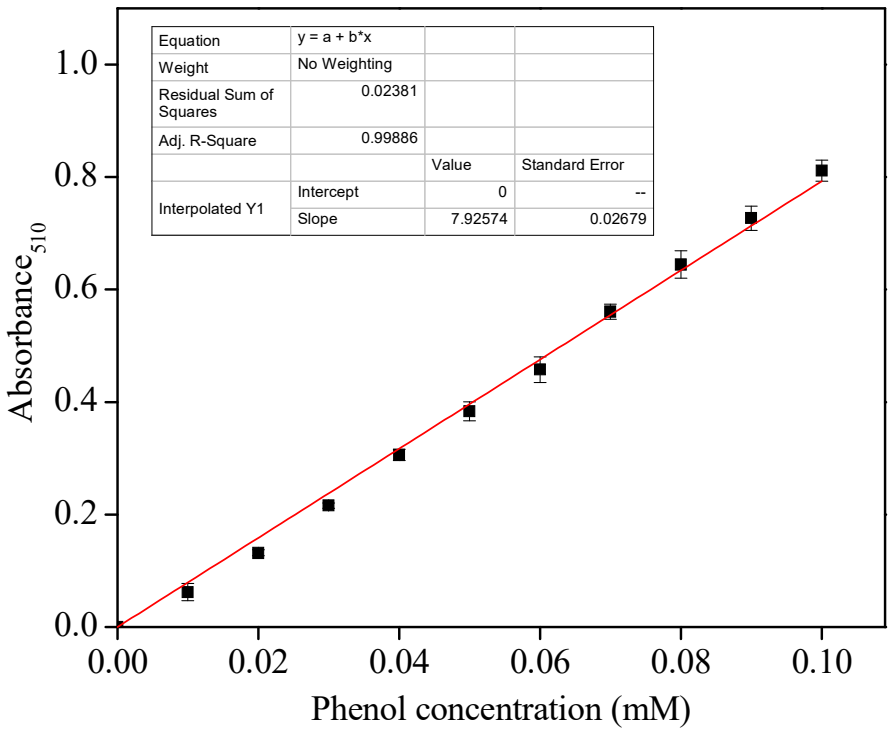

Figure A. 1: Standard curve of phenol concentrations.

2) Standard curve of BSA protein concentrations:

Table A. 2: Raw data for protein concentration standard curve.

Protein concentration, mg/mL	Absorbance, A_{595nm}	Net A_{595nm}
0	0.4989	0.0000
0.01	0.5128	0.0220
0.025	0.5559	0.0570
0.05	0.6284	0.1295
0.1	0.7572	0.2583
0.2	0.9829	0.4840

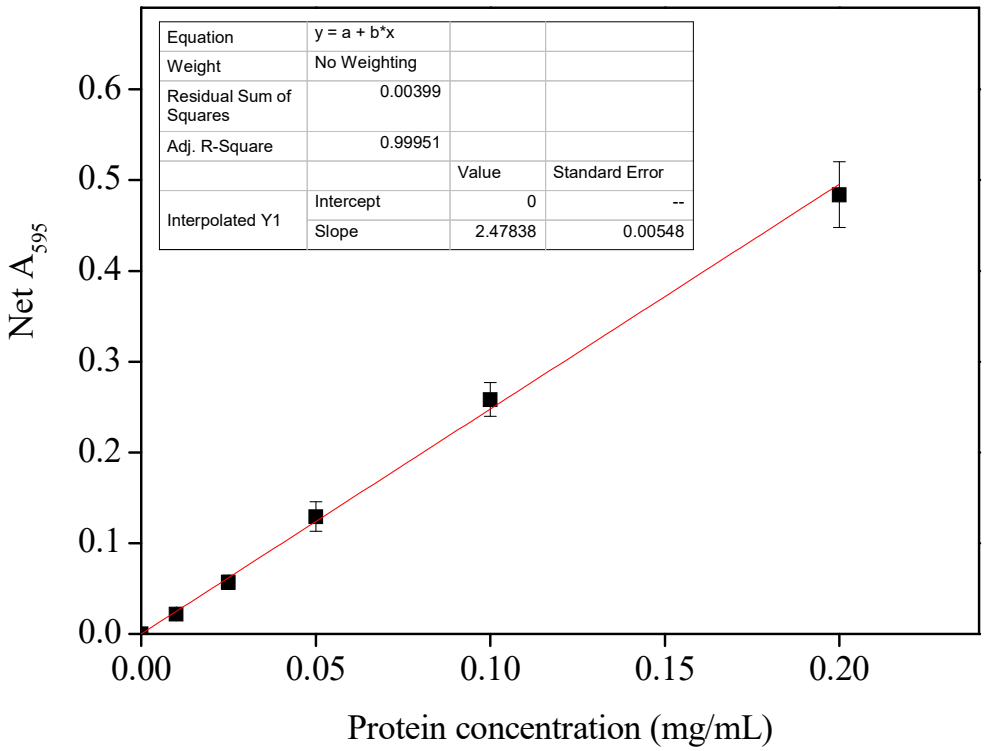

Figure A. 2: Standard curve of protein concentrations.

APPENDIX B

Calculation of phenol and H_2O_2 concentrations under Section 4.9.

Total volume of pH 6 sodium phosphate buffer solution (0.1 M) = 200 mL

a) After adding 2 mL of 0.1 M phenol stock solution into the buffer solution, the concentration of phenol in the reaction mixture is:

$$M_1V_1 = M_2V_2$$
$$0.1\ \text{M} \times 2\ \text{mL} = M_2 \times 202\ \text{mL}$$
$$M_2 = 0.99\ \text{mM}$$
$$= \sim 1\ \text{mM}$$

b) After adding 1 mL of 0.2 M H_2O_2 stock solution into the reaction mixture to initiate the enzymatic process, the concentration of phenol in the reaction mixture becomes:

$$M_1V_1 = M_2V_2$$
$$0.99\ \text{mM} \times 202\ \text{mL} = M_2 \times 203\ \text{mL}$$
$$M_2 = 0.985\ \text{mM}$$
$$\text{Percentage of change in phenol concentration} = \frac{0.99 - 0.985}{0.99} \times 100\%$$
$$= 0.5\%$$

c) Concentration of H_2O_2 solution in the reaction mixture:

$$M_1V_1 = M_2V_2$$
$$0.2\ \text{M} \times 1\ \text{mL} = M_2 \times 203\ \text{mL}$$
$$M_2 = 0.985\ \text{mM}$$
$$= \sim 1\ \text{mM}$$